Effect of Slot Spacing on Single Plate Connections with Long Slots

by

Drake S. Taxon

A Report Submitted to the Faculty of the

Milwaukee School of Engineering

In Partial Fulfillment of the

Requirements for the Degree of

Master of Science in Civil Engineering

Milwaukee, Wisconsin

May 2021

Abstract

Single plate shear connections with extra-long slots are commonly used at interfaces between concrete cores and steel framing. Differences in construction tolerances require compensation at these interfaces and this difference is often accounted for in the connection by using extra-long slots. However, there is an extremely limited body of knowledge on the effect these long slots have on this type of connection. This report seeks to begin contributing to the knowledge and offer recommendations for future work by examining the effect of varied slot spacing on the connection.

To study this connection, an experimental program consisting of specimens with varied spacings of 3.0 in. (76 mm), 3.5 in. (89 mm), 4.0 in. (102 mm), and 4.5 in. (114 mm) center to center were used. The tests were carried out under monotonic loading and global displacement data were analyzed to determine a tested capacity for each specimen.

The results of the experimental program indicate a positive correlation between slot spacing and connection capacity – as the slot spacing in increased, the capacity of the connection increases. The results of this study are limited though and offer a starting point for this work. Future research studying different parameters of the connection such as plate thickness, number of bolt rows, and end distances should be carried out as well as developing a more accurate calculation of the capacity and creating an inelastic finite element model to observe behavior of the connection not measurable in experimental testing.

Acknowledgments

This capstone report would not have been possible without the help of many people and groups. I would start off by thanking Steve Herlache and Casey Peterson at Computerized Structural Design for bringing this research topic to light. It was exciting working on a project that is centered around a real-world issue. I would also like to thank Zalk Josephs Fabricators in Stoughton, WI for generously donating the test specimens and custom test setup components.

I would like to thank my advisor, Dr. Christopher Raebel, for helping me throughout the project with his guidance and helpful feedback. Thank you to my committee members, Dr. Pouria Bahmani at the Milwaukee School of Engineering and Michael Kempfert at Computerized Structural Design for providing insightful comments and helping me think deeper about the work for this report.

I would also like to thank Cassidy Jackson for her work alongside mine as we worked through the experimental setup and testing portions of this project in tandem.

Lastly, I would like to thank my family and friends for encouraging me throughout my time at MSOE.

Table of Contents

List of Figures ... 7

List of Tables ... 14

Nomenclature ... 15

Glossary ... 17

Chapter 1: Introduction ... 18

Chapter 2: Literature Review and Current Practices ... 21

2.1 AISC *Specification for Structural Steel Buildings* ... 21

2.2 Behavior of Extra-Long Slots by Wollenslegel ... 22

2.3 Analysis of Long-Slotted Holes in Single Plate Connections by Peterson ... 27

2.4 Beam-to-Column Shear Connections with Slotted Holes by Man, Grondin, and Driver ... 29

Chapter 3: Experimental Program ... 33

3.1 Introduction ... 33

3.2 Hypothesis ... 33

3.3 Experimental Specimens ... 34

3.3.1 Overview ... 34

3.3.2 Test Nomenclature ... 36

3.4 Experimental Specimen Expected Capacities ... 36

3.4.1 Discussion of Expected Capacities ... 38

3.5 Test Setup Overview and Design ... 40

3.6 Shop Drawings ... 48

3.7 Material Testing ... 48

3.8 Instrumentation ... 49

3.8.1 Displacements ... 49

3.8.2 Strain Gauges ... 53

3.8.3 Load Cell ... 56

3.9 Data Acquisition System and Wiring ... 56

3.9.1 Data Acquisition System Wiring ... 58

3.10 Experimental Procedure ... 61

Chapter 4: Experimental Results ... 68

4.1 Experimental Specimen Behavior ... 68

4.2 Specimen Plate Displacement Data ... 70

4.3 Strain Gauges ... 83

4.4 Base Plate Displacement ... 84

4.5 Access to Raw Experimental Data ... 84

Chapter 5: Data Analysis and Comparison ... 85

5.1 Introduction ... 85

5.2 Alternate Analysis Methods Considered ... 85

5.3 Analysis Procedure ... 86

5.3.1 Manual Prefiltering of Raw Data ... 86

5.3.2 MATLAB Operations ... 86

5.3.3 Manual Capacity Determination ... 90

5.4 Tested Capacities ... 92

5.5 Comparison of Expected Capacities and Tested Capacities ... 104

Chapter 6: Discussion and Conclusions ... 108

6.1 Discussion of Experimental Instrumentation and Procedure 108
6.1.1 Specimen Anchorage Improvements 108
6.1.2 Removal of One Sandwich Plate 108
6.1.3 Experimental Setup of Connection 108
6.1.4 Additional Displacement Measurement 109
6.1.5 Alternate Rosette Location 109
6.2 Recommendations for Future Work 110
6.2.1 Varied Specimen Properties 110
6.2.2 Determine Behavior Model for Slots 111
6.2.3 Inelastic Finite Element Model 111
6.3 Conclusions 112
References 113
Appendix A : Calculations for the Expected Capacity of the Experimental Specimens 115
Appendix B : Calculations for the Custom Yoke 141
Appendix C : Calculations for the Sandwich Plates 146
Appendix D : Shop Drawings 152
Appendix E : Material Testing Report 164
Appendix F : Experimental Specimen Dimensions 166
Appendix G : Post-Test Specimen Photos 171
Appendix H : Load versus Strain Plots 194
Appendix I : Summary of Changes Made to LVDT 1 Data During Prefilter Step 202
Appendix J : MATLAB Code 206

List of Figures

Figure 1-1: Common Detail of Single Shear Plate for Beam to Column Connection. 18

Figure 1-2: Construction Tolerance and Its Effect on Single Plate Shear Connections. .. 20

Figure 2.2-1: Wollenslegel Test Setup 23

Figure 2.2-2: Test Specimen Series. 24

Figure 2.2-3: Failed Test Specimens E-04A (a) and F-04A (b) 26

Figure 2.3-1: Finite Element Mesh 27

Figure 2.3-2: Axial Stress Patterns (a) and Deformed Model (b). 28

Figure 2.4-1: Clip Angle Test Setup 30

Figure 2.4-2: Failed Test Specimens 1L9 (a), 1L1 (b), and 2L3 (c) 32

Figure 3.3-1: Parametric Elevation of Experimental Specimen. 35

Figure 3.3-2: Bolt Group Positions Within Long Slots. 36

Figure 3.3-3: Experimental Specimen Nomenclature Explanation. 36

Figure 3.4.1-1: Expected Capacity Versus Slot Spacing. 39

Figure 3.5-1: Schematic Drawing of Test Setup. 40

Figure 3.5-2: Support Beam in Test Setup 41

Figure 3.5-3: Reaction Plates in Test Setup. 41

Figure 3.5-4: Enerpac RRH606 “Hollow-Core” Actuator. 42

Figure 3.5-5: Sensotec 41-A530-01-03 Load Cell. 43

Figure 3.5-6: Load Cell Plate. 43

Figure 3.5-7: A307 Grade B Threaded Rod. 44

Figure 3.5-8: Custom Designed Yoke. 45

Figure 3.5-9: Sandwich Plates. 46

Figure 3.5-10: Filler Plate Used Between Sandwich Plates. 47

Figure 3.5-11: Steel Shim Plate. 48

Figure 3.8.1-1: Attachment of LVDT 1 to Experimental Specimen................................ 50

Figure 3.8.1-2: Location of LVDTs on Experimental Specimen..................................... 51

Figure 3.8.1-3: LVDT 1 (a) and LVDT 2 (b) with Signal Conditioner. 52

Figure 3.8.2-1: A Single Rosette, Close up. 53

Figure 3.8.2-2: Placement of Rosette on Specimen. 54

Figure 3.8.2-3: Rosette Adhered to Specimen. 55

Figure 3.9-1: cDAQ-9178 CompactDAQ Chassis... 57

Figure 3.9-2: NI-9215 Voltage Input Module... 57

Figure 3.9-3: NI-9235 Strain/Bridge Module 58

Figure 3.9.1-1: Schematic Plan View of Data Acquisition System Wiring...................... 60

Figure 3.10-1: Specimen Dimensions. 61

Figure 3.10-2: TONE® Shear Wrench. 64

Figure 3.10-3: Plexiglass Shield. 65

Figure 4.2-1: Load Versus Specimen Displacement for Specimen S30P100.................. 73

Figure 4.2-2: Load Versus Specimen Displacement for Specimen S35P100.................. 73

Figure 4.2-3: Load Versus Specimen Displacement for Specimen S40P100.................. 74

Figure 4.2-4: Load Versus Specimen Displacement for Specimen S45P100.................. 74

Figure 4.2-5: Load Versus Specimen Displacement for Specimen S30P075.................. 75

Figure 4.2-6: Load Versus Specimen Displacement for Specimen S35P075.................. 75

Figure 4.2-7: Load Versus Specimen Displacement for Specimen S40P075.................. 76

Figure 4.2-8: Load Versus Specimen Displacement for Specimen S45P075.................. 76

Figure 4.2-9: Load Versus Specimen Displacement for Specimen S30P050.................. 77

Figure 4.2-10: Load Versus Specimen Displacement for Specimen S35P050................ 77

Figure 4.2-11: Load Versus Specimen Displacement for Specimen S40P050................ 78

Figure 4.2-12: Load Versus Specimen Displacement for Specimen S45P050................ 78

Figure 4.2-13: Load Versus Specimen Displacement for Specimen S30P025................ 79

Figure 4.2-14: Load Versus Specimen Displacement for Specimen S35P025................ 79

Figure 4.2-15: Load Versus Specimen Displacement for Specimen S40P025................ 80

Figure 4.2-16: Load Versus Specimen Displacement for Specimen S45P025................ 80

Figure 4.2-17: Load Versus Specimen Displacement for Specimen S30P000................ 81

Figure 4.2-18: Load Versus Specimen Displacement for Specimen S35P000................ 81

Figure 4.2-19: Load Versus Specimen Displacement for Specimen S40P000................ 82

Figure 4.2-20: Load Versus Specimen Displacement for Specimen S45P000................ 82

Figure 4.3-1: Representative Strain Data (from Specimen S40P100). 83

Figure 4.3-2: Strain Gauge Numbering and Positioning. 84

Figure 5.3.2.1-1: Effect of Additional Median Filter on Specimen S30P100. 88

Figure 5.3.2.2-1: Effect of Smoothing Parameter on Curve Fit Function. 89

Figure 5.3.3-1: Explanation of “Region of Interest”... 91

Figure 5.4-1: Load Versus Specimen Displacement for Specimen S30P100.................. 94

Figure 5.4-2: Load Versus Specimen Displacement for Specimen S35P100.................. 94

Figure 5.4-3: Load Versus Specimen Displacement for Specimen S40P100.................. 95

Figure 5.4-4: Load Versus Specimen Displacement for Specimen S45P100.................. 95

Figure 5.4-5: Load Versus Specimen Displacement for Specimen S30P075.................. 96

Figure 5.4-6: Load Versus Specimen Displacement for Specimen S35P075.................. 96

Figure 5.4-7: Load Versus Specimen Displacement for Specimen S40P075................... 97

Figure 5.4-8: Load Versus Specimen Displacement for Specimen S45P075................... 97

Figure 5.4-9: Load Versus Specimen Displacement for Specimen S30P050................... 98

Figure 5.4-10: Load Versus Specimen Displacement for Specimen S35P050................. 98

Figure 5.4-11: Load Versus Specimen Displacement for Specimen S40P050................. 99

Figure 5.4-12: Load Versus Specimen Displacement for Specimen S45P050................. 99

Figure 5.4-13: Load Versus Specimen Displacement for Specimen S30P025............... 100

Figure 5.4-14: Load Versus Specimen Displacement for Specimen S35P025............... 100

Figure 5.4-15: Load Versus Specimen Displacement for Specimen S40P025............... 101

Figure 5.4-16: Load Versus Specimen Displacement for Specimen S45P025............... 101

Figure 5.4-17: Load Versus Specimen Displacement for Specimen S30P000............... 102

Figure 5.4-18: Load Versus Specimen Displacement for Specimen S35P000............... 102

Figure 5.4-19: Load Versus Specimen Displacement for Specimen S40P000............... 103

Figure 5.4-20: Load Versus Specimen Displacement for Specimen S45P000............... 103

Figure 5.5-1: Tested Capacity Versus Slot Spacing. 107

Figure F-1: Specimen Dimensions.. 167

Figure G-1: Specimen S30P100 Post-Test, Front... 172

Figure G-2: Specimen S30P100 Post-Test, Loaded Edge. 172

Figure G-3: Specimen S35P100 Post-Test, Front... 173

Figure G-4: Specimen S35P100 Post-Test, Loaded Edge. 173

Figure G-5: Specimen S40P100 Post-Test, Front... 174

Figure G-6: Specimen S40P100 Post-Test, Loaded Edge. 174

Figure G-7: Specimen S45P100 Post-Test, Front... 175

Figure G-8: Specimen S45P100 Post-Test, Loaded Edge. 175

Figure G-9: Specimen S30P075 Post-Test, Front. 176

Figure G-10: Specimen S30P075 Post-Test, Loaded Edge. 176

Figure G-11: Specimen S35P075 Post-Test, Front. 177

Figure G-12: Specimen S35P075 Post-Test, Loaded Edge. 177

Figure G-13: Specimen S35P075 Post-Test, Plate Tearing. 178

Figure G-14: Specimen S40P075 Post-Test, Front. 179

Figure G-15: Specimen S40P075 Post-Test, Loaded Edge. 179

Figure G-16: Specimen S45P075 Post-Test, Front. 180

Figure G-17: Specimen S45P075 Post-Test, Loaded Edge. 180

Figure G-18: Specimen S30P050 Post-Test, Front. 181

Figure G-19: Specimen S30P050 Post-Test, Loaded Edge. 181

Figure G-20: Specimen S30P050 Post-Test, Plate Tearing. 182

Figure G-21: Specimen S35P050 Post-Test, Front. 183

Figure G-22: Specimen S35P050 Post-Test, Loaded Edge. 183

Figure G-23: Specimen S40P050 Post-Test, Front. 184

Figure G-24: Specimen S40P050 Post-Test, Loaded Edge. 184

Figure G-25: Specimen S45P050 Post-Test, Front. 185

Figure G-26: Specimen S45P050 Post-Test, Loaded Edge. 185

Figure G-27: Specimen S30P025 Post-Test, Front. 186

Figure G-28: Specimen S30P025 Post-Test, Loaded Edge. 186

Figure G-29: Specimen S35P025 Post-Test, Front. 187

Figure G-30: Specimen S35P025 Post-Test, Loaded Edge. 187

Figure G-31: Specimen S40P025 Post-Test, Front. 188
Figure G-32: Specimen S40P025 Post-Test, Loaded Edge. 188
Figure G-33: Specimen S45P025 Post-Test, Front. 189
Figure G-34: Specimen S45P025 Post-Test, Loaded Edge. 189
Figure G-35: Specimen S30P000 Post-Test, Front. 190
Figure G-36: Specimen S30P000 Post-Test, Loaded Edge. 190
Figure G-37: Specimen S35P000 Post-Test, Front. 191
Figure G-38: Specimen S35P000 Post-Test, Loaded Edge. 191
Figure G-39: Specimen S40P000 Post-Test, Front. 192
Figure G-40: Specimen S40P000 Post-Test, Loaded Edge. 192
Figure G-41: Specimen S45P000 Post-Test, Front. 193
Figure G-42: Specimen S45P000 Post-Test, Loaded Edge. 193
Figure H-1: Load Versus Strain Plot for Specimen S30P100.. 195
Figure H-2: Load Versus Strain Plot for Specimen S35P100.. 195
Figure H-3: Load Versus Strain Plot for Specimen S40P100.. 196
Figure H-4: Load Versus Strain Plot for Specimen S45P100.. 196
Figure H-5: Load Versus Strain Plot for Specimen S30P075.. 197
Figure H-6: Load Versus Strain Plot for Specimen S30P050.. 197
Figure H-7: Load Versus Strain Plot for Specimen S35P050.. 198
Figure H-8: Load Versus Strain Plot for Specimen S40P050.. 198
Figure H-9: Load Versus Strain Plot for Specimen S45P050.. 199
Figure H-10: Load Versus Strain Plot for Specimen S30P025...................................... 199
Figure H-11: Load Versus Strain Plot for Specimen S30P000...................................... 200

Figure H-12: Load Versus Strain Plot for Specimen S35P000....................................... 200

Figure H-13: Load Versus Strain Plot for Specimen S40P000....................................... 201

Figure H-14: Load Versus Strain Plot for Specimen S45P000....................................... 201

List of Tables

Table 2.2-1: Results of Testing 25

Table 2.4-1: Test Specimen Summary 31

Table 3.4-1: Expected Capacities and Failure Mode of Each Experimental Specimen. .. 38

Table 4.1-1: Maximum Load and Relative Observed Experimental Specimen Behavior.70

Table 5.4-1: Tested Capacities for Each Experimental Specimen. 93

Table 5.5-1: Comparison of Expected and Tested Capacity for Each Specimen. 104

Table 5.5-2: Percent Differences, Expected Failure Mode, and Observed Behaviors. .. 105

Table F-1: Experimental Specimen Dimensions. 168

Nomenclature

Symbols

C_x Percent difference between step x and step $x - 1$, %

D_x Edge distance x, in. (mm)

E Modulus of elasticity, ksi (GPa)

E_x Edge distance x, in. (mm)

F_u Ultimate tensile stress, ksi (MPa)

F_y Yield stress, ksi (MPa)

L_{sx} Length of slot x, in. (mm)

L_v Vertical edge distance, in. (mm)

P Bolt position, %

S Slot spacing, in. (mm)

S_x Distance between slots x, in. (mm)

d_{hx} Width of slot x, in. (mm)

d_p Depth of plate, in. (mm)

h_p Height of plate, in. (mm)

n Number of bolt rows

t_p Plate thickness, in. (mm)

Abbreviations

ACI	American Concrete Institute
AISC	American Institute of Steel Construction
ANSI	American National Standards Institute
ASTM	American Society for Testing Materials
BNC	Bayonet Neill-Concelman [Connector]
ft	feet
GPa	Gigapascal
in.	inch
kip	kilopound (1000 pounds)
kN	kilonewton
ksi	kips per square inch
LVDT	Linear Variable Displacement Transducer
m	meter
mm	millimeter
MPa	Megapascal
P/N	Part Number
STD	Standard
USB	Universal Serial Bus

Glossary

Butterworth Filter A filter designed to have a frequency response as flat as possible in the passband [1]

Median Filter A filter in which each output value is computed as the median value of the input values in the considered window

[1] Butterworth, S. (1930). "On the Theory of Filter Amplifiers". *Experimental Wireless and the Wireless Engineer, Vol. 7, pp.* 536-541.

Chapter 1: Introduction

Single plate shear connections are commonly used in structural steel applications. They are a simple method of connecting beams to girders and girders to columns. Figure 1-1 shows a common detail of this type of this connection.

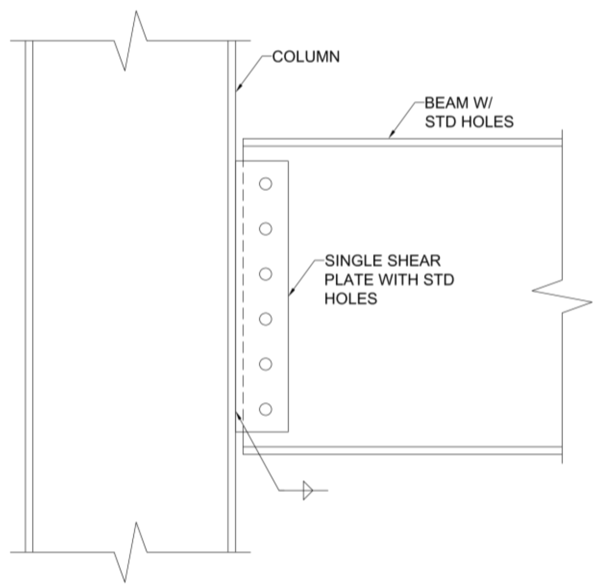

Figure 1-1: Common Detail of Single Shear Plate for Beam to Column Connection.

Single plate shear connections can also be used for connecting steel elements to concrete elements, such as a concrete wall as part of a full-height stair tower or elevator shaft. However, because construction tolerances differ between steel and concrete, there is a potential for fit-up difficulties in the field. The American Concrete Institute's (ACI) document, ACI 117-10 *Specification for Tolerance of Concrete Construction and Materials*, gives the maximum allowable deviation in all directions for cast-in-place concrete as ± 1 in. (25 mm) (ACI, 2010). The American National Standards Institute (ANSI) and the American Institute of Steel Construction (AISC) in their document, ANSI/AISC 303-16 *Code of Standard Practice for Steel Buildings and Bridges,* provide a fabrication tolerance for members up to 30 ft (9.1 m) in length an allowable deviation of

± $^{1}/_{16}$ in. (1.6 mm) (AISC, 2016a, p.16.3-32). Together, these tolerances create the need for connections that utilize long slots to ensure the steel members can frame into the concrete structure in the field. Figure 1-2 and the following description details how the construction and fabrication tolerances create the need for this type of connection.

Figure 1-2a shows a wall that was built exactly where it was supposed to be per the plans (the face of the wall is in line with the red line). If this happened every time a concrete wall was built, there would be no need to add long slots to the single shear plate. Figure 1-2b and Figure 1-2c show what happens to the connection if the wall is 1 in. (25 mm) to the right or 1 in. (25 mm) to the left of where the plans show it. As shown, the bolts move to the one extreme end or the other of the slots. This allows the other end of the beam to frame in with no issues. Without these slots, field work would need to be done to make the beam fit or a new beam, cut to the correct length, would need to be fabricated and shipped to the site. It should be noted that if at some point construction tolerances for concrete are reduced to the same ± $^{1}/_{16}$ in. (1.6 mm) as the steel tolerances, the issue presented in this report would disappear entirely.

There has been significant research done on the behavior of standard single shear plate connections with standard holes (like the one shown in Figure 1-1) or short slots in the plate, but the body of knowledge regarding the effect of long slots on the connection is limited. This capstone project report examines the effect of slot spacing on single shear plate connections with long slots.

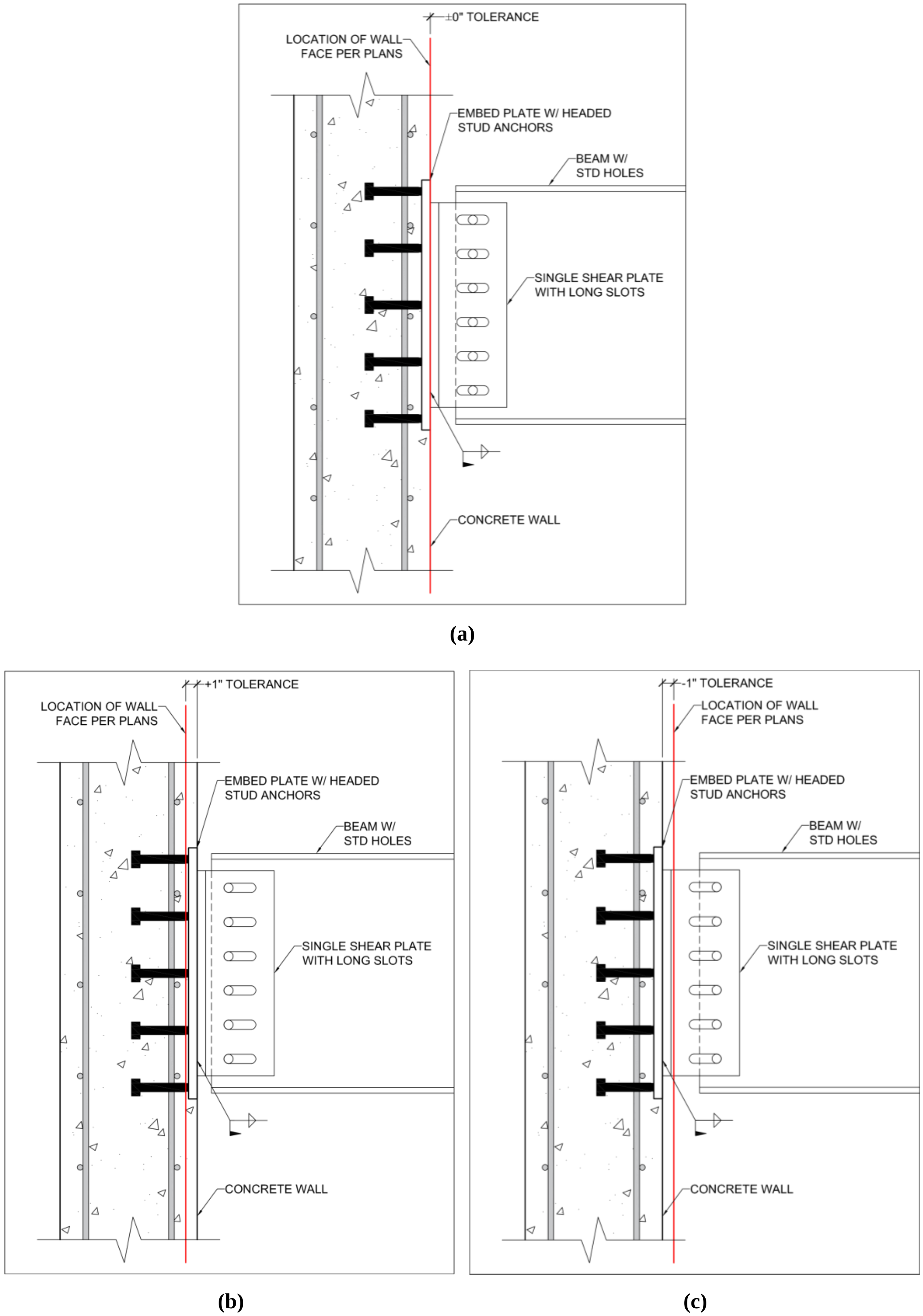

Figure 1-2: Construction Tolerance and Its Effect on Single Plate Shear Connections.

Chapter 2: Literature Review and Current Practices

Currently, connections involving long slots in plates are designed with a significant emphasis on engineering judgement. The current AISC *Specification for Structural Steel Buildings*, hereafter referred to as the AISC *Specification,* provides little guidance on how to design such connections (AISC, 2016b). This results in connections that may be underdesigned or unnecessarily conservative. In either case, understanding how the connection behaves is critical to proper design.

Significant research has been done on single shear plate connections with standard holes and short slots for decades, but there has been little research on the effects of long slots in steel connections. A summary of the applicable past research and current practice is included herein.

2.1 AISC *Specification for Structural Steel Buildings*

The AISC *Specification* describes standards to be used in bolted connections. According to Table J3.3 of the AISC *Specification*, the maximum slot dimension for a $^{3}/_{4}$-in.-diameter bolt is $^{13}/_{16}$ in. x 1 $^{7}/_{8}$ in. (21mm x 48mm) (AISC, 2016b, p. 16.1-130). This limit does not account for the construction tolerance previously discussed between steel and concrete. However, J3.2(b) states, “Standard holes or short-slotted holes transverse to the direction of the load shall be provided in accordance with the provisions of this Specification, unless... long-slotted holes are approved by the engineer of record” (AISC, 2016b, p. 16.1-128). This can be interpreted as the ability to use atypical slot lengths if the engineer of record adequately designs such connections.

In an attempt to practice good judgement, engineers can follow the provisions of the AISC *Specification* and add additional checks to confirm the design. Applicable limit states from the AISC *Specification* would include bolt shear (J3.6), bolt bearing and tearout (J3.10), plate shear yield and plate shear rupture (J4.2), block shear strength (J4.3), flexural strength of the connecting elements (J4.5), and weld strength (J2) (AISC 2016b, 2016).

All these limit states are straightforward to check except for the flexural strength limit states. The behavior at the extended slots cannot be easily predicted. Understanding this behavior is a primary goal of this research initiative.

2.2 Behavior of Extra-Long Slots by Wollenslegel

Wollenslegel (2020) studied the effects of extra-long slots in plate connections. Thirty-three different configurations were tested with slots of varying lengths (2.5, 4, and 6 times the bolt diameter) and different spacings (2 $^{1}/_{4}$ in. and 3 in. (57mm and 76mm)) to gain an understanding of the effect long slots have on connections. The specimens were loaded both parallel and perpendicular to the slots and the ultimate capacity was determined. Figure 2.2-1 shows the testing setup used to test the specimens and Figure 2.2-2 shows the different series of specimens.

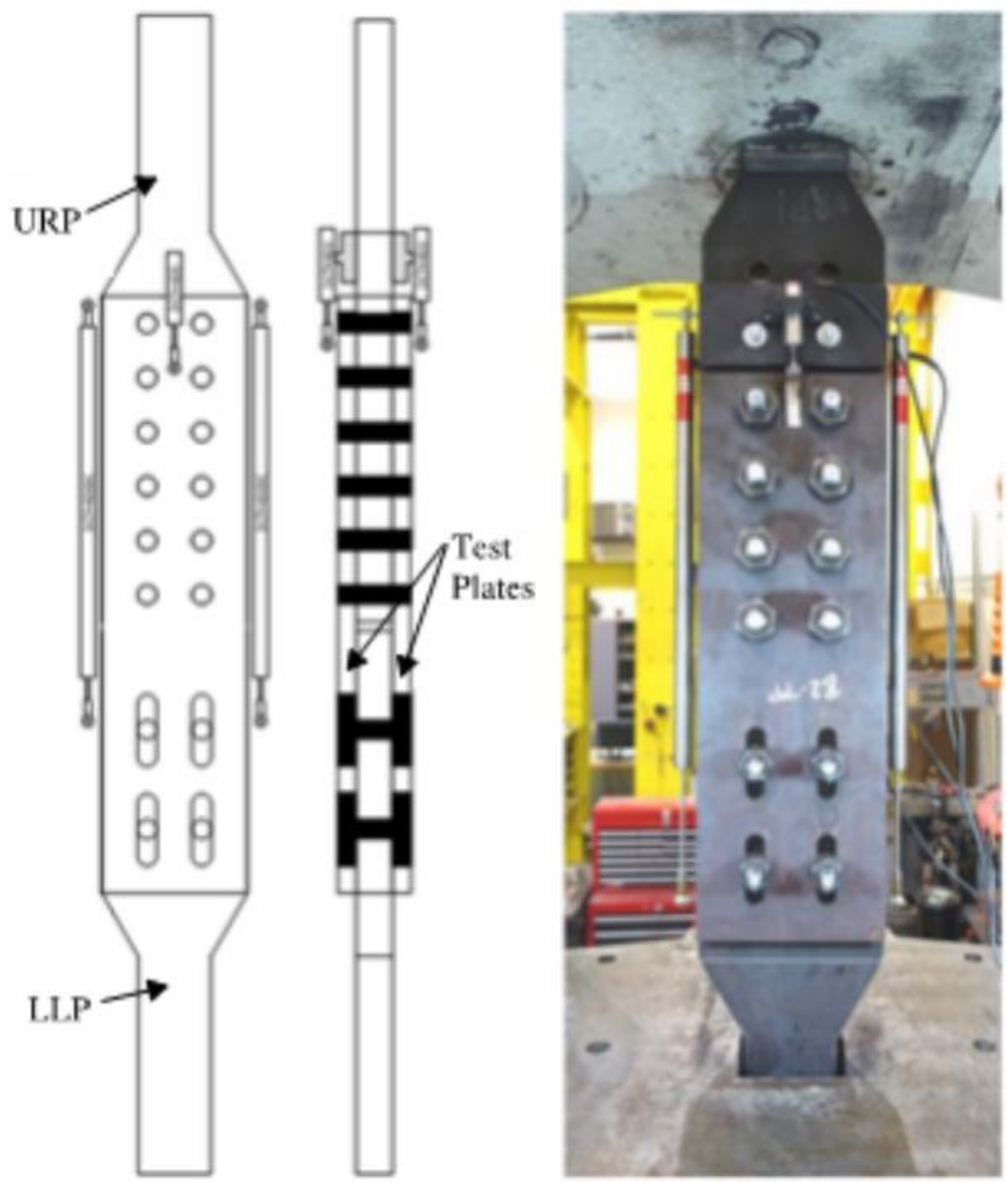

Figure 2.2-1: Wollenslegel Test Setup (Wollenslegel, 2020).

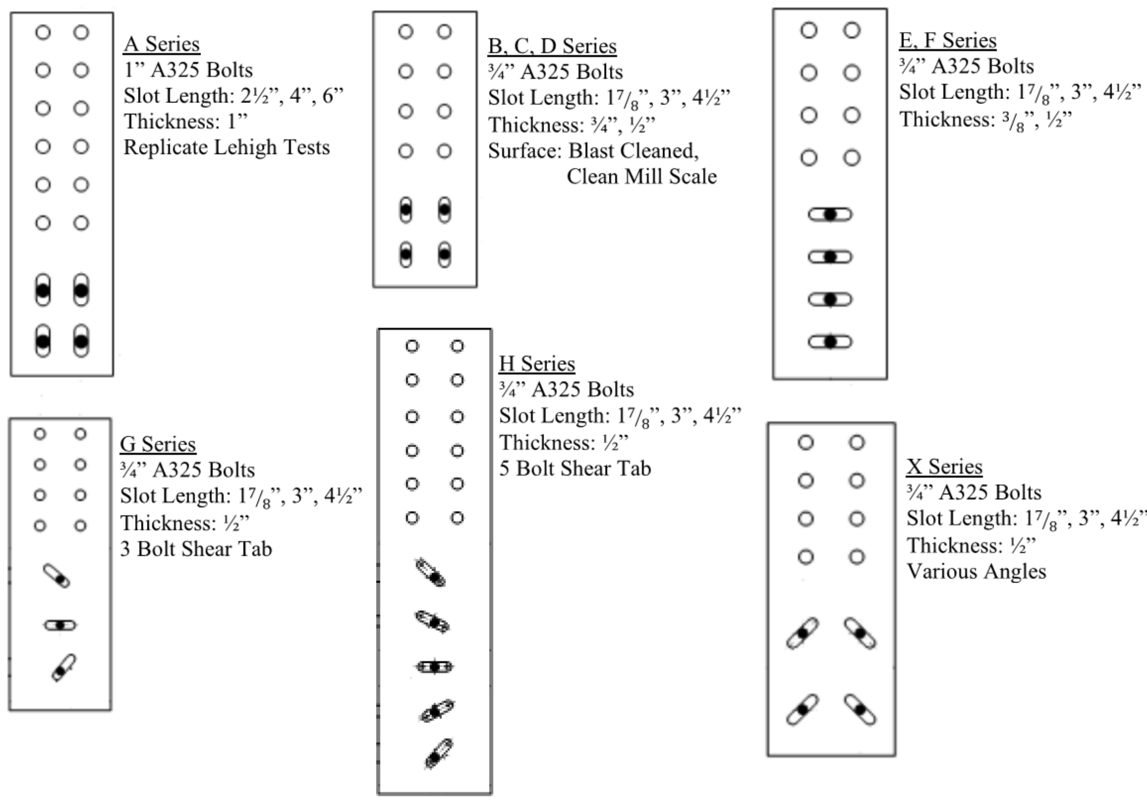

Figure 2.2-2: Test Specimen Series (Wollenslegel, 2020).

The E-series and F-series relate most closely to the experimental program in this capstone project report as the slots are perpendicular to the applied load; however, the specimens were supported at both edges of the plate. The E-series tests used $^{1}/_{2}$ in. (13 mm) plate and the F-series tests used $^{3}/_{8}$ in. (10 mm) plate. The results of the tests show that as slot length increased, the capacity decreased, and as slot spacing increased, the capacity increased. The trends are not significant but are noticeable from the data.

See Figure 2.2-3 for photos of the failed specimens. Table 2.2-1 provides a summary of the applicable results from Wollenslegel's thesis. The author also noted that at the time the paper was written, the research was ongoing, and the conclusions presented may “differ somewhat from those presented in the report and publications that are yet to be written” (Wollenslegel, 2020, p. 63).

Table 2.2-1: Results of Testing (Wollenslegel, 2020).

Joint ID	Number of Bolts	Bolt Diameter	Slot Spacing	Slot Length	Plate Thickness	Ultimate Machine Load
		in.	*in. (mm)*	*in. (mm)*	*in. (mm)*	*kips (kN)*
E-01	4	3/4	3 (76)	1 7/8 (48)	1/2 (13)	347.0 (1544)
E-02	4	3/4	3 (76)	3 (76)		343.4 (1528)
E-03	4	3/4	3 (76)	4 ½ (114)		343.2 (1527)
E-04	4	3/4	2 1/4 (57)	4 ½ (114)		333.4 (1483)
F-01	4	3/4	3 (76)	1 7/8 (48)	3/8 (10)	277.8 (1236)
F-02	4	3/4	3 (76)	3 (76)		262.0 (1165)
F-03	4	3/4	3 (76)	4 ½ (114)		269.6 (1199)
F-04	4	3/4	2 1/4 (57)	4 ½ (114)		259.7 (1155)

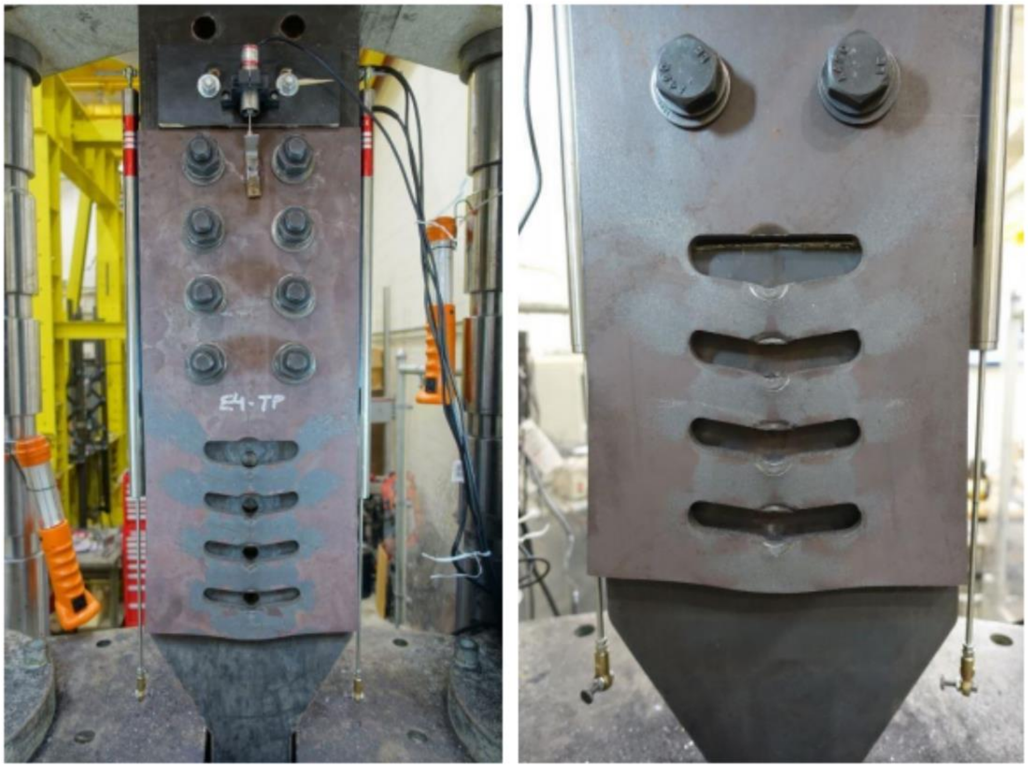

(a)

(b)

Figure 2.2-3: Failed Test Specimens E-04A (a) and F-04A (b) (Wollenslegel, 2020).

2.3 Analysis of Long-Slotted Holes in Single Plate Connections by Peterson

Peterson (2014) conducted a finite element analysis of the type of connection considered in this report. This analysis considered a 2D plate model with slots of varying number of bolt rows, lengths, and spacings. The base model used $^{1}/_{2}$ in. x 6 in. (13 mm x 152 mm) plate with $^{13}/_{16}$ in. x 3 in. (21 mm x 76 mm) slots. An image of the model is shown in Figure 2.3-1. The model was analyzed with a force of 23.8 kips (106 kN) per slot, the unfactored shear strength of a $^{3}/_{4}$-in.-diameter A325-N bolt. Peterson noted that applying this force to individual nodes in the model would not accurately reflect how the force distributes into the connection and alternatively utilizes "compression only springs [to link] between the centers of the bolt locations to the surrounding nodes" (Peterson, 2014, p.22). This can also be seen in Figure 2.3-1.

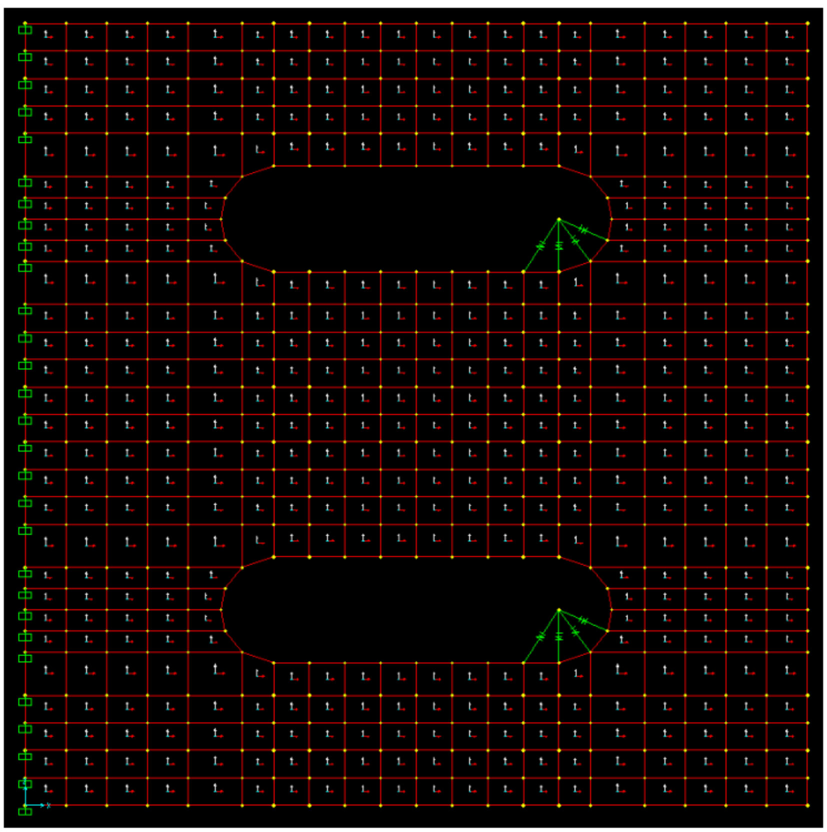

Figure 2.3-1: Finite Element Mesh (Peterson, 2014).

The results of this analysis gave very small deflections of the plate, but very high stresses as shown in Figure 2.3-2. The stress at the top left corner of the bottom slot is reported as 139.6 ksi (963 MPa) and stress at the lower left corner of the plate, at the fixed end condition, is 119.7 ksi (825 MPa). These values are the maximum stresses in the plate "ignoring the stress concentration at the bolt loading" (Peterson, 2014, p. 22). Based on the stress concentrations exhibited by the model, Peterson (2014) believes that the sections of material between the slots are acting like cantilever beams. As more rows of slots were added to the connection, the force distributed itself differently. More slots meant there were more elements with equal stiffness to share the load more evenly.

Peterson concludes by commenting on the limitations of the elastic model created and suggesting creating a set of experiments to test this type of connection to better observe the behavior of these connections. "... [running experimental tests] may present failure modes that are different [than] those that have already been considered..." (Peterson, 2014, p. 28).

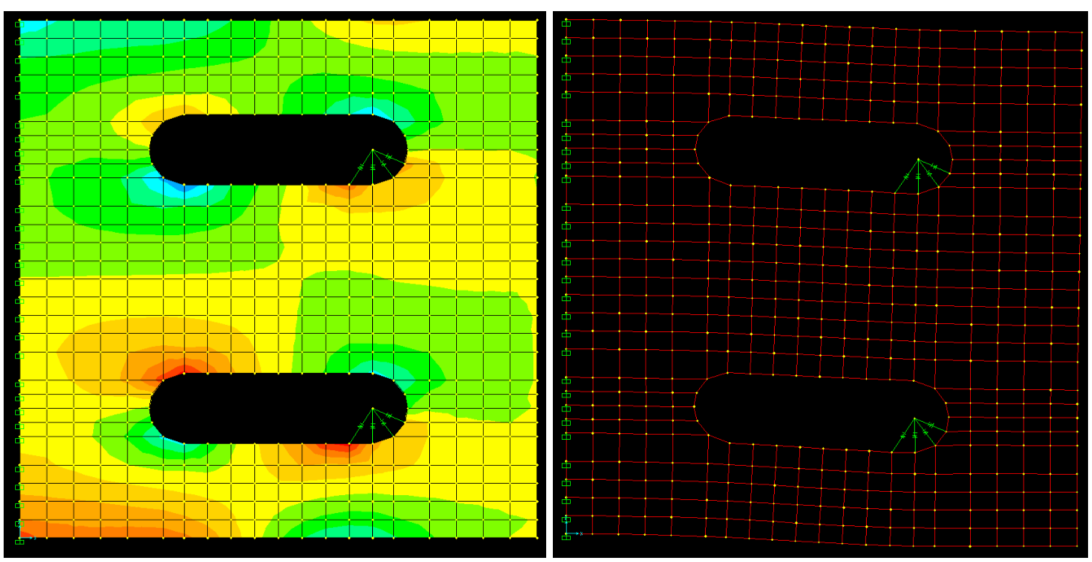

(a) (b)

Figure 2.3-2: Axial Stress Patterns (a) and Deformed Model (b) (Peterson, 2014).

2.4 Beam-to-Column Shear Connections with Slotted Holes by Man, Grondin, and Driver

Man *et al.* (2006) investigated the effects of long and short slots on clip angle shear connections. The variables considered included end distances, edge distances, and cope dimensions. The experimental program subjected single- and double-clip angles to shear loading. Like the current capstone project, the research conducted by Man *et al.* was intended to begin gathering experimental data on a connection with little research available.

Specimens consisted of a wide flange beam with either one or two clip angles supporting it at the loaded end. Load was applied 400 mm (15 $^{3}/_{4}$ in.) from the connection end. A reaction support was located 2400 mm (94 $^{1}/_{2}$ in.) from the connection. Figure 2.4-1 shows an elevation of the test setup.

The results showed two key findings that are relevant to the current research initiative. First, larger spacing between the bolts did not significantly increase the capacity of the connection, "except for double angle specimens that failed by tension and shear block" (Man *et al.*, 2006, p. 60). This is because the single angle specimens failed by "angle end tearing" and the spacing between the bolts did not affect this failure mode. Second, Man *et al.* state that "single angles with short slots showed a 41% higher angle capacity than connections with long slots that failed by angle end tearing" (Man *et al.*, 2006, p. 60). While the length of the slot is not a variable investigated in the current capstone project, this conclusion shows that the length of the slot does affect connection capacity and might be something to consider in future work.

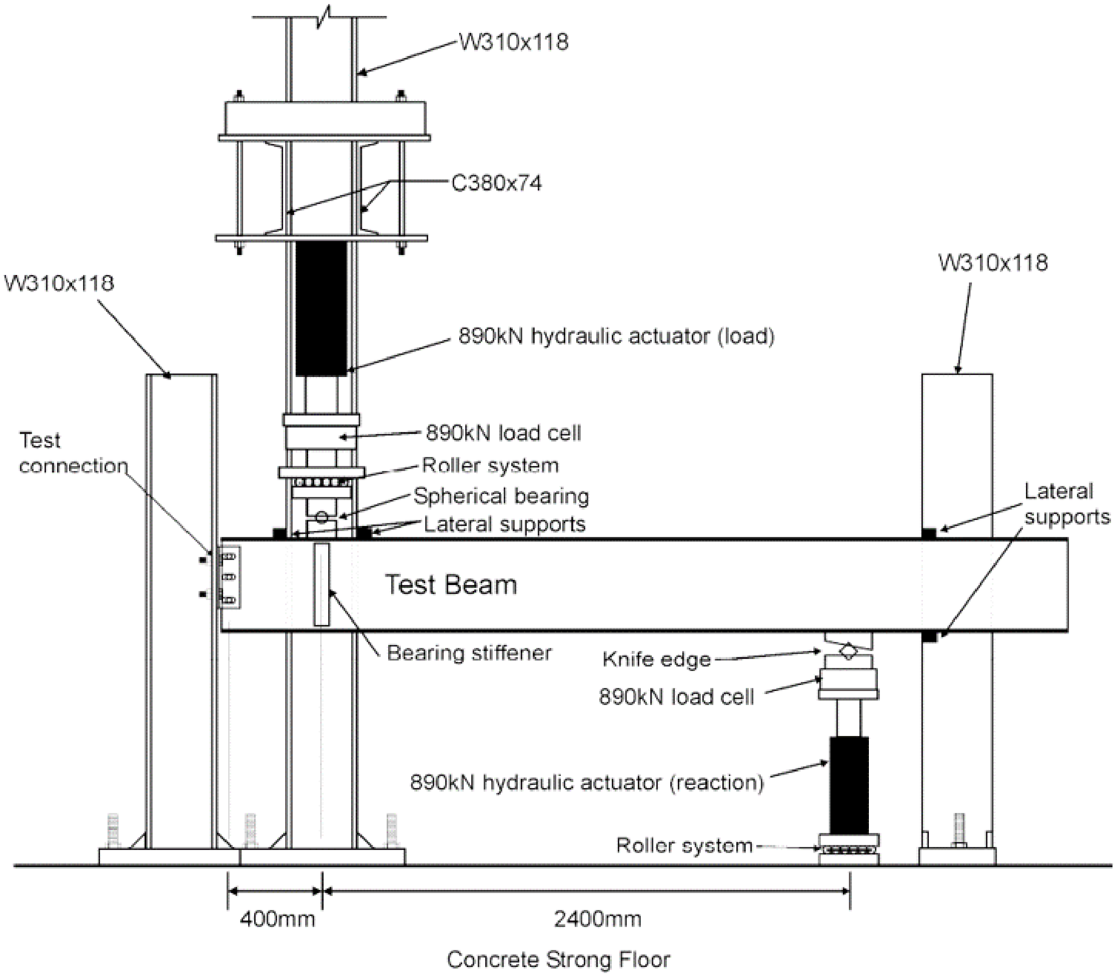

Figure 2.4-1: Clip Angle Test Setup (Man *et al.*, 2006).

The behavior of the failed specimens from single and double clip angle connections is noteworthy. Figure 2.4-2 shows some of the failed angles from the experimental program by Man *et al.* (2006). Table 2.4-1 provides a summary of relevant test parameters and the peak test capacity. In this table, the conclusions mentioned above can be confirmed; slot spacing has little effect on the capacity and shorter slots result in higher capacities. One other interesting thing to note is that the connections with double angles only had about 30% more capacity than single angle connections.

Table 2.4-1: Test Specimen Summary (Man *et al.*, 2006).

Test Specimen	Number of Angles	Slot Length	Bolt Pitch	Peak Test Capacity
		mm (in.)	*mm (in.)*	*kN (kip)*
1L9	1	28 (1.10)	102 (4.02)	360 (80.9)
1L1	1	55 (2.17)	76 (2.99)	306 (68.8)
1L8	1	55 (2.17)	76 (2.99)	290 (65.2)
2L1	2	55 (2.17)	76 (2.99)	400 (89.9)
2L7	2	55 (2.17)	76 (2.99)	347 (78.0)
1L2	1	55 (2.17)	102 (4.02)	346 (77.8)
1L3	1	55 (2.17)	102 (4.02)	430 (96.7)
1L6	1	55 (2.17)	102 (4.02)	368 (82.7)
2L2	2	55 (2.17)	102 (4.02)	482 (108)
2L3	2	55 (2.17)	102 (4.02)	574 (129)

(a)

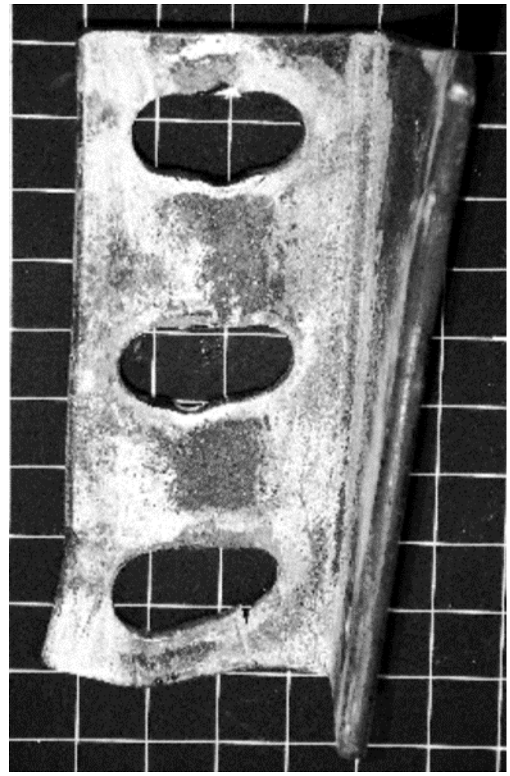

(b)

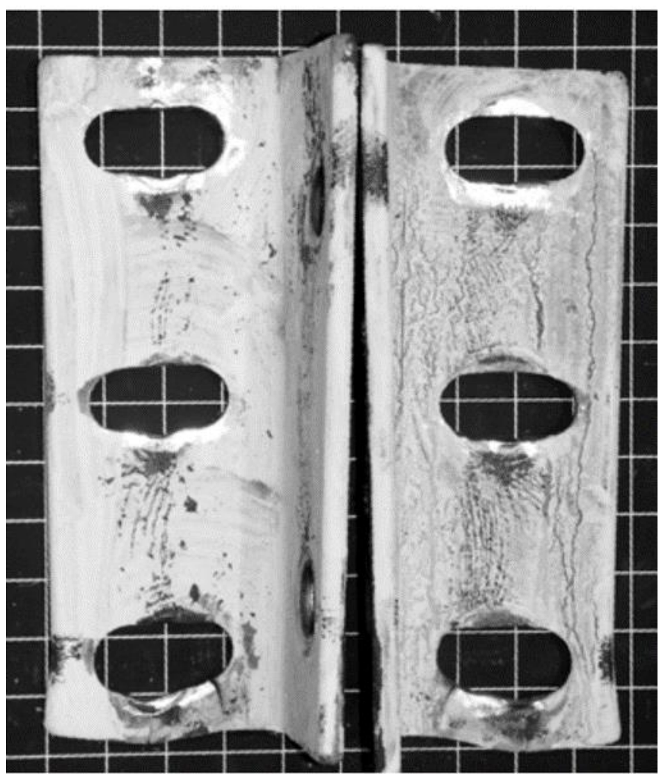

(c)

Figure 2.4-2: Failed Test Specimens 1L9 (a), 1L1 (b), and 2L3 (c) (Man *et al.*, 2006).

Chapter 3: Experimental Program

Based on the literature discussed, this experimental program sought to investigate a key variable in the behavior of extended single plate connections with long slots: the spacing between slots. The hypothesis and experimental program focused on isolating this variable to understand its effect on the connection.

3.1 Introduction

Experimental testing was conducted at the Structures Laboratory in the Construction Science and Engineering Center (CSEC) at Milwaukee School of Engineering (MSOE). The objective of this experiment was to collect initial data on extended shear plate connections with long slots and begin to gain an understanding of the connection behavior. It is the author's understanding that no prior experimental research has been done on this connection and this research initiative will be the first. As such, special attention was given to the setup to ensure the tests were conducted in a suitable fashion and data were gathered appropriately.

3.2 Hypothesis

Based on the literature review conducted, a hypothesis was formulated to guide the specimen design and test setup. The hypothesis for this experimental program is as follows: by increasing the spacing between the rows of long slots in a single plate shear connection, the capacity of the connection will increase. The material between the slots is expected to behave as a cantilever and the additional capacity will result from a deeper cross-section resisting the load.

3.3 Experimental Specimens

The primary objective of this experimental program is to determine the effect of spacing between slots in connections with long slotted holes, so the test specimens were configured in such a way to isolate that variable.

3.3.1 Overview

The experimental program for this research initiative consisted of 20 specimens. All specimens used a $^{1}/_{4}$ in.-thick (6 mm) shear plate welded to a 1 in.-thick (25 mm) base plate or embed plate. The thick base plate was intended to approximate the fixity of a concrete wall without requiring concrete in the test setup. This plate had eight standard holes to attach the specimen to the test setup. The $^{1}/_{4}$ in.-thick (6 mm) plate had three slots in it. Each slot measured $^{13}/_{16}$ in. x 2 $^{13}/_{16}$ in. (21 mm x 71mm). This is $^{15}/_{16}$ in. (24 mm) longer than the “long slot” length of 1 $^{7}/_{8}$ in. (48 mm) provided in Table J3.3 of the AISC *Specification* and recognizes the two inches of construction tolerance previously discussed (AISC 2016b).

To capture the effect of the slot spacing, the three slots were spaced at four spacings of 3.0 in. (76 mm), 3.5 in. (89 mm), 4.0 in. (102 mm), and 4.5 in. (114 mm) center to center. All the specimens had a consistent end distance of 2 in. (51 mm) and plate height of 6 in. (152 mm) – making the clear edge distance for all tests 1 $^{9}/_{32}$ in. (33 mm). Figure 3.3-1 shows a parametric illustration of the test specimens.

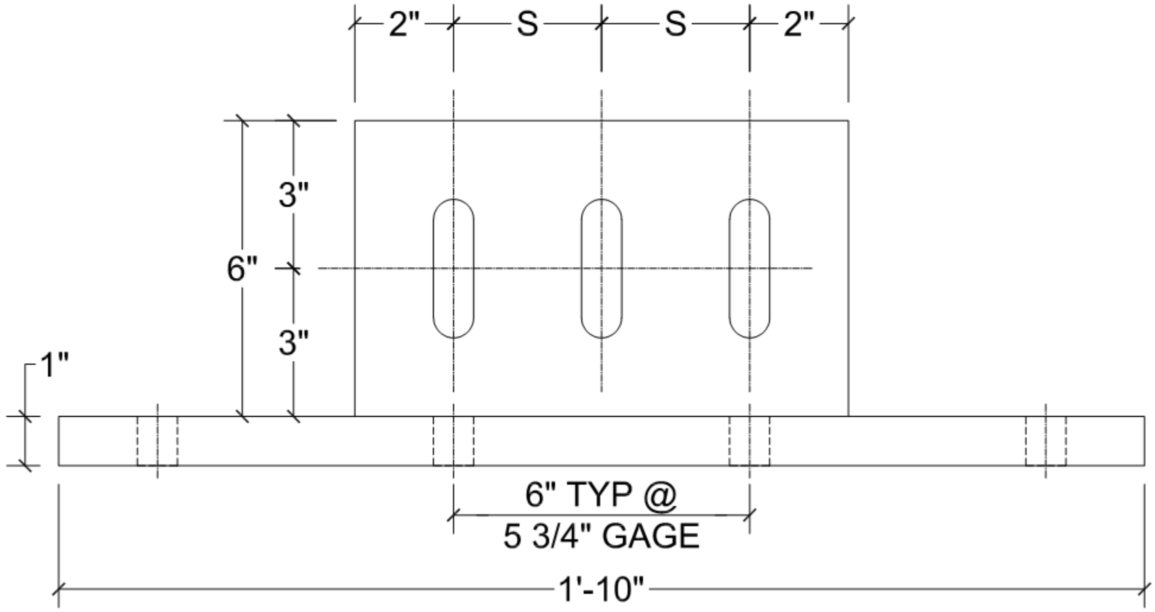

SLOT SPACING "S"
in. (mm)
3.0 (76)
3.5 (89)
4.0 (102)
4.5 (114)

Figure 3.3-1: Parametric Elevation of Experimental Specimen.

The tests for the experimental program were conducted in conjunction with work by Jackson (2021), so the specimens were also used to gather data for Jackson's capstone project which investigates the effect of bolt position within the slot. As such, each of the four spacings had five tests performed on it with the bolt group in varying positions within the slots. The positions consisted of the bolts located closest to the welded edge, farthest from the welded edge, and at quarter points within the slot. These were referred to by a percentage of the slot length relative to the lowest position the bolts could be in. So, the five positions were 0% for the bolts closest to the weld, 100% for the bolts farthest from the welded edge, and 25%, 50%, and 75% for the bolts located at quarter points. Figure 3.3-2 shows the layout of the bolt positions within the slots.

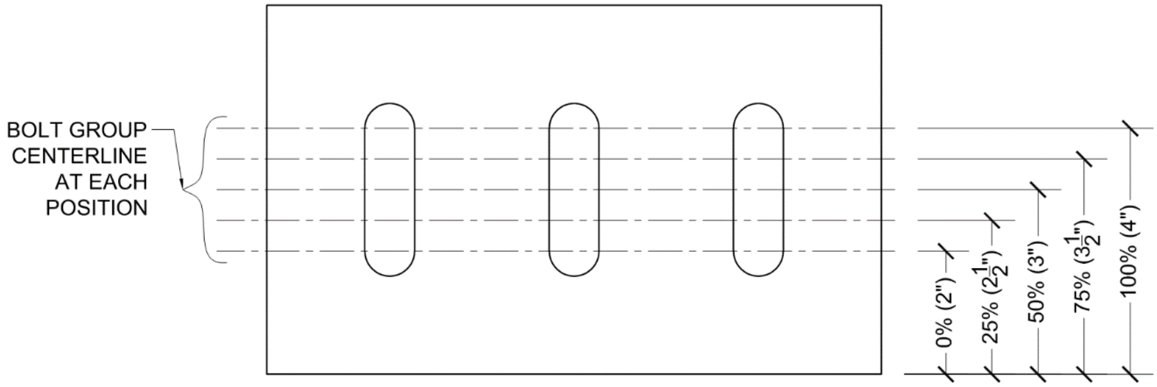

Figure 3.3-2: Bolt Group Positions Within Long Slots.

3.3.2 Test Nomenclature

A seven-digit alphanumeric identifier was assigned to each of the 20 tests in the experimental program. Figure 3.3-3 shows a sample test ID and explains the structure of the tag. This nomenclature was used for all tests in this experimental program.

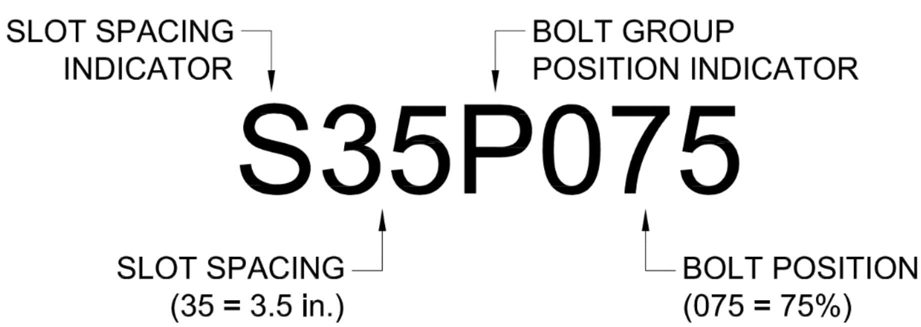

Figure 3.3-3: Experimental Specimen Nomenclature Explanation.

3.4 Experimental Specimen Expected Capacities

The specimens for the experimental program were designed following the provisions in the AISC *Specification* and some additional checks. The limits checked were bolt shear (J3.6), bolt bearing and tearout (J3.10), plate shear yield and plate shear rupture (J4.2), block shear strength (J4.3), flexural strength of the connecting elements (J4.5), and weld strength (J2). These checks represent an approach that appropriately uses engineering judgement and the AISC *Specification* to design this type of connection.

The bolts in this connection are assumed to be type N bolts (threads not excluded from the shear plane) and to not have any slip resistance. While this may not be the condition found in buildings using this connection, it is certainly a possible condition for the connection. This assumption also changes the way the connection behaves. If the bolts are slip critical, then the behavior of the slots likely does not matter since the connection is considered to have failed once the bolts slip. However, if the plate was thin enough and the bolts were large enough, it is possible that the bolts would clamp onto the plate enough to deform it as it is loaded. The test setup, however, ensured a bearing condition was created. There will be more discussion on the test setup in Section 3.5.

The material properties used in the calculations for the plate with the long slots were taken from material testing performed on coupons from the material used to fabricate the specimens. The plates were specified as ASTM A572 Grade 50 plates and had a tested yield stress, F_y, of 62.7 ksi (432 MPa) and ultimate strength, F_u, of 72.9 ksi (502 MPa). The calculations use these values to determine the expected capacity of each specimen. The modulus of elasticity, E, for steel was taken as 29,000 ksi (200 GPa). This value did not come from the material testing results. More discussion on the material testing can be found in Section 3.7.

Table 3.4-1 summarizes the expected capacity of each connection as well as the expected failure mode.

A sample set of calculations for specimen S30P100 along with a summary sheet for each of the remaining 19 specimens is provided in Appendix A. The complete set of calculations for every test is available from the author upon request.

Table 3.4-1: Expected Capacities and Failure Mode of Each Experimental Specimen.

Test ID	**Expected Capacity**	**Expected Failure Mode**
	kip (kN)	
S30P100	22.1 (98.1)	Bolt Plate Flexure
S35P100	31.6 (141)	Bolt Plate Flexure
S40P100	43.1 (192)	Bolt Plate Flexure
S45P100	56.6 (252)	Bolt Plate Flexure
S30P075	29.4 (131)	Bolt Plate Flexure
S35P075	42.1 (187)	Bolt Plate Flexure
S40P075	57.5 (256)	Bolt Plate Flexure
S45P075	59.1 (263)	Bolt Bearing/Bolt Plate Flexure
S30P050	44.1 (196)	Bolt Plate Flexure
S35P050	61.3 (273)	Bolt Bearing/Bolt Plate Flexure
S40P050	61.3 (273)	Bolt Bearing/Bolt Plate Flexure
S45P050	61.3 (273)	Bolt Bearing/Bolt Plate Flexure
S30P025	60.8 (270)	Plate Shear Rupture
S35P025	67.9 (302)	Bolt Bearing/Bolt Plate Flexure
S40P025	67.9 (302)	Bolt Bearing/Bolt Plate Flexure
S45P025	67.9 (302)	Bolt Bearing/Bolt Plate Flexure
S30P000	60.8 (270)	Plate Shear Rupture
S35P000	71.7 (319)	Plate Shear Rupture
S40P000	82.0 (365)	Bolt Bearing
S45P000	82.0 (365)	Bolt Bearing

3.4.1 Discussion of Expected Capacities

Table 3.4-1 shows that, based on the calculations performed, bolt plate flexure is the governing limit state for almost every test. This limit is predicting the yield of the material between the slots as it bends like a cantilevered beam. For the tests that list “Bolt Bearing/Bolt Plate Flexure” as the failure mode, this indicates that one bolt (the bottom bolt) will fail in plate flexure as previously discussed and the remaining bolts will fail in bolt bearing. The methodology used is identical to the effective fastener strength often used to calculate the strength of a group of bolts based on the limits of bolt shear, bolt bearing, and bolt tearout, but also adds bolt plate flexure to the combination of strengths. For the tests with the bolts in the 0% position, there is no length for the slots to bend over, so the plate flexure limit state cannot govern, which is why shear and bearing failures are expected.

Figure 3.4.1-1 shows a plot of expected capacity versus slot spacing grouped by bolt position. Increasing the slot spacing is expected to increase the capacity of the connection.

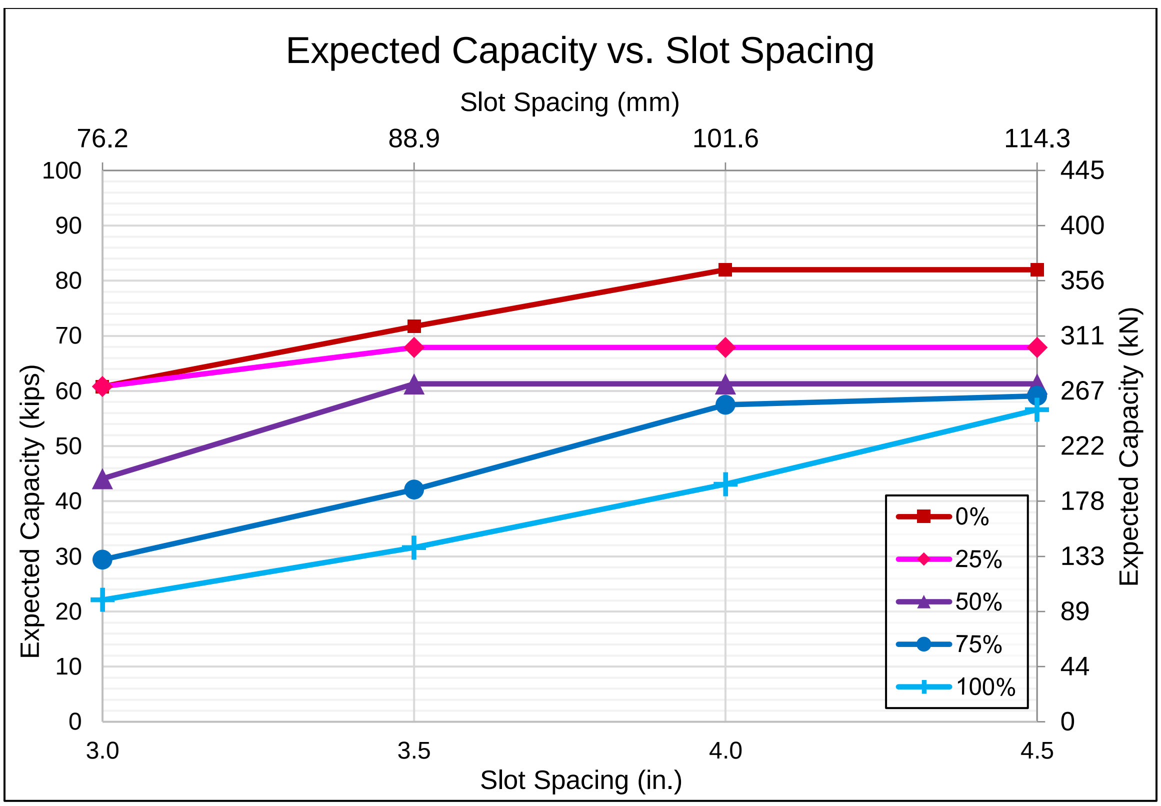

Figure 3.4.1-1: Expected Capacity Versus Slot Spacing.

3.5 Test Setup Overview and Design

The test setup for this experimental program was created to make the testing procedure as efficient as possible while adequately approximating the conditions this connection is typically found in. The following sections outline how the components of the test setup were pieced together and designed. Figure 3.5-1 shows a schematic layout of the complete test setup. It will be referenced further in the rest of this section.

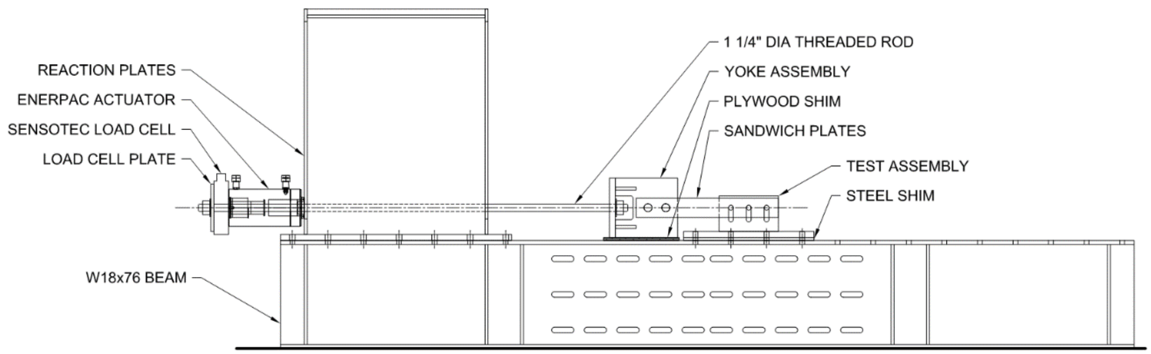

Figure 3.5-1: Schematic Drawing of Test Setup.

The support for this test was provided by a W18×76 beam that had been used for previous testing in the CSEC. The steel beam had a set of eight $^{13}/_{16}$ in. diameter holes drilled in the top flange to accommodate the holes in the experimental specimen base plate that were previously mentioned. The slots in the beam web, seen in Figure 3.5-2, are left over from a previous test and served no purpose in this experimental program. After careful consideration, it was determined embedding the specimens in concrete was unnecessary as long as the fixity the concrete would provide was well approximated. The flange of the W18×76 was seen as sufficiently rigid and the specimens were attached directly to it. Instrumentation was added to confirm this rigid condition was met. More discussion of this is provided in Section 3.8.1. At the left end of the beam were two large reaction plates, shown in Figure 3.5-3, that were bolted to the beam flange with (14) $^3/_4$ in. bolts. These plates resisted the load that was applied to the specimens.

Figure 3.5-2: Support Beam in Test Setup.

Figure 3.5-3: Reaction Plates in Test Setup.

The actuator used for this experimental setup was an Enerpac RRH606 “Hollow-Core” actuator with a maximum capacity of 120 kips (534 kN). Figure 3.5-4 shows an image of this actuator. This was the strongest actuator available in the CSEC and had a higher capacity than the all expected capacities of the specimens. An Enerpac PER 2042 hydraulic pump fed the actuator. The actuator was mounted directly to the large reaction plates with two bolts and positioned such that the threaded rod was level with the beam flange. A Sensotec 41-A530-01-03 load cell, shown in Figure 3.5-5, was attached to the back of the actuator with a 1 in. (25 mm)-thick load cell plate, shown in Figure 3.5-6, to measure the load applied to the specimen. The load cell will be discussed further in Section 3.8.3.

Figure 3.5-4: Enerpac RRH606 “Hollow-Core” Actuator.

Figure 3.5-5: Sensotec 41-A530-01-03 Load Cell.

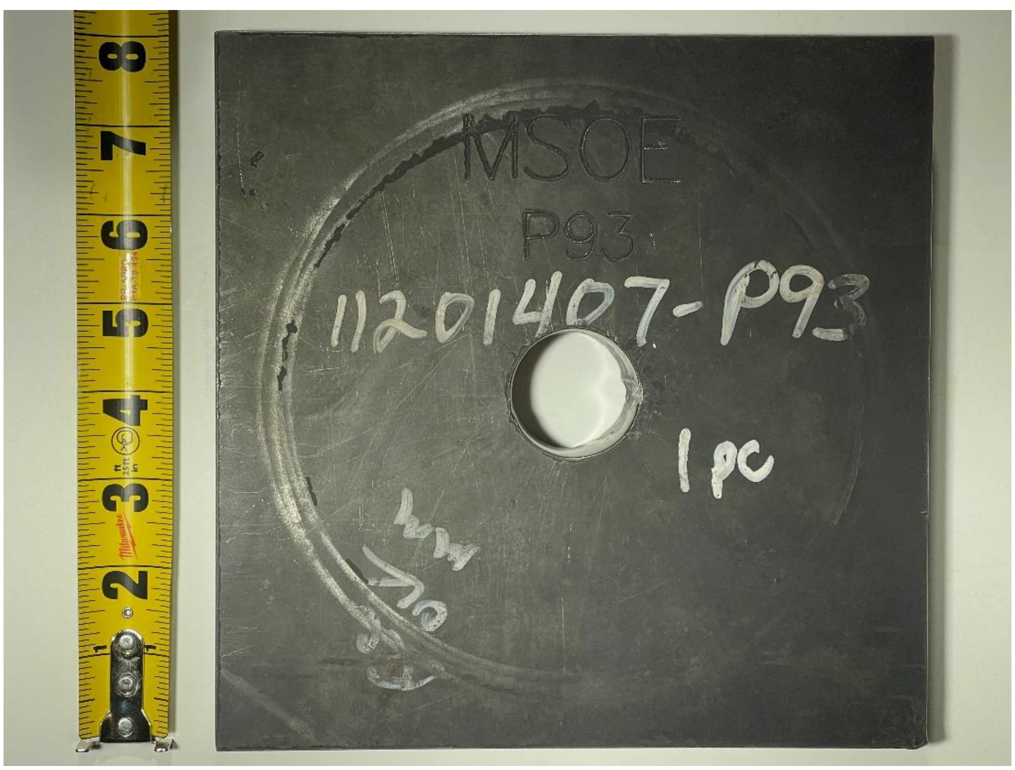

Figure 3.5-6: Load Cell Plate.

From the actuator, the load was transferred to an 8 ft (2.44 m)-long $1^1/_4$ in. (32 mm) A307 Grade B threaded rod, shown in Figure 3.5-7. The rod went through the actuator and between the reaction plates to connect to the rest of the setup. This rod was selected based on the sizes and materials readily available. There is a possibility that this rod yielded during testing as loads approached 100 kips (445 kN), but it would not have affected results of the tests.

Figure 3.5-7: A307 Grade B Threaded Rod.

The threaded rod then transferred the force to a custom designed yoke. The yoke was fabricated from ASTM A572 Grade 50 plate and is shown in Figure 3.5-8. The back plate of the yoke was 1 in. (25 mm) thick and had a $1^3/_8$ in. (35 mm) diameter hole for the threaded rod. The yoke plates were checked for tensile yielding, bolt bearing, bolt tearout, block shear, and reduced section yielding. These calculations adequately captured the realistic limit states for the yoke. The plates were connected to the back plate of the yoke with CJP welds to develop the full strength of the plates and the stiffener plates were attached with $^5/_{16}$ in. (8 mm) fillet welds. Calculations for the yoke are provided in Appendix B.

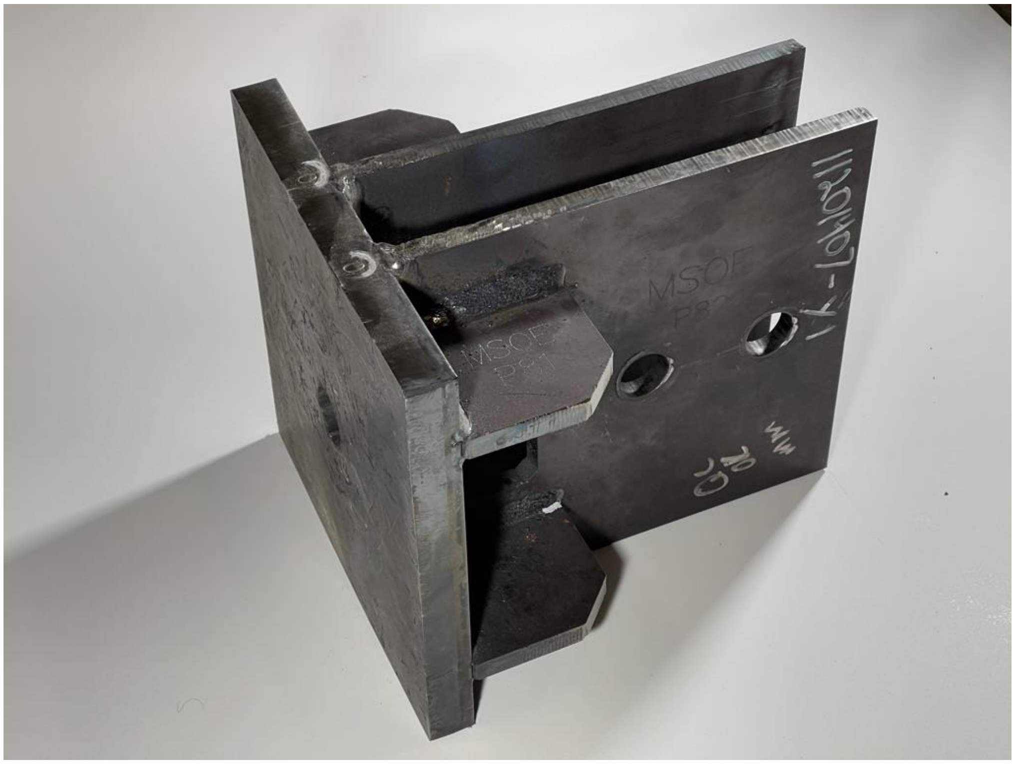

Figure 3.5-8: Custom Designed Yoke.

The yoke transferred the load to two sandwich plates that were connected to the experimental specimen. By using a plate on either side of the specimen, the specimen plate was almost completely laterally braced and eliminated the eccentricity the connection would see if only one plate was used. Four pairs of sandwich plates, shown in Figure 3.5-9, were fabricated for each of the four slot spacings used in the experimental specimens. Each sandwich plate was 1 in. (25 mm) x $3^{1}/_{4}$ in. (83 mm) but varied in length to accommodate the changing slot spacing. The sandwich plates were connected to the yoke with two 1 in.-diameter A325-N bolts. This connection was checked for bolt shear, bolt bearing in the sandwich plate, bolt tearout in the sandwich plate, yielding of the sandwich plate, net tension rupture of the sandwich plate, and block shear of the sandwich plate. Because the plates could only be $3^{1}/_{4}$ in. (83 mm) tall to allow clearance at the weld in the lowest bolt position, the net cross section at the bolt holes was greatly reduced and tension rupture governed requiring the use of the 1 in. (25 mm) plate. Calculations for the sandwich plates are provided in Appendix C.

Figure 3.5-9: Sandwich Plates.

There was a $^{1}/_{4}$ in. (6 mm) filler plate between the sandwich plates in the yoke to account for the separation from the specimen plate. The filler plate is shown in Figure 3.5-10. Multiple $^{1}/_{2}$ in. (13 mm) steel plates were used to raise the test and effectively lower the bolt position within the slot. A single shim was used under the tests at the highest bolt position to align the bolts with the actuator and one shim was added to move to the next bolt position. The tests with bolts at the 0% bolt position used a total of five shims. A single shim is shown in Figure 3.5-11. Additionally, to keep the yoke in line vertically with the expected bolt position, a $^{1}/_{2}$ in. (13 mm) plywood shim was placed below the yoke. This is shown in Figure 3.5-1. Plywood was used at this location to lower the coefficient of friction between the shim and steel beam.

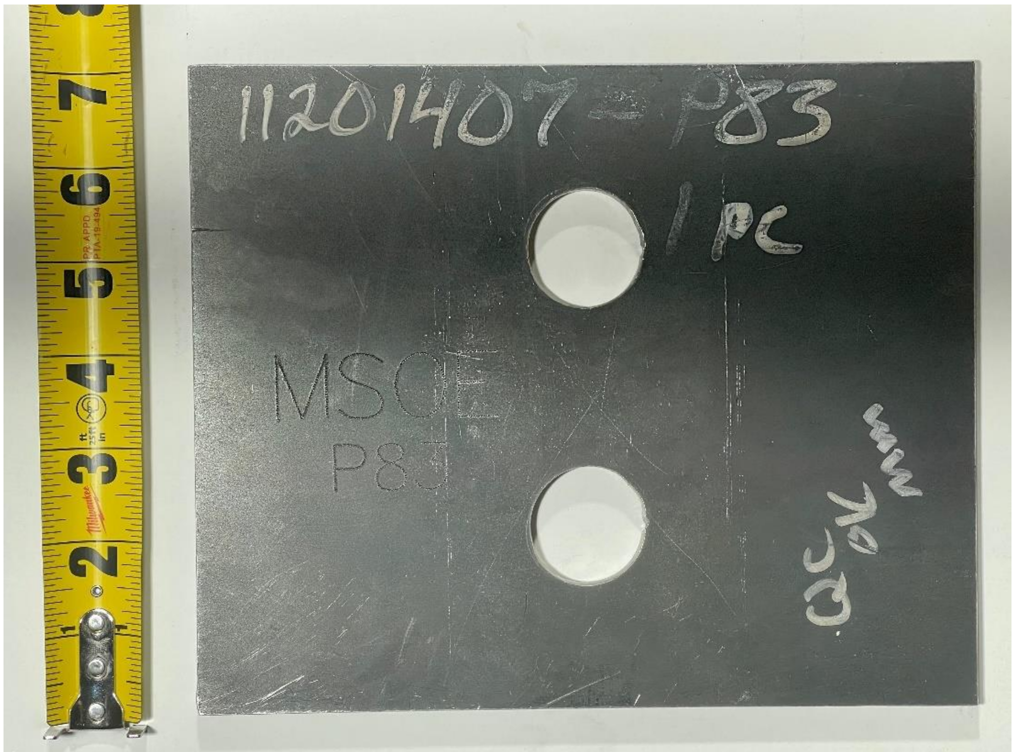

Figure 3.5-10: Filler Plate Used Between Sandwich Plates.

Figure 3.5-11: Steel Shim Plate.

3.6 Shop Drawings

After the calculations for the specimens and test setup components were complete, drawings for fabrication were created in conjunction with Jackson. These drawings showed all critical dimensions for the specimens and test setup components. They also included drawings for material test specimen coupons of the plate material used in the specimens. These coupons will be discussed further in Section 3.7. The complete set of drawings is provided in Appendix D.

3.7 Material Testing

Material test specimen coupons were provided with the experimental specimens and test setup components. The six samples measured $1^1/_2$ in. (38 mm) x 12 in. (305 mm). A note on the shop drawings indicated that these pieces were to be cut from the same ¼ in. (6 mm) plate used for the specimens. These plates were sent to Metallurgical

Associates, Inc. in Waukesha, Wisconsin where they were tested to determine the true yield and ultimate stress of the plates used in the experiment. Although ASTM A572 Grade 50 steel has a minimum yield stress of 50 ksi (345 MPa) and minimum ultimate stress of 65 ksi (448 MPa), the steel used to fabricate the specimens had an average yield stress of 62.7 ksi (432 MPa) and an average ultimate stress of 72.9 ksi (502 MPa). Because these values accurately reflect the strength of the plate used to create the specimens, these were the values used to calculate the expected capacities for each specimen as discussed in Section 3.4. A copy of the material testing report is included in Appendix E.

3.8 Instrumentation

This experimental program utilized three different data acquisition devices to capture the results of each of the 20 tests. Because this is the first experimental program to investigate this connection, there was no good reference for how to instrument these tests, so careful consideration was given to the expected behavior of the connection and how the anticipated data could be analyzed to answer the hypothesis for this research initiative.

3.8.1 Displacements

The first data acquisition device used was a linear variable displacement transducer (LVDT). Two LVDTs were used to measure and record displacement data on each test. LVDT 1 (a Sensotec P/N 060-3618-02 with $^{+}/_{-}$ 1.0 in. (25 mm) stroke) was located at the top corner of the unloaded edge of the plate to measure the lateral deformation of the specimen plate. These data were expected to indicate loss of stiffness of the plate as the specimen was loaded. Placing the LVDT in the same location on every test would allow for meaningful comparisons to be made between all 20 tests. LVDT 1 was attached to the plate using a rare earth magnet and a small nut to ensure it did not come off as the specimen deflected. Figure 3.8.1-1 shows how LVDT 1 was attached to the specimens. LVDT 1 is marked with red tape in all photos of the experimental program.

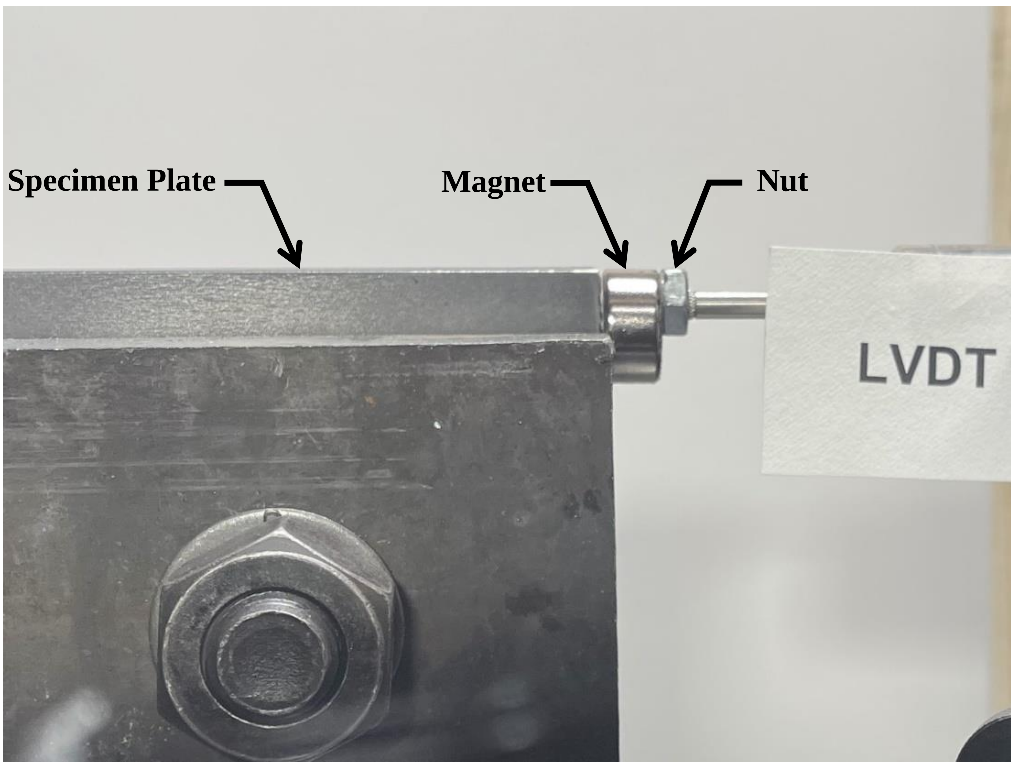

Figure 3.8.1-1: Attachment of LVDT 1 to Experimental Specimen.

LVDT 2 (Honeywell P/N 060-3590-07 with $^{+}/_{-}$ 0.5 in. (13 mm) stroke) was used to measure the vertical displacement in the base plate at the row of bolts farthest from the loaded edge. These data were expected to indicate if the experimental setup accurately approximated the fixed condition that is provided by the concrete in a real application of this connection. LVDT 2 is marked with blue tape in all photos of the experimental program. Figure 3.8.1-2 shows the locations for the two LVDTs used in this experimental program.

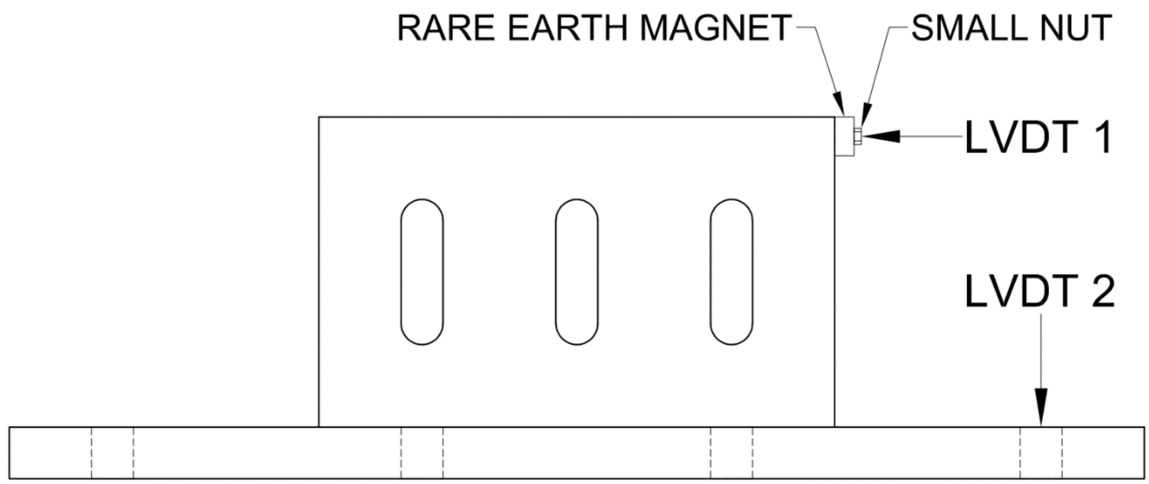

Figure 3.8.1-2: Location of LVDTs on Experimental Specimen.

Both LVDTs were connected to their own Sensotec model DM060-3157-01 Signal Conditioner that displayed the displacements in real time and output voltage to the data acquisition system. These signal conditioners were calibrated using a micrometer and multimeter before the testing began to ensure the correct voltage was being sent to the data acquisition system based on the LVDT stroke. The two LVDTs and their accompanying signal conditioners are shown in Figure 3.8.1-3.

(a)

(b)

Figure 3.8.1-3: LVDT 1 (a) and LVDT 2 (b) with Signal Conditioner.

3.8.2 Strain Gauges

Rosettes were applied to 14 of the 20 experimental specimens to collect strain data. The rosettes chosen for this program were type FRAB-1-11-5LJB-F manufactured by Tokyo Measuring Instruments Laboratory Company and consisted of three 1 mm gauges oriented 45 degrees apart. Figure 3.8.2-1 shows a single rosette. The rosettes were placed at the bottom of the slot and centered between the two slots closest to the load. Figure 3.8.2-2 shows the location of the rosette on a specimen. This position was chosen because it could be accurately repeated on each test and because of the anticipated bending behavior that was discussed in Section 2.3; the centerline between the slots should exhibit no axial strain if that section of the plate behaves like a cantilevered beam.

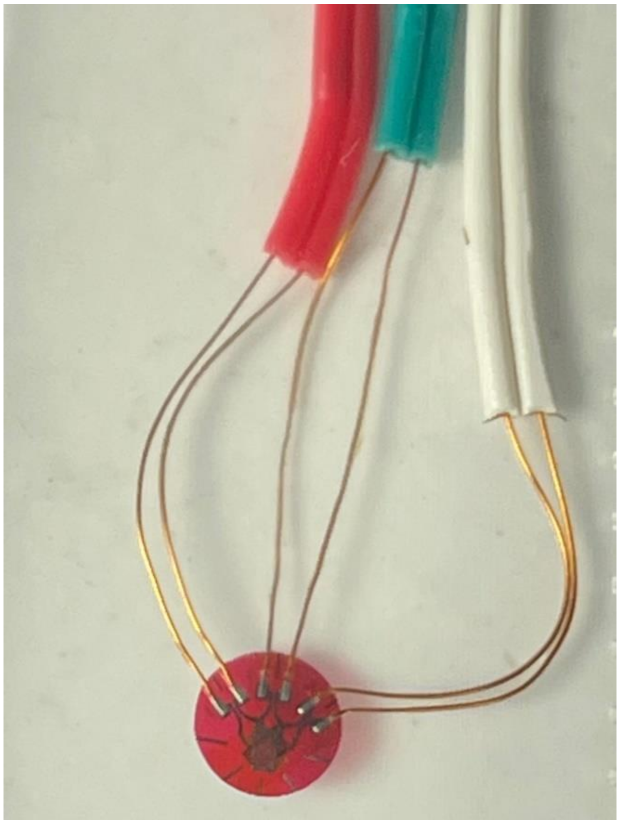

Figure 3.8.2-1: A Single Rosette, Close up.

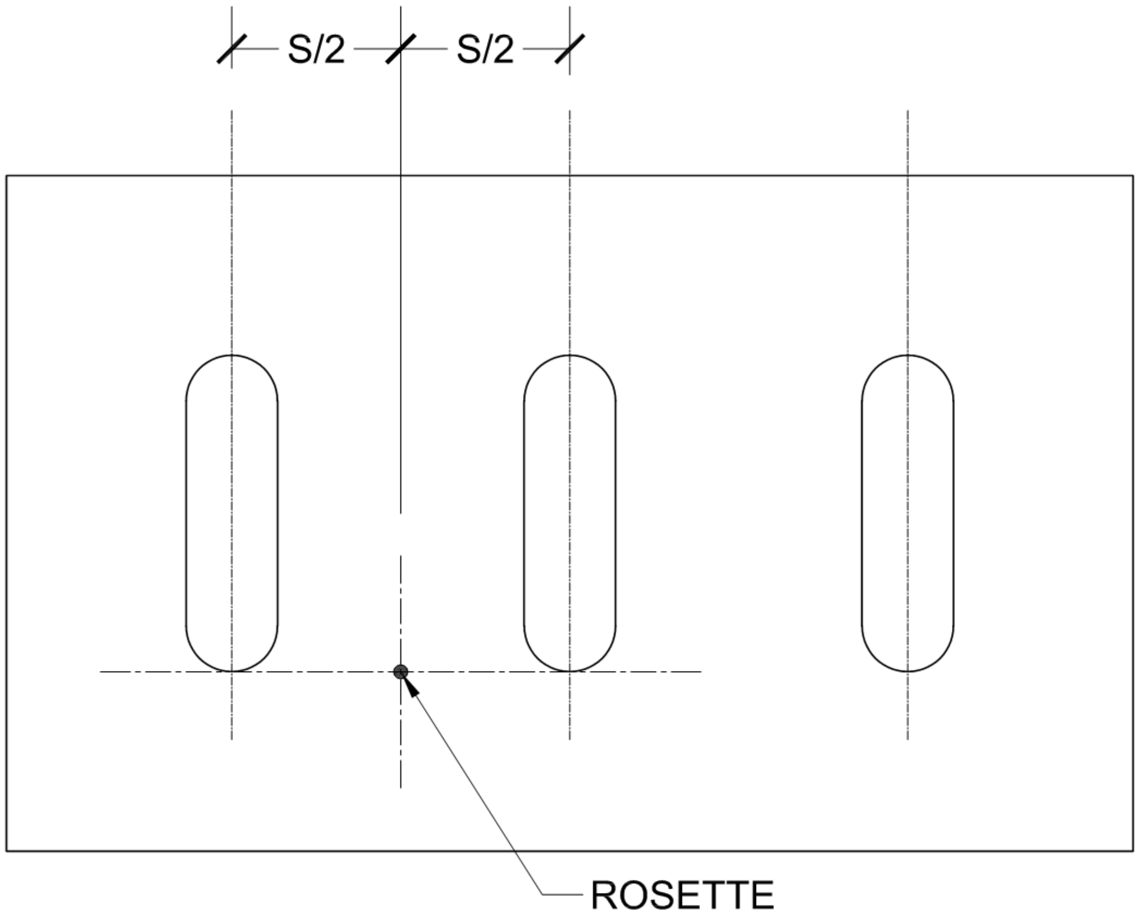

Figure 3.8.2-2: Placement of Rosette on Specimen.

To adhere the rosettes to the specimens, the following process was used:

1. Grind off mill scale and surface debris from the specimen where the rosette is to be placed
2. Sand the area with 120 grit sandpaper
3. Sand the area with 220 grit sandpaper
4. Polish the area using polishing wheel
5. Gently re-roughen the surface with 220 grit sandpaper
6. Mark location of rosette with straightedge and razor blade

7. Thoroughly clean the area using cotton swabs and acetone. Allow the area to dry completely before starting step 9.
8. Affix rosette to long strip of clear tape
9. Clean back of rosette with a cotton swab and acetone and apply cyanoacrylate adhesive
10. Align rosette with previously marked location
11. Press firmly and securely tape rosette to specimen

This process was used for all 14 tests that had a rosette. The prepared area was always significantly larger than was needed for the rosette to ensure the tape would hold the rosette in place as the cyanoacrylate adhesive dried. Figure 3.8.2-3 shows a rosette adhered to a specimen.

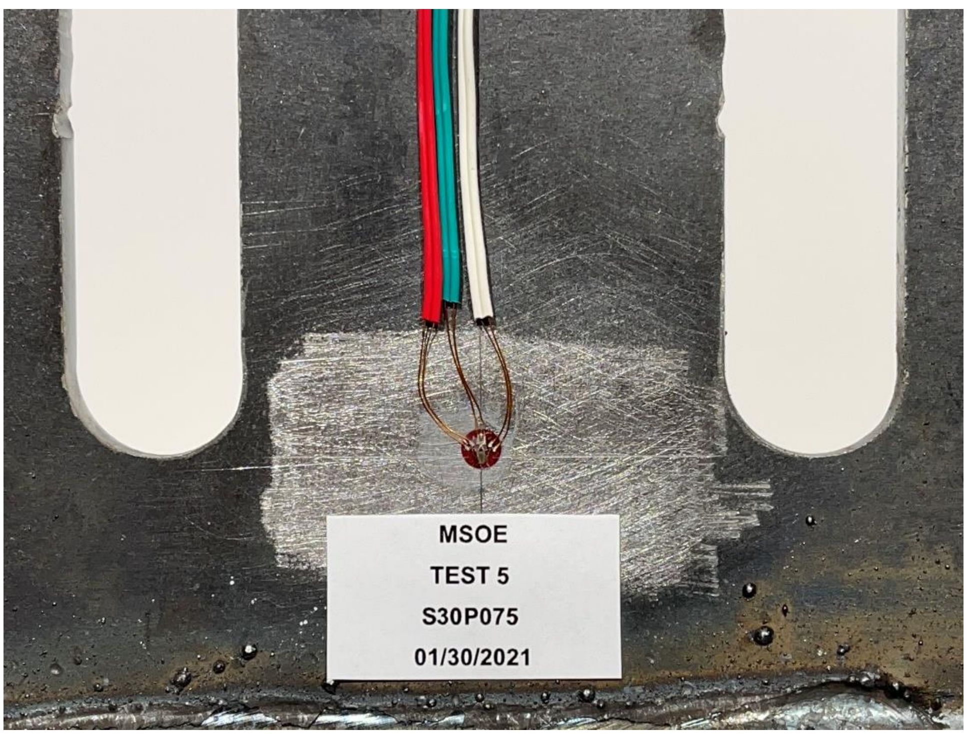

Figure 3.8.2-3: Rosette Adhered to Specimen.

3.8.3 Load Cell

A Sensotec 41-A530-01-03 load cell was used to measure and record the force applied during each test. This load cell has a maximum capacity of 100 kips (445 kN). Because this is less than the 120-kip (534 kN) capacity of the actuator, this capacity limited how much load could be applied to the specimens during the tests. The load cell was connected to a Sensotec 060-6834-03 Signal Conditioner that displayed the applied load in real time and output voltage to the data acquisition system.

3.9 Data Acquisition System and Wiring

To record the data from each test, the instrumentation was connected to a National Instruments cDAQ-9178 CompactDAQ Chassis with a NI-9215 Voltage Input Module for the load cell and LVDTs and a NI-9325 Strain/Bridge Input Module for the three strain gauges in the rosette. These three pieces of hardware are shown in Figure 3.9-1, Figure 3.9-2, and Figure 3.9-3 respectively. This system was connected to a laptop running National Instruments LabVIEW software to capture, display, and log the data for each test.

Figure 3.9-1: cDAQ-9178 CompactDAQ Chassis (National Instruments, 2021).

Figure 3.9-2: NI-9215 Voltage Input Module (National Instruments, 2021).

Figure 3.9-3: NI-9235 Strain/Bridge Module (National Instruments, 2021).

3.9.1 Data Acquisition System Wiring

Because of the positioning of the various pieces of equipment and instrumentation around the test setup, the author decided to include a brief discussion on the how the components of the data acquisition system were connected. The components of the data acquisition system previously discussed were pulled away from the test setup to allow the measurements to be observed while the test was running without placing the operator in the potential path of flying objects.

The rosettes used had 16.4 ft (5 m) lead wires that allowed plenty of flexibility in running them around and out of the way of the test setup. The three wires loosely ran behind the support beam, up and over the flange, and to a terminal block connected to the data acquisition system.

The load cell had a cable that was sufficiently long to reach to signal conditioner and the bulk of it was coiled underneath the load cell. The signal conditioner for the load cell was placed adjacent to the data acquisition system and the BNC cables from the conditioner plugged directly into the data acquisition system.

The two LVDTs were placed a bit farther from the data acquisition system and in order to maintain a clean and safe work area in the lab, extension cables that were approximately 25 ft (7.6 m) were added to both LVDTs to extend the cables to the data acquisition system. These cables were run on the ground behind the support beam, around the left side of the beam, and to the data acquisition system. Because additional wire length has the potential to add resistance and reduce the voltage at the data acquisition system, both LVDTs were rechecked to ensure that they were producing the appropriate voltage at the end of the extension cable.

See Figure 3.9.1-1 for a schematic plan of the data acquisition system wiring.

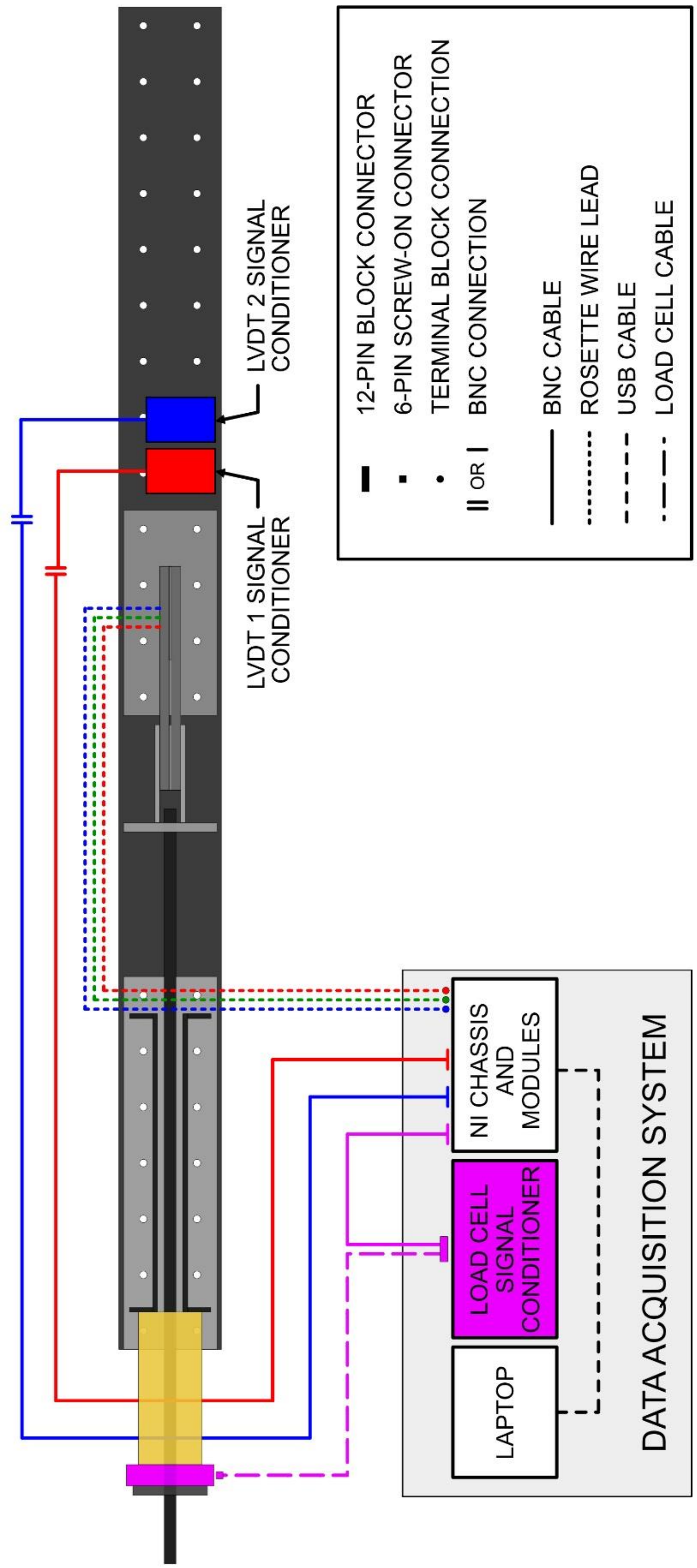

Figure 3.9.1-1: Schematic Plan View of Data Acquisition System Wiring.

3.10 Experimental Procedure

Prior to testing, a detailed procedure was developed to ensure the 20 tests were conducted in a consistent manner. The process was tested on an extra specimen – not one of the 20 used for the experimental program – to make sure it worked and was repeatable. Small adjustments were made as found necessary during the testing process.

The following procedure was used. Whole number steps indicate steps for the original procedure.

1. Measure all the specimen dimensions shown in Figure 3.10-1 and record them in the measurement spreadsheet. See Appendix F for the specimen dimensions.

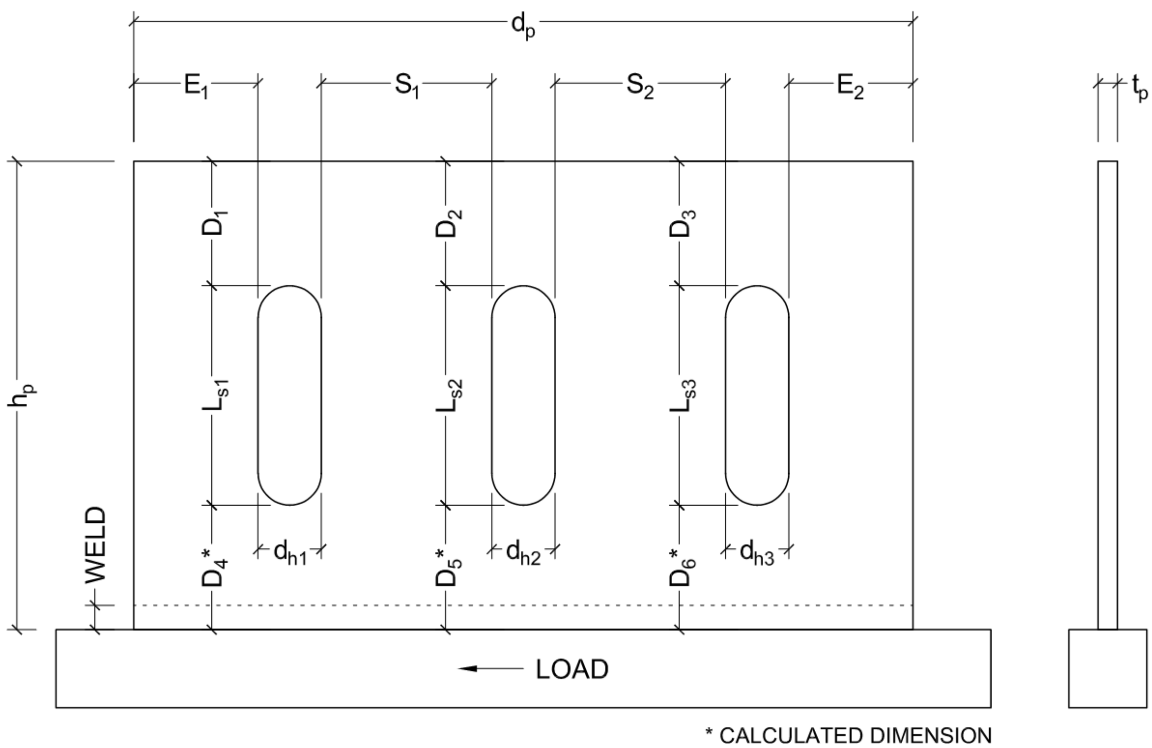

Figure 3.10-1: Specimen Dimensions.

2. Take photos of the specimen with test ID cards. Photos should include a specimen plate elevation, top view, loaded edge elevation, and close-up of rosette location where applicable.
3. Slide the yoke assembly away from the area where the experimental specimen will sit to give ample room to work.
4. Stack the appropriate number of shims for the test. All tests need a minimum of one shim. One additional shim is required for each “step” down in bolt position.
5. Place the experimental specimen onto the shim stack.
6. Insert (8) $^3/_4$ in. A325 tension control bolts from the top of the base plate down into the beam flange. The bolt length will vary based on number of shims required. Place a washer and nut onto the bolts and leave loose to allow for adjustment in the following steps.
7. Select the correct set of sandwich plates for the specimen. Insert (3) $^3/_4$ in. A325 heavy hex bolts through one of the plates from the back side and into the specimen plate. Place a flat washer on the bolts, directly against the specimen plate, to protect the rosette from being damaged. Add these washers even if there is no rosette on the test. Place the second sandwich plate onto the bolts and add a washer and nut to each bolt and leave loose.
8. Slide the yoke assembly to the specimen. Slide the yoke plate over the sandwich plates and add the filler plate. Use a spud wrench to align the holes in the yoke, sandwich plates, and filler plate and insert (2) 1 in. A325 heavy hex bolts. Add a washer and nut and finger tighten.

9. Raise or lower the sandwich plates at the specimen side to level them using a torpedo level. This will ensure the bolts pull at the expected bolt position. Fully tighten the (2) bolts in the yoke. Lightly tighten the (3) bolts at the specimen with spud wrenches (about a quarter- to a half-turn past finger tight). Slip resistance should be avoided at this interface. Leave the level on the front sandwich plate.
10. Pull any extra length of threaded rod back through the actuator and lightly tighten the nut at the left end against the load cell plate. Do not overtighten the nut as this will offset the load data at the start of the test.
11. Hand tighten the (8) tension control bolts, then fully tighten them using a shear wrench (TONE® Model S-61EZ). The shear wrench used is shown in Figure 3.10-2. Slip resistance here is expected and ideal. In tests with higher expected capacities, it is necessary to “pre-slip” the specimen base plate so that the specimen does not slip at a high load and cause a jump in the data. To do this, after finger tightening the bolts, apply approximately 0.5 kip (2.2 kN) of force using the actuator, then tighten the bolts fully with a shear wrench. Release the load from the actuator once all the bolts are fully tightened. The load will have increased after the bolts are tightened.

Figure 3.10-2: TONE® Shear Wrench.

12. Place LVDT 1 in its position at the top corner of the non-loaded edge, setting the tip inside the magnet LVDT holder. Make the LVDT body as normal to the specimen edge as possible. The LVDT should be just less than its full stroke inward to allow ample extension of the LVDT as the specimen plate deflects
13. Place LVDT 2 in its position centered between the tension control bolts farthest from the loaded edge. Make the LVDT body as normal to the base plate as possible. The LVDT should be approximately centered in its stroke at the start of the test.

14. Connect the rosette wires to the data acquisition system as applicable. Make sure the order is the same for every test (left to right: red, green, white).
15. Place (2) test ID cards on the test specimen. One is attached to the front-facing sandwich plate. One is attached to the base plate.
16. Clean and set the plexiglass shield (seen in Figure 3.10-3) around the test to contain any components that may break during the test and protect observers.

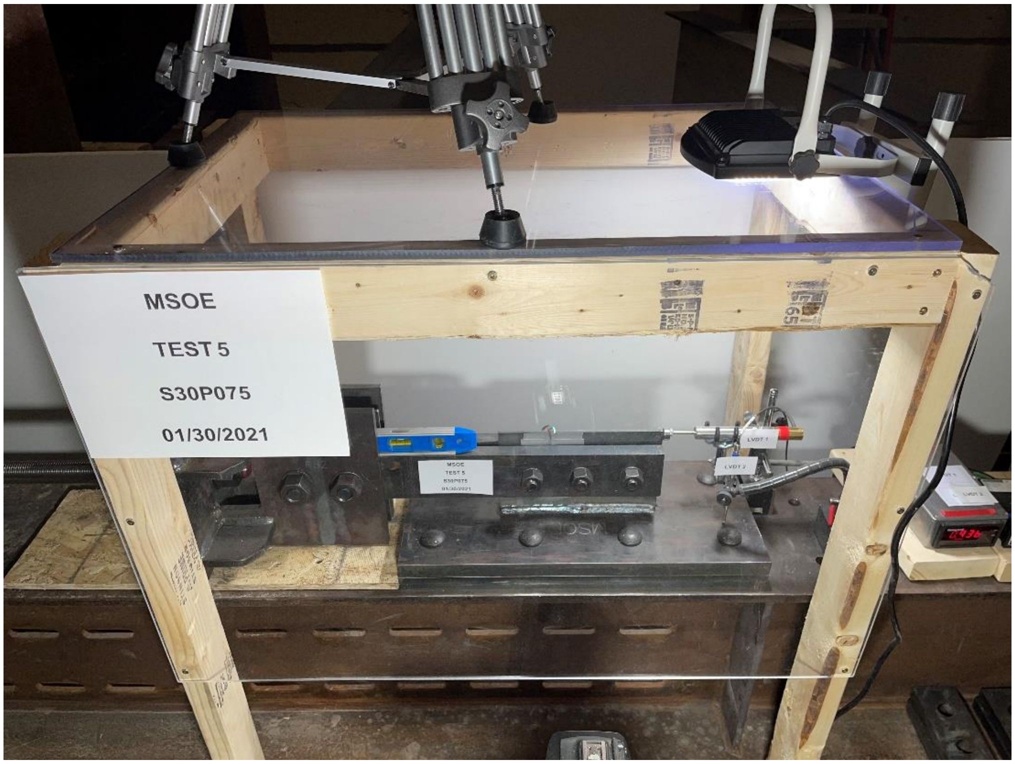

Figure 3.10-3: Plexiglass Shield.

17. Set up lights and video cameras to record the test. One camera will get placed level with the specimen and the other will get placed on top of the plexiglass shield looking down at the specimen. The test ID cards and level should be visible in the videos.

18. Take photos of completed test setup including an overall photo of the specimen in the setup, a close-up of the LVDT positions, and elevation of the specimen with the sandwich plates attached.
19. Ensure all instrumentation is reporting to the data acquisition software. Confirm LVDT readings in the software with the display on the signal conditioners.
20. Double check that all steps up to this point have been completed.
21. Simultaneously begin recording on video cameras and data acquisition system to make aligning the data with the video easier during analysis.
22. Ensure any observers are away from the longitudinal axis of the test to protect them from potential flying objects. Apply load to the specimen using the hand control for the actuator. Use consistent pulses to achieve the most monotonic load application possible. Monitor a load versus LVDT 1 plot in the software to determine when the specimen has failed. Once the plot has sufficiently turned over, the test is complete. If the test does not sufficiently turn over, the test is complete when the load reaches 100 kips (445 kN). Stop the data collection.
23. Release the load from the specimen until there is no more force on the specimen. At this point, stop the video cameras, remove the shield, and remove the specimen from the test setup. Reset the actuator position so it is retracted fully.
24. Take photos of the specimen with test ID cards again. Photos should be similar to those taken before the specimen was tested.

25. Repeat the procedure for the remaining specimens.

Chapter 4: Experimental Results

This chapter will provide a summary of the results from the experimental program, both observed and measured.

4.1 Experimental Specimen Behavior

The 20 experimental specimens primarily behaved in two ways, plate flexure and bolt bearing, and each test displayed varying levels of these behaviors. Table 4.1-1 provides a summary of each test's maximum applied load, observed behaviors, and the referring figure number in Appendix G. The observations are made relative to the full experimental program and are impacted by the ultimate load seen by each specimen. This is to say that specimens that saw higher load may have seen a direct increase in either plate flexure, bolt bearing, or both.

A few other observations of the specimens include:

- The top right corner of the plate turned up in nearly every single test. The magnitude of this displacement was different depending on the configuration, but this was observed on every specimen *except* specimens S45P025, S40P000, and S45P000. Figure G-2 shows a good example of this observation. One possible explanation for this behavior is that the material between the slots and along the non-welded edge behave as a frame rather than independent members.
- The top of the loaded edge of the specimen plate buckled towards one of the sandwich plates in every test. Because there were washers adjacent to the specimen on only one side, there was a slight eccentricity and space for the specimen plate to buckle.

- At the bottom of the loaded edge, approximately 1 in. (25 mm) up from the weld, a local buckling of the specimen plate was observed on all 12 specimens with the bolts at the 50% position and higher and S30P025 (a total of 13 specimens). The magnitude again varied with the configuration.
- Tearing of the plate occurred on specimens S35P075 and S30P050. These tests both had extreme plate flexure and once the slots were not able to deform anymore, the plate tore to allow the specimen to continue deforming. Most of the specimens would have likely exhibited this behavior if they had been loaded more.

All these observations can be seen in the post-test specimen photos in Appendix G. Because the specimen plate could not be observed during the testing procedure and these observations were made after the test was complete, it is not possible to determine the true failure mode for each specimen.

The four levels of observed behaviors from least to greatest are “minimal”, “moderate”, “significant”, and “extreme”. “Minimal” indicates that relative to all the specimens in the experiment, there was none or very little of the behavior. “Extreme” indicates the specimen saw the most exaggerated behavior of all the specimens. This level was reserved for no more than three specimens for each behavior. The “moderate” and “significant” designations were based on judgement between these two.

Table 4.1-1: Maximum Load and Relative Observed Experimental Specimen Behavior.

Test ID	Observed Plate Flexure	Observed Bolt Bearing	Maximum Applied Load	Figure
			kip (kN)	
S30P100	Moderate	Minimal	62.9 (280)	Figure G-1
S35P100	Significant	Moderate	84.2 (375)	Figure G-3
S40P100	Moderate	Minimal	89.3 (397)	Figure G-5
S45P100	Moderate	Moderate	96.5 (429)	Figure G-7
S30P075	Significant	Minimal	73.1 (325)	Figure G-9
S35P075	Extreme	Significant	87.3 (388)	Figure G-11
S40P075	Moderate	Moderate	95.9 (426)	Figure G-14
S45P075	Moderate	Moderate	100 (445)	Figure G-16
S30P050	Extreme	Extreme	85.7 (381)	Figure G-18
S35P050	Significant	Moderate	92.3 (410)	Figure G-21
S40P050	Moderate	Moderate	98.9 (440)	Figure G-23
S45P050	Minimal	Moderate	99.9 (444)	Figure G-25
S30P025	Extreme	Extreme	88.5 (394)	Figure G-27
S35P025	Moderate	Moderate	91.9 (409)	Figure G-29
S40P025	Moderate	Significant	99.9 (444)	Figure G-31
S45P025	Minimal	Significant	99.9 (444)	Figure G-33
S30P000	Significant	Extreme	92.3 (410)	Figure G-35
S35P000	Minimal	Significant	99.9 (444)	Figure G-37
S40P000	Minimal	Significant	99.9 (444)	Figure G-39
S45P000	Minimal	Significant	99.9 (444)	Figure G-41

4.2 Specimen Plate Displacement Data

The raw displacement data from LVDT 1, the instrument measuring horizontal displacement of the specimen plate, provides consistent results among the 20 tests. However, the load versus displacement plots require a brief explanation to clarify what is being shown. Figure 4.2-1 through Figure 4.2-20 provide plots of applied load versus specimen displacement for each test and a line showing the expected capacity for the specimen. The axis limits for all the plots are the same to allow the reader to easily compare them. As such, the horizontal axis' limit of 0.6 in. (15.2 mm) may not extend to the final, maximum displacement of a test.

The first thing to point out is that the LVDT or signal conditioner appears to have some small issue that produced a fair bit of noise in the experimental data. However, the noisy data did not affect the results as there were still strong, observable trends in every test. The large lateral spikes seen on some of the plots are single data points and are also likely related to the same issue.

One other common artifact on these plots is extra data at the bottom of the graphs, along the horizontal axis. This happened because the data acquisition system was started before load was applied and the LVDT was flickering around, creating extra data. These data points were removed prior to analyzing the data, as will be discussed in Section 5.3.1.

The last common note across multiple tests is crisscrossing lines after the plots have turned over. This overlapping portion is most likely due to either a pause in load application that allowed some load to be released from the specimen or the same internal issue with the LVDT or signal conditioner. This fuzziness in the data does not affect the results of the test because it was beyond the “region of interest” that will be discussed in Section 5.3.3.

On specimens S45P075, S35P050, and S40P025, there is a large horizontal shift at the bottom of the plot. This was due to the LVDT settling into the LVDT holder as the test began. All the jumps happened below 6.0 kips (26.7 kN) and had no impact on the remainder of the test.

On specimen S45P075, there is a nearly horizontal shift around 80 kips (356 kN). There was no visible shift in the specimen in the video of the test, so this shift was likely due to something internal to the LVDT.

On specimen S45P000, there is a significant horizontal jog in the data around 88 kips (391 kN). Upon reviewing the video of this test, the specimen did deflect in this range and the jump was not due to the whole specimen shifting in the setup. The author is unsure of what caused this behavior in the specimen. The specimen still had stiffness left after this quick deflection and continued to gather load until the load cell capacity was reached.

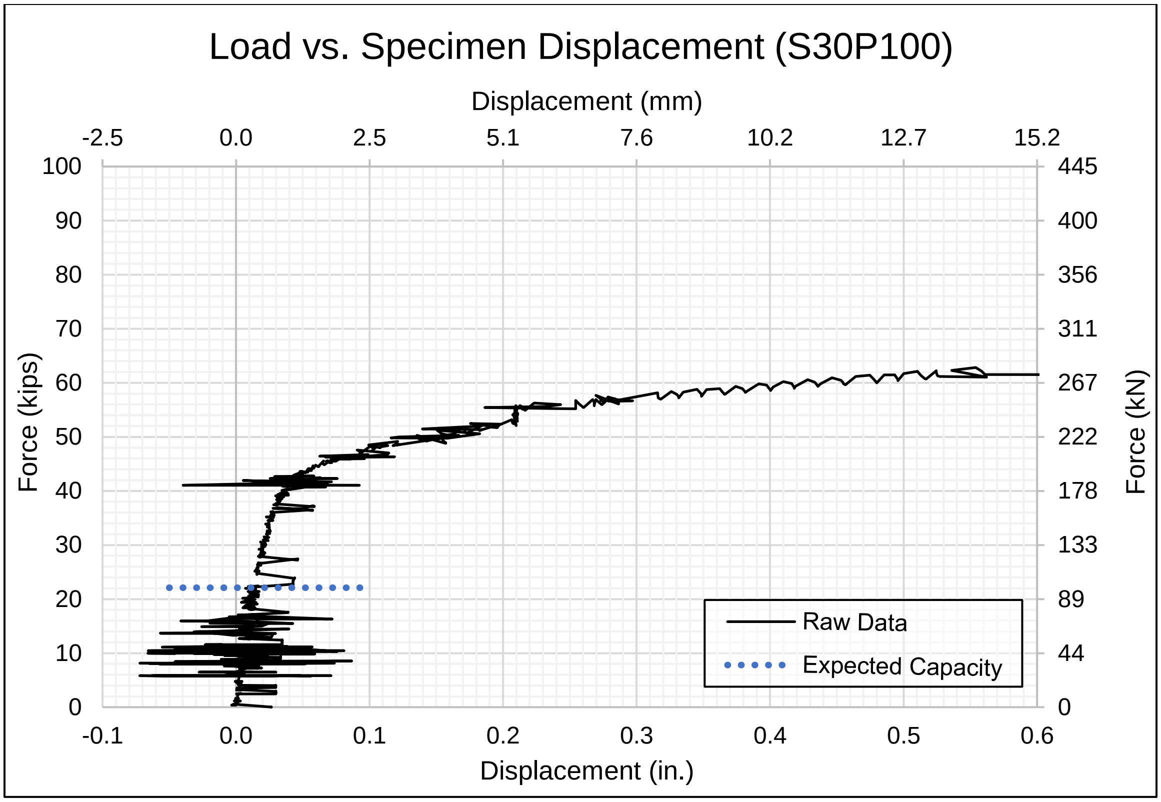

Figure 4.2-1: Load Versus Specimen Displacement for Specimen S30P100.

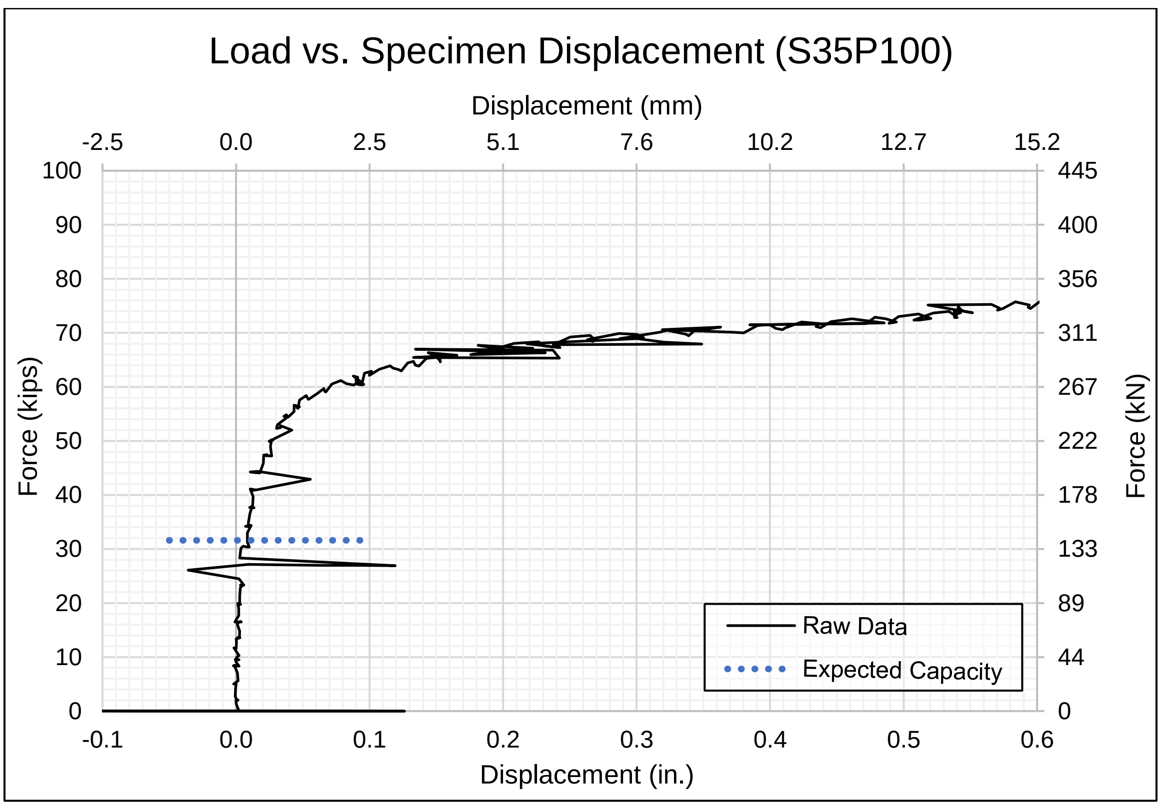

Figure 4.2-2: Load Versus Specimen Displacement for Specimen S35P100.

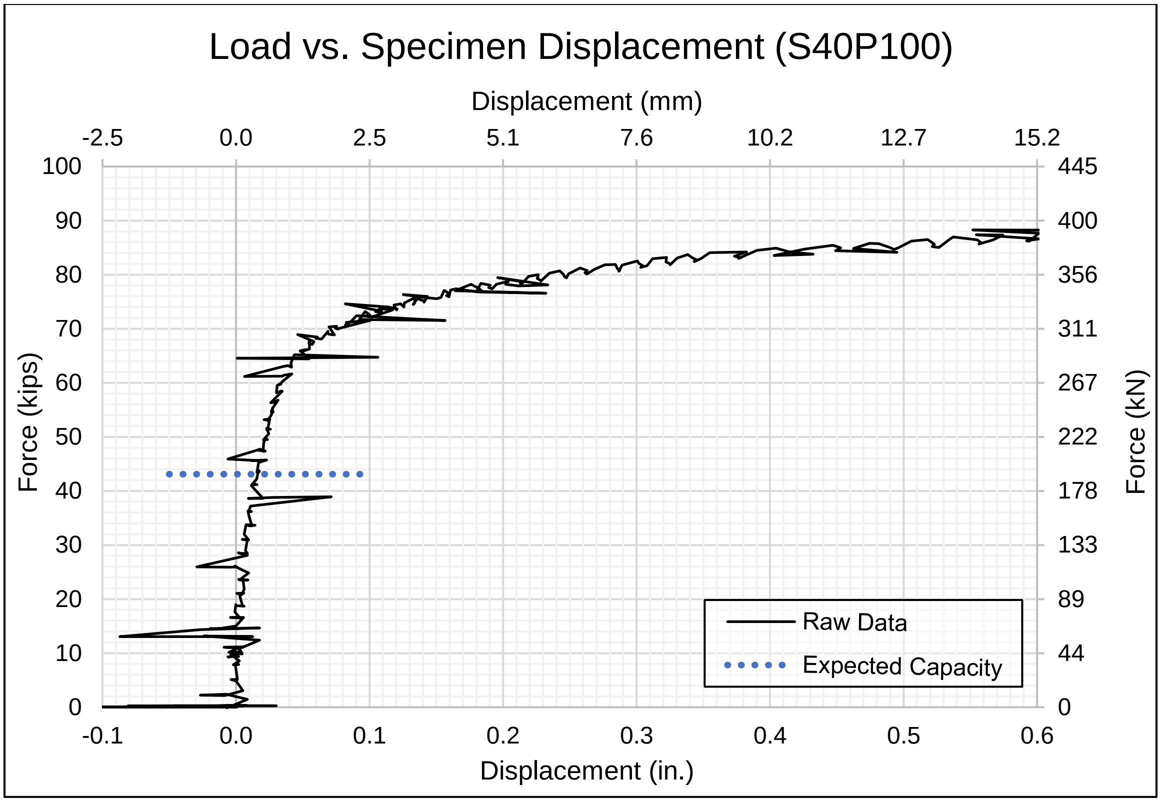

Figure 4.2-3: Load Versus Specimen Displacement for Specimen S40P100.

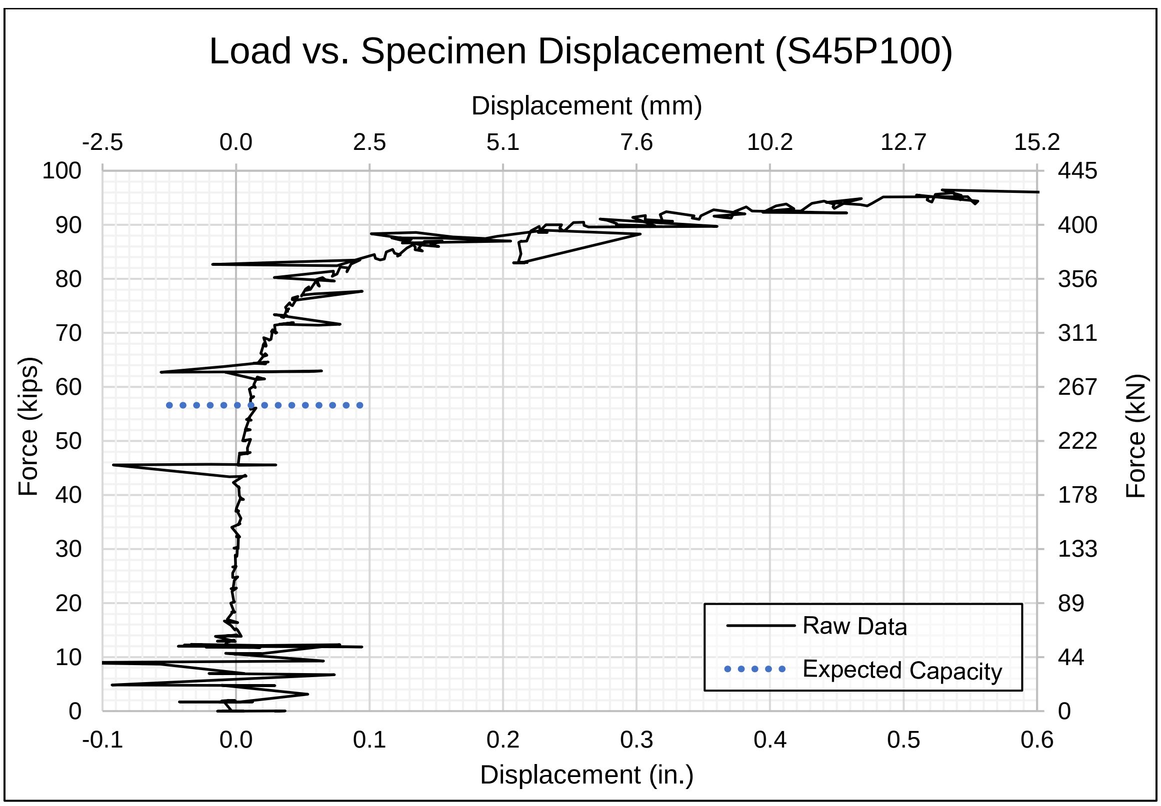

Figure 4.2-4: Load Versus Specimen Displacement for Specimen S45P100.

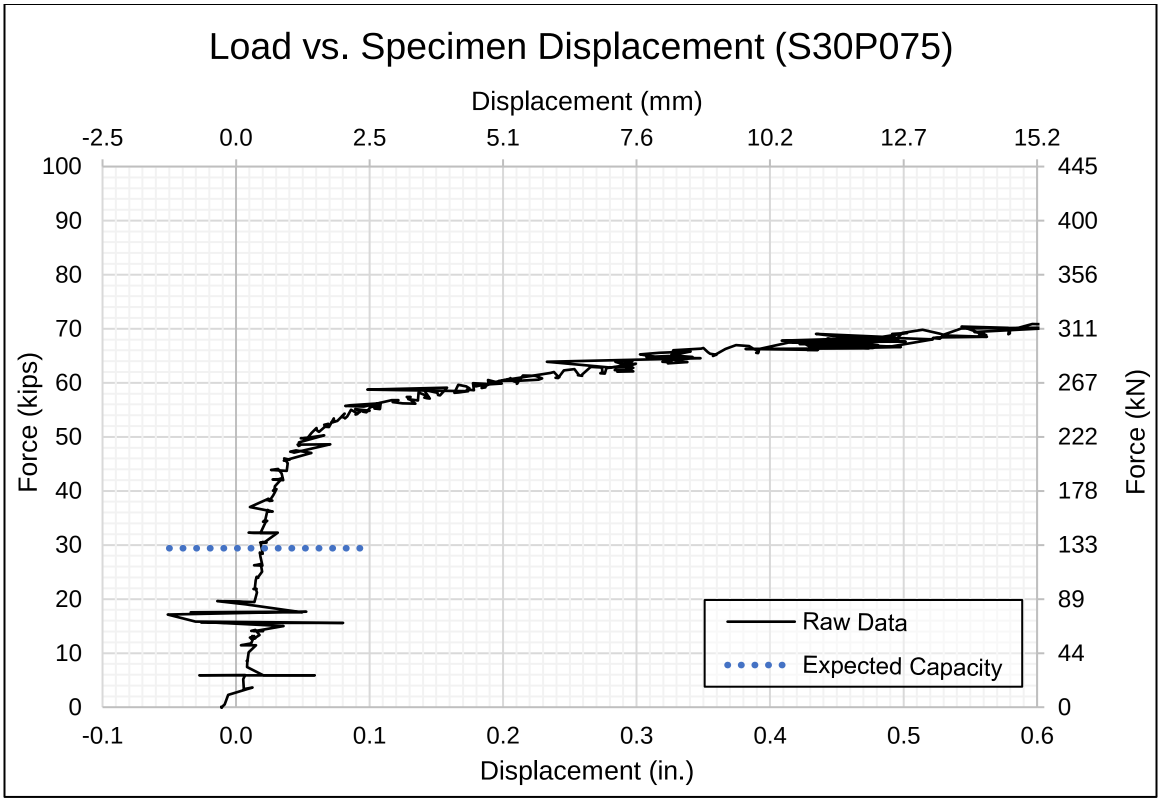

Figure 4.2-5: Load Versus Specimen Displacement for Specimen S30P075.

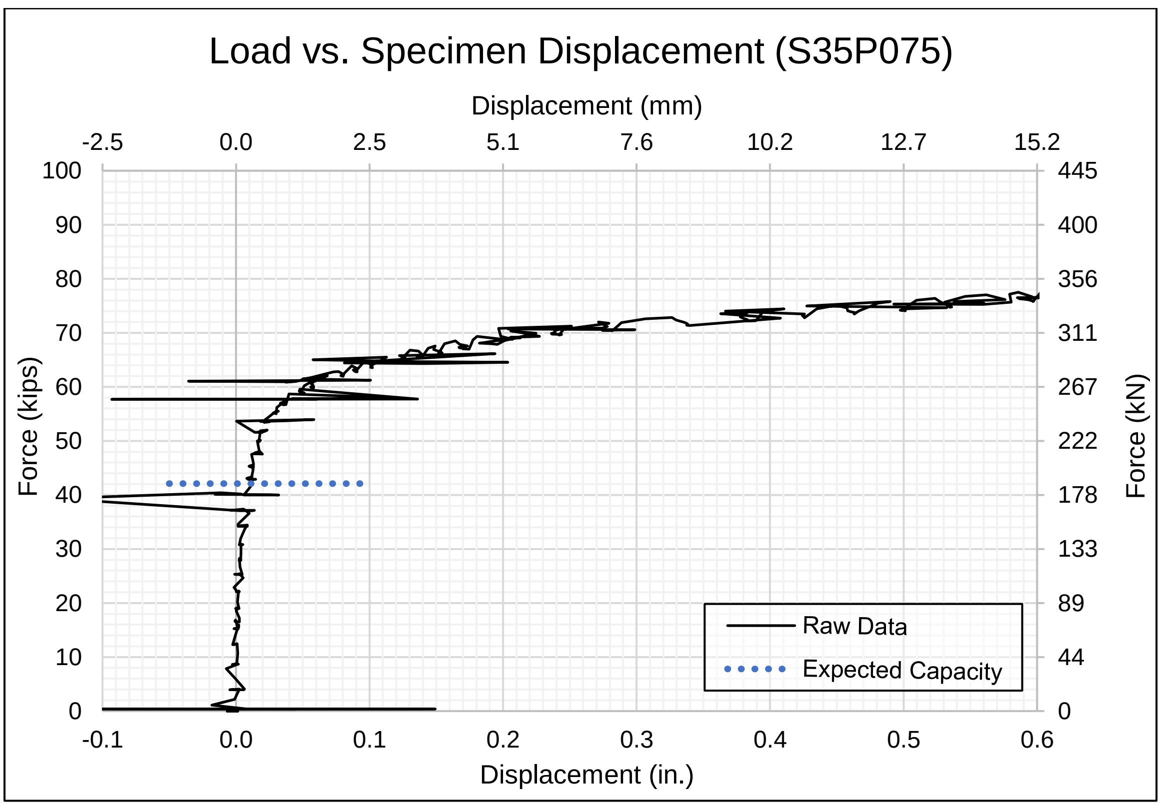

Figure 4.2-6: Load Versus Specimen Displacement for Specimen S35P075.

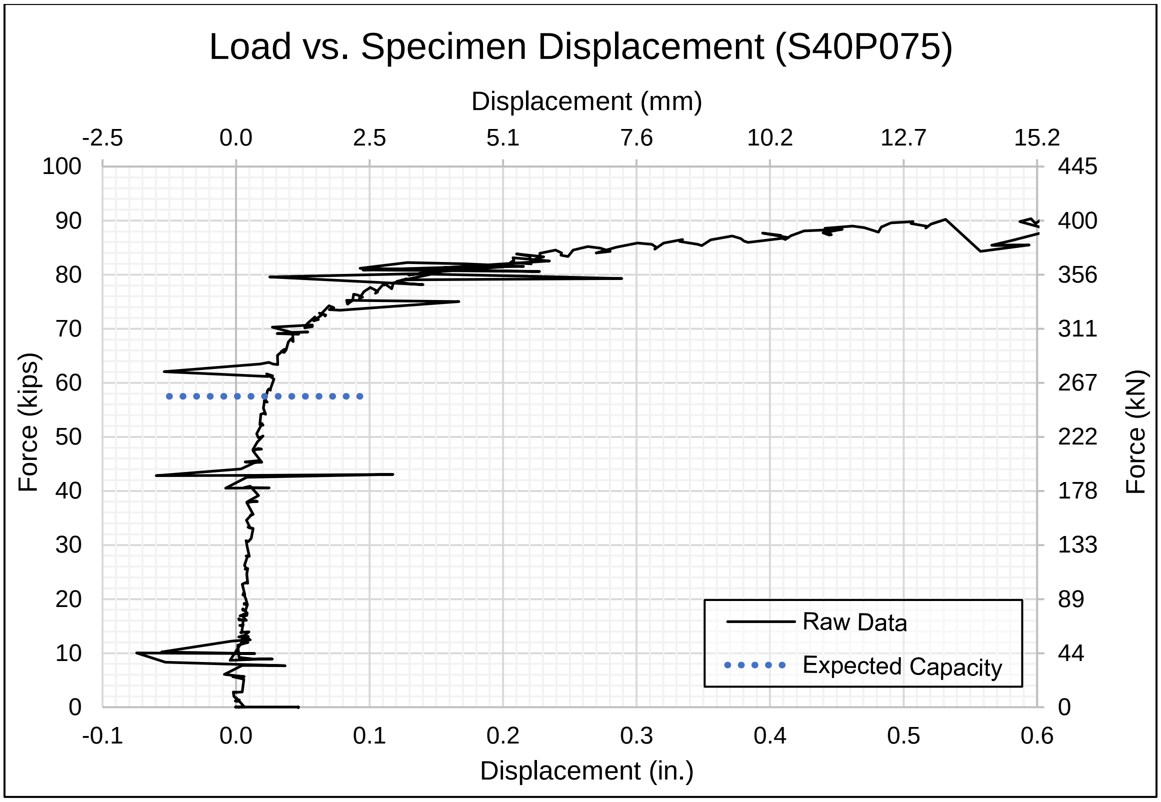

Figure 4.2-7: Load Versus Specimen Displacement for Specimen S40P075.

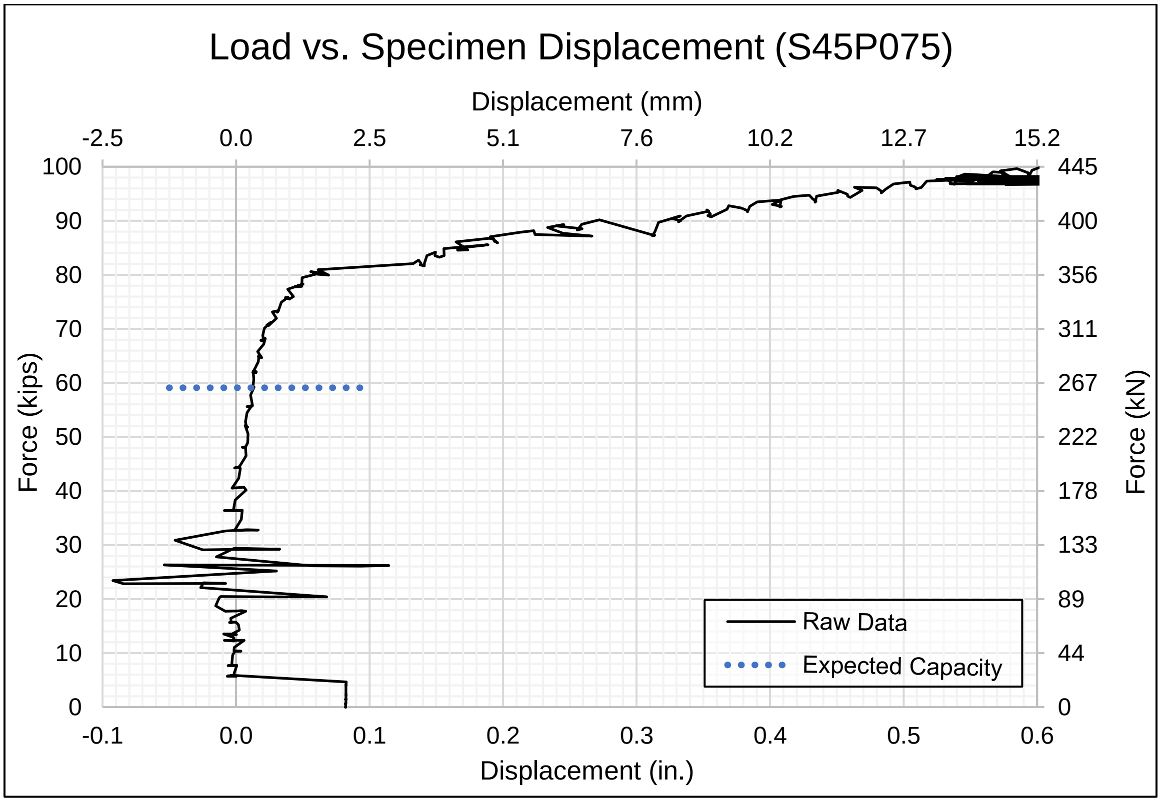

Figure 4.2-8: Load Versus Specimen Displacement for Specimen S45P075.

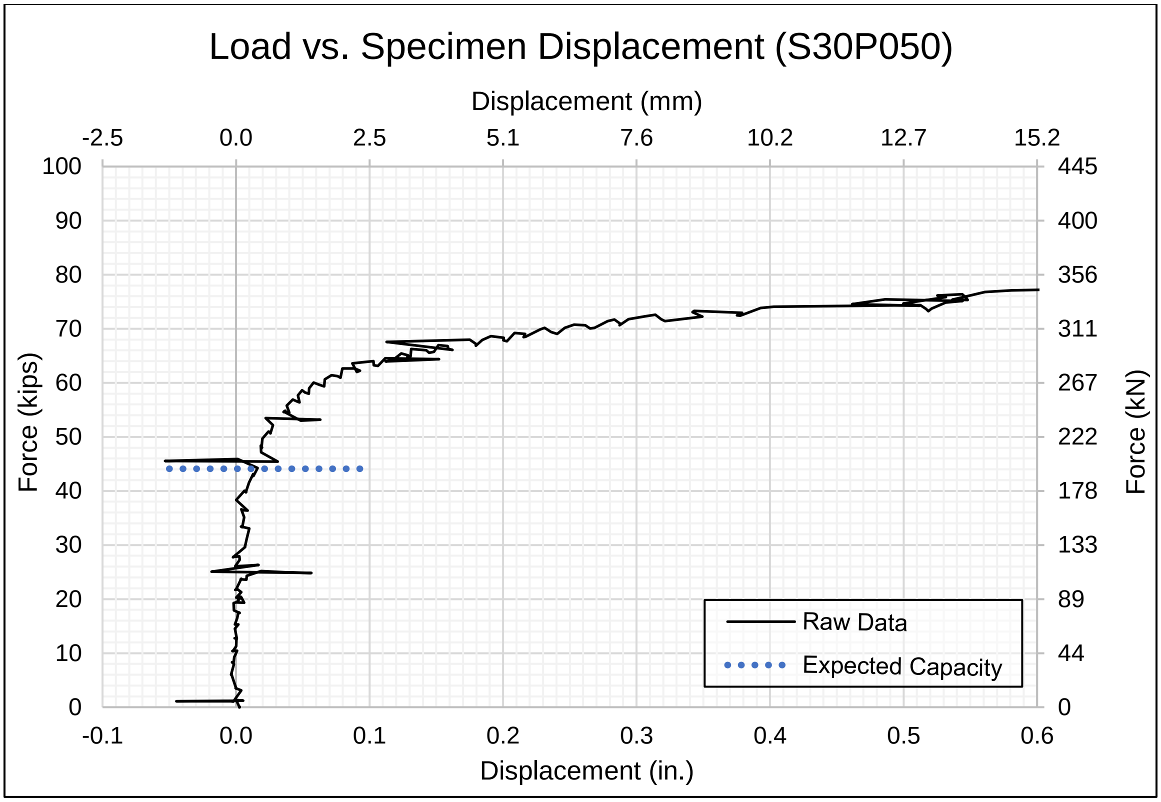

Figure 4.2-9: Load Versus Specimen Displacement for Specimen S30P050.

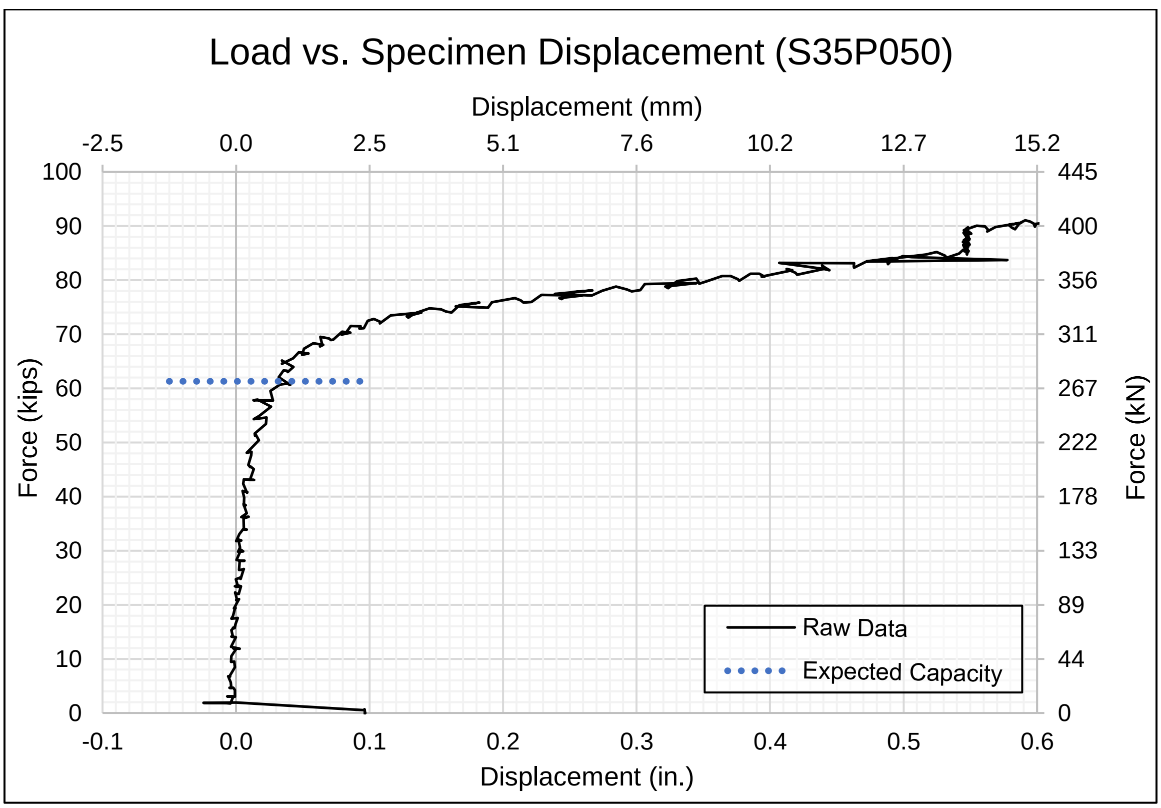

Figure 4.2-10: Load Versus Specimen Displacement for Specimen S35P050.

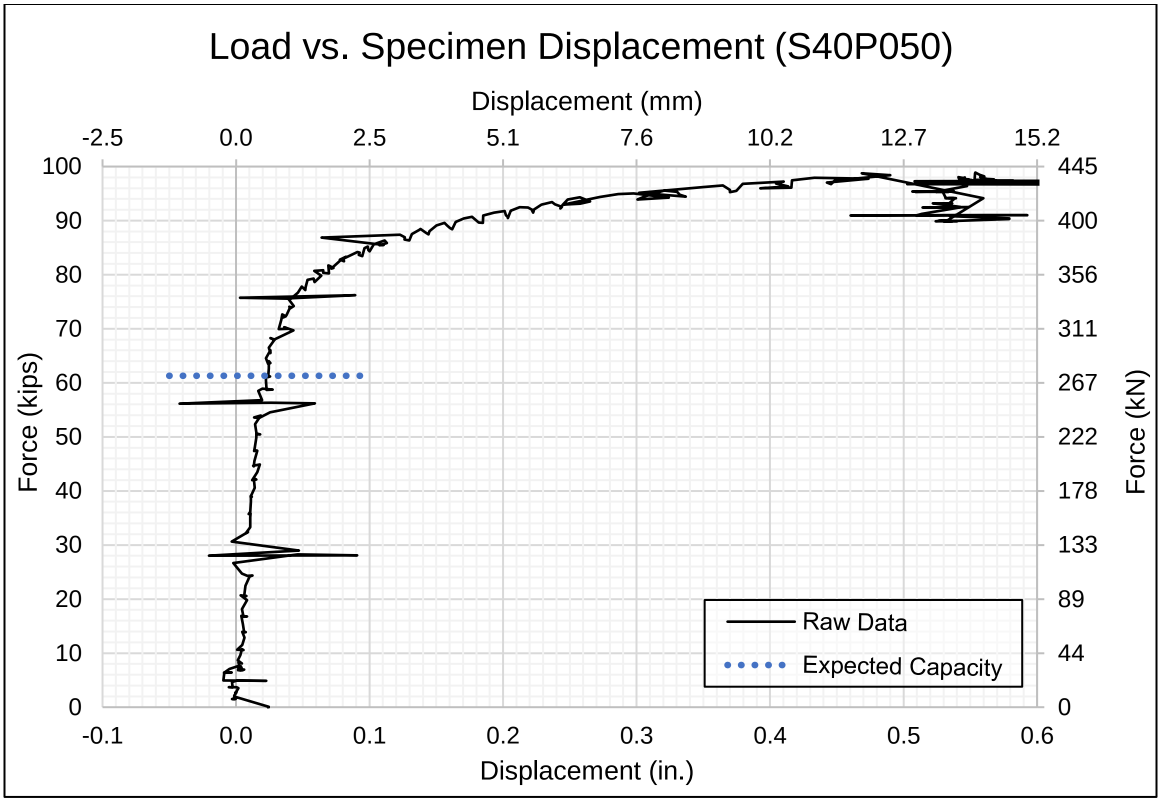

Figure 4.2-11: Load Versus Specimen Displacement for Specimen S40P050.

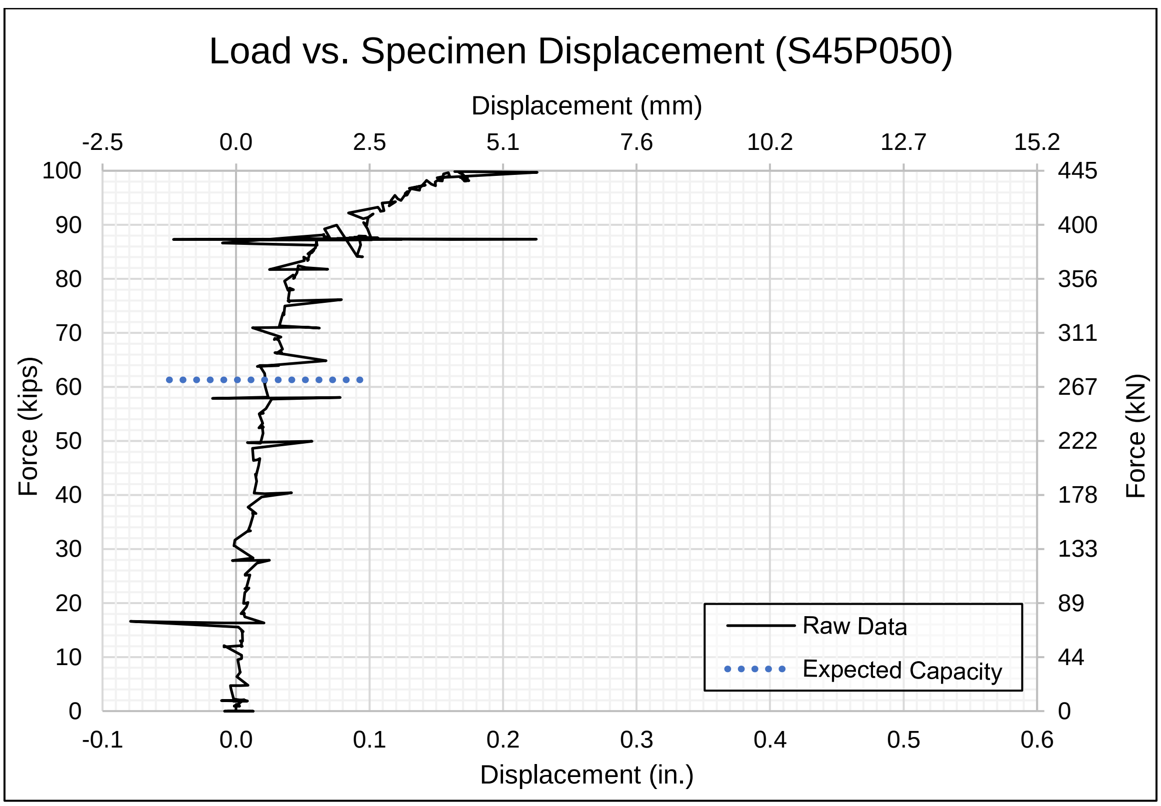

Figure 4.2-12: Load Versus Specimen Displacement for Specimen S45P050.

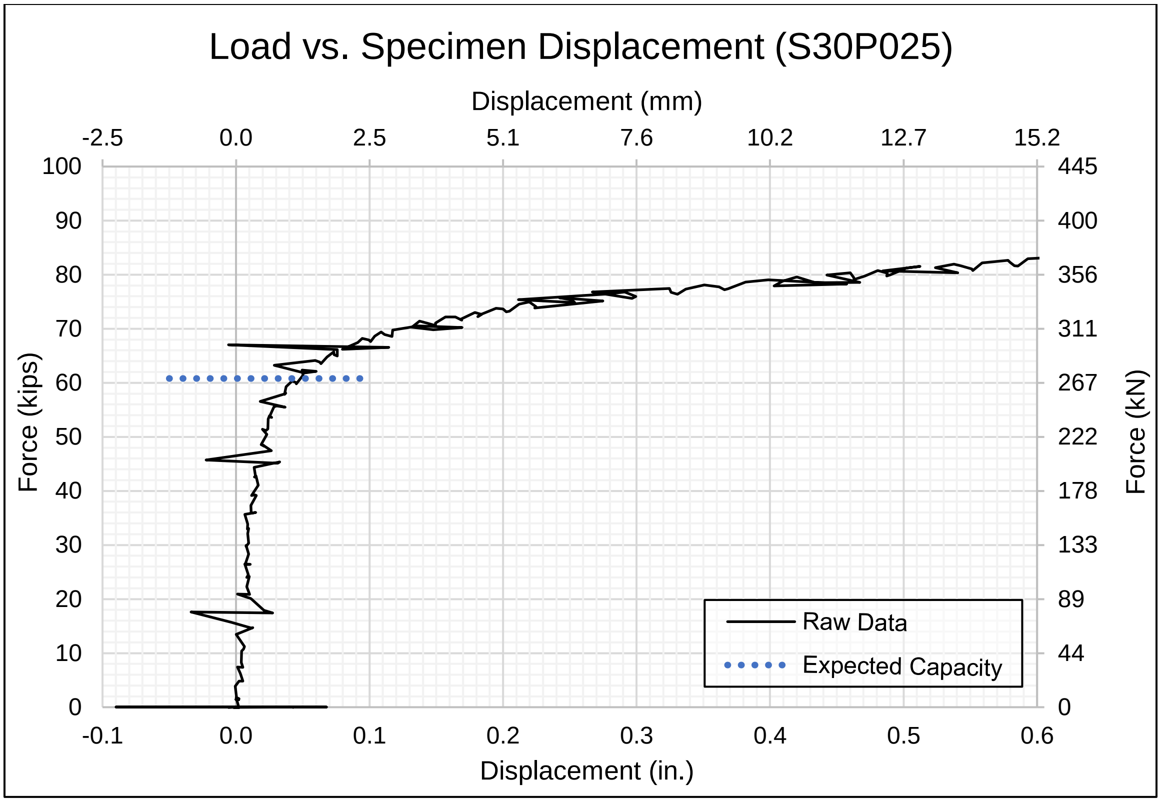

Figure 4.2-13: Load Versus Specimen Displacement for Specimen S30P025.

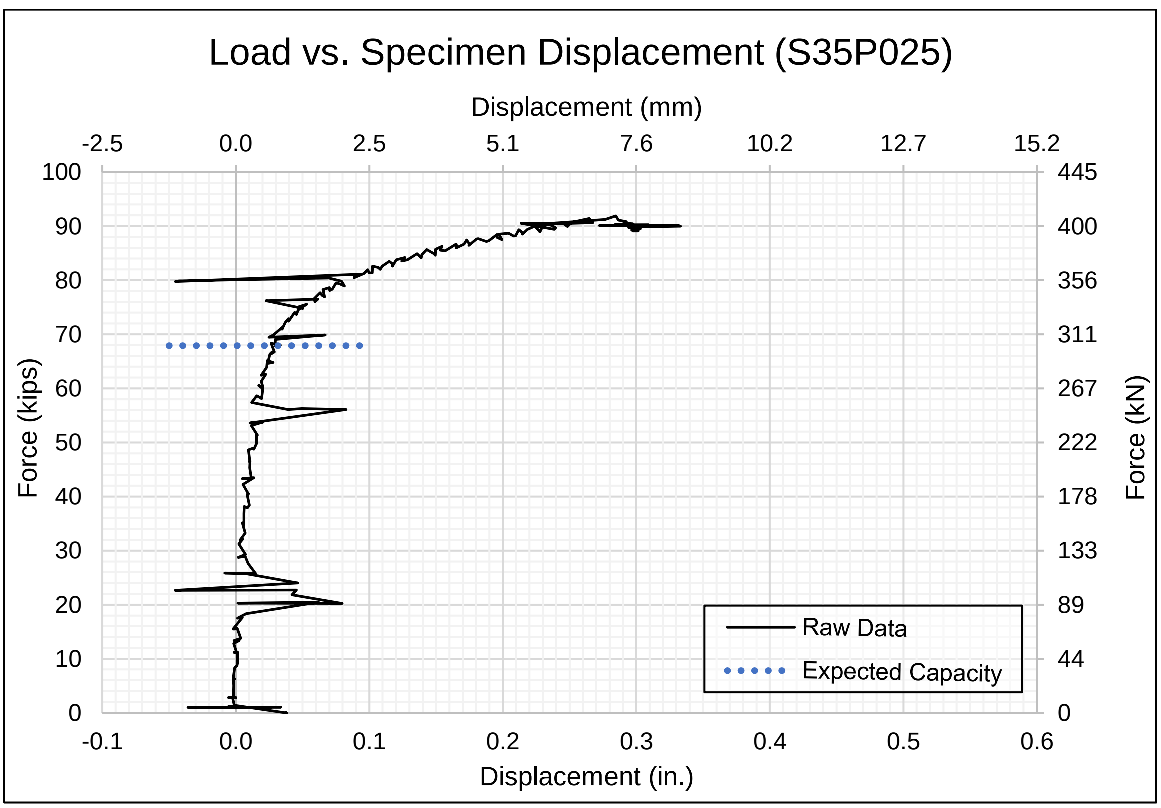

Figure 4.2-14: Load Versus Specimen Displacement for Specimen S35P025.

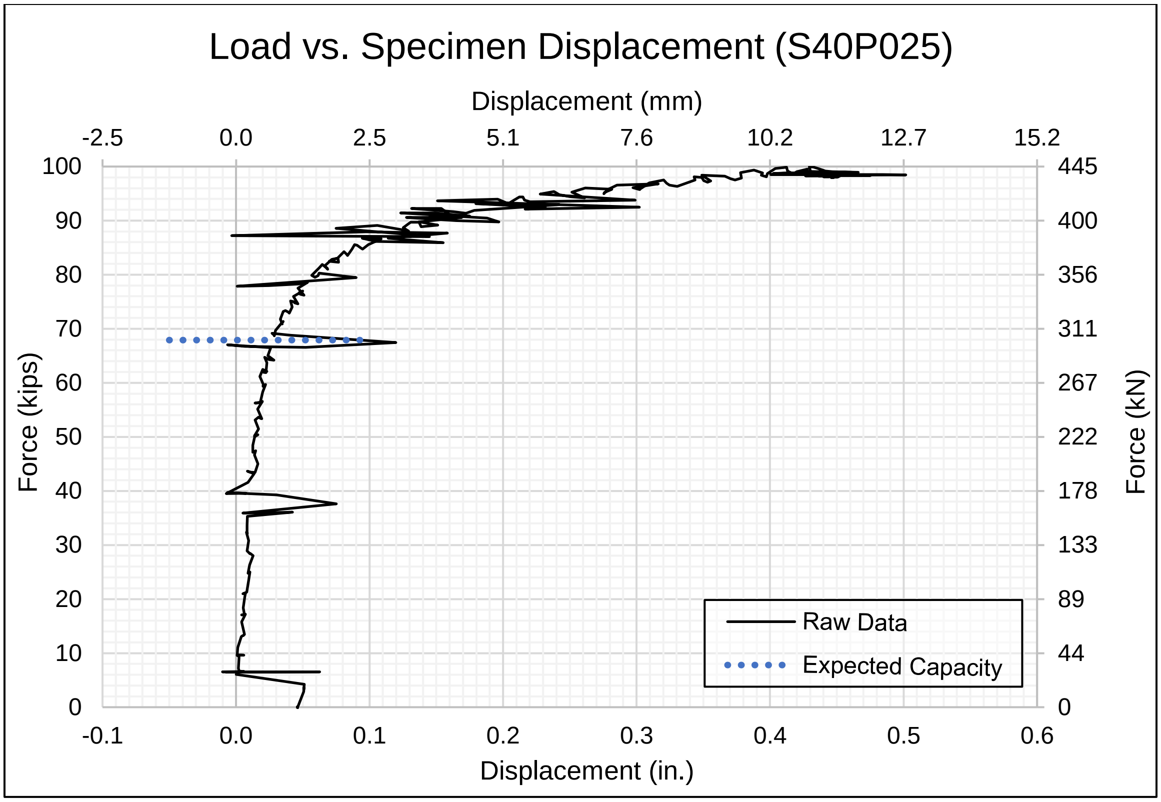

Figure 4.2-15: Load Versus Specimen Displacement for Specimen S40P025.

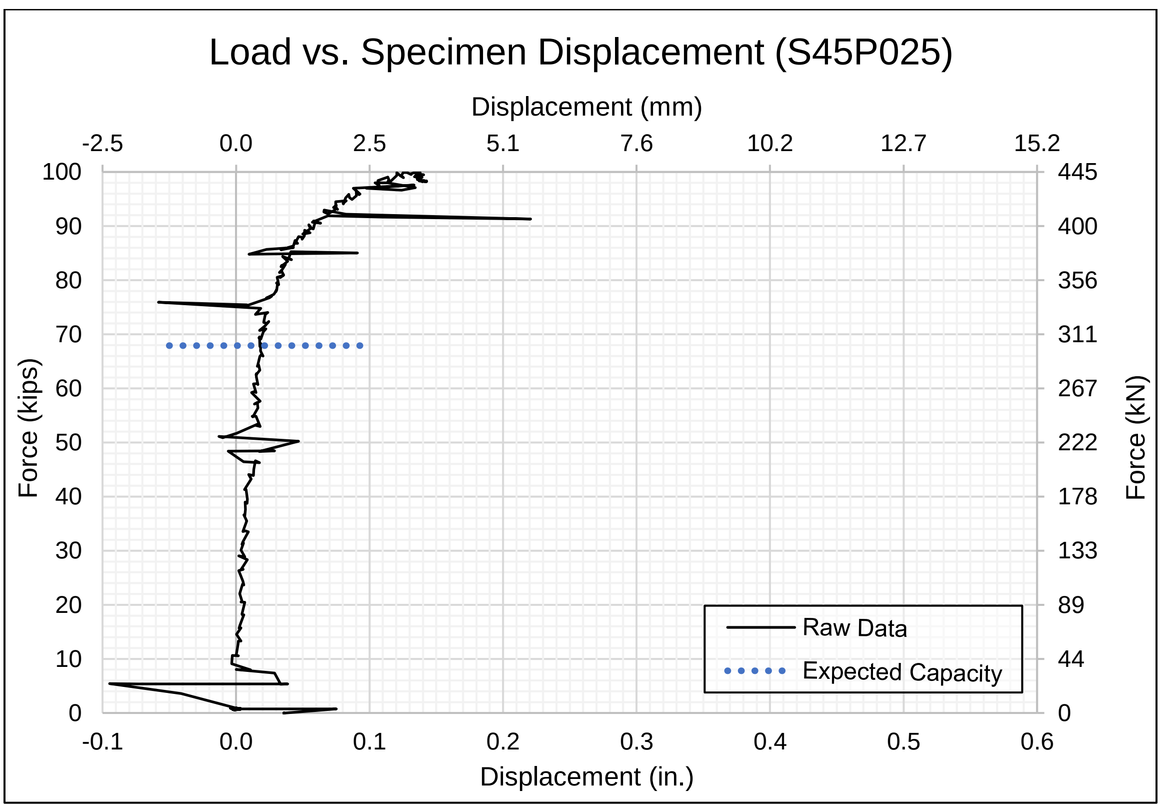

Figure 4.2-16: Load Versus Specimen Displacement for Specimen S45P025.

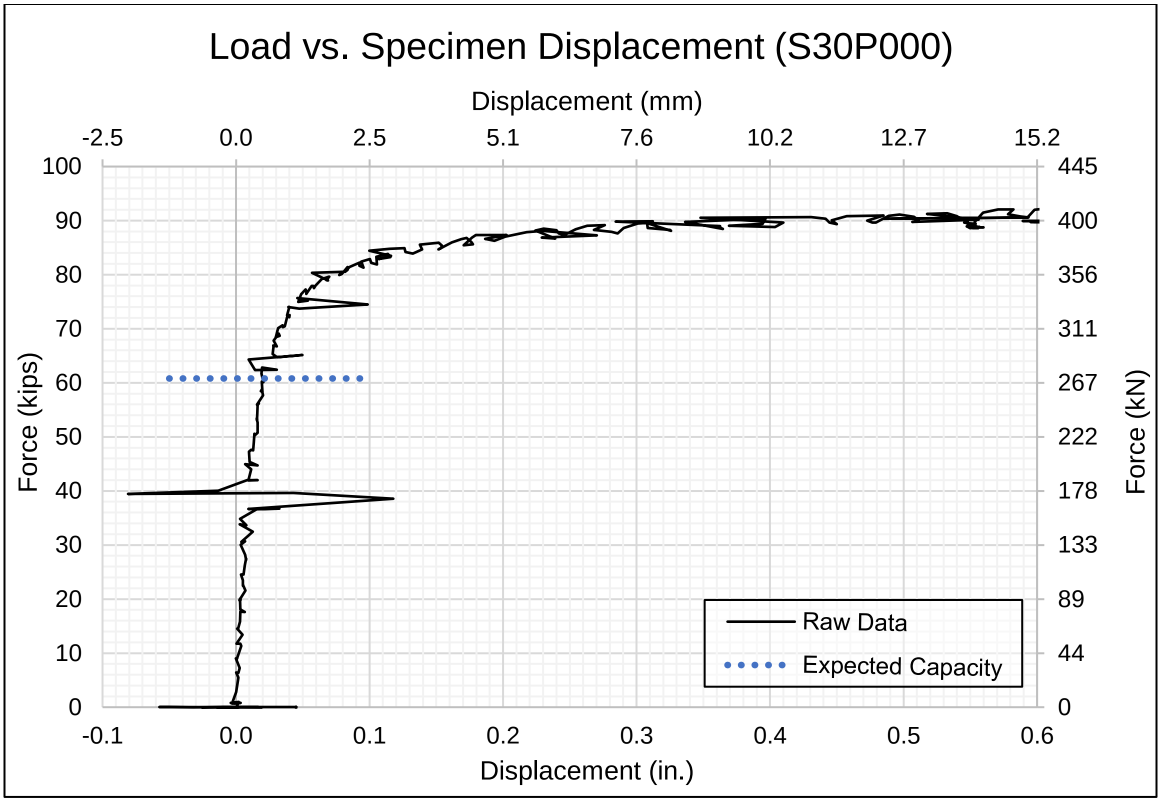

Figure 4.2-17: Load Versus Specimen Displacement for Specimen S30P000.

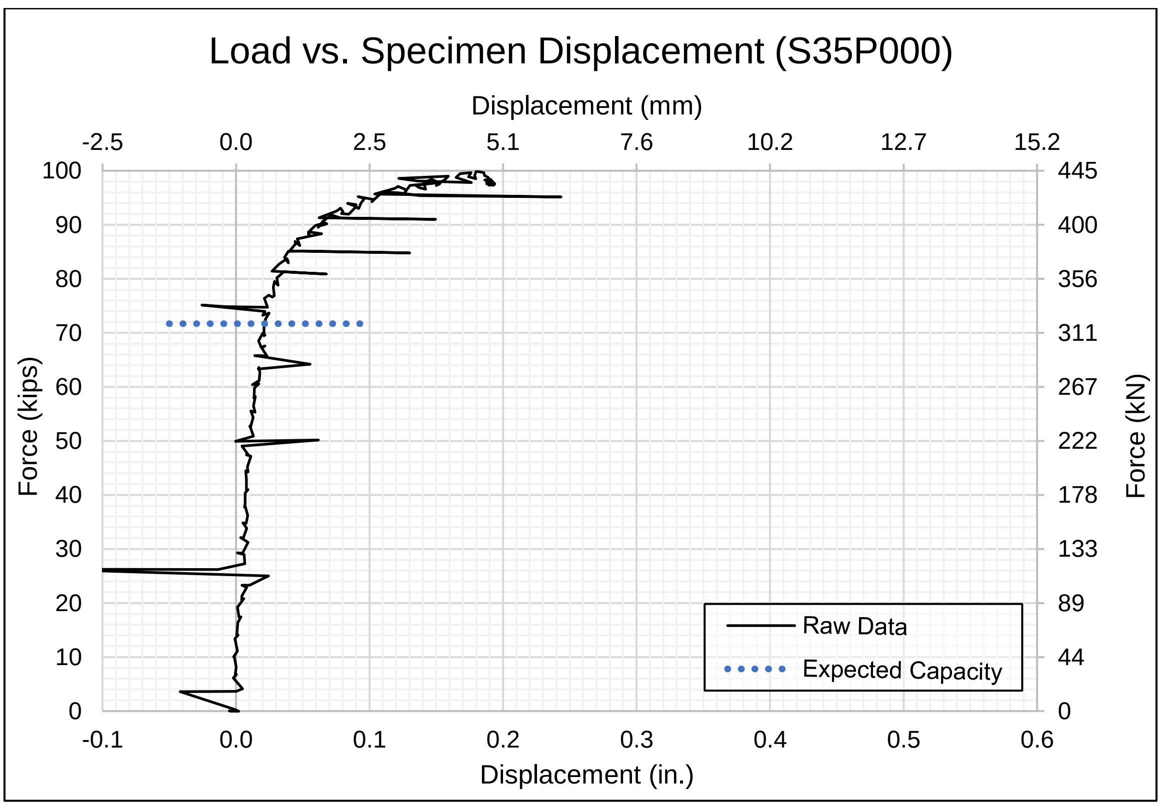

Figure 4.2-18: Load Versus Specimen Displacement for Specimen S35P000.

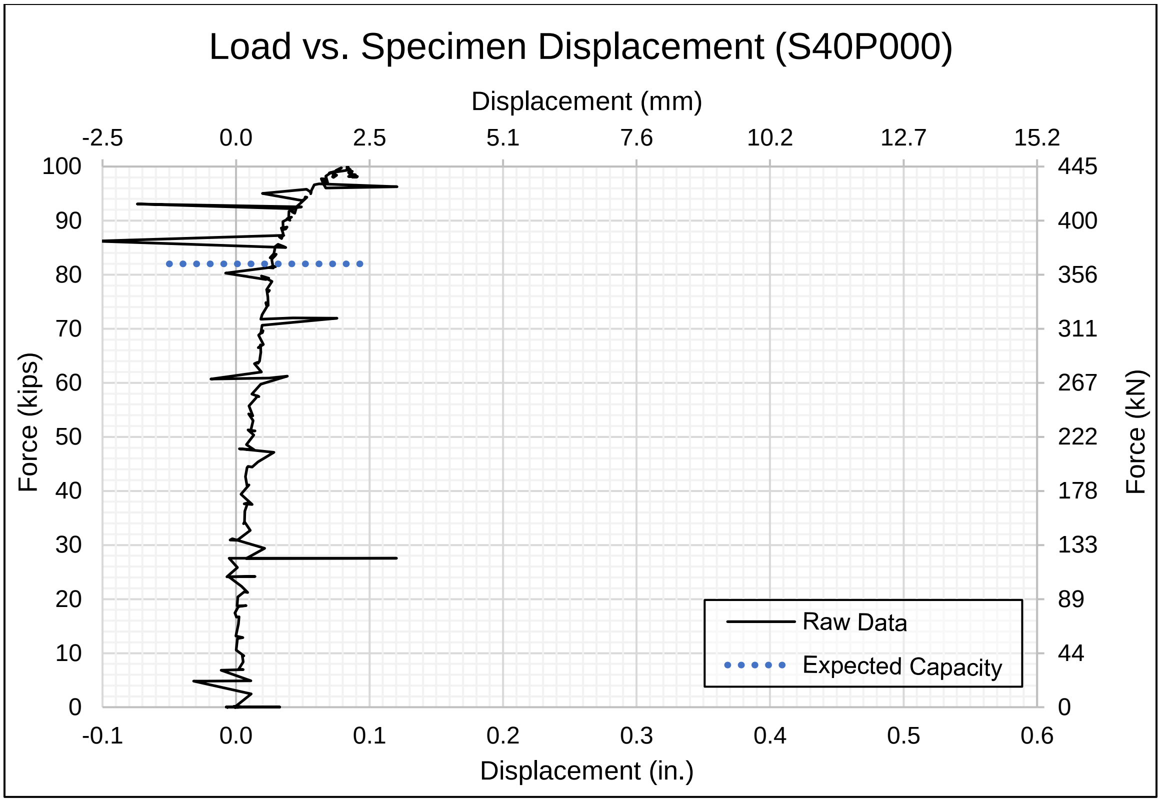

Figure 4.2-19: Load Versus Specimen Displacement for Specimen S40P000.

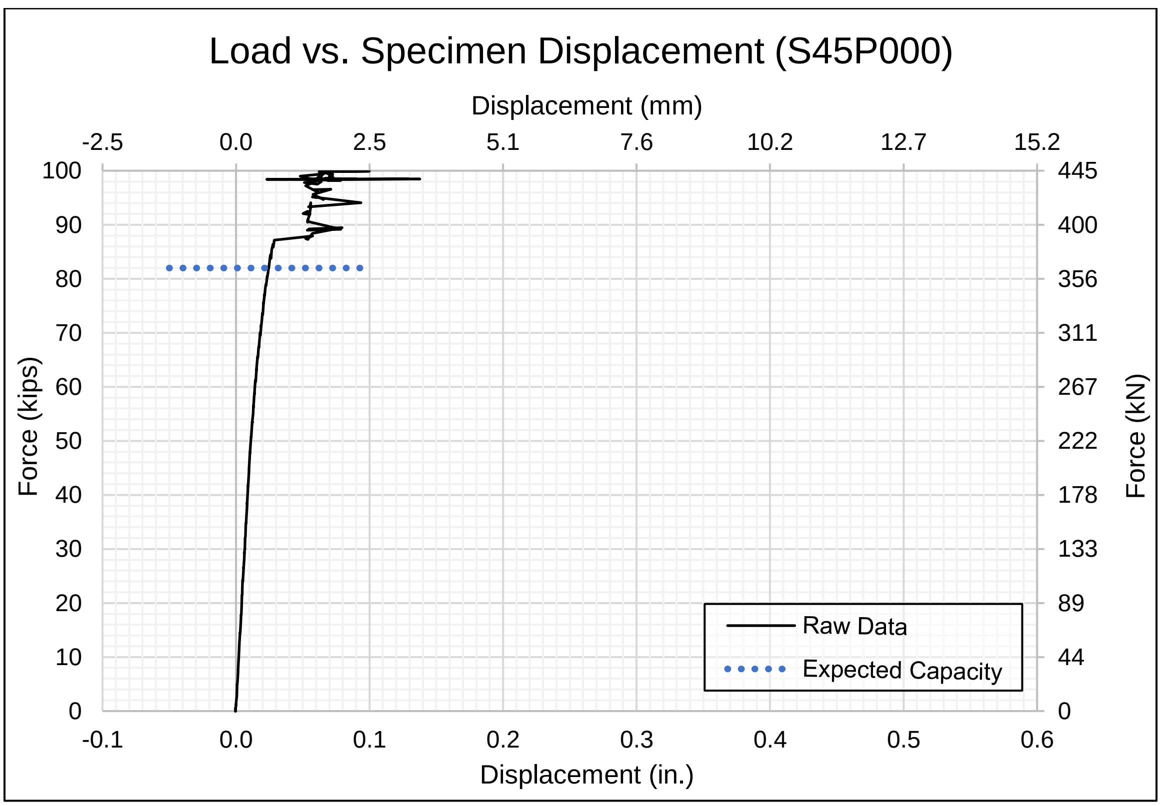

Figure 4.2-20: Load Versus Specimen Displacement for Specimen S45P000.

4.3 Strain Gauges

Strain data were collected for each of the 14 tests that had a rosette attached. The results from these tests were also very consistent between tests. The load versus strain plot for specimen S40P100 provides a good representation of the trends seen across all 14 tests and is shown in Figure 4.3-1. Strain gauge 1 was angled 45 degrees towards the load, strain gauge 2 was vertical, and strain gauge 3 was angled 45 degrees away from the load. This configuration is shown in Figure 4.3-2 and is the same for every test. All the load versus strain plots are provided in Appendix H.

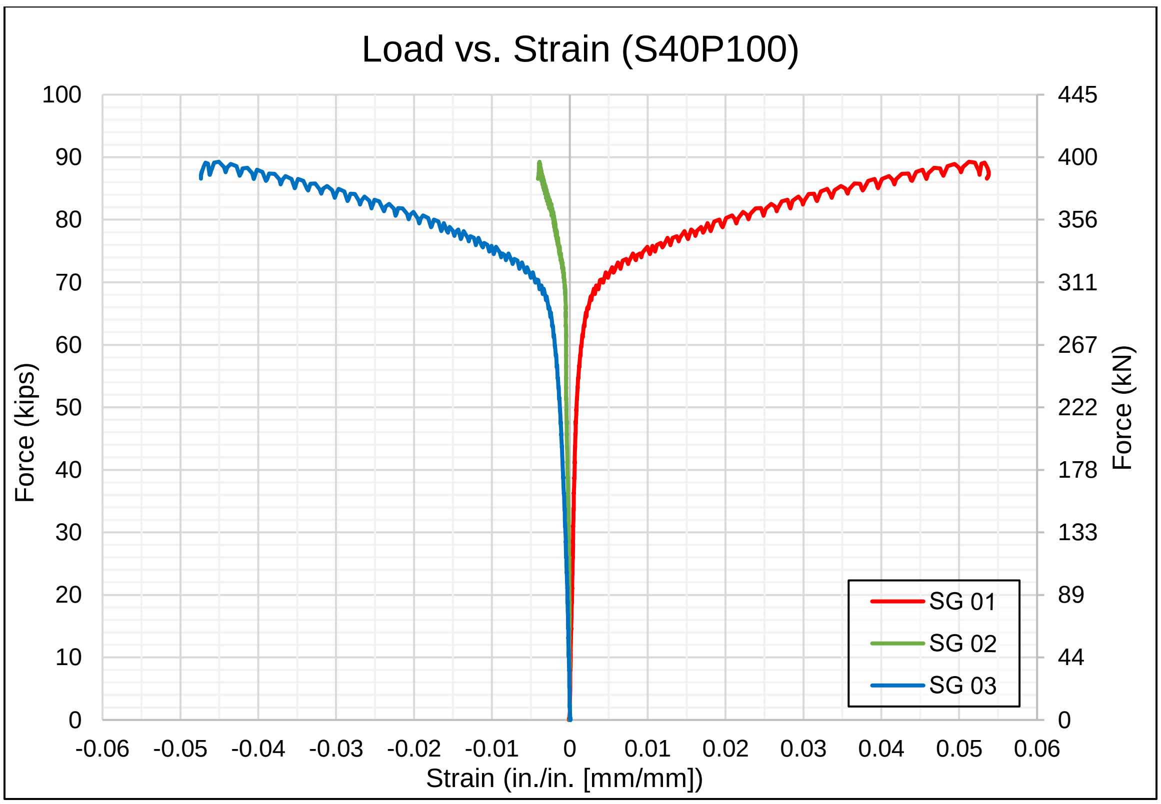

Figure 4.3-1: Representative Strain Data (from Specimen S40P100).

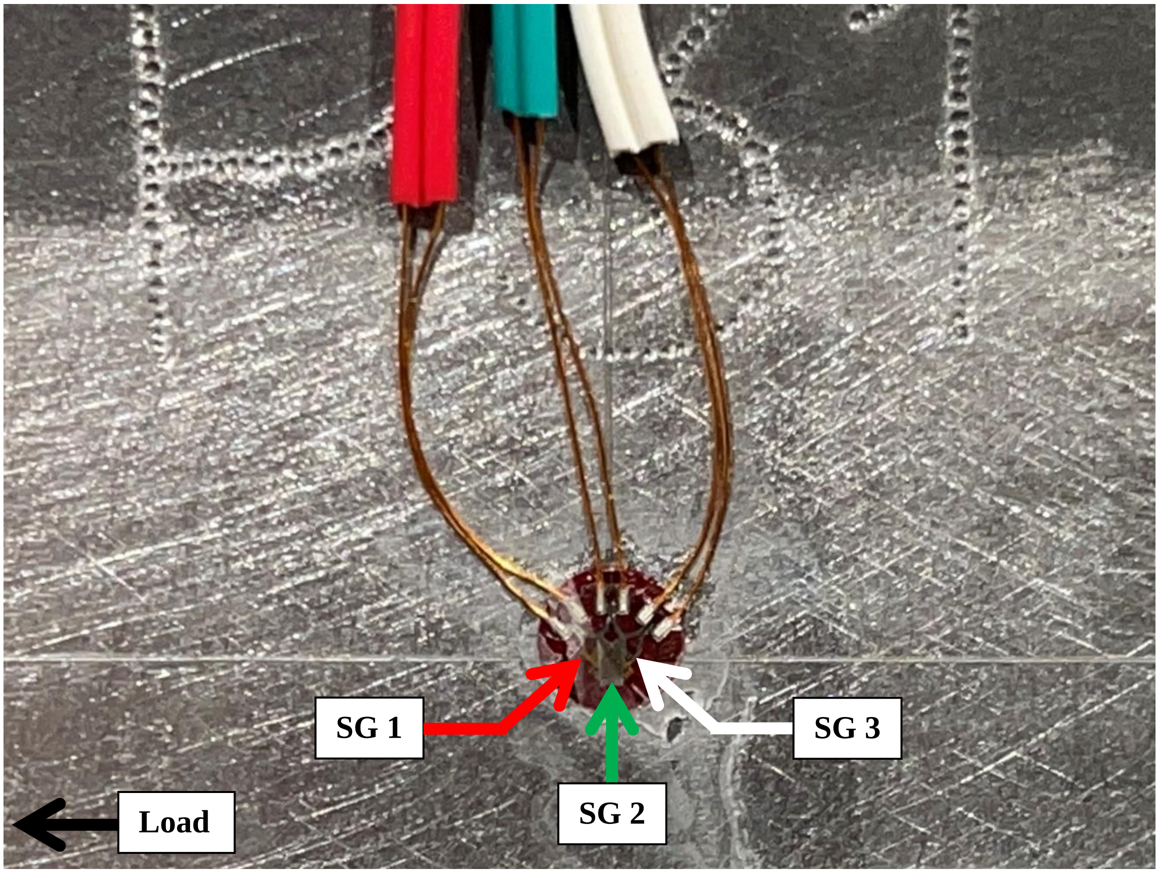

Figure 4.3-2: Strain Gauge Numbering and Positioning.

4.4 Base Plate Displacement

The last data collected were from LVDT 2, the instrument that measured vertical displacement of the specimen base plate. The maximum base plate displacement across the 20 experimental specimens was less than 0.005 in. (0.13 mm), indicating the test setup approximated the fixity as expected. No further discussion of these data is required.

4.5 Access to Raw Experimental Data

The raw data from this experimental program is available from the author upon request.

Chapter 5: Data Analysis and Comparison

5.1 Introduction

The data analysis portion of this research initiative required careful thought and consideration to make sense of what the data show and what conclusions could be drawn. Multiple different approaches for determining an experimental capacity were considered and tried before deciding on the procedure outlined in this chapter. Ultimately it was decided that the data from LVDT 1 would provide the best analysis of the connection to be able to determine the effect the slot spacing had on this connection. As such, the data from the rosettes were not used to determine a failure capacity of the specimens.

5.2 Alternate Analysis Methods Considered

One of the analysis options considered included analyzing the strain data using a Mohr's circle stress transformation and determining a failure point based on stresses in the material; however, this was not an ideal method, as an evaluation of the finite element results from Peterson (2014) indicates the highest stresses were not at the midpoint between the slots, but rather around the edge of the slots. The purpose of the rosettes was to gain an understanding of the behavior of the material between the slots, not determine failure of the specimens. As such, the strain data gathered on these specimens would not have accurately reflected a failure point in the specimens.

Another method would be to use a time-lapse of the videos that were taken to determine when bolt bearing occurred versus when plate flexure occurred, but that would not prove to be a reliable method.

The last alternate method of analyzing the data to find a failure point involved approximating the load versus specimen displacement data (from LVDT 1) with straight lines, indicating an “elastic” region, a “plastic” region, and a “transition” region between the two. However, because this method would be difficult to apply consistently across the 20 tests, this was not chosen as the analysis option.

5.3 Analysis Procedure

The analysis of the experimental data was comprised of three main steps: manually prefiltering the data, processing the prefiltered data through a series of filters in MATLAB, and finally manually determining the connection capacity.

5.3.1 Manual Prefiltering of Raw Data

The first step in the data analysis was manually prefiltering the raw LVDT 1 data. This primarily consisted of removing the outlier data points (spikes) to allow the following filtering operation to be more effective. The points that were removed clearly did not reflect actual specimen behavior. Additionally, on the specimens that had large shifts in the LVDT data at the bottom of the plots, the difference between the two segments was calculated and the misaligned data were shifted to align with the data closer to the vertical axis. Lastly, on tests that had extra data along the horizontal axis, the data before load was applied were removed, and the clean-up of the data was passed into the next step. Appendix I provides a summary of all the changes made to the raw data during the prefiltering step.

5.3.2 MATLAB Operations

5.3.2.1 Butterworth and Median Filters

This step was thoughtfully crafted to maintain the integrity of the data while smoothing it in such a way that made analysis possible. The prefiltered LVDT 1 displacement data were first passed through a 10^{th}-order Butterworth filter. This filter removed the crisscrossing data and started smoothing the noisy data. The output of the Butterworth filter was then passed through a median filter. The order of the median filter was equal to $^{1}/_{15}$ the number of data points, rounded to the nearest integer (e.g. a test with 439 data points would have an order of 29). The order for the median filter is the number of points the filter looks at in each step. This value changed for each test to make the effect of the filter consistent across the 20 data sets in which each had varying amounts of data.

This process was used as stated for every specimen except S30P100. Because of the exceptionally noisy data at the start of the test, it was necessary to pass the raw data through a median filter with the same parameters as described previously before passing it into the Butterworth filter. This step significantly reduced the noise at the start of the test and allowed the Butterworth and second median filter to be more effective. Figure 5.3.2.1-1 shows what the results of the second median filter look like with and without the initial median filter. The plot showing the data with the extra filter follows the trend of the unfiltered data better than the plot without the extra filter.

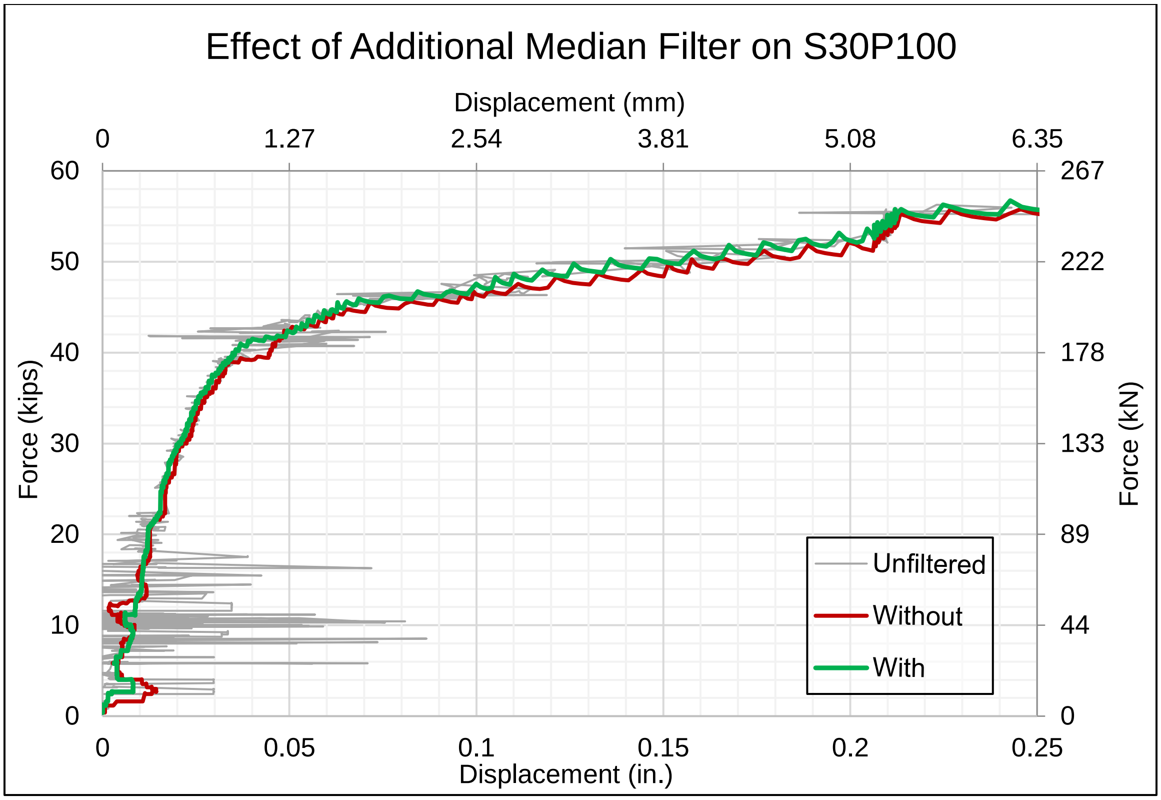

Figure 5.3.2.1-1: Effect of Additional Median Filter on Specimen S30P100.

5.3.2.2 Curve-Fitting

After the data had been passed through the Butterworth and median filters, the data were sent to a curve fitting function in MATLAB. The "fit" function has various types of curve-fitting functions including quadratic polynomial curves, piecewise cubic interpolation, and smoothing spline (a piecewise polynomial function). Because of the nature of the data in this experimental program, the smoothing spline offered the best flexibility to fit the data. The function's inputs were the output from the median filter(s) (displacements, X-values), the column vector of loads (Y-values), the type of fit (smoothing spline), and lastly a smoothing parameter. This parameter determines how smooth the fitted curve is. A value of 1 simply traces over the input data and does not actually produce a new curve. After trying different values, it was found that the output of the "fit" function using the smoothing spline is very sensitive to this smoothing parameter. Anything less than 0.999 produced a drastically different curve. After tuning this parameter across a few of the tests, a value of 0.9999999 was determined to adequately fit and smooth the data while still showing the trend of the data. Figure 5.3.2.2-1 provides an example of the effect of the smoothing parameter on a data set.

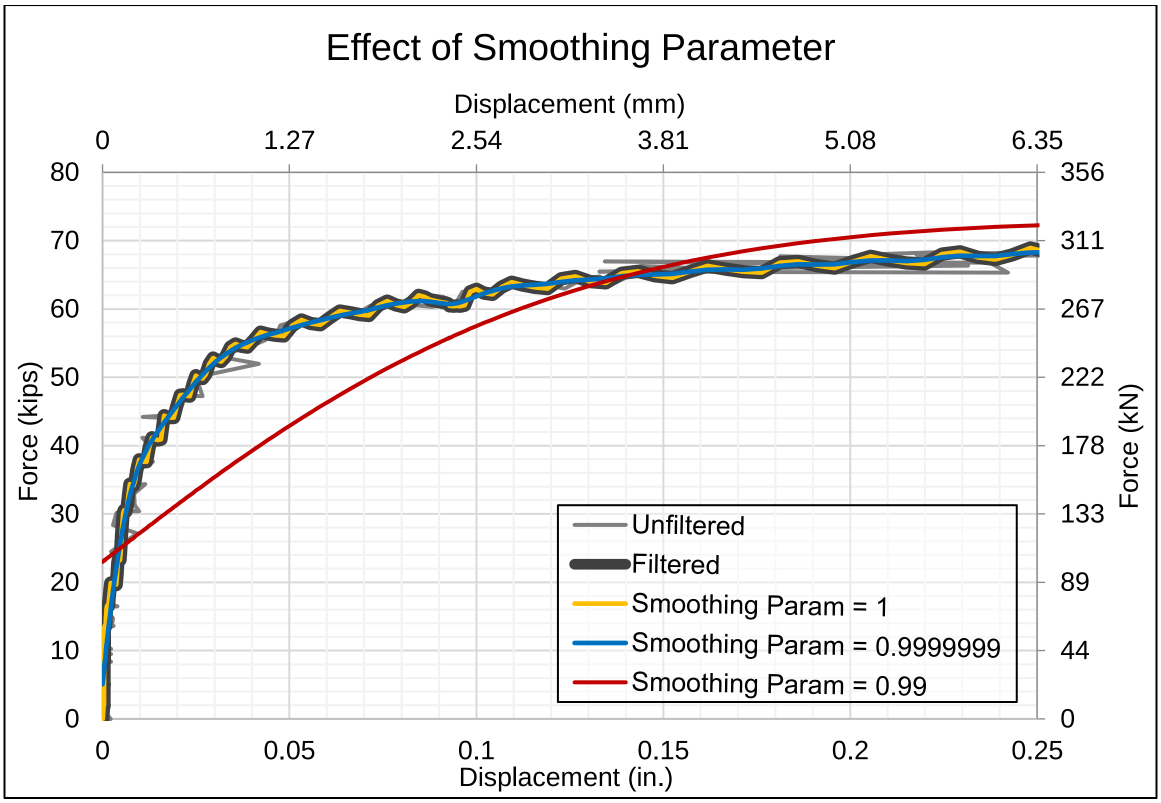

Figure 5.3.2.2-1: Effect of Smoothing Parameter on Curve Fit Function.

After the curve-fitting was complete, the curve-fit data (new Y-values) and filtered displacement values from the filtering steps were exported from MATLAB back into an Excel file for the final analysis step.

The MATLAB code used to analyze the data is provided in Appendix J.

5.3.3 Manual Capacity Determination

After the filtering step was complete, the data were brought back into Excel to determine the tested capacity of the specimen. This step required careful consideration to create a procedure for selecting the capacity in a consistent and appropriate manner based on the curve-fit data.

The first step was defining failure for these specimens. Failure of the specimen was defined as the point at which the specimen accumulated significant reduction in stiffness. Graphically, this point is represented by the change from the mostly vertical portion to the mostly horizontal portion of the load versus displacement graph. As seen in the plots of raw LVDT data (beginning at Figure 4.2-1), this point is not easily selected because there is a transition region between the two segments of the graph. This led to the development of a “region of interest” that focused on the range bounding the transition portion. Figure 5.3.3-1 shows an example of the limits of a “region of interest”.

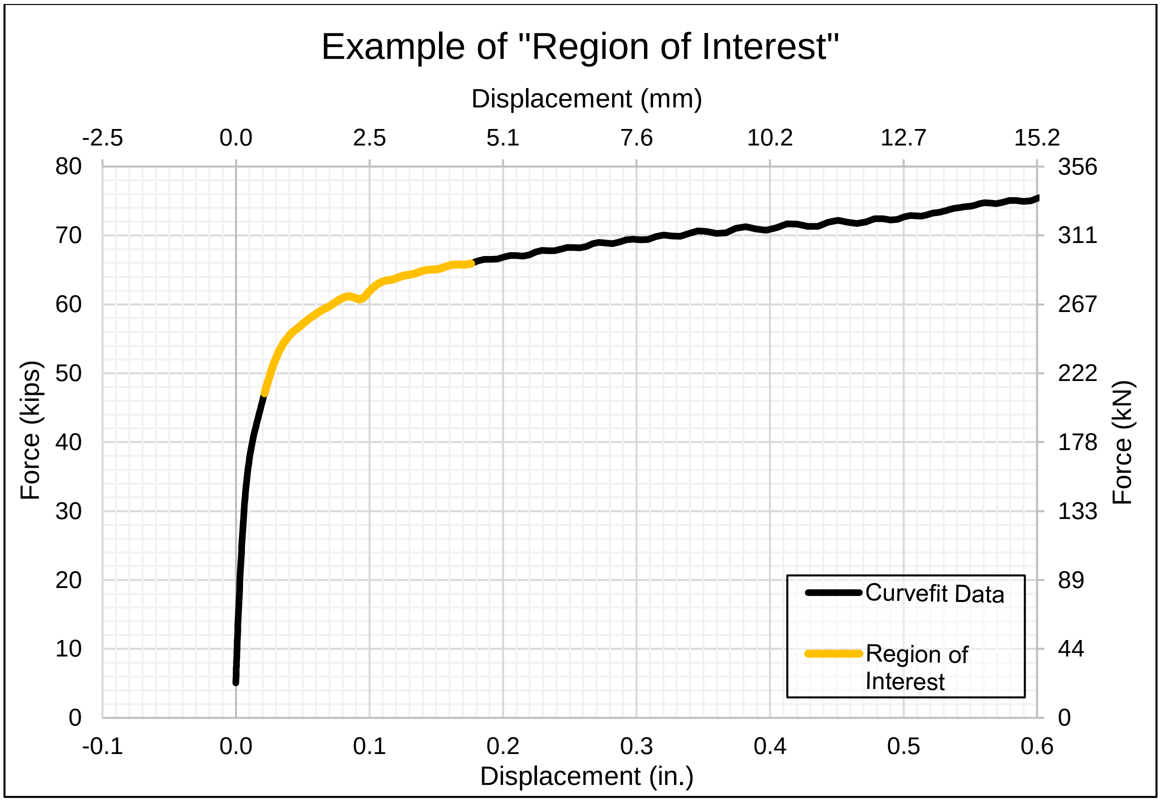

Figure 5.3.3-1: Explanation of "Region of Interest".

To find the location at which the specimen had accumulated significant loss of stiffness, a simple percent difference calculation was used to find the point of maximum rate of change in the curve-fit data. The percent difference at any step, *i*, was calculated as:

$$C_i = \frac{m_{i-1} - m_i}{m_{i-1}} \tag{5.3-1}$$

where

$$m_i = \frac{\Delta P_i}{\Delta D_i} \quad , \tag{5.3-2}$$

$$\Delta P_i = P_i - P_{i-1} \quad , \tag{5.3-3}$$

$$\Delta D_i = D_i - D_{i-1} \quad , \tag{5.3-4}$$

P_i = load at step *i*, kip (kN),

D_i = displacement at step *i*, in. (mm).

This calculation yields the percent difference in the slope to one data point from the previous data point. Determining where this value is at a maximum indicates where the connection saw the peak rate of reduction in stiffness and is where the connection is determined to have failed.

However, even after filtering and fitting a curve to the data, there were still some bumps and jogs that caused the maximum percent difference to correlate to a connection capacity that did not make any sense. This is where the "region of interest" helped. The connection capacity was determined by finding the maximum percent difference within the "region of interest." Manually limiting the range that the maximum capacity could fall in allowed the method to be applied consistently across all the tests.

5.4 Tested Capacities

Table 5.4-1 provides a summary of the tested capacity for each specimen. The following plots in Figure 5.4-1 through Figure 5.4-20 help visualize the analyzed data and tested capacity. The axis limits for all the plots are the same to allow the reader to easily compare them. Each plot shows the raw data, prefiltered data, curve-fit data, expected capacity, and tested capacity. The raw data and prefiltered data lay directly on top of one another. The locations where the raw data curve can be seen indicates data points that were removed from the data set during the manual prefiltering operation.

Table 5.4-1: Tested Capacities for Each Experimental Specimen.

Test ID	**Tested Capacity**
	kip (kN)
S30P100	45.7 (203)
S35P100	54.7 (244)
S40P100	68.4 (304)
S45P100	68.7 (306)
S30P075	51.1 (227)
S35P075	55.3 (246)
S40P075	65.8 (293)
S45P075	76.0 (338)
S30P050	53.1 (236)
S35P050	63.1 (281)
S40P050	72.1 (321)
S45P050	84.1 (374)
S30P025	60.2 (268)
S35P025	72.8 (324)
S40P025	81.1 (362)
S45P025	86.9 (386
S30P000	76.8 (342)
S35P000	79.4 (353)
S40P000	91.4 (407)
S45P000	--- (---)*
*A tested capacity for specimen S45P000 could not be determined because the specimen was not loaded high enough to turn the load versus displacement plot over definitively.	

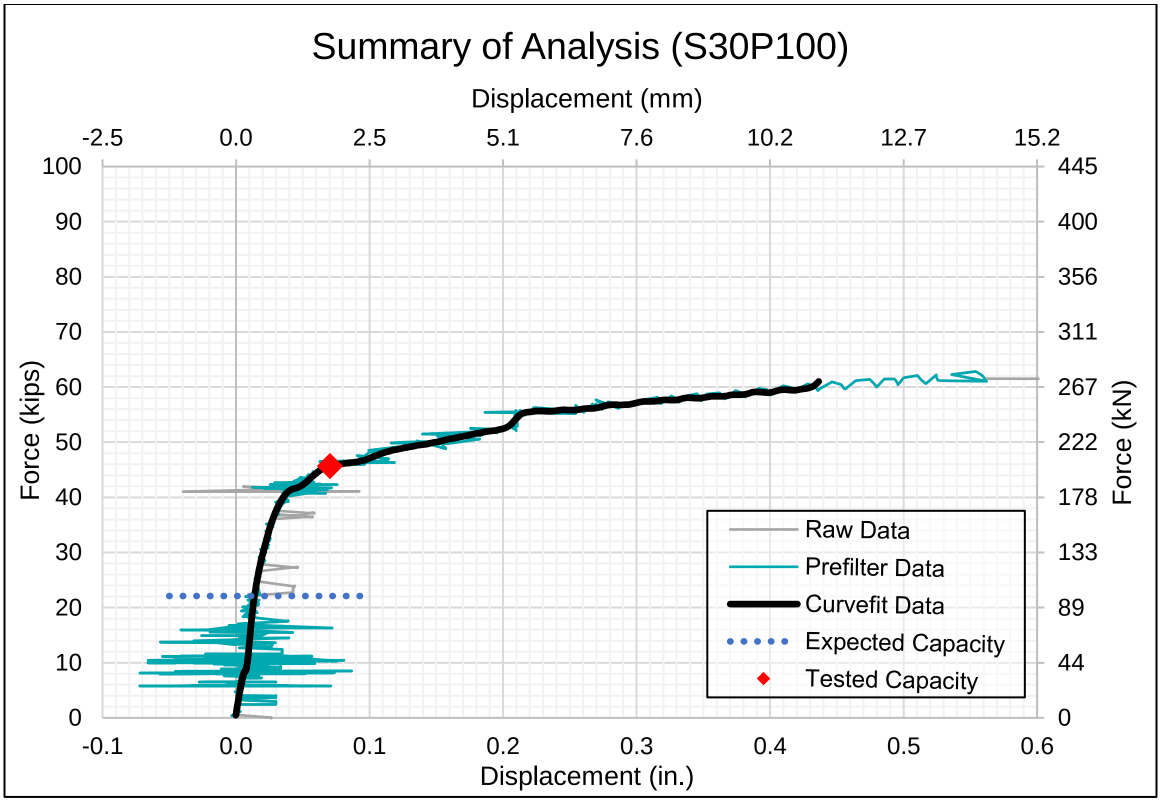

Figure 5.4-1: Load Versus Specimen Displacement for Specimen S30P100.

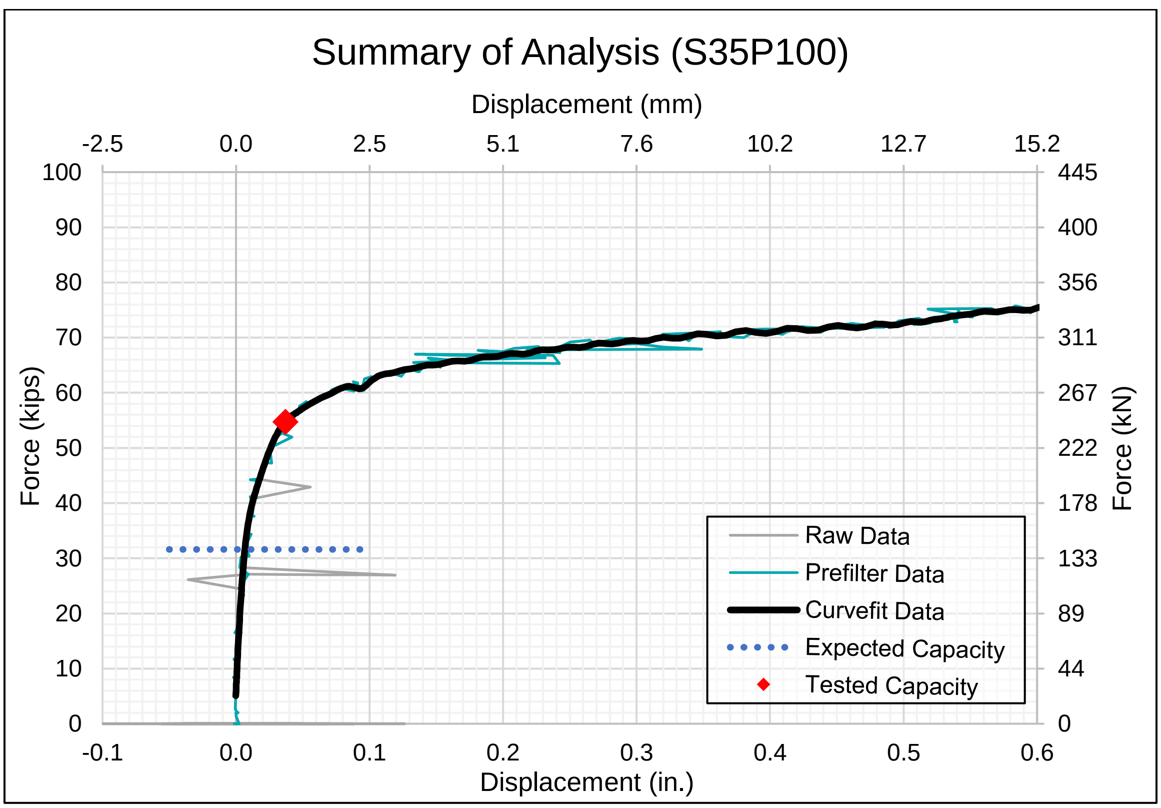

Figure 5.4-2: Load Versus Specimen Displacement for Specimen S35P100.

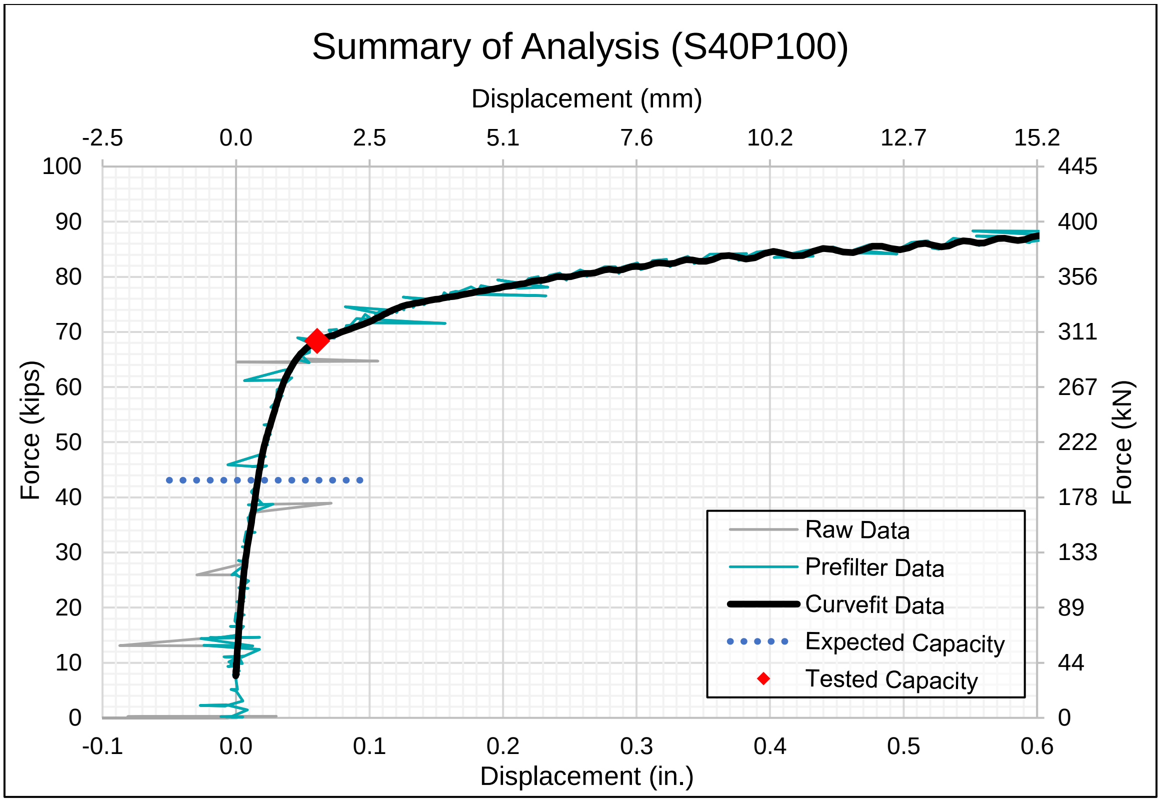

Figure 5.4-3: Load Versus Specimen Displacement for Specimen S40P100.

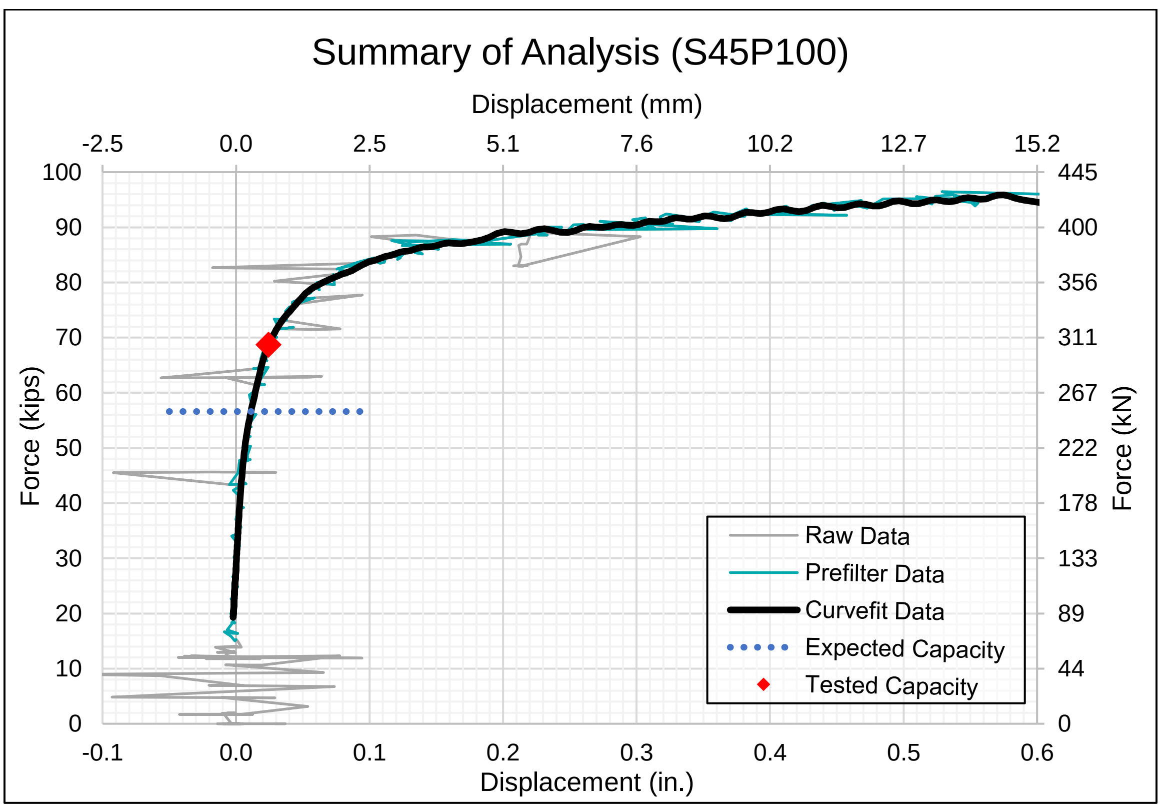

Figure 5.4-4: Load Versus Specimen Displacement for Specimen S45P100.

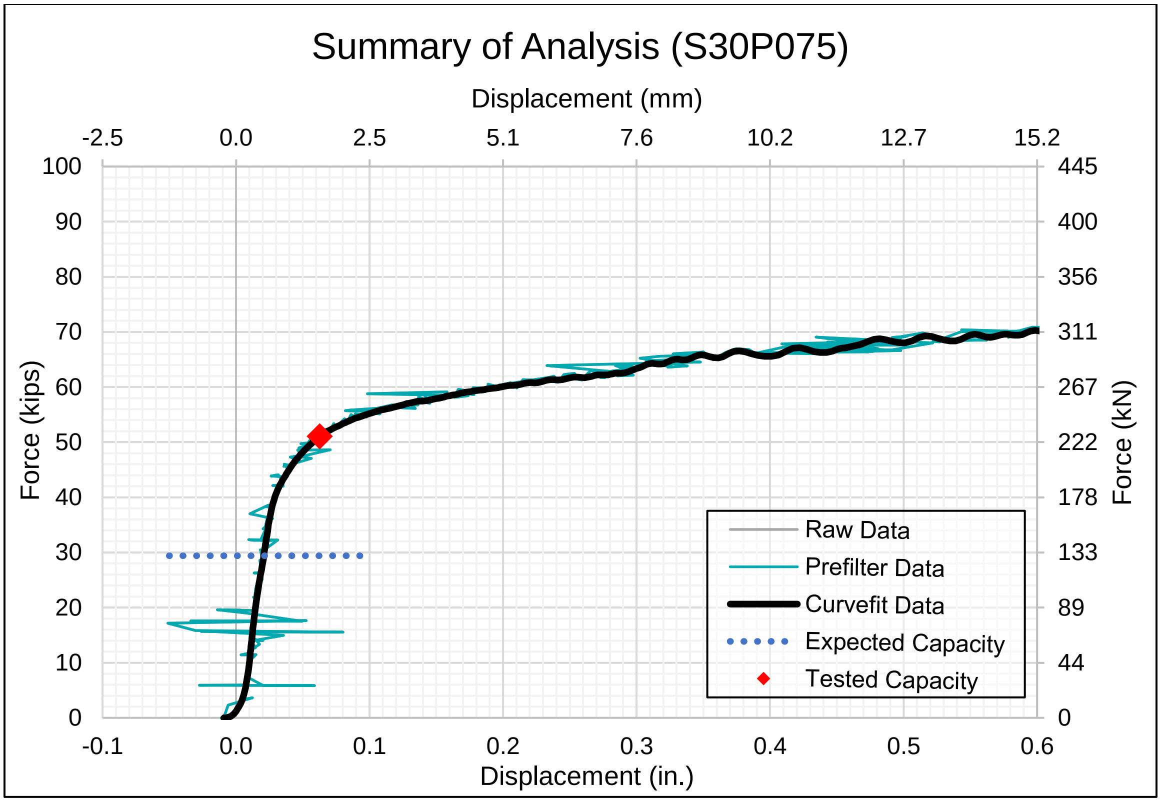

Figure 5.4-5: Load Versus Specimen Displacement for Specimen S30P075.

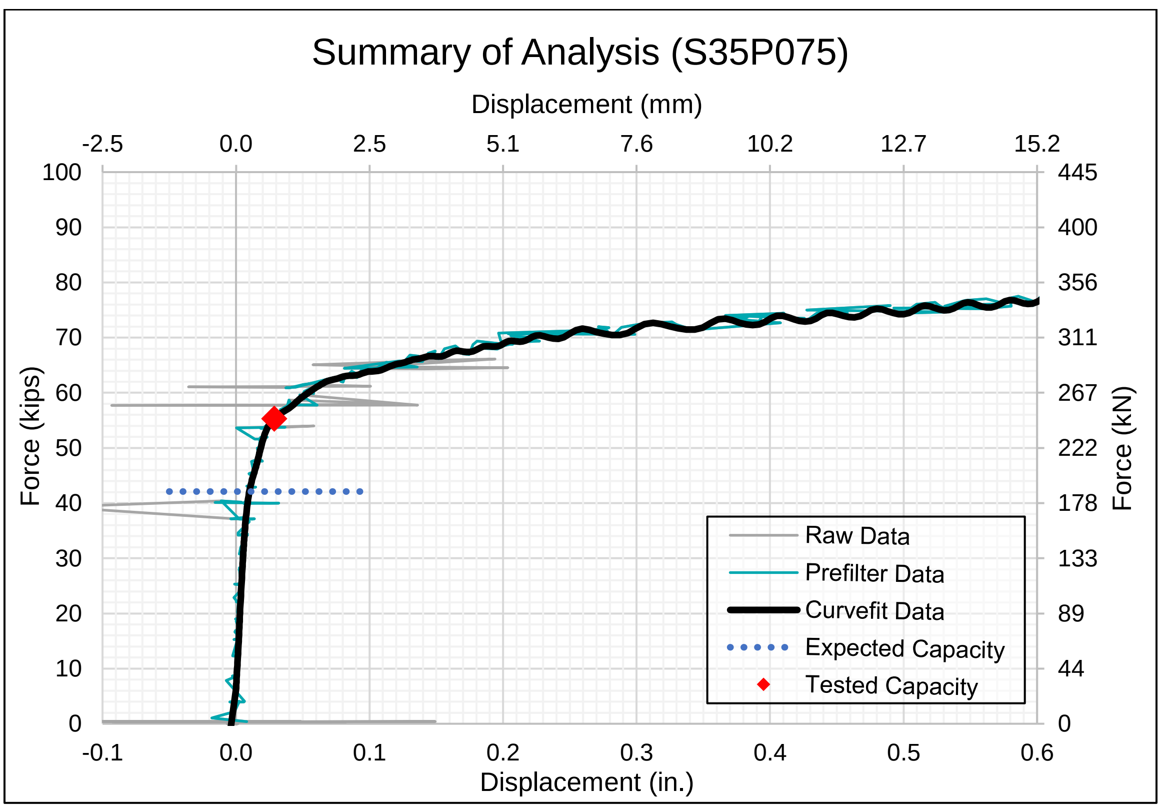

Figure 5.4-6: Load Versus Specimen Displacement for Specimen S35P075.

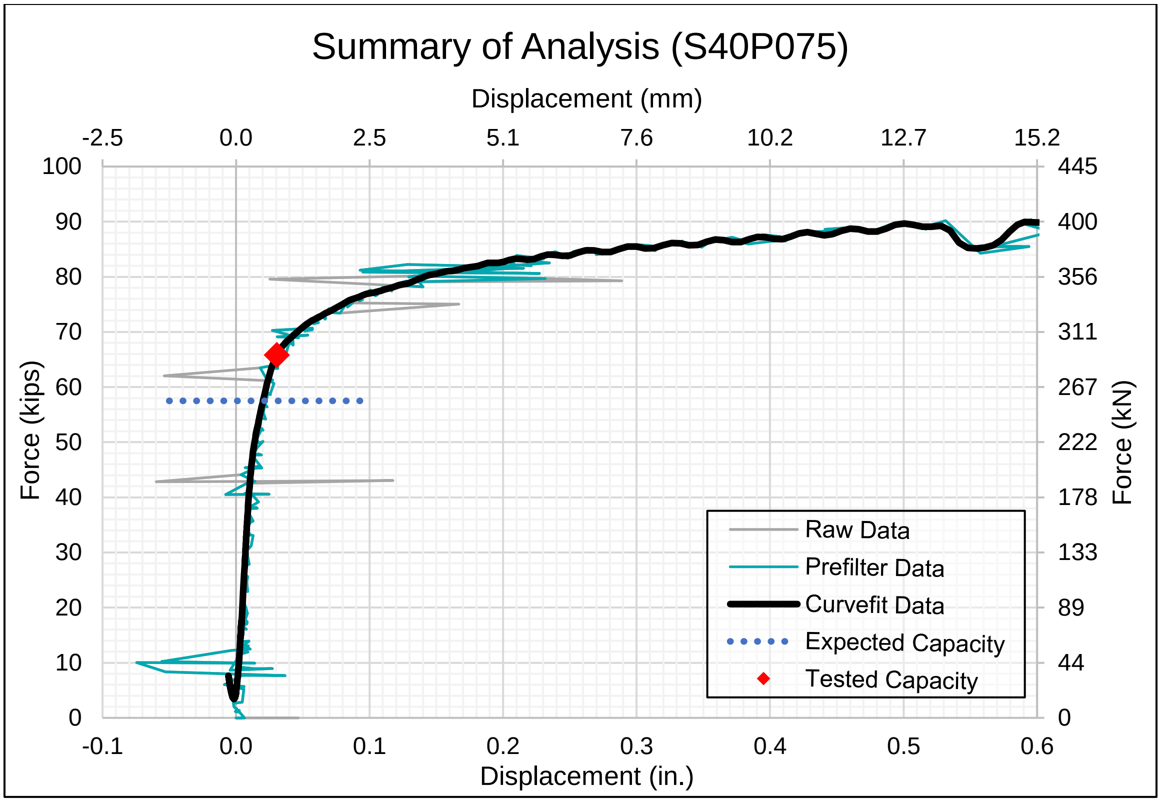

Figure 5.4-7: Load Versus Specimen Displacement for Specimen S40P075.

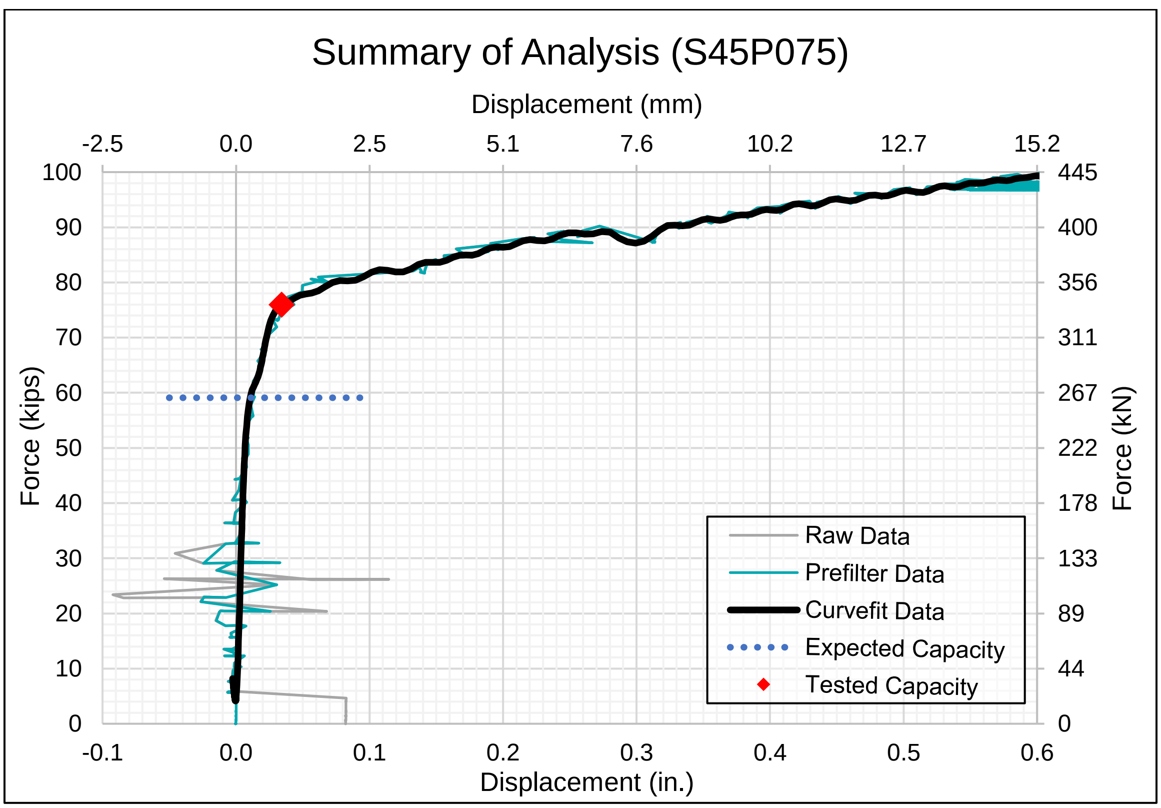

Figure 5.4-8: Load Versus Specimen Displacement for Specimen S45P075.

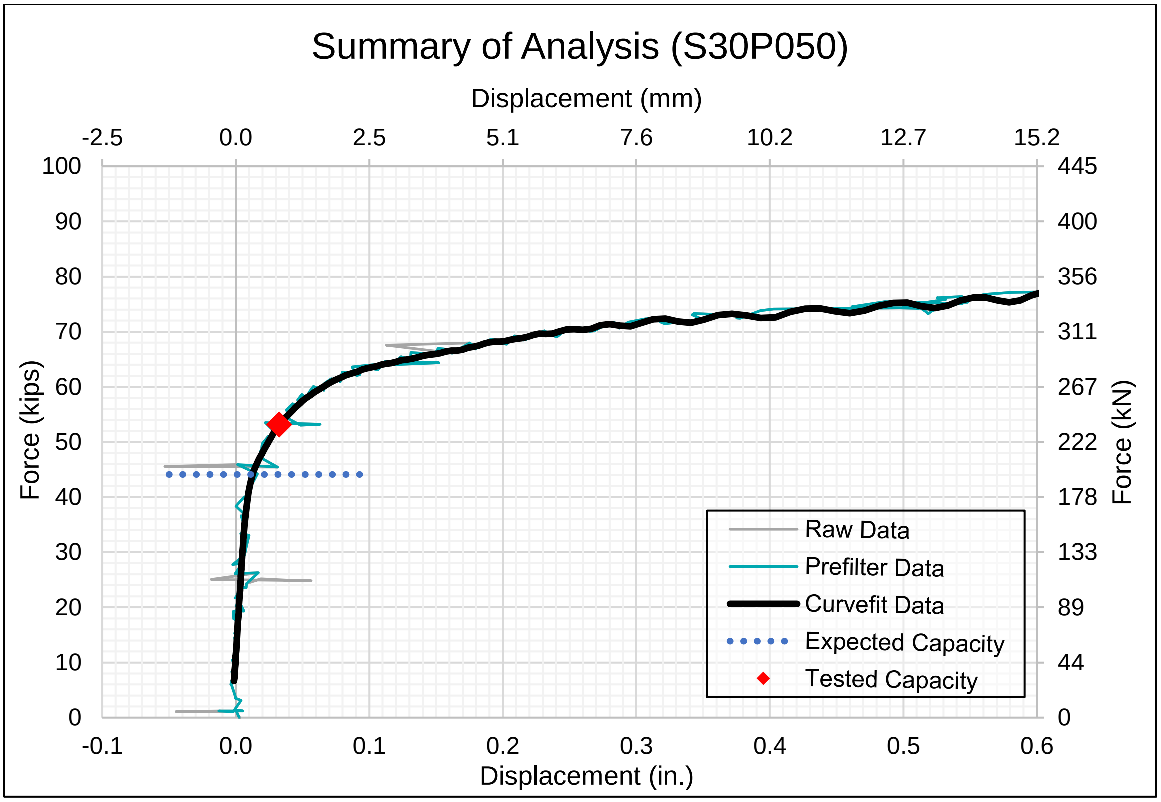

Figure 5.4-9: Load Versus Specimen Displacement for Specimen S30P050.

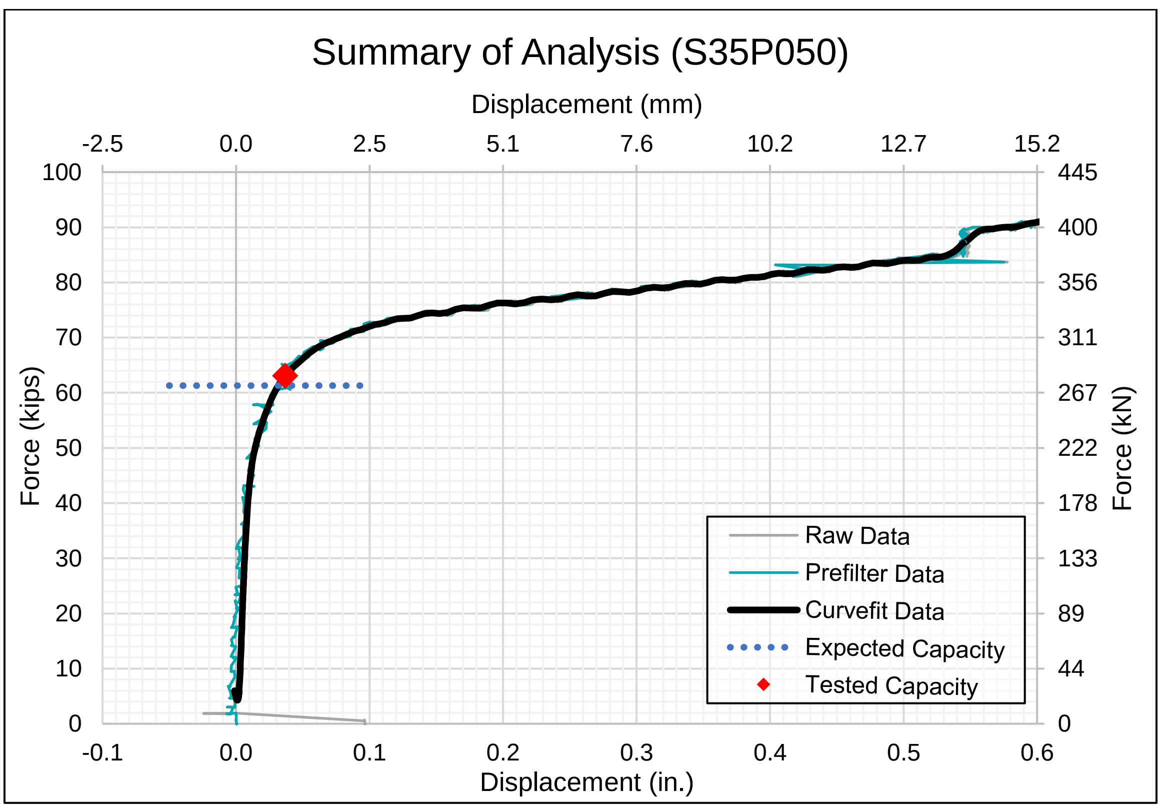

Figure 5.4-10: Load Versus Specimen Displacement for Specimen S35P050.

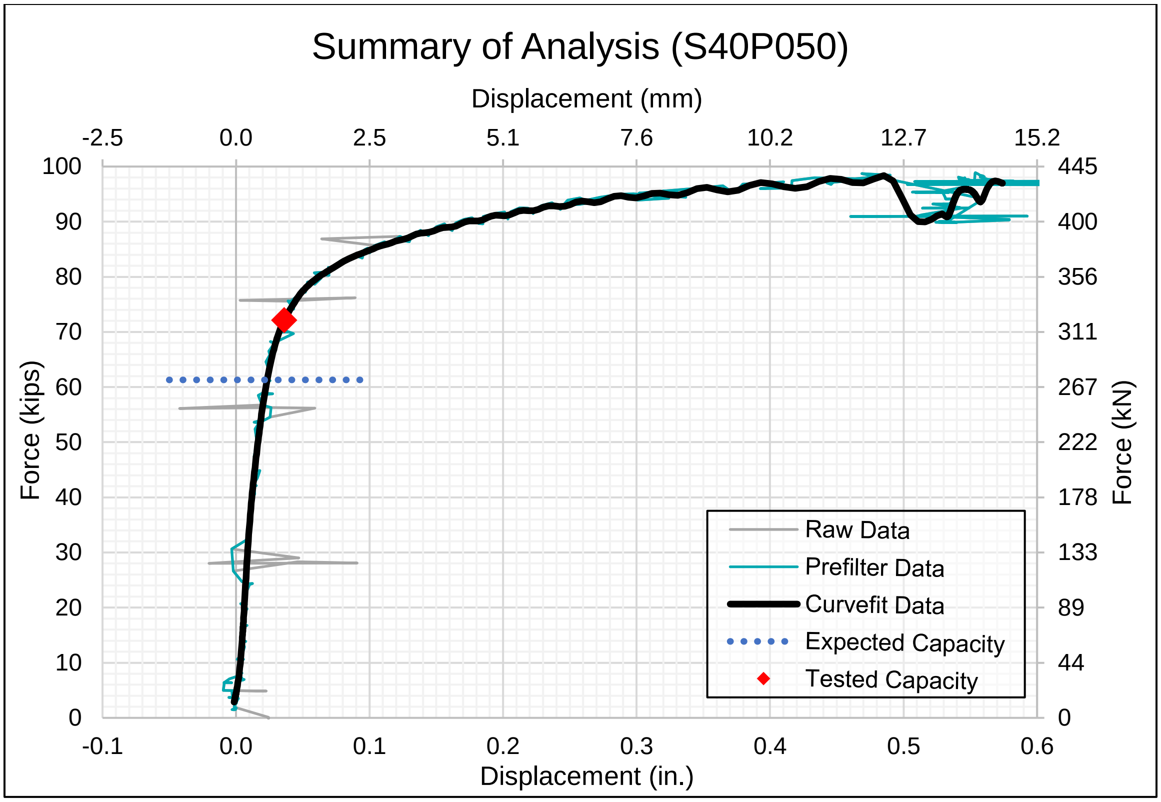

Figure 5.4-11: Load Versus Specimen Displacement for Specimen S40P050.

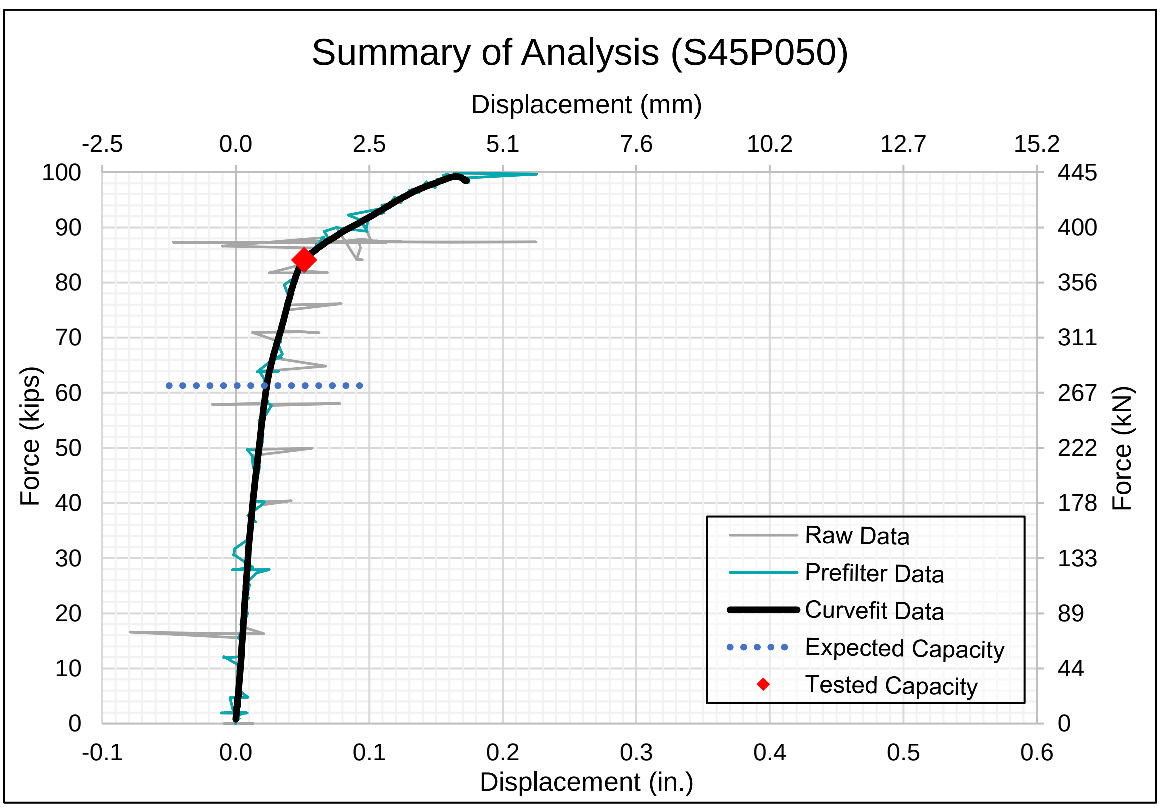

Figure 5.4-12: Load Versus Specimen Displacement for Specimen S45P050.

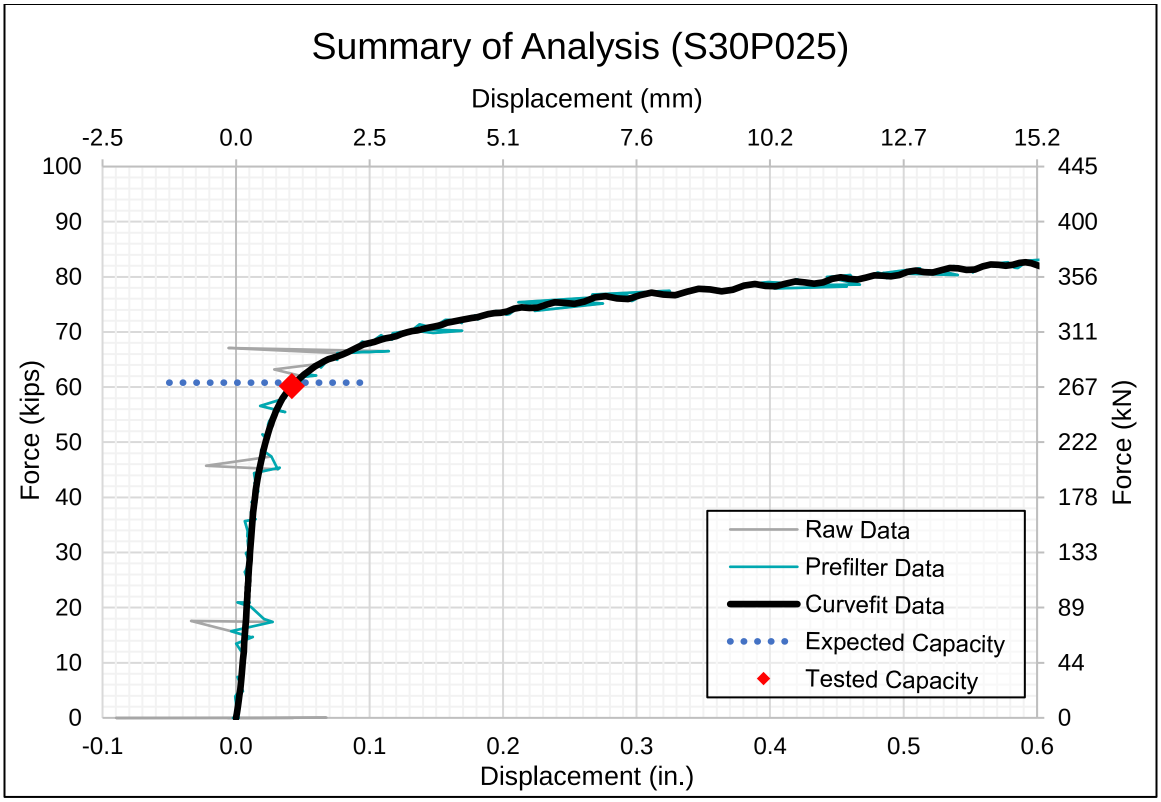

Figure 5.4-13: Load Versus Specimen Displacement for Specimen S30P025.

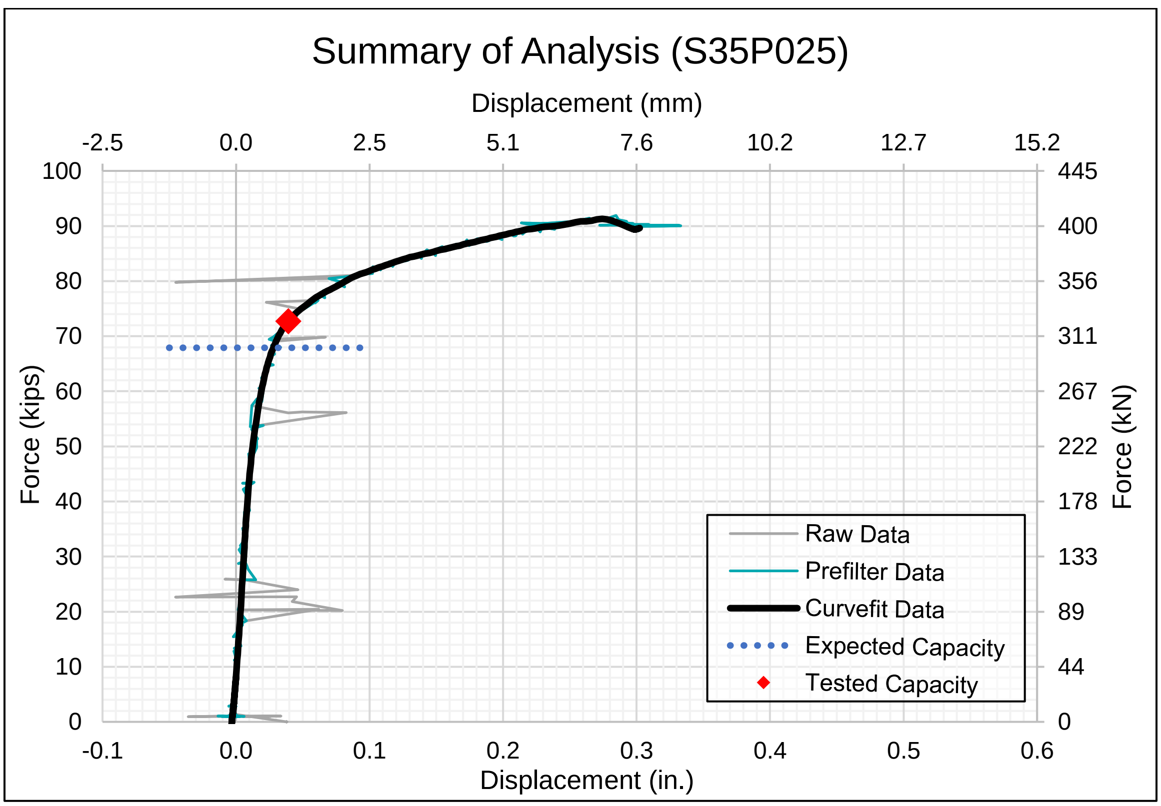

Figure 5.4-14: Load Versus Specimen Displacement for Specimen S35P025.

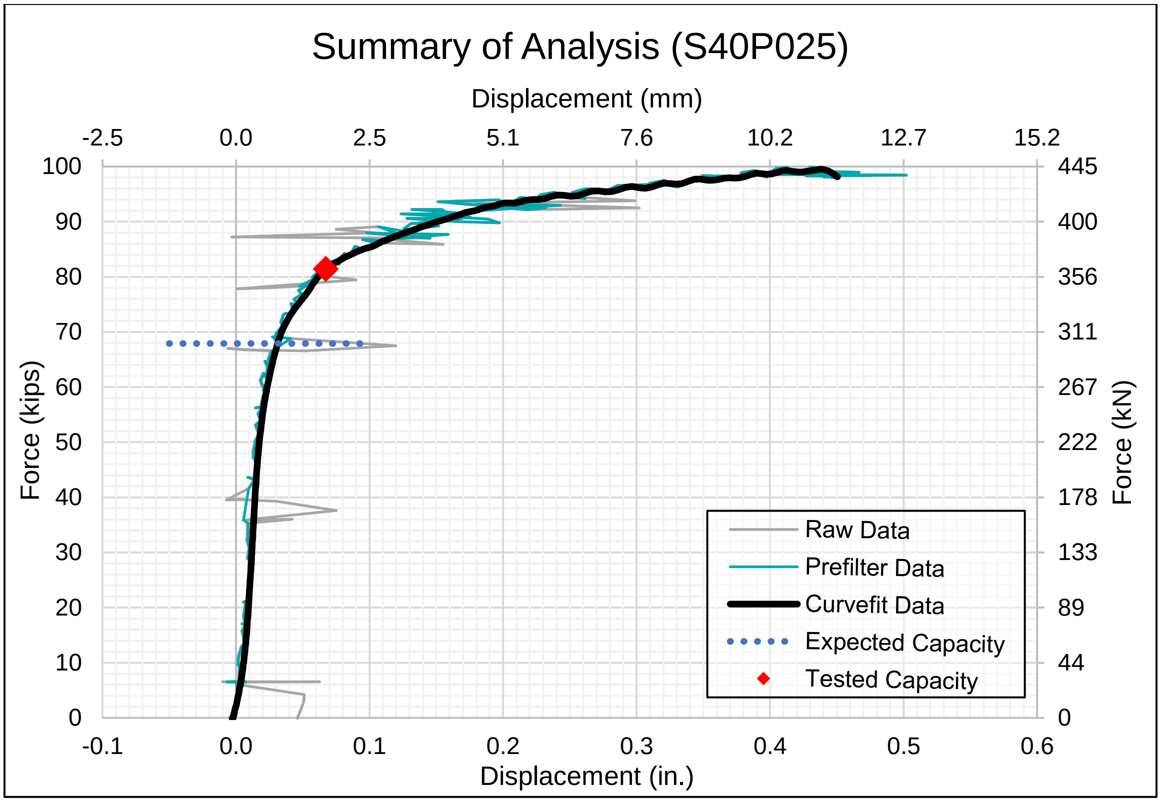

Figure 5.4-15: Load Versus Specimen Displacement for Specimen S40P025.

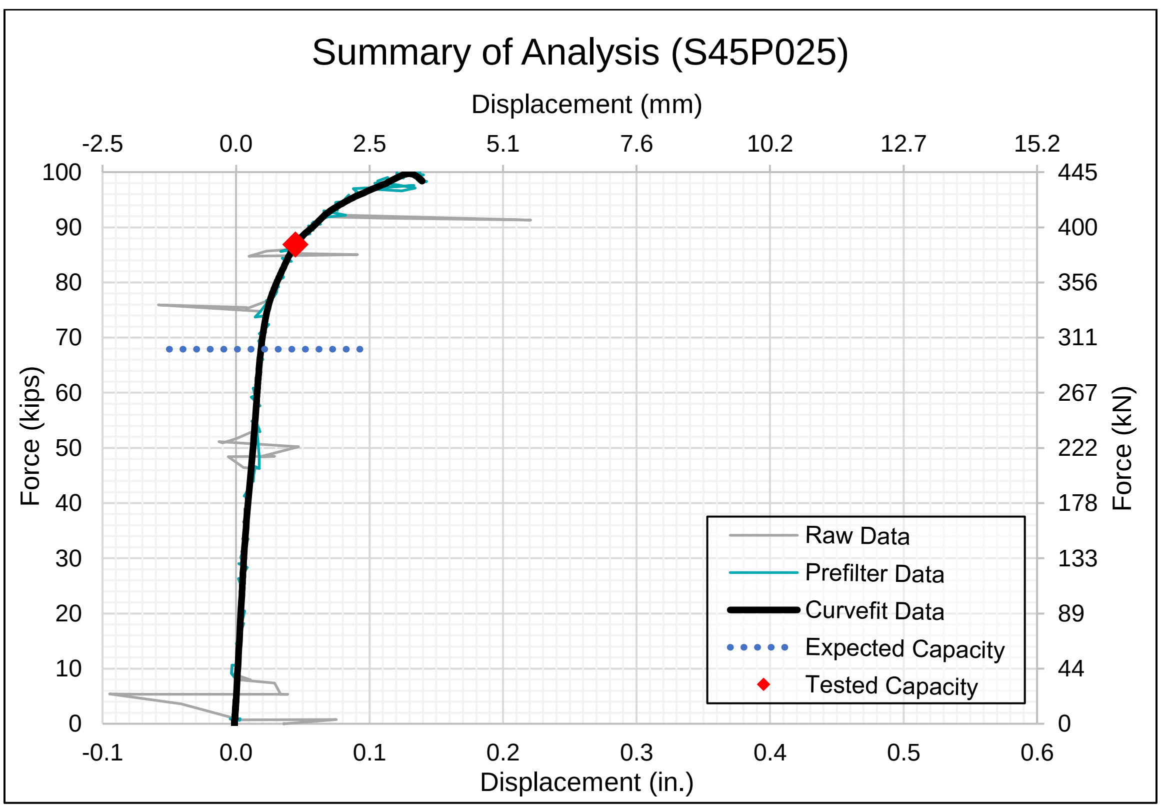

Figure 5.4-16: Load Versus Specimen Displacement for Specimen S45P025.

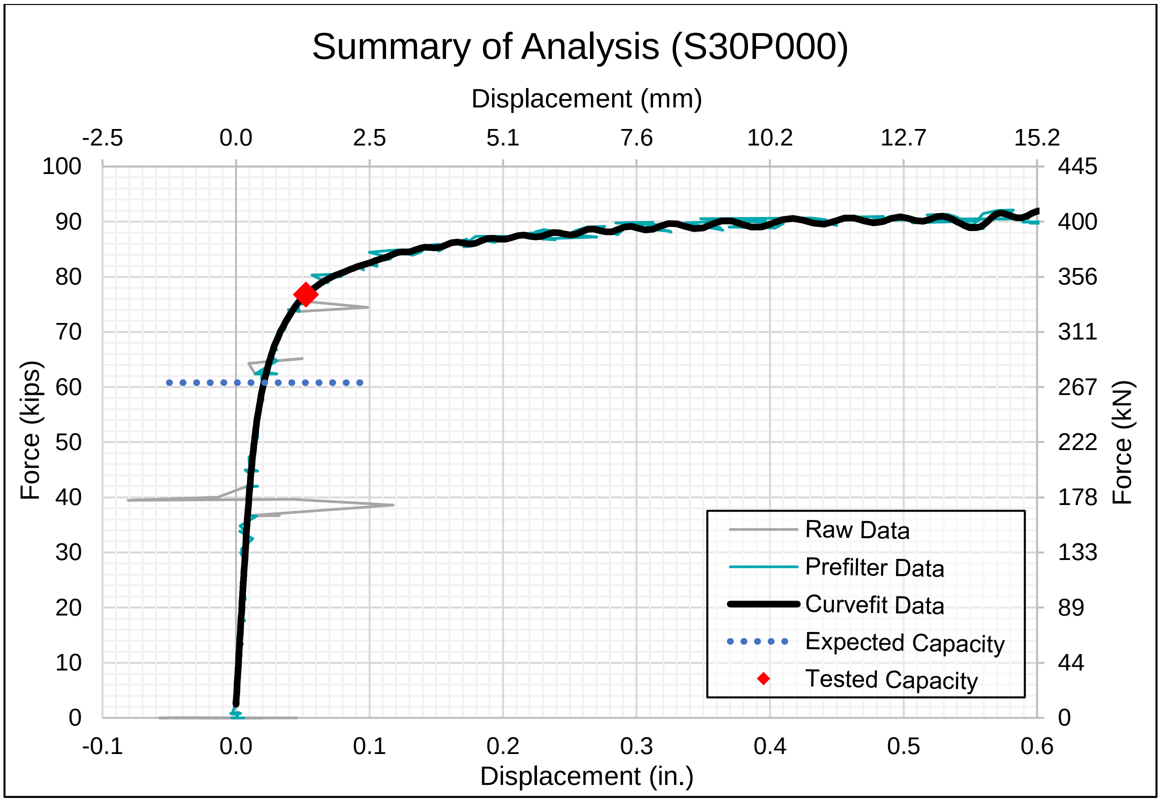

Figure 5.4-17: Load Versus Specimen Displacement for Specimen S30P000.

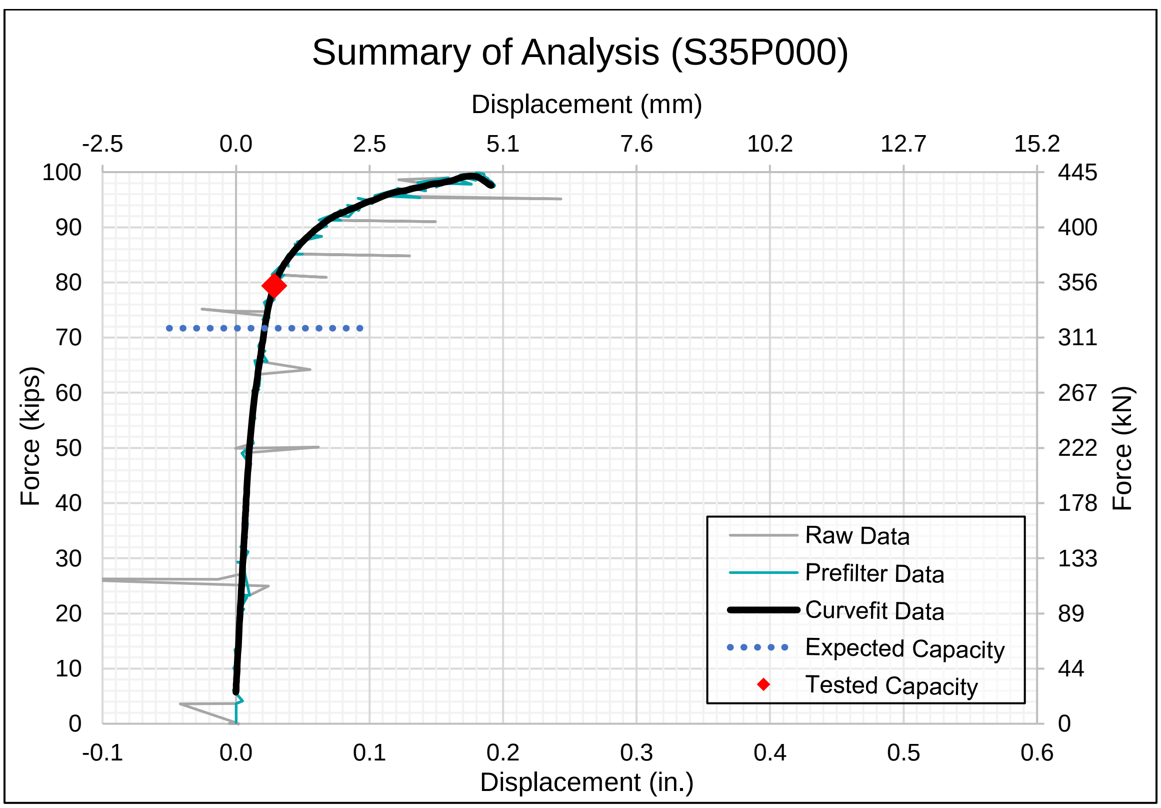

Figure 5.4-18: Load Versus Specimen Displacement for Specimen S35P000.

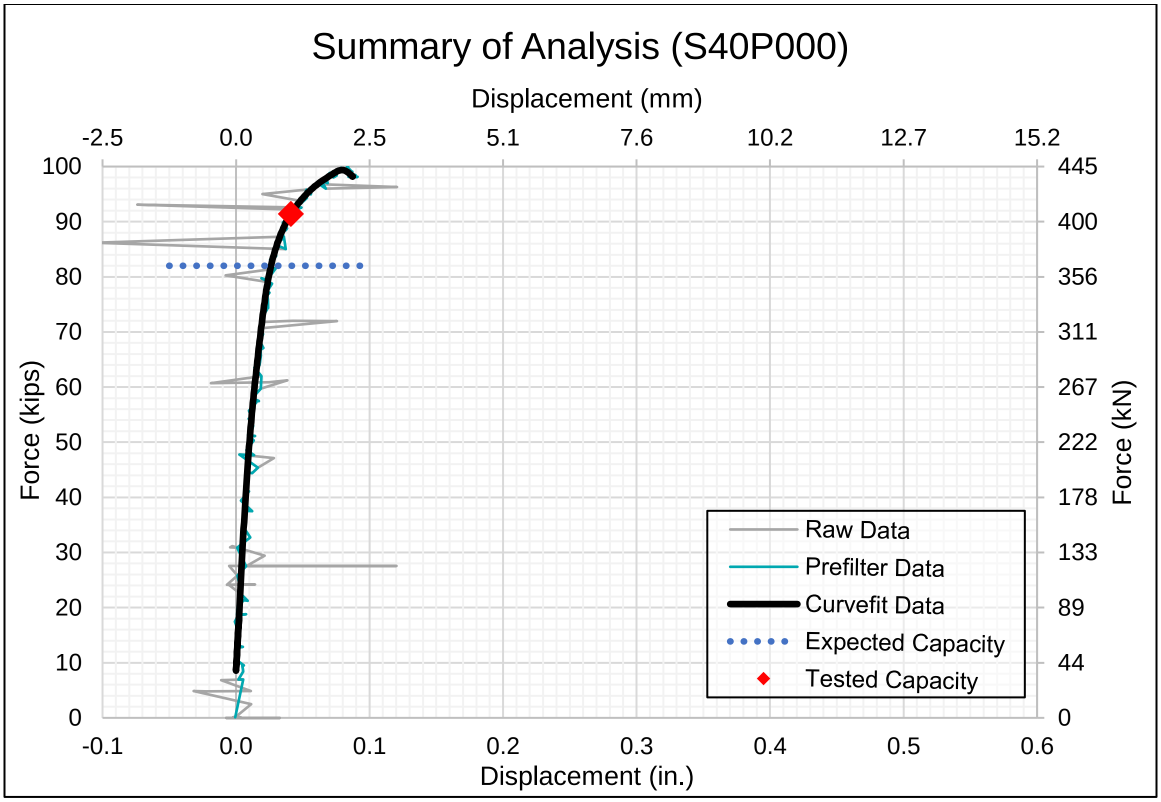

Figure 5.4-19: Load Versus Specimen Displacement for Specimen S40P000.

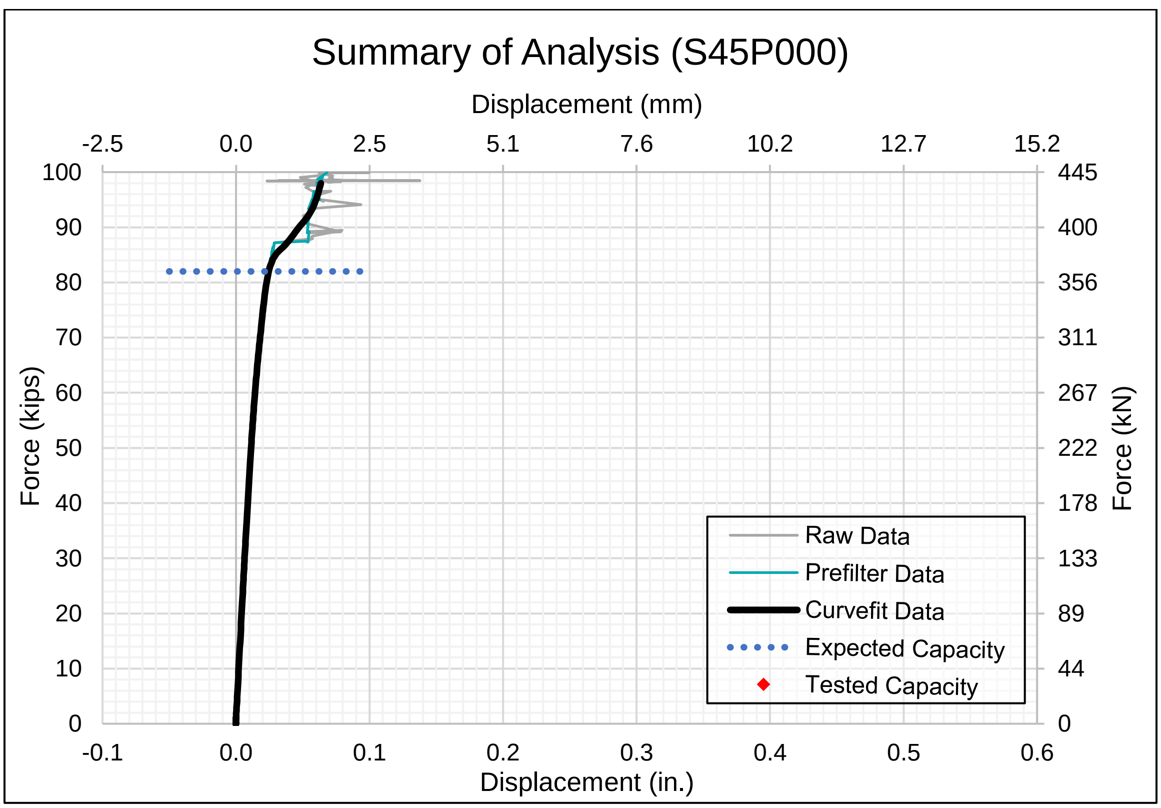

Figure 5.4-20: Load Versus Specimen Displacement for Specimen S45P000.

5.5 Comparison of Expected Capacities and Tested Capacities

Nearly every test in this experimental program exceeded the expected capacity. Table 5.5-1 provides a summary of the expected capacity, tested capacity, and percent difference for each test. A positive percent difference indicates the tested capacity exceeded the expected capacity. Table 5.5-2 shows the percent differences from Table 5.5-1 along with the observed specimen behaviors from Table 4.1-1.

Table 5.5-1: Comparison of Expected and Tested Capacity for Each Specimen.

Test ID	Expected Capacity	Tested Capacity	Percent Difference
	kip (kN)	*kip (kN)*	
S30P100	22.1 (98.1)	45.7 (203)	107%
S35P100	31.6 (141)	54.7 (244)	73.2%
S40P100	43.1 (192)	68.4 (304)	58.6%
S45P100	56.6 (252)	68.7 (306)	21.5%
S30P075	29.4 (131)	51.1 (227)	73.8%
S35P075	42.1 (187)	55.3 (246)	31.4%
S40P075	57.5 (256)	65.8 (293)	14.4%
S45P075	59.1 (263)	76.0 (338)	28.6%
S30P050	44.1 (196)	53.1 (236)	20.5%
S35P050	61.3 (273)	63.1 (281)	2.98%
S40P050	61.3 (273)	72.1 (321)	17.7%
S45P050	61.3 (273)	84.1 (374)	37.2%
S30P025	60.8 (270)	60.2 (268)	-1.01%
S35P025	67.9 (302)	72.8 (324)	7.15%
S40P025	67.9 (302)	81.1 (362)	19.9%
S45P025	67.9 (302)	86.9 (386	28.0%
S30P000	60.8 (270)	76.8 (342)	26.3%
S35P000	71.7 (319)	79.4 (353)	10.7%
S40P000	82.0 (365)	91.4 (407)	11.5%
S45P000	82.0 (365)	--- (---)	N/A

Table 5.5-2: Percent Differences, Expected Failure Mode, and Observed Behaviors.

Test ID	Percent Difference	Expected Failure Mode	Observed Plate Flexure	Observed Bolt Bearing
S30P100	107%	Bolt Plate Flexure	Moderate	Minimal
S35P100	73.2%	Bolt Plate Flexure	Significant	Moderate
S40P100	58.6%	Bolt Plate Flexure	Moderate	Minimal
S45P100	21.5%	Bolt Plate Flexure	Moderate	Moderate
S30P075	73.8%	Bolt Plate Flexure	Significant	Minimal
S35P075	31.4%	Bolt Plate Flexure	Extreme	Significant
S40P075	14.4%	Bolt Plate Flexure	Moderate	Moderate
S45P075	28.6%	Bolt Bearing/Bolt Plate Flexure	Moderate	Moderate
S30P050	20.5%	Bolt Plate Flexure	Extreme	Extreme
S35P050	2.98%	Bolt Bearing/Bolt Plate Flexure	Significant	Moderate
S40P050	17.7%	Bolt Bearing/Bolt Plate Flexure	Moderate	Moderate
S45P050	37.2%	Bolt Bearing/Bolt Plate Flexure	Minimal	Moderate
S30P025	-1.01%	Plate Shear Rupture	Extreme	Extreme
S35P025	7.15%	Bolt Bearing/Bolt Plate Flexure	Moderate	Moderate
S40P025	19.9%	Bolt Bearing/Bolt Plate Flexure	Moderate	Significant
S45P025	28.0%	Bolt Bearing/Bolt Plate Flexure	Minimal	Significant
S30P000	26.3%	Plate Shear Rupture	Significant	Extreme
S35P000	10.7%	Plate Shear Rupture	Minimal	Significant
S40P000	11.5%	Bolt Bearing	Minimal	Significant
S45P000	N/A	Bolt Bearing	Minimal	Significant

There is large variation in the percent difference between expected and tested capacities for these specimens. As mentioned previously in Section 4.1, it was not possible to determine the first failure mode of the specimens because the sandwich plates blocked the view of the slots during the test. As such, the specimen may have reached a limit state, such as bolt bearing, prior to the load versus displacement plot showing significant reduction in connection stiffness. The data from LVDT 1 may not have captured this other limit state fully and resulted in a higher tested capacity.

There are no observable trends between the slot spacing and percent difference. A trend here could indicate the calculation for the expected capacity was appropriate for the specimens. Because there is no trend, a different method of determining the expected capacity should be investigated. However, the method used in this research initiative is relatively conservative still and considers additional limit states that are not directly prescribed by the AISC *Specification*, resulting in a design that an engineer can be comfortable using.

Table 5.5-2 does show a slight correlation between observed specimen behavior and percent difference. The specimens that saw “Significant” or “Extreme” observed bolt bearing generally have a lower percent difference compared to those with “Minimal” or “Moderate” observed bolt bearing. This correlation could be because there is a better understanding of bolt bearing failures and the flexural failure observed was not accurately predicted by the expected capacity calculation. This may also indicate that a different method of determining the expected capacity should be investigated.

Overall, the tested capacity versus slot spacing plot, shown in Figure 5.5-1, yields a strong trend that indicates increasing the slot spacing increases the connection capacity, even if the exact failure mode is unknown. This plot shows the tested capacity for all the specimens except S45P000, which did not have a determined tested capacity. This conclusion supports the hypothesis presented in Section 3.2. Recommendations for the continuation of this work will be presented in the next chapter.

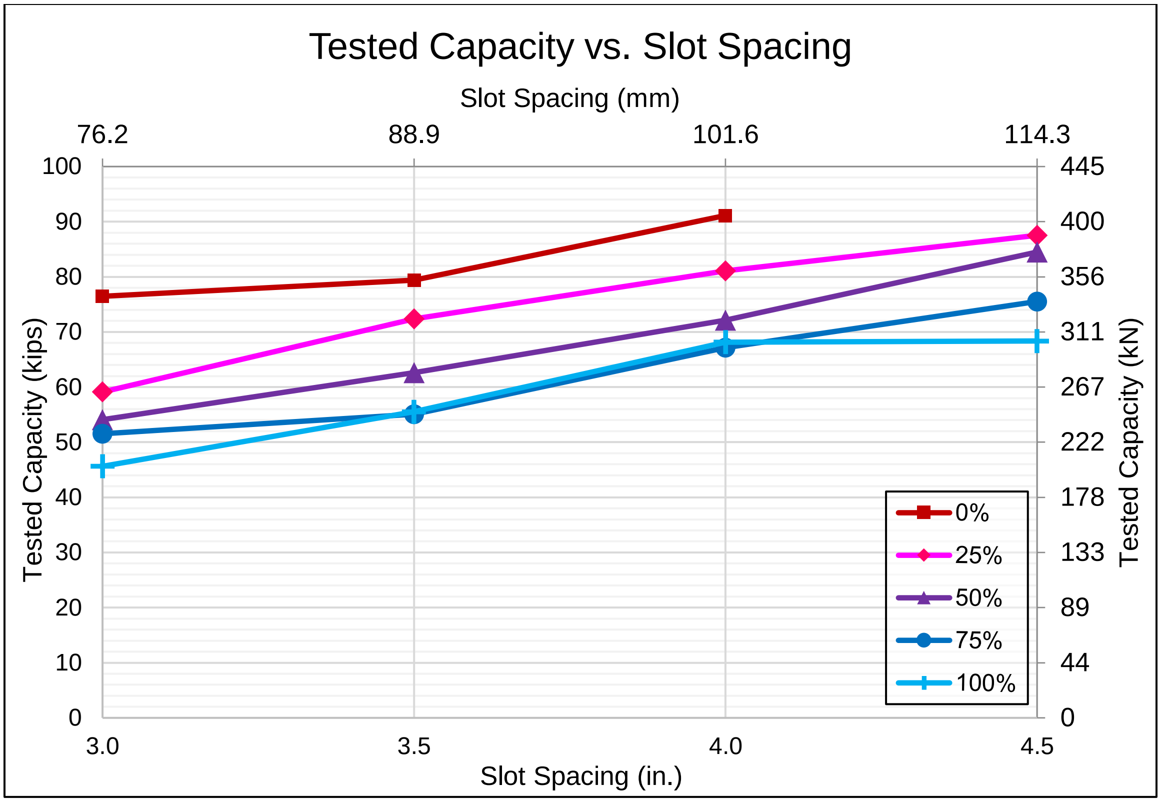

Figure 5.5-1: Tested Capacity Versus Slot Spacing.

Chapter 6: Discussion and Conclusions

6.1 Discussion of Experimental Instrumentation and Procedure

The experimental instrumentation and procedure as described in Sections 3.8 and 3.10 respectively were adequate for determining the effect of slot spacing in this connection. However, as the experimental procedure was carried out, a few things were noted that could be improved or changed in future testing.

6.1.1 Specimen Anchorage Improvements

The slip-critical connection worked well for anchoring the specimen in the setup if the specimen was “pre-slipped” as described in Section 3.5. However, an alternate method of holding the specimen down may leave less room for problems. Welding the specimen into the setup or clamping it in some fashion may eliminate the potential for it to slip as high loads are applied. If the slip-critical connection is still desired, achieving the proper surface preparation would also help achieve the required resistance.

6.1.2 Removal of One Sandwich Plate

Because there was a sandwich plate on both sides of the specimen, it was impossible to see the behavior of the specimen as the test progressed. One way to be able to observe the specimen would be to remove the sandwich plate from one side of the connection. Doing this would add some inherent moment to the connection, although this condition would be more reflective of the true condition this connection would see and would not necessarily drastically affect the results.

6.1.3 Experimental Setup of Connection

Another change that could benefit the research of this connection would be testing the specimens in a more common configuration. This experimental program sought to investigate the single variable of slot spacing and as such, had an experimental setup that intentionally isolated that variable. To gain a better understanding of how this connection behaves in practical applications, a revised test setup that rotates the connection so it is vertical and uses a beam instead of sandwich plates may provide a better understanding of the behavior of the connection as a whole.

6.1.4 Additional Displacement Measurement

As previously discussed in Section 5.5, the true failure mode of the specimen was unable to be determined for the specimens. One option to potentially gain some insight into the behavior of the specimen plate would be to add a horizontal LVDT to the end of one of the sandwich plates to be able to see the displacement of the bolts relative to the corner of the specimen. If these displacements were equal for the duration of the test, it would indicate that plate flexure is the primary failure mode. If the sandwich plates move before the specimen plate does, that would indicate the bolts have engaged in bearing in the plate prior to a flexural failure of the plate.

6.1.5 Alternate Rosette Location

The rosette data from the specimens in this experimental program did not aid in understanding the behavior of the connection. As such, in future research programs, the rosettes should be placed in different locations on the specimens. Also, using more rosettes may provide a better understanding of the behavior of the plate. An inelastic finite element model of the specimen, discussed further in Section 6.2.3, could be useful in determining where the rosettes should be placed to adequately capture the behavior of the specimen.

6.2 Recommendations for Future Work

After completing the analysis for this experimental program, thought was given to the limits of the completed research and what should be investigated in future experimental and analytical research initiatives to further the body of knowledge on this connection.

6.2.1 Varied Specimen Properties

The specimens in this experimental program were limited in size and dimensions by the equipment available in the testing laboratory. Future work should expand on the specimen group investigated in this capstone project to specimens with thicker plates, different edge distances, and more rows of bolts. Thicker plates would be a better representation of the connections used in practice – $^{1}/_{4}$ in. (6mm) plate is a thin plate to use in this connection. Adding bolt rows would also reflect real-world practices for this connection in applications with deeper beams. Also, adding more bolt rows could change the distribution of load and thus the overall behavior of the connection. Lastly, the distance to the loaded edge of the specimen plate was the same for every specimen in this experimental program. By increasing the end distance, the bottom bolt should gain strength and add capacity to the connection according to the calculations used in this report. It is possible that a way to make this connection stronger would be to simply add plate material below the bottom bolt.

Another parameter that could be changed is the slot length. Longer slots would not necessarily be needed in the example of an embed plate in a concrete wall, but there could be another situation that would require a single plate connection with longer slots.

6.2.2 Determine Behavior Model for Slots

The calculations used to determine the expected capacity for each specimen in this experimental program did not accurately predict the results of the analysis. As such, more investigation should go into determining a more accurate model for the slot behavior. One possible option for this model, based on the observed specimen behavior, would be to analyze the remaining material between the slots and at the edges of the plate as a frame. Because the top edge of the specimens did not deform, it appears that the top edge resists the rotation at the end of the material remaining between the slots. Another option would be to consider each slot individually as a fixed end beam that does not allow rotation at the end and determine a capacity like the procedure in the calculations in the report. However, this would produce higher capacities than were already seen, so further exploration would be required to determine if a different length should be considered as the span or a different cross section should be considered to resist the load.

6.2.3 Inelastic Finite Element Model

Another need for future research is creating and analyzing a series of inelastic finite element models of these connections. A set of parametric models that reflect the specimens in this study would be a good place to start as displacement and strain data from this experimental program can be used to calibrate the model and validate the results. Then additional models with varying dimensions and parameters, like plate thickness, number of slots, and end distances, can be analyzed. The goal of this analytical work would be to limit the need for experimental tests as well as gain insight into the connection that cannot be easily obtained through experimental testing. These models could provide insight into the specimen behavior and help determine what behavior model is most appropriate for the connection – cantilevered beam, frame, etc.

6.3 Conclusions

This experimental research initiative marks the start of an investigation into single plate connections with long slots. The results of the experiments conducted as part of this research initiative yield a strong trend that indicates increasing the slot spacing increases the connection capacity, even if the exact failure mode is unknown. The results also provide valuable insight into the behaviors of this connection.

Investigating a frame model to determine the flexural capacity of this connection would be the best next step based on the results of the experiments conducted in this research initiative. The observed specimen behavior strongly suggests that the slots act together in some fashion and that they should be analyzed together.

Additionally, the insight into what changes should be made to the experimental design should help future research initiatives overcome some of the issues faced in this experimental program. These connections are common and understanding how they behave is critical to designing them safely and economically.

References

American Concrete Institute (ACI). (2010). *Specification for Tolerance of Concrete Construction and Materials*. ACI 117-10. American Concrete Institute. Farmington Hills, Michigan.

American Institute of Steel Construction (AISC). (2016a). *Code of Standard Practice for Steel Buildings and Bridges*. ANSI/AISC 303-16. American Institute of Steel Construction. Chicago, Illinois.

American Institute of Steel Construction (AISC). (2016b). *Specification for Structural Steel Buildings*. ANSI/AISC 360-16. American Institute of Steel Construction. Chicago, Illinois.

Jackson, C. (2021). *Effects of Bolt Position within Long Slots on Extended Single Plate Connections*. Master of Science in Structural Engineering (MSAE) Capstone Report, Milwaukee School of Engineering.

Man, J. C. Y., Grondin, G. Y., & Driver, R. G. (2006). Beam-to-Column Shear Connections with Slotted Holes (Structural Engineering Report No. 260). University of Alberta, Department of Civil & Environmental Engineering. https://doi.org/10.7939/R3FF3M04W

National Instruments. (2021). [Image of cDAQ-9178] [Photograph]. www.ni.com. https://www.ni.com/en-us/support/model.cdaq-9178.html.

National Instruments. (2021). [Image of NI-9215] [Photograph]. www.ni.com. https://www.ni.com/en-us/support/model.ni-9215.html.

National Instruments. (2021). [Image of NI-9235]] [Photograph]. www.ni.com. https://www.ni.com/en-us/support/model.ni-9235.html.

Peterson, C. (2014). “Analysis of Long-Slotted Holes in Single Plate Connections.” Master of Science in Structural Engineering (MSST) Capstone Paper, Milwaukee School of Engineering.

Wollenslegel, B. (2020). *Behavior of Extra-Long Slots*. Master’s thesis, University of Cincinnati. https://etd.ohiolink.edu/.

Appendix A:

Calculations for the Expected Capacity of the Experimental Specimens

S30P100 Expected Capacity

Goemetry and Material Properties

Single Plate Properties

Single Plate Thickness	$t_p := .25in$	
Vertical Edge Distance	$L_v := 2in$	From center of long slot
Horizontal Edge Distance	$L_h := 3in$	From center of long slot
Yield Strength	$F_y := 62.65ksi$	From material test data
Ultimate Strength	$F_u := 72.85ksi$	From material test data
Modulus of Elasticity	$E := 29000ksi$	From material test data
Slot Length	$L_s := \left(2 + \frac{13}{16}\right)in = 2\frac{13}{16}\ in$	
Bolt Position Relative to Welded Edge	$P_b := 100\%$	

Bolt Properties

A325-N Bolts

Number of Slots in a Row	$n := 3$	
Nominal Bolt Diameter	$d_b := .75in$	
Slot Spacing	$s := 3in$	
Slot Width	$d_h := d_b + \frac{1}{16}in = \frac{13}{16}\ in$	
Location of Bolt Relative to Welded Edge	$L_e := \left(L_h - \frac{L_s}{2}\right) + \frac{d_h}{2} + P_b \cdot \left(L_s - d_h\right) = 4\ in$	
Location of Bolt Relative to Slot End	$L_b := \frac{d_h}{2} + P_b \cdot \left(L_s - d_h\right) = 2\frac{13}{32}\ in$	

Embed Plate Properties

Embed Plate Thickness	$t_e := 1in$	
Embed Plate Eccentricity	$e := L_e = 4\ in$	Distance to Bolts from Face of Support
Yield Stress	$F_{ye} := 50ksi$	
Ultimate Stres	$F_{ue} := 65ksi$	

Single Plate Checks

Plate Properties

Plate Depth $d_p := (n - 1) \cdot s + 2 \cdot L_v = 10\,in$

Gross Shear Area $A_{gv} := d_p \cdot t_p = 2.5\,in^2$

Net Shear Area $A_{nv} := \left[d_p - (n) \cdot \left(d_h\right) - L_v\right] \cdot t_p = 1.39\,in^2$

Number of Shear Planes $n_{sp} := 1$

Plastic Section Modulus $Z_x := n_{sp} \cdot \frac{t_p \cdot d_p^{\,2}}{4} = 6.25\,in^3$

Shear and Flexure Checks

Shear Yielding $R_{n.PlShearYield} := 0.6 \cdot F_y A_{gv} = 94.0\,kip$ EQN J4-3

Flexural Yielding $R_{n.PlFlexureYield} := \frac{F_y \cdot Z_x}{e} = 97.9\,kip$

Combined Shear and Flexure Check

$$R_{n.PlShearFlexureYield} := \frac{1}{\sqrt{\left(\frac{1}{R_{n.PlShearYield}}\right)^2 + \left(\frac{1}{R_{n.PlFlexureYield}}\right)^2}}$$

$R_{n.PlShearFlexureYield} = 67.8\,kip$

Net Shear Rupture $R_{n.PlShearRupt} := 0.60 \cdot F_u \cdot A_{nv} = 60.78\,kip$ EQN J4-4

Buckling Checks

Flexural Coefficient

$$\lambda := \frac{d_p \cdot \sqrt{F_y \cdot \frac{in^2}{kip}}}{10 \cdot t_p \cdot \sqrt{475 + 280\left(\frac{d_p}{e}\right)^2}} = 0.671$$

Muir and Hewitt Equation

Flexural Buckling Coefficient

$$Q := \begin{cases} 1.0 & \text{if } \lambda \le 0.7 \\ (1.34 - .486\lambda) & \text{if } 0.7 < \lambda \le 1.41 \\ \frac{1.3}{\lambda^2} & \text{if } \lambda > 1.41 \end{cases} = 1.00$$

Critical Buckling Stress $F_{bx} := F_y \cdot Q = 62.65\,ksi$

Elastic Section Modulus $S_x := n_{sp} \cdot \frac{t_p \cdot d_p^{\,2}}{6} = 4.17\,in^3$

Plate Buckling Strength $R_{n.PlBuckling} := \frac{F_{bx} \cdot S_x}{e} = 65.3\,kip$

Block Shear Check

Gross Shear Length $L_{gv} := (n-1)\cdot s + L_v = 8\,in$

Net Shear Length $L_{nv} := L_{gv} - (n - .5)\cdot d_h = 5.97\,in$

Gross Tension Length $L_{gt} := L_v = 2\,in$

Net Tension Length $L_{nt} := L_{gt} - \frac{L_s}{2} = 0.59375\,in$

Gross Shear Area $A_{gv} := L_{gv}\cdot t_p = 2\,in^2$

Net Shear Area $A_{nv} := L_{nv}\cdot t_p = 1.49\,in^2$

Gross Tension Area $A_{gt} := L_{gt}\cdot t_p = 0.5\,in^2$

Net Tension Area $A_{nt} := L_{nt}\cdot t_p = 0.15\cdot in^2$

Block Shear Capacity $R_{n.PlBlockShear} := F_u\cdot A_{nt} + min\left(0.6\cdot F_u\cdot A_{nv}, 0.6\cdot F_y\cdot A_{gv}\right)$ EQN J4-5

$R_{n.PlBlockShear} = 76.04\,kip$

Bolt Checks

Bolt Shear

Area of Bolt $A_{bolt} := \pi\cdot\frac{{d_b}^2}{4} = 0.44\,in^2$

Bolt Shear Stress $F_{nv} := 54ksi$ AISC Table J3.2, P. 16.1-129

Number of Shear Planes $n_{sp} := 2$ 2 Sandwich Plates

Bolt Shear Strength $R_{n.BoltShear} := n\cdot n_{sp}\cdot F_{nv}\cdot A_{bolt} = 143.14\cdot kip$ EQN J3-1

Plate Bearing/Tearout at Bottom Bolt

Clear Edge Distance $L_{c.pl} := L_v - \frac{d_h}{2} = 1.59\,in$

Number of Shear Planes $n_{sp} := 1$

Bolt Tearout Strength $R_{n.BoltTearout.PlBot} := n_{sp}\cdot 1\cdot L_{c.pl}\cdot t_p\cdot F_u = 29.03\cdot kip$ EQN J3-6F

Bolt Bearing Strength $R_{n.BoltBearing.PlBot} := n_{sp}\cdot 2\cdot d_b\cdot t_p\cdot F_u = 27.32\cdot kip$ EQN J3-6E

Botom Bolt Capacity $R_{n.Bolt.PlBottom} := min\left(R_{n.BoltTearout.PlBot}, R_{n.BoltBearing.PlBot}\right)$

$R_{n.Bolt.PlBottom} = 27.32\,kip$

Plate Bearing/Tearout at Remaining Bolts

Clear Distance Between Slots $L_{c.pl} := s - d_h = 2.19\,in$

Number of Shear Planes $n_{sp} := 1$

Bolt Tearout Strength $R_{n.BoltTearout.PlMid} := (n-1)\cdot n_{sp}\cdot 1\cdot L_{c.pl}\cdot t_p\cdot F_u = 79.68\cdot kip$ EQN J3-6F

Bolt Bearing Strength $R_{n.BoltBearing.PlMid} := (n-1)\cdot n_{sp}\cdot 2\cdot d_b\cdot t_p\cdot F_u = 54.64\cdot kip$ EQN J3-6E

Remaining Bolt Capacity $R_{n.Bolt.PlMid} := \min\left(R_{n.BoltTearout.PlMid}, R_{n.BoltBearing.PlMid}\right)$

$R_{n.Bolt.PlMid} = 54.64\,kip$

Plate Flexure at Bottom Bolt

Clear Edge Distance $L_{c.pl} := L_v - \frac{d_h}{2} = 1.59375\,in$

Elastic Section Modulus $S_x := \frac{t_p\cdot L_{c.pl}^2}{6} = 0.105835\,in^3$

"Beam" Span Length $Span := L_b - \frac{13}{32}in = 2\,in$

$Span := \begin{cases} 0.001in & \text{if } Span \le 0 \\ Span & \text{if } Span > 0 \end{cases} = 2\cdot in$ Used 0.001 in. in equation to avoid dividing by 0

Plate Flexure Capacity at Bottom Bolt $R_{n.BoltPlFlexure.Bot} := \frac{F_y\cdot S_x}{Span} = 3.32\cdot kip$

Plate Flexure at Remaining Bolts

Clear Distance Between Slots $L_{c.pl} := s - d_h = 2.19\,in$

Elastic Section Modulus $S_x := \frac{t_p\cdot L_{c.pl}^2}{4} = 0.3\,in^3$

"Beam" Span Length $Span := L_b - \frac{13}{32}in = 2\,in$

$Span := \begin{cases} 0.001in & \text{if } Span \le 0 \\ Span & \text{if } Span > 0 \end{cases} = 2\cdot in$ Used 0.001 in. in equation to avoid dividing by 0

Plate Flexure Capacity at Remaining Bolts $R_{n.BoltPlFlexure.Mid} := \frac{(n-1)F_y\cdot S_x}{Span} = 18.74\cdot kip$

Single Plate to Embed Plate Weld

Minimum Weld Metal Strength $F_{EXX} := 70ksi$

Effective Weld Length $L_w := d_p - 2 \cdot .25in = 9.5\,in$

Minimum Plate Thickness $t_{min} := min(t_p, t_e) = 0.25\,in$

Minimum Weld Sixe

$$w_{min} := \begin{vmatrix} \frac{1}{4}in \;\; if \;\; t_{min} \le .75in \\ \frac{3}{16}in \;\; if \;\; t_{min} \le .5in \\ \frac{1}{8}in \;\; if \;\; t_{min} \le .25in \\ \frac{5}{16}in \;\; otherwise \end{vmatrix} = \frac{1}{8} \cdot in$$

Design Weld Size $w_{des} := max\left(w_{min}, Ceil\left(\frac{5 \cdot t_{min}}{8}, \frac{1}{16}in\right)\right) = \frac{3}{16}\,in$

Design Weld Size $w_{des} := \frac{1}{4}in$

Resultant Load Angle

$$\theta := atan\left[\frac{\frac{3 \cdot e}{L_w^{\,2}}}{\left(\frac{1}{2L_w}\right)}\right] = 68.4 \cdot deg$$

Weld Directional Increase $F := 1 + 0.5 \cdot \left(sin(\theta)^{1.5}\right) = 1.45$

Weld Strength $F_w := F \cdot 0.6 \cdot F_{EXX} = 60.83 \cdot ksi$

Weld Stress $F_{w.des} := \frac{F_w}{\sqrt{2}} = 43.01\,ksi$

Combined Weld Stress $F_{r.all} := w_{des} \cdot F_{w.des} = 10.75 \cdot kpi$

Start of Solve Block *Given*

$$F_{r.all} = \sqrt{\left(\frac{P}{2 \cdot L_w}\right)^2 + \left(P \cdot e \cdot \frac{3}{L_w^{\,2}}\right)^2}$$

$P := Find(P)\;float, 5 \;\rightarrow (-902338.0 \cdot in \cdot plf \quad 902338.0 \cdot in \cdot plf\,)$

Weld Strength $R_{n.weld} := max(P) = 75.2 \cdot kip$

S30P100 Expected Capacity Summary

$R_{n.PlShearYield} = 93.98\,kip$

$R_{n.PlFlexureYield} = 97.89\,kip$

$R_{n.PlShearFlexureYield} = 67.79\,kip$

$R_{n.PlShearRupt} = 60.78\,kip$

$R_{n.PlBuckling} = 65.26\,kip$

$R_{n.PlBlockShear} = 76.04\,kip$

$R_{n.BoltShear} = 143.14\,kip$

$R_{n.BoltTearout.PlBot} = 29.03\,kip$

$R_{n.BoltTearout.PlMid} = 79.68\,kip$

$R_{n.BoltTearout} := R_{n.BoltTearout.PlBot} + R_{n.BoltTearout.PlMid} = 108.71\,kip$

$R_{n.BoltBearing.PlBot} = 27.32\,kip$

$R_{n.BoltBearing.PlMid} = 54.64\,kip$

$R_{n.BoltBearing} := R_{n.BoltBearing.PlBot} + R_{n.BoltBearing.PlMid} = 81.96\,kip$

$R_{n.BoltPlFlexure.Bot} = 3.32\,kip$

$R_{n.BoltPlFlexure.Mid} = 18.74\,kip$

$R_{n.Bolt.PlFlexure} := R_{n.BoltPlFlexure.Bot} + R_{n.BoltPlFlexure.Mid} = 22.05\,kip$

$$R_{n.Bolt.Bot} := \begin{pmatrix} R_{n.BoltTearout.PlBot} \\ R_{n.BoltBearing.PlBot} \\ R_{n.BoltPlFlexure.Bot} \end{pmatrix} = \begin{pmatrix} 29.03 \\ 27.32 \\ 3.32 \end{pmatrix} kip$$

$$R_{n.Bolt.Mid} := \begin{pmatrix} R_{n.BoltTearout.PlMid} \\ R_{n.BoltBearing.PlMid} \\ R_{n.BoltPlFlexure.Mid} \end{pmatrix} = \begin{pmatrix} 79.68 \\ 54.64 \\ 18.74 \end{pmatrix} kip$$

$R_{n.Bolts} := min(R_{n.Bolt.Bot}) + min(R_{n.Bolt.Mid}) = 22.05\,kip$

$R_{n.weld} = 75.19\,kip$

$w_{des} = \frac{1}{4}\,in$

$s = 3\,in$

$P_b = 100 \cdot \%$

$Capacity = 22.05\,kip$ $\quad Capacity = 98.09 \cdot kN$ $\quad LimitState = \begin{pmatrix} \text{"R.Bolt.PLFlexure"} \\ \text{"R.Bolts"} \end{pmatrix}$

S35P100 Expected Capacity Summary

$R_{n.PlShearYield} = 103.37\,kip$

$R_{n.PlFlexureYield} = 118.45\,kip$

$R_{n.PlShearFlexureYield} = 77.88\,kip$

$R_{n.PlShearRupt} = 71.71\,kip$

$R_{n.PlBuckling} = 78.97\,kip$

$R_{n.PlBlockShear} = 86.96\,kip$

$R_{n.BoltShear} = 143.14\,kip$

$R_{n.BoltTearout.PlBot} = 29.03\,kip$

$R_{n.BoltTearout.PlMid} = 97.89\,kip$

$R_{n.BoltTearout} := R_{n.BoltTearout.PlBot} + R_{n.BoltTearout.PlMid} = 126.92\,kip$

$R_{n.BoltBearing.PlBot} = 27.32\,kip$

$R_{n.BoltBearing.PlMid} = 54.64\,kip$

$R_{n.BoltBearing} := R_{n.BoltBearing.PlBot} + R_{n.BoltBearing.PlMid} = 81.96\,kip$

$R_{n.BoltPlFlexure.Bot} = 3.32\,kip$

$R_{n.BoltPlFlexure.Mid} = 28.28\,kip$

$R_{n.Bolt.PlFlexure} := R_{n.BoltPlFlexure.Bot} + R_{n.BoltPlFlexure.Mid} = 31.6\,kip$

$$R_{n.Bolt.Bot} := \begin{pmatrix} R_{n.BoltTearout.PlBot} \\ R_{n.BoltBearing.PlBot} \\ R_{n.BoltPlFlexure.Bot} \end{pmatrix} = \begin{pmatrix} 29.03 \\ 27.32 \\ 3.32 \end{pmatrix} kip$$

$$R_{n.Bolt.Mid} := \begin{pmatrix} R_{n.BoltTearout.PlMid} \\ R_{n.BoltBearing.PlMid} \\ R_{n.BoltPlFlexure.Mid} \end{pmatrix} = \begin{pmatrix} 97.89 \\ 54.64 \\ 28.28 \end{pmatrix} kip$$

$R_{n.Bolts} := min(R_{n.Bolt.Bot}) + min(R_{n.Bolt.Mid}) = 31.6\,kip$

$R_{n.weld} = 89.89\,kip$

$w_{des} = \frac{1}{4}\,in$

$s = 3.5\,in$ $\quad Capacity = 31.6\,kip \quad Capacity = 140.55 \cdot kN \quad LimitState = \begin{pmatrix} \text{"R.Bolt.PLFlexure"} \\ \text{"R.Bolts"} \end{pmatrix}$

$P_b = 100 \cdot \%$

S40P100 Expected Capacity Summary

$R_{n.PlShearYield} = 112.77\ kip$

$R_{n.PlFlexureYield} = 140.96\ kip$

$R_{n.PlShearFlexureYield} = 88.06\ kip$

$R_{n.PlShearRupt} = 82.64\ kip$

$R_{n.PlBuckling} = 93.97\ kip$

$R_{n.PlBlockShear} = 97.89\ kip$

$R_{n.BoltShear} = 143.14\ kip$

$R_{n.BoltTearout.PlBot} = 29.03\ kip$

$R_{n.BoltTearout.PlMid} = 116.1\ kip$

$R_{n.BoltTearout} := R_{n.BoltTearout.PlBot} + R_{n.BoltTearout.PlMid} = 145.13\ kip$

$R_{n.BoltBearing.PlBot} = 27.32\ kip$

$R_{n.BoltBearing.PlMid} = 54.64\ kip$

$R_{n.BoltBearing} := R_{n.BoltBearing.PlBot} + R_{n.BoltBearing.PlMid} = 81.96\ kip$

$R_{n.BoltPlFlexure.Bot} = 3.32\ kip$

$R_{n.BoltPlFlexure.Mid} = 39.78\ kip$

$R_{n.Bolt.PlFlexure} := R_{n.BoltPlFlexure.Bot} + R_{n.BoltPlFlexure.Mid} = 43.1\ kip$

$$R_{n.Bolt.Bot} := \begin{pmatrix} R_{n.BoltTearout.PlBot} \\ R_{n.BoltBearing.PlBot} \\ R_{n.BoltPlFlexure.Bot} \end{pmatrix} = \begin{pmatrix} 29.03 \\ 27.32 \\ 3.32 \end{pmatrix} kip$$

$$R_{n.Bolt.Mid} := \begin{pmatrix} R_{n.BoltTearout.PlMid} \\ R_{n.BoltBearing.PlMid} \\ R_{n.BoltPlFlexure.Mid} \end{pmatrix} = \begin{pmatrix} 116.1 \\ 54.64 \\ 39.78 \end{pmatrix} kip$$

$R_{n.Bolts} := min(R_{n.Bolt.Bot}) + min(R_{n.Bolt.Mid}) = 43.1\ kip$

$R_{n.weld} = 105.39\ kip$

$w_{des} = \frac{1}{4}\ in$

$s = 4\ in$

$P_b = 100 \cdot \%$

$Capacity = 43.1\ kip$ $\quad Capacity = 191.71 \cdot kN$ $\quad LimitState = \begin{pmatrix} \text{"R.Bolt.PLFlexure"} \\ \text{"R.Bolts"} \end{pmatrix}$

S45P100 Expected Capacity Summary

$R_{n.PlShearYield} = 122.17\ kip$

$R_{n.PlFlexureYield} = 165.44\ kip$

$R_{n.PlShearFlexureYield} = 98.28\ kip$

$R_{n.PlShearRupt} = 93.57\ kip$

$R_{n.PlBuckling} = 110.13\ kip$

$R_{n.PlBlockShear} = 108.82\ kip$

$R_{n.BoltShear} = 143.14\ kip$

$R_{n.BoltTearout.PlBot} = 29.03\ kip$

$R_{n.BoltTearout.PlMid} = 134.32\ kip$

$R_{n.BoltTearout} := R_{n.BoltTearout.PlBot} + R_{n.BoltTearout.PlMid} = 163.34\ kip$

$R_{n.BoltBearing.PlBot} = 27.32\ kip$

$R_{n.BoltBearing.PlMid} = 54.64\ kip$

$R_{n.BoltBearing} := R_{n.BoltBearing.PlBot} + R_{n.BoltBearing.PlMid} = 81.96\ kip$

$R_{n.BoltPlFlexure.Bot} = 3.32\ kip$

$R_{n.BoltPlFlexure.Mid} = 53.24\ kip$

$R_{n.Bolt.PlFlexure} := R_{n.BoltPlFlexure.Bot} + R_{n.BoltPlFlexure.Mid} = 56.56\ kip$

$$R_{n.Bolt.Bot} := \begin{pmatrix} R_{n.BoltTearout.PlBot} \\ R_{n.BoltBearing.PlBot} \\ R_{n.BoltPlFlexure.Bot} \end{pmatrix} = \begin{pmatrix} 29.03 \\ 27.32 \\ 3.32 \end{pmatrix} kip$$

$$R_{n.Bolt.Mid} := \begin{pmatrix} R_{n.BoltTearout.PlMid} \\ R_{n.BoltBearing.PlMid} \\ R_{n.BoltPlFlexure.Mid} \end{pmatrix} = \begin{pmatrix} 134.32 \\ 54.64 \\ 53.24 \end{pmatrix} kip$$

$R_{n.Bolts} := min(R_{n.Bolt.Bot}) + min(R_{n.Bolt.Mid}) = 56.56\ kip$

$R_{n.weld} = 121.55\ kip$

$w_{des} = \frac{1}{4}\ in$

$s = 4.5\ in$ $\quad$ $Capacity = 56.56\ kip$ $\quad$ $Capacity = 251.59 \cdot kN$ $\quad$ $LimitState = \begin{pmatrix} \text{"R.Bolt.PLFlexure"} \\ \text{"R.Bolts"} \end{pmatrix}$

$P_b = 100 \cdot \%$

S30P075 Expected Capacity Summary

$R_{n.PlShearYield} = 93.98\,kip$

$R_{n.PlFlexureYield} = 111.88\,kip$

$R_{n.PlShearFlexureYield} = 71.96\,kip$

$R_{n.PlShearRupt} = 60.78\,kip$

$R_{n.PlBuckling} = 74.58\,kip$

$R_{n.PlBlockShear} = 76.04\,kip$

$R_{n.BoltShear} = 143.14\,kip$

$R_{n.BoltTearout.PlBot} = 29.03\,kip$

$R_{n.BoltTearout.PlMid} = 79.68\,kip$

$R_{n.BoltTearout} := R_{n.BoltTearout.PlBot} + R_{n.BoltTearout.PlMid} = 108.71\,kip$

$R_{n.BoltBearing.PlBot} = 27.32\,kip$

$R_{n.BoltBearing.PlMid} = 54.64\,kip$

$R_{n.BoltBearing} := R_{n.BoltBearing.PlBot} + R_{n.BoltBearing.PlMid} = 81.96\,kip$

$R_{n.BoltPlFlexure.Bot} = 4.42\,kip$

$R_{n.BoltPlFlexure.Mid} = 24.98\,kip$

$R_{n.Bolt.PlFlexure} := R_{n.BoltPlFlexure.Bot} + R_{n.BoltPlFlexure.Mid} = 29.4\,kip$

$$R_{n.Bolt.Bot} := \begin{pmatrix} R_{n.BoltTearout.PlBot} \\ R_{n.BoltBearing.PlBot} \\ R_{n.BoltPlFlexure.Bot} \end{pmatrix} = \begin{pmatrix} 29.03 \\ 27.32 \\ 4.42 \end{pmatrix} kip$$

$$R_{n.Bolt.Mid} := \begin{pmatrix} R_{n.BoltTearout.PlMid} \\ R_{n.BoltBearing.PlMid} \\ R_{n.BoltPlFlexure.Mid} \end{pmatrix} = \begin{pmatrix} 79.68 \\ 54.64 \\ 24.98 \end{pmatrix} kip$$

$R_{n.Bolts} := min\left(R_{n.Bolt.Bot}\right) + min\left(R_{n.Bolt.Mid}\right) = 29.4\,kip$

$R_{n.weld} = 83.42\,kip$

$w_{des} = \frac{1}{4}\,in$

$s = 3\,in$

$P_b = 75 \cdot \%$

$Capacity = 29.4\,kip$ $Capacity = 130.79 \cdot kN$ $LimitState = \begin{pmatrix} \text{"R.Bolt.PLFlexure"} \\ \text{"R.Bolts"} \end{pmatrix}$

S35P075 Expected Capacity Summary

$R_{n.PlShearYield} = 103.37\,kip$

$R_{n.PlFlexureYield} = 135.37\,kip$

$R_{n.PlShearFlexureYield} = 82.16\,kip$

$R_{n.PlShearRupt} = 71.71\,kip$

$R_{n.PlBuckling} = 90.25\,kip$

$R_{n.PlBlockShear} = 86.96\,kip$

$R_{n.BoltShear} = 143.14\,kip$

$R_{n.BoltTearout.PlBot} = 29.03\,kip$

$R_{n.BoltTearout.PlMid} = 97.89\,kip$

$R_{n.BoltTearout} := R_{n.BoltTearout.PlBot} + R_{n.BoltTearout.PlMid} = 126.92\,kip$

$R_{n.BoltBearing.PlBot} = 27.32\,kip$

$R_{n.BoltBearing.PlMid} = 54.64\,kip$

$R_{n.BoltBearing} := R_{n.BoltBearing.PlBot} + R_{n.BoltBearing.PlMid} = 81.96\,kip$

$R_{n.BoltPlFlexure.Bot} = 4.42\,kip$

$R_{n.BoltPlFlexure.Mid} = 37.71\,kip$

$R_{n.Bolt.PlFlexure} := R_{n.BoltPlFlexure.Bot} + R_{n.BoltPlFlexure.Mid} = 42.13\,kip$

$$R_{n.Bolt.Bot} := \begin{pmatrix} R_{n.BoltTearout.PlBot} \\ R_{n.BoltBearing.PlBot} \\ R_{n.BoltPlFlexure.Bot} \end{pmatrix} = \begin{pmatrix} 29.03 \\ 27.32 \\ 4.42 \end{pmatrix} kip$$

$$R_{n.Bolt.Mid} := \begin{pmatrix} R_{n.BoltTearout.PlMid} \\ R_{n.BoltBearing.PlMid} \\ R_{n.BoltPlFlexure.Mid} \end{pmatrix} = \begin{pmatrix} 97.89 \\ 54.64 \\ 37.71 \end{pmatrix} kip$$

$R_{n.Bolts} := min(R_{n.Bolt.Bot}) + min(R_{n.Bolt.Mid}) = 42.13\,kip$

$R_{n.weld} = 99.22\,kip$

$w_{des} = \frac{1}{4}\,in$

$s = 3.5\,in$

$P_b = 75 \cdot \%$

$Capacity = 42.13\,kip$ $\quad$ $Capacity = 187.4\,kN$ $\quad$ $LimitState = \begin{pmatrix} \text{"R.Bolt.PLFlexure"} \\ \text{"R.Bolts"} \end{pmatrix}$

S40P075 Expected Capacity Summary

$R_{n.PlShearYield} = 112.77\,kip$

$R_{n.PlFlexureYield} = 161.1\,kip$

$R_{n.PlShearFlexureYield} = 92.38\,kip$

$R_{n.PlShearRupt} = 82.64\,kip$

$R_{n.PlBuckling} = 107.4\,kip$

$R_{n.PlBlockShear} = 97.89\,kip$

$R_{n.BoltShear} = 143.14\,kip$

$R_{n.BoltTearout.PlBot} = 29.03\,kip$

$R_{n.BoltTearout.PlMid} = 116.1\,kip$

$R_{n.BoltTearout} := R_{n.BoltTearout.PlBot} + R_{n.BoltTearout.PlMid} = 145.13\,kip$

$R_{n.BoltBearing.PlBot} = 27.32\,kip$

$R_{n.BoltBearing.PlMid} = 54.64\,kip$

$R_{n.BoltBearing} := R_{n.BoltBearing.PlBot} + R_{n.BoltBearing.PlMid} = 81.96\,kip$

$R_{n.BoltPlFlexure.Bot} = 4.42\,kip$

$R_{n.BoltPlFlexure.Mid} = 53.04\,kip$

$R_{n.Bolt.PlFlexure} := R_{n.BoltPlFlexure.Bot} + R_{n.BoltPlFlexure.Mid} = 57.46\,kip$

$$R_{n.Bolt.Bot} := \begin{pmatrix} R_{n.BoltTearout.PlBot} \\ R_{n.BoltBearing.PlBot} \\ R_{n.BoltPlFlexure.Bot} \end{pmatrix} = \begin{pmatrix} 29.03 \\ 27.32 \\ 4.42 \end{pmatrix} kip$$

$$R_{n.Bolt.Mid} := \begin{pmatrix} R_{n.BoltTearout.PlMid} \\ R_{n.BoltBearing.PlMid} \\ R_{n.BoltPlFlexure.Mid} \end{pmatrix} = \begin{pmatrix} 116.1 \\ 54.64 \\ 53.04 \end{pmatrix} kip$$

$R_{n.Bolts} := min(R_{n.Bolt.Bot}) + min(R_{n.Bolt.Mid}) = 57.46\,kip$

$R_{n.weld} = 115.71\,kip$

$w_{des} = \frac{1}{4}\,in$

$s = 4\,in$

$P_b = 75 \cdot \%$

$Capacity = 57.46\,kip$ $\quad Capacity = 255.62 \cdot kN$ $\quad LimitState = \begin{pmatrix} \text{"R.Bolt.PLFlexure"} \\ \text{"R.Bolts"} \end{pmatrix}$

S45P075 Expected Capacity Summary

$R_{n.PlShearYield} = 122.17\ kip$

$R_{n.PlFlexureYield} = 189.07\ kip$

$R_{n.PlShearFlexureYield} = 102.61\ kip$

$R_{n.PlShearRupt} = 93.57\ kip$

$R_{n.PlBuckling} = 126.05\ kip$

$R_{n.PlBlockShear} = 108.82\ kip$

$R_{n.BoltShear} = 143.14\ kip$

$R_{n.BoltTearout.PlBot} = 29.03\ kip$

$R_{n.BoltTearout.PlMid} = 134.32\ kip$

$R_{n.BoltTearout} := R_{n.BoltTearout.PlBot} + R_{n.BoltTearout.PlMid} = 163.34\ kip$

$R_{n.BoltBearing.PlBot} = 27.32\ kip$

$R_{n.BoltBearing.PlMid} = 54.64\ kip$

$R_{n.BoltBearing} := R_{n.BoltBearing.PlBot} + R_{n.BoltBearing.PlMid} = 81.96\ kip$

$R_{n.BoltPlFlexure.Bot} = 4.42\ kip$

$R_{n.BoltPlFlexure.Mid} = 70.99\ kip$

$R_{n.Bolt.PlFlexure} := R_{n.BoltPlFlexure.Bot} + R_{n.BoltPlFlexure.Mid} = 75.41\ kip$

$$R_{n.Bolt.Bot} := \begin{pmatrix} R_{n.BoltTearout.PlBot} \\ R_{n.BoltBearing.PlBot} \\ R_{n.BoltPlFlexure.Bot} \end{pmatrix} = \begin{pmatrix} 29.03 \\ 27.32 \\ 4.42 \end{pmatrix} kip$$

$$R_{n.Bolt.Mid} := \begin{pmatrix} R_{n.BoltTearout.PlMid} \\ R_{n.BoltBearing.PlMid} \\ R_{n.BoltPlFlexure.Mid} \end{pmatrix} = \begin{pmatrix} 134.32 \\ 54.64 \\ 70.99 \end{pmatrix} kip$$

$R_{n.Bolts} := min\left(R_{n.Bolt.Bot}\right) + min\left(R_{n.Bolt.Mid}\right) = 59.06\ kip$

$R_{n.weld} = 132.75\ kip$

$w_{des} = \frac{1}{4}\ in$

$s = 4.5\ in$ $\quad$ $Capacity = 59.06\ kip$ $\quad$ $Capacity = 262.7 \cdot kN$ $\quad$ $LimitState = (\text{"R.Bolts"})$

$P_b = 75 \cdot \%$

S30P050 Expected Capacity Summary

$R_{n.PlShearYield} = 93.98\,kip$

$R_{n.PlFlexureYield} = 130.52\,kip$

$R_{n.PlShearFlexureYield} = 76.26\,kip$

$R_{n.PlShearRupt} = 60.78\,kip$

$R_{n.PlBuckling} = 87.01\,kip$

$R_{n.PlBlockShear} = 76.04\,kip$

$R_{n.BoltShear} = 143.14\,kip$

$R_{n.BoltTearout.PlBot} = 29.03\,kip$

$R_{n.BoltTearout.PlMid} = 79.68\,kip$

$R_{n.BoltTearout} := R_{n.BoltTearout.PlBot} + R_{n.BoltTearout.PlMid} = 108.71\,kip$

$R_{n.BoltBearing.PlBot} = 27.32\,kip$

$R_{n.BoltBearing.PlMid} = 54.64\,kip$

$R_{n.BoltBearing} := R_{n.BoltBearing.PlBot} + R_{n.BoltBearing.PlMid} = 81.96\,kip$

$R_{n.BoltPlFlexure.Bot} = 6.63\,kip$

$R_{n.BoltPlFlexure.Mid} = 37.47\,kip$

$R_{n.Bolt.PlFlexure} := R_{n.BoltPlFlexure.Bot} + R_{n.BoltPlFlexure.Mid} = 44.1\,kip$

$$R_{n.Bolt.Bot} := \begin{pmatrix} R_{n.BoltTearout.PlBot} \\ R_{n.BoltBearing.PlBot} \\ R_{n.BoltPlFlexure.Bot} \end{pmatrix} = \begin{pmatrix} 29.03 \\ 27.32 \\ 6.63 \end{pmatrix} kip$$

$$R_{n.Bolt.Mid} := \begin{pmatrix} R_{n.BoltTearout.PlMid} \\ R_{n.BoltBearing.PlMid} \\ R_{n.BoltPlFlexure.Mid} \end{pmatrix} = \begin{pmatrix} 79.68 \\ 54.64 \\ 37.47 \end{pmatrix} kip$$

$R_{n.Bolts} := min(R_{n.Bolt.Bot}) + min(R_{n.Bolt.Mid}) = 44.1\,kip$

$R_{n.weld} = 93.22\,kip$

$w_{des} = \frac{1}{4}\,in$

$s = 3\,in$

$P_b = 50 \cdot \%$

$Capacity = 44.1\,kip$ $\quad Capacity = 196.19 \cdot kN$ $\quad LimitState = \begin{pmatrix} \text{"R.Bolt.PLFlexure"} \\ \text{"R.Bolts"} \end{pmatrix}$

S35P050 Expected Capacity Summary

$R_{n.PlShearYield} = 103.37\ kip$

$R_{n.PlFlexureYield} = 157.93\ kip$

$R_{n.PlShearFlexureYield} = 86.49\ kip$

$R_{n.PlShearRupt} = 71.71\ kip$

$R_{n.PlBuckling} = 105.29\ kip$

$R_{n.PlBlockShear} = 86.96\ kip$

$R_{n.BoltShear} = 143.14\ kip$

$R_{n.BoltTearout.PlBot} = 29.03\ kip$

$R_{n.BoltTearout.PlMid} = 97.89\ kip$

$R_{n.BoltTearout} := R_{n.BoltTearout.PlBot} + R_{n.BoltTearout.PlMid} = 126.92\ kip$

$R_{n.BoltBearing.PlBot} = 27.32\ kip$

$R_{n.BoltBearing.PlMid} = 54.64\ kip$

$R_{n.BoltBearing} := R_{n.BoltBearing.PlBot} + R_{n.BoltBearing.PlMid} = 81.96\ kip$

$R_{n.BoltPlFlexure.Bot} = 6.63\ kip$

$R_{n.BoltPlFlexure.Mid} = 56.56\ kip$

$R_{n.Bolt.PlFlexure} := R_{n.BoltPlFlexure.Bot} + R_{n.BoltPlFlexure.Mid} = 63.19\ kip$

$$R_{n.Bolt.Bot} := \begin{pmatrix} R_{n.BoltTearout.PlBot} \\ R_{n.BoltBearing.PlBot} \\ R_{n.BoltPlFlexure.Bot} \end{pmatrix} = \begin{pmatrix} 29.03 \\ 27.32 \\ 6.63 \end{pmatrix} kip$$

$$R_{n.Bolt.Mid} := \begin{pmatrix} R_{n.BoltTearout.PlMid} \\ R_{n.BoltBearing.PlMid} \\ R_{n.BoltPlFlexure.Mid} \end{pmatrix} = \begin{pmatrix} 97.89 \\ 54.64 \\ 56.56 \end{pmatrix} kip$$

$R_{n.Bolts} := min(R_{n.Bolt.Bot}) + min(R_{n.Bolt.Mid}) = 61.27\ kip$

$R_{n.weld} = 110.1\ kip$

$w_{des} = \frac{1}{4}\ in$

$s = 3.5\ in$

$P_b = 50 \cdot \%$

$Capacity = 61.27\ kip$ $Capacity = 272.53 \cdot kN$ $LimitState = (\text{"R.Bolts"})$

S40P050 Expected Capacity Summary

$R_{n.PlShearYield} = 112.77\ kip$

$R_{n.PlFlexureYield} = 187.95\ kip$

$R_{n.PlShearFlexureYield} = 96.7\ kip$

$R_{n.PlShearRupt} = 82.64\ kip$

$R_{n.PlBuckling} = 125.3\ kip$

$R_{n.PlBlockShear} = 97.89\ kip$

$R_{n.BoltShear} = 143.14\ kip$

$R_{n.BoltTearout.PlBot} = 29.03\ kip$

$R_{n.BoltTearout.PlMid} = 116.1\ kip$

$R_{n.BoltTearout} := R_{n.BoltTearout.PlBot} + R_{n.BoltTearout.PlMid} = 145.13\ kip$

$R_{n.BoltBearing.PlBot} = 27.32\ kip$

$R_{n.BoltBearing.PlMid} = 54.64\ kip$

$R_{n.BoltBearing} := R_{n.BoltBearing.PlBot} + R_{n.BoltBearing.PlMid} = 81.96\ kip$

$R_{n.BoltPlFlexure.Bot} = 6.63\ kip$

$R_{n.BoltPlFlexure.Mid} = 79.57\ kip$

$R_{n.Bolt.PlFlexure} := R_{n.BoltPlFlexure.Bot} + R_{n.BoltPlFlexure.Mid} = 86.2\ kip$

$$R_{n.Bolt.Bot} := \begin{pmatrix} R_{n.BoltTearout.PlBot} \\ R_{n.BoltBearing.PlBot} \\ R_{n.BoltPlFlexure.Bot} \end{pmatrix} = \begin{pmatrix} 29.03 \\ 27.32 \\ 6.63 \end{pmatrix} kip$$

$$R_{n.Bolt.Mid} := \begin{pmatrix} R_{n.BoltTearout.PlMid} \\ R_{n.BoltBearing.PlMid} \\ R_{n.BoltPlFlexure.Mid} \end{pmatrix} = \begin{pmatrix} 116.1 \\ 54.64 \\ 79.57 \end{pmatrix} kip$$

$R_{n.Bolts} := min(R_{n.Bolt.Bot}) + min(R_{n.Bolt.Mid}) = 61.27\ kip$

$R_{n.weld} = 127.5\ kip$

$w_{des} = \frac{1}{4}\ in$

$s = 4\ in$

$P_b = 50 \cdot \%$

$Capacity = 61.27\ kip$ $Capacity = 272.53 \cdot kN$ $LimitState = (\text{"R.Bolts"})$

S45P050 Expected Capacity Summary

$R_{n.PlShearYield} = 122.17\ kip$

$R_{n.PlFlexureYield} = 220.58\ kip$

$R_{n.PlShearFlexureYield} = 106.87\ kip$

$R_{n.PlShearRupt} = 93.57\ kip$

$R_{n.PlBuckling} = 147.05\ kip$

$R_{n.PlBlockShear} = 108.82\ kip$

$R_{n.BoltShear} = 143.14\ kip$

$R_{n.BoltTearout.PlBot} = 29.03\ kip$

$R_{n.BoltTearout.PlMid} = 134.32\ kip$

$R_{n.BoltTearout} := R_{n.BoltTearout.PlBot} + R_{n.BoltTearout.PlMid} = 163.34\ kip$

$R_{n.BoltBearing.PlBot} = 27.32\ kip$

$R_{n.BoltBearing.PlMid} = 54.64\ kip$

$R_{n.BoltBearing} := R_{n.BoltBearing.PlBot} + R_{n.BoltBearing.PlMid} = 81.96\ kip$

$R_{n.BoltPlFlexure.Bot} = 6.63\ kip$

$R_{n.BoltPlFlexure.Mid} = 106.49\ kip$

$R_{n.Bolt.PlFlexure} := R_{n.BoltPlFlexure.Bot} + R_{n.BoltPlFlexure.Mid} = 113.12\ kip$

$$R_{n.Bolt.Bot} := \begin{pmatrix} R_{n.BoltTearout.PlBot} \\ R_{n.BoltBearing.PlBot} \\ R_{n.BoltPlFlexure.Bot} \end{pmatrix} = \begin{pmatrix} 29.03 \\ 27.32 \\ 6.63 \end{pmatrix} kip$$

$$R_{n.Bolt.Mid} := \begin{pmatrix} R_{n.BoltTearout.PlMid} \\ R_{n.BoltBearing.PlMid} \\ R_{n.BoltPlFlexure.Mid} \end{pmatrix} = \begin{pmatrix} 134.32 \\ 54.64 \\ 106.49 \end{pmatrix} kip$$

$R_{n.Bolts} := min\left(R_{n.Bolt.Bot}\right) + min\left(R_{n.Bolt.Mid}\right) = 61.27\ kip$

$R_{n.weld} = 145.28\ kip$

$w_{des} = \frac{1}{4}\ in$

$s = 4.5\ in$ $\quad$ $Capacity = 61.27\ kip$ $\quad$ $Capacity = 272.53 \cdot kN$ $\quad$ $LimitState = (\text{"R.Bolts"})$

$P_b = 50 \cdot \%$

S30P025 Expected Capacity Summary

$R_{n.PlShearYield} = 93.98\,kip$

$R_{n.PlFlexureYield} = 156.63\,kip$

$R_{n.PlShearFlexureYield} = 80.58\,kip$

$R_{n.PlShearRupt} = 60.78\,kip$

$R_{n.PlBuckling} = 104.42\,kip$

$R_{n.PlBlockShear} = 76.04\,kip$

$R_{n.BoltShear} = 143.14\,kip$

$R_{n.BoltTearout.PlBot} = 29.03\,kip$

$R_{n.BoltTearout.PlMid} = 79.68\,kip$

$R_{n.BoltTearout} := R_{n.BoltTearout.PlBot} + R_{n.BoltTearout.PlMid} = 108.71\,kip$

$R_{n.BoltBearing.PlBot} = 27.32\,kip$

$R_{n.BoltBearing.PlMid} = 54.64\,kip$

$R_{n.BoltBearing} := R_{n.BoltBearing.PlBot} + R_{n.BoltBearing.PlMid} = 81.96\,kip$

$R_{n.BoltPlFlexure.Bot} = 13.26\,kip$

$R_{n.BoltPlFlexure.Mid} = 74.95\,kip$

$R_{n.Bolt.PlFlexure} := R_{n.BoltPlFlexure.Bot} + R_{n.BoltPlFlexure.Mid} = 88.21\,kip$

$$R_{n.Bolt.Bot} := \begin{pmatrix} R_{n.BoltTearout.PlBot} \\ R_{n.BoltBearing.PlBot} \\ R_{n.BoltPlFlexure.Bot} \end{pmatrix} = \begin{pmatrix} 29.03 \\ 27.32 \\ 13.26 \end{pmatrix} kip$$

$$R_{n.Bolt.Mid} := \begin{pmatrix} R_{n.BoltTearout.PlMid} \\ R_{n.BoltBearing.PlMid} \\ R_{n.BoltPlFlexure.Mid} \end{pmatrix} = \begin{pmatrix} 79.68 \\ 54.64 \\ 74.95 \end{pmatrix} kip$$

$R_{n.Bolts} := min\left(R_{n.Bolt.Bot}\right) + min\left(R_{n.Bolt.Mid}\right) = 67.9\,kip$

$R_{n.weld} = 104.78\,kip$

$w_{des} = \frac{1}{4}\,in$

$s = 3\,in$

$P_b = 25 \cdot \%$

$Capacity = 60.78\,kip$ $Capacity = 270.38 \cdot kN$ $LimitState = (\text{"Cap.PLShearRupt"})$

S35P025 Expected Capacity Summary

$R_{n.PlShearYield} = 103.37\ kip$

$R_{n.PlFlexureYield} = 189.52\ kip$

$R_{n.PlShearFlexureYield} = 90.75\ kip$

$R_{n.PlShearRupt} = 71.71\ kip$

$R_{n.PlBuckling} = 126.34\ kip$

$R_{n.PlBlockShear} = 86.96\ kip$

$R_{n.BoltShear} = 143.14\ kip$

$R_{n.BoltTearout.PlBot} = 29.03\ kip$

$R_{n.BoltTearout.PlMid} = 97.89\ kip$

$R_{n.BoltTearout} := R_{n.BoltTearout.PlBot} + R_{n.BoltTearout.PlMid} = 126.92\ kip$

$R_{n.BoltBearing.PlBot} = 27.32\ kip$

$R_{n.BoltBearing.PlMid} = 54.64\ kip$

$R_{n.BoltBearing} := R_{n.BoltBearing.PlBot} + R_{n.BoltBearing.PlMid} = 81.96\ kip$

$R_{n.BoltPlFlexure.Bot} = 13.26\ kip$

$R_{n.BoltPlFlexure.Mid} = 113.12\ kip$

$R_{n.Bolt.PlFlexure} := R_{n.BoltPlFlexure.Bot} + R_{n.BoltPlFlexure.Mid} = 126.39\ kip$

$$R_{n.Bolt.Bot} := \begin{pmatrix} R_{n.BoltTearout.PlBot} \\ R_{n.BoltBearing.PlBot} \\ R_{n.BoltPlFlexure.Bot} \end{pmatrix} = \begin{pmatrix} 29.03 \\ 27.32 \\ 13.26 \end{pmatrix} kip$$

$$R_{n.Bolt.Mid} := \begin{pmatrix} R_{n.BoltTearout.PlMid} \\ R_{n.BoltBearing.PlMid} \\ R_{n.BoltPlFlexure.Mid} \end{pmatrix} = \begin{pmatrix} 97.89 \\ 54.64 \\ 113.12 \end{pmatrix} kip$$

$R_{n.Bolts} := min(R_{n.Bolt.Bot}) + min(R_{n.Bolt.Mid}) = 67.9\ kip$

$R_{n.weld} = 122.56\ kip$

$w_{des} = \frac{1}{4}\ in$

$s = 3.5\ in$ $\quad Capacity = 67.9\ kip \quad Capacity = 302.03 \cdot kN \quad LimitState = (\text{"R.Bolts"})$

$P_b = 25 \cdot \%$

S40P025 Expected Capacity Summary

$R_{n.PlShearYield} = 112.77\ kip$

$R_{n.PlFlexureYield} = 225.54\ kip$

$R_{n.PlShearFlexureYield} = 100.86\ kip$

$R_{n.PlShearRupt} = 82.64\ kip$

$R_{n.PlBuckling} = 150.36\ kip$

$R_{n.PlBlockShear} = 97.89\ kip$

$R_{n.BoltShear} = 143.14\ kip$

$R_{n.BoltTearout.PlBot} = 29.03\ kip$

$R_{n.BoltTearout.PlMid} = 116.1\ kip$

$R_{n.BoltTearout} := R_{n.BoltTearout.PlBot} + R_{n.BoltTearout.PlMid} = 145.13\ kip$

$R_{n.BoltBearing.PlBot} = 27.32\ kip$

$R_{n.BoltBearing.PlMid} = 54.64\ kip$

$R_{n.BoltBearing} := R_{n.BoltBearing.PlBot} + R_{n.BoltBearing.PlMid} = 81.96\ kip$

$R_{n.BoltPlFlexure.Bot} = 13.26\ kip$

$R_{n.BoltPlFlexure.Mid} = 159.13\ kip$

$R_{n.Bolt.PlFlexure} := R_{n.BoltPlFlexure.Bot} + R_{n.BoltPlFlexure.Mid} = 172.39\ kip$

$$R_{n.Bolt.Bot} := \begin{pmatrix} R_{n.BoltTearout.PlBot} \\ R_{n.BoltBearing.PlBot} \\ R_{n.BoltPlFlexure.Bot} \end{pmatrix} = \begin{pmatrix} 29.03 \\ 27.32 \\ 13.26 \end{pmatrix} kip$$

$$R_{n.Bolt.Mid} := \begin{pmatrix} R_{n.BoltTearout.PlMid} \\ R_{n.BoltBearing.PlMid} \\ R_{n.BoltPlFlexure.Mid} \end{pmatrix} = \begin{pmatrix} 116.1 \\ 54.64 \\ 159.13 \end{pmatrix} kip$$

$R_{n.Bolts} := min\left(R_{n.Bolt.Bot}\right) + min\left(R_{n.Bolt.Mid}\right) = 67.9\ kip$

$R_{n.weld} = 140.62\ kip$

$w_{des} = \frac{1}{4}\ in$

$s = 4\ in$ $\quad$ $Capacity = 67.9\ kip$ $\quad$ $Capacity = 302.03 \cdot kN$ $\quad$ $LimitState = (\text{"R.Bolts"})$

$P_b = 25 \cdot \%$

S45P025 Expected Capacity Summary

$R_{n.PlShearYield} = 122.17\ kip$

$R_{n.PlFlexureYield} = 264.7\ kip$

$R_{n.PlShearFlexureYield} = 110.92\ kip$

$R_{n.PlShearRupt} = 93.57\ kip$

$R_{n.PlBuckling} = 176.46\ kip$

$R_{n.PlBlockShear} = 108.82\ kip$

$R_{n.BoltShear} = 143.14\ kip$

$R_{n.BoltTearout.PlBot} = 29.03\ kip$

$R_{n.BoltTearout.PlMid} = 134.32\ kip$

$R_{n.BoltTearout} := R_{n.BoltTearout.PlBot} + R_{n.BoltTearout.PlMid} = 163.34\ kip$

$R_{n.BoltBearing.PlBot} = 27.32\ kip$

$R_{n.BoltBearing.PlMid} = 54.64\ kip$

$R_{n.BoltBearing} := R_{n.BoltBearing.PlBot} + R_{n.BoltBearing.PlMid} = 81.96\ kip$

$R_{n.BoltPlFlexure.Bot} = 13.26\ kip$

$R_{n.BoltPlFlexure.Mid} = 212.97\ kip$

$R_{n.Bolt.PlFlexure} := R_{n.BoltPlFlexure.Bot} + R_{n.BoltPlFlexure.Mid} = 226.23\ kip$

$$R_{n.Bolt.Bot} := \begin{pmatrix} R_{n.BoltTearout.PlBot} \\ R_{n.BoltBearing.PlBot} \\ R_{n.BoltPlFlexure.Bot} \end{pmatrix} = \begin{pmatrix} 29.03 \\ 27.32 \\ 13.26 \end{pmatrix} kip$$

$$R_{n.Bolt.Mid} := \begin{pmatrix} R_{n.BoltTearout.PlMid} \\ R_{n.BoltBearing.PlMid} \\ R_{n.BoltPlFlexure.Mid} \end{pmatrix} = \begin{pmatrix} 134.32 \\ 54.64 \\ 212.97 \end{pmatrix} kip$$

$R_{n.Bolts} := min(R_{n.Bolt.Bot}) + min(R_{n.Bolt.Mid}) = 67.9\ kip$

$R_{n.weld} = 158.83\ kip$

$w_{des} = \frac{1}{4}\ in$

$s = 4.5\ in$ $\quad$ $Capacity = 67.9\ kip$ $\quad$ $Capacity = 302.03 \cdot kN$ $\quad$ $LimitState = (\text{"R.Bolts"})$

$P_b = 25 \cdot \%$

S30P000 Expected Capacity Summary

$R_{n.PlShearYield} = 93.98\,kip$

$R_{n.PlFlexureYield} = 195.78\,kip$

$R_{n.PlShearFlexureYield} = 84.72\,kip$

$R_{n.PlShearRupt} = 60.78\,kip$

$R_{n.PlBuckling} = 130.52\,kip$

$R_{n.PlBlockShear} = 76.04\,kip$

$R_{n.BoltShear} = 143.14\,kip$

$R_{n.BoltTearout.PlBot} = 29.03\,kip$

$R_{n.BoltTearout.PlMid} = 79.68\,kip$

$R_{n.BoltTearout} := R_{n.BoltTearout.PlBot} + R_{n.BoltTearout.PlMid} = 108.71\,kip$

$R_{n.BoltBearing.PlBot} = 27.32\,kip$

$R_{n.BoltBearing.PlMid} = 54.64\,kip$

$R_{n.BoltBearing} := R_{n.BoltBearing.PlBot} + R_{n.BoltBearing.PlMid} = 81.96\,kip$

$R_{n.BoltPlFlexure.Bot} = 6630.56\,kip$

$R_{n.BoltPlFlexure.Mid} = 37473.75\,kip$

$R_{n.Bolt.PlFlexure} := R_{n.BoltPlFlexure.Bot} + R_{n.BoltPlFlexure.Mid} = 44104.32\,kip$

$$R_{n.Bolt.Bot} := \begin{pmatrix} R_{n.BoltTearout.PlBot} \\ R_{n.BoltBearing.PlBot} \\ R_{n.BoltPlFlexure.Bot} \end{pmatrix} = \begin{pmatrix} 29.03 \\ 27.32 \\ 6630.56 \end{pmatrix} kip$$

$$R_{n.Bolt.Mid} := \begin{pmatrix} R_{n.BoltTearout.PlMid} \\ R_{n.BoltBearing.PlMid} \\ R_{n.BoltPlFlexure.Mid} \end{pmatrix} = \begin{pmatrix} 79.68 \\ 54.64 \\ 37473.75 \end{pmatrix} kip$$

$R_{n.Bolts} := min(R_{n.Bolt.Bot}) + min(R_{n.Bolt.Mid}) = 81.96\,kip$

$R_{n.weld} = 117.96\,kip$

$w_{des} = \frac{1}{4}\,in$

$s = 3\,in$

$P_b = 0 \cdot \%$

$Capacity = 60.78\,kip$ $Capacity = 270.38 \cdot kN$ $LimitState = ($"Cap.PLShearRupt"$)$

S35P000 Expected Capacity Summary

$R_{n.PlShearYield} = 103.37\,kip$

$R_{n.PlFlexureYield} = 236.9\,kip$

$R_{n.PlShearFlexureYield} = 94.74\,kip$

$R_{n.PlShearRupt} = 71.71\,kip$

$R_{n.PlBuckling} = 157.93\,kip$

$R_{n.PlBlockShear} = 86.96\,kip$

$R_{n.BoltShear} = 143.14\,kip$

$R_{n.BoltTearout.PlBot} = 29.03\,kip$

$R_{n.BoltTearout.PlMid} = 97.89\,kip$

$R_{n.BoltTearout} := R_{n.BoltTearout.PlBot} + R_{n.BoltTearout.PlMid} = 126.92\,kip$

$R_{n.BoltBearing.PlBot} = 27.32\,kip$

$R_{n.BoltBearing.PlMid} = 54.64\,kip$

$R_{n.BoltBearing} := R_{n.BoltBearing.PlBot} + R_{n.BoltBearing.PlMid} = 81.96\,kip$

$R_{n.BoltPlFlexure.Bot} = 6630.56\,kip$

$R_{n.BoltPlFlexure.Mid} = 56562.43\,kip$

$R_{n.Bolt.PlFlexure} := R_{n.BoltPlFlexure.Bot} + R_{n.BoltPlFlexure.Mid} = 63192.99\,kip$

$$R_{n.Bolt.Bot} := \begin{pmatrix} R_{n.BoltTearout.PlBot} \\ R_{n.BoltBearing.PlBot} \\ R_{n.BoltPlFlexure.Bot} \end{pmatrix} = \begin{pmatrix} 29.03 \\ 27.32 \\ 6630.56 \end{pmatrix} kip$$

$$R_{n.Bolt.Mid} := \begin{pmatrix} R_{n.BoltTearout.PlMid} \\ R_{n.BoltBearing.PlMid} \\ R_{n.BoltPlFlexure.Mid} \end{pmatrix} = \begin{pmatrix} 97.89 \\ 54.64 \\ 56562.43 \end{pmatrix} kip$$

$R_{n.Bolts} := min\left(R_{n.Bolt.Bot}\right) + min\left(R_{n.Bolt.Mid}\right) = 81.96\,kip$

$R_{n.weld} = 136.19\,kip$

$w_{des} = \frac{1}{4}\,in$

$s = 3.5\,in$ $\quad$ $Capacity = 71.71\,kip$ $\quad$ $Capacity = 318.99 \cdot kN$ $\quad$ $LimitState = (\text{"Cap.PLShearRupt"})$

$P_b = 0 \cdot \%$

S40P000 Expected Capacity Summary

$R_{n.PlShearYield} = 112.77\,kip$

$R_{n.PlFlexureYield} = 281.93\,kip$

$R_{n.PlShearFlexureYield} = 104.7\,kip$

$R_{n.PlShearRupt} = 82.64\,kip$

$R_{n.PlBuckling} = 187.95\,kip$

$R_{n.PlBlockShear} = 97.89\,kip$

$R_{n.BoltShear} = 143.14\,kip$

$R_{n.BoltTearout.PlBot} = 29.03\,kip$

$R_{n.BoltTearout.PlMid} = 116.1\,kip$

$R_{n.BoltTearout} := R_{n.BoltTearout.PlBot} + R_{n.BoltTearout.PlMid} = 145.13\,kip$

$R_{n.BoltBearing.PlBot} = 27.32\,kip$

$R_{n.BoltBearing.PlMid} = 54.64\,kip$

$R_{n.BoltBearing} := R_{n.BoltBearing.PlBot} + R_{n.BoltBearing.PlMid} = 81.96\,kip$

$R_{n.BoltPlFlexure.Bot} = 6630.56\,kip$

$R_{n.BoltPlFlexure.Mid} = 79566.72\,kip$

$R_{n.Bolt.PlFlexure} := R_{n.BoltPlFlexure.Bot} + R_{n.BoltPlFlexure.Mid} = 86197.28\,kip$

$$R_{n.Bolt.Bot} := \begin{pmatrix} R_{n.BoltTearout.PlBot} \\ R_{n.BoltBearing.PlBot} \\ R_{n.BoltPlFlexure.Bot} \end{pmatrix} = \begin{pmatrix} 29.03 \\ 27.32 \\ 6630.56 \end{pmatrix} kip$$

$$R_{n.Bolt.Mid} := \begin{pmatrix} R_{n.BoltTearout.PlMid} \\ R_{n.BoltBearing.PlMid} \\ R_{n.BoltPlFlexure.Mid} \end{pmatrix} = \begin{pmatrix} 116.1 \\ 54.64 \\ 79566.72 \end{pmatrix} kip$$

$R_{n.Bolts} := min(R_{n.Bolt.Bot}) + min(R_{n.Bolt.Mid}) = 81.96\,kip$

$R_{n.weld} = 154.4\,kip$

$w_{des} = \frac{1}{4}\,in$

$s = 4\,in$

$P_b = 0 \cdot \%$

$Capacity = 81.96\,kip$ $Capacity = 364.56 \cdot kN$ $LimitState = \begin{pmatrix} \text{"R.BoltBearing"} \\ \text{"R.Bolts"} \end{pmatrix}$

S45P000 Expected Capacity Summary

$R_{n.PlShearYield} = 122.17\,kip$

$R_{n.PlFlexureYield} = 330.87\,kip$

$R_{n.PlShearFlexureYield} = 114.6\,kip$

$R_{n.PlShearRupt} = 93.57\,kip$

$R_{n.PlBuckling} = 220.58\,kip$

$R_{n.PlBlockShear} = 108.82\,kip$

$R_{n.BoltShear} = 143.14\,kip$

$R_{n.BoltTearout.PlBot} = 29.03\,kip$

$R_{n.BoltTearout.PlMid} = 134.32\,kip$

$R_{n.BoltTearout} := R_{n.BoltTearout.PlBot} + R_{n.BoltTearout.PlMid} = 163.34\,kip$

$R_{n.BoltBearing.PlBot} = 27.32\,kip$

$R_{n.BoltBearing.PlMid} = 54.64\,kip$

$R_{n.BoltBearing} := R_{n.BoltBearing.PlBot} + R_{n.BoltBearing.PlMid} = 81.96\,kip$

$R_{n.BoltPlFlexure.Bot} = 6630.56\,kip$

$R_{n.BoltPlFlexure.Mid} = 106486.65\,kip$

$R_{n.Bolt.PlFlexure} := R_{n.BoltPlFlexure.Bot} + R_{n.BoltPlFlexure.Mid} = 113117.21\,kip$

$$R_{n.Bolt.Bot} := \begin{pmatrix} R_{n.BoltTearout.PlBot} \\ R_{n.BoltBearing.PlBot} \\ R_{n.BoltPlFlexure.Bot} \end{pmatrix} = \begin{pmatrix} 29.03 \\ 27.32 \\ 6630.56 \end{pmatrix} kip$$

$$R_{n.Bolt.Mid} := \begin{pmatrix} R_{n.BoltTearout.PlMid} \\ R_{n.BoltBearing.PlMid} \\ R_{n.BoltPlFlexure.Mid} \end{pmatrix} = \begin{pmatrix} 134.32 \\ 54.64 \\ 106486.65 \end{pmatrix} kip$$

$R_{n.Bolts} := min(R_{n.Bolt.Bot}) + min(R_{n.Bolt.Mid}) = 81.96\,kip$

$R_{n.weld} = 172.48\,kip$

$w_{des} = \frac{1}{4}\,in$

$s = 4.5\,in$ $\quad$ $Capacity = 81.96\,kip$ $\quad$ $Capacity = 364.56 \cdot kN$ $\quad$ $LimitState = \begin{pmatrix} \text{"R.BoltBearing"} \\ \text{"R.Bolts"} \end{pmatrix}$

$P_b = 0 \cdot \%$

Appendix B:

Calculations for the Custom Yoke

Yoke Design

Plate P82 Checks

Plate Thickness	$t := .5in$	
Plate Width	$w := 10in$	
Plate Length	$l := 10.5in$	Portion of plate with notch is excluded
Plate Yield Stress	$F_y := 50ksi$	
Plate Ultimate Stress	$F_u := 65ksi$	
Number of Bolt Rows	$n_{Rows} := 1$	Parallel to Load
Number of Bolt Columns	$n_{Cols} := 2$	Perpendicular to Load
Number of Bolts	$N := n_{Rows} \cdot n_{Cols} = 2$	
Bolt Col Spacing	$s_h := 3in$	Horizontal Spacing
Bolt Row Spacing	$s_v := 0in$	Vertical Spacing
Bolt Strength	$F_{nv} := 54ksi$	A325 Bolt
Bolt Diameter	$d_b := 1in$	
Hole Diameter	$d_{hole} := d_b + \frac{1}{8}in = 1.13\,in$	
Horizontal Edge Distance	$l_h := 2in$	
Clear Horizontal Edge Distance	$l_{eh} := l_h - \frac{\left(d_b + \frac{1}{8}in\right)}{2} = 1.438\,in$	
Vertical Edge Distance	$l_v := \frac{w - s_v}{2} = 5\,in$	
Clear Vertical Edge Distance	$l_{ev} := l_v - \frac{\left(d_b + \frac{1}{8}in\right)}{2} = 4.438\,in$	
Applied Load	$P := 120kip$	Maximum actuator capacity

Tensile Yielding

Strength Reduction Factor $\phi := 0.9$

Gross Area $A_g := t \cdot w = 5\ in^2$

Tensile Yielding Capacity $Cap_{TenYield} := \phi \cdot F_y \cdot A_g = 225 \cdot kip$ Eqn. J4-1

Check $Check_{TenYield} := \begin{cases} \text{"OK"} & \text{if } Cap_{TenYield} \geq P \\ \text{"No Good"} & \text{otherwise} \end{cases} = \text{"OK"}$

Tensile Rupture

Strength Reduction Factor $\phi := 0.75$

Net Area $A_n := t \cdot (w - n_{Rows} \cdot d_{hole}) = 4.44\ in^2$

Shear Lag Factor $U := 1.0$ AISC Table D3.1, P. 16.1-30

Effective Area $A_e := U \cdot A_n = 4.44\ in^2$

Tensile Rupture Capacity $Cap_{TenRupt} := \phi \cdot F_u \cdot A_e = 216.33 \cdot kip$ Eqn. J4-2

Check $Check_{TenRupt} := \begin{cases} \text{"OK"} & \text{if } Cap_{TenRupt} \geq P \\ \text{"No Good"} & \text{otherwise} \end{cases} = \text{"OK"}$

Bearing at Bolt Hole

Strength Reduction Factor $\phi := 0.75$

Number of Shear Planes $N_{sp} := 2$

Capacity of Bolt Bearing $Cap_{BoltBearing} := N_{sp} \cdot N \cdot \phi \cdot 2.4 \cdot d_b \cdot t \cdot F_u = 234 \cdot kip$ Eqn. J3-6a

Check $Check_{BoltBearing} := \begin{cases} \text{"OK"} & \text{if } Cap_{BoltBearing} \geq P \\ \text{"No Good"} & \text{otherwise} \end{cases} = \text{"OK"}$

Tearout at Bolt Hole

Strength Reduction Factor $\phi := 0.75$

Number of Shear Planes $N_{sp} := 2$

Capacity of Bolt Tearout $Cap_{BoltTearout} := N_{sp} \cdot N \cdot \phi \cdot 1.2 \cdot l_{eh} \cdot t \cdot F_u = 168.19 \cdot kip$ Eqn. J3-6c

Check $Check_{BoltBearing} := \begin{cases} \text{"OK"} & \text{if } Cap_{BoltTearout} \geq P \\ \text{"No Good"} & \text{otherwise} \end{cases} = \text{"OK"}$

Block Shear Check

Shear Lag Factor	$U_{bs} := 1.0$
Strength Reduction Factor	$\phi := 0.75$

Failure Path: L-Shape

Shear Length	$l_{Shear} := l_h + s_h = 5\,in$	
Number of Shear Planes	$n_{SP} := 1$	
Number of Bolt Holes in Shear Plane	$n_{BoltSP} := 1.5$	
Net Shear Area	$A_{nv} := t \cdot n_{SP} \cdot \left[l_{Shear} - n_{BoltSP} \cdot \left(d_{hole} + \frac{1}{16} in \right) \right] = 1.61\,in^2$	
Gross Shear Area	$A_{gv} := t \cdot n_{SP} \cdot l_{Shear} = 2.5\,in^2$	
Tension Length	$l_{Tension} := s_v + l_v = 5\,in$	
Number of Bolt Holes in Tension Plane	$n_{BoltTen} := .5$	
Net Tension Area	$A_{nt} := t \cdot \left[l_{Tension} - n_{BoltTen} \cdot \left(d_{hole} + \frac{1}{16} in \right) \right] = 2.2\,in^2$	
	$Cap_{BS1} := 0.60 \cdot F_u \cdot A_{nv} + U_{bs} \cdot F_u \cdot A_{nt} = 205.97 \cdot kip$	Eqn. J4-5
	$Cap_{BS2} := 0.60 \cdot F_y \cdot A_{gv} + U_{bs} \cdot F_u \cdot A_{nt} = 218.2 \cdot kip$	Eqn. J4-5
Block Shear Capacity	$Cap_{BS} := min\left(Cap_{BS1}, Cap_{BS2} \right) = 205.97 \cdot kip$	
Check	$Check_{BlockShear} := \begin{cases} \text{"OK"} & \text{if } Cap_{BS} \geq P \\ \text{"No Good"} & \text{otherwise} \end{cases} = \text{"OK"}$	

Weld at Connection to P64

Strength Reduction Factor $\phi := 0.75$

Available Weld Length $l_{Weld} := 3in$

Number of Weld Lines $n_{Lines} := 8$

Weld Size $s_{Weld} := \frac{5}{16}in$

Effective Weld Length $l_{WeldEff} := n_{Lines} \cdot (l_{Weld} - 2 \cdot s_{Weld}) = 19\,in$

Electrode Grade $F_{EXX} := 70ksi$

Available Weld Strength $Cap_{Weld} := \phi \cdot 0.60 \cdot F_{EXX} \cdot \left(\frac{\sqrt{2}}{2}\right) \cdot s_{Weld} \cdot l_{WeldEff} = 132.25 \cdot kip$ Eqn. 8-1

Check $Check_{Weld} := \begin{cases} \text{"OK"} & \text{if } Cap_{Weld} \geq P \\ \text{"No Good"} & \text{otherwise} \end{cases} = \text{"OK"}$

Plate Reduced Section Yielding

Strength Reduction Factor $\phi := 0.90$

Length at Reduced Section $l_{Tension} := 6in$

Tension Area $A_{Tension} := t \cdot l_{Tension} = 3\,in^2$

Plate Yielding Capacity $Cap_{PlateYield} := \phi \cdot F_y \cdot A_{Tension} = 135 \cdot kip$

Check $Check_{PlateYield} := \begin{cases} \text{"OK"} & \text{if } Cap_{PlateYield} \geq P \\ \text{"No Good"} & \text{otherwise} \end{cases} = \text{"OK"}$

Appendix C:

Calculations for the Sandwich Plates

Sandwich Plate Design

Input

Plate Dimensions

Plate Length	$w := 24in$
Plate Width	$b := 3.25in$
Plate Thickness	$t := 1in$
Gross Area	$A_g := b \cdot t = 3.25\, in^2$
Horizontal Edge Distance	$L_h := 2in$
Vertical Edge Distance	$L_v := 1.625in$
Test Side Hole Spacing	$S_T := 3in$
Test Side Bolt Diameter	$d_{bT} := \frac{3}{4}in$
Test Side Number of Bolts	$N_T := 3$
Test Side Hole Diameter	$d_{hT} := d_{bT} + \frac{1}{16}in = 0.81\, in$
Yoke Side Hole Spacing	$S_Y := 3in$
Yoke Side Bolt Diameter	$d_{bY} := 1in$
Yoke Side Number of Bolts	$N_Y := 2$
Yoke Side Hole Diameter	$d_{hY} := d_{bY} + \frac{1}{8}in = 1.13\, in$

Material Properties

Yield Stress	$F_y := 50ksi$	
Ultimate Stress	$F_u := 65ksi$	
Bolt Strength	$F_{nv} := 54ksi$	A325 Bolt

Bolt Shear

Area of Test Side Bolt $A_{bT} := \frac{\pi \cdot d_{bT}^2}{4} = 0.44\ in^2$

Area of Yoke Side Bolt $A_{bY} := \frac{\pi \cdot d_{bY}^2}{4} = 0.79\ in^2$

Number of Shear Planes $N_{sp} := 2$ Bolts are in double shear

Strength Reduction Factor $\phi := 0.75$

Test Side Bolt Strength $Cap_{BoltShear.T} := \left(N_T \cdot N_{sp}\right) \cdot \phi \cdot F_{nv} \cdot A_{bT} = 107.35\ kip$ Eqn J3-1

Yoke Side Bolt Strength $Cap_{BoltShear.Y} := \left(N_Y \cdot N_{sp}\right) \cdot \phi \cdot F_{nv} \cdot A_{bY} = 127.23\ kip$ Eqn J3-1

Bearing and Tearout

Number of Shear Planes $N_{sp} := 2$

Strength Reduction Factor $\phi := 0.75$

Test Side Bearing $Cap_{BoltBearing.T} := N_{sp} \cdot N_T \cdot \phi \cdot 2.4 \cdot d_{bT} \cdot t \cdot F_u = 526.5\ kip$ Eqn J3-6a

Test Side Clear Distance $L_c := L_h - 0.5 \cdot d_{hT} = 1.59\ in$

Test Side Tearout $Cap_{BoltTearout.T} := N_{sp} \cdot N_T \cdot \phi \cdot 1.2 \cdot L_c \cdot t \cdot F_u = 559.41\ kip$ Eqn J3-6c

Yoke Side Bearing $Cap_{BoltBearing.Y} := N_{sp} \cdot N_Y \cdot \phi \cdot 2.4 \cdot d_{bY} \cdot t \cdot F_u = 468\ kip$ Eqn J3-6a

Yoke Side Clear Distance $L_c := L_h - 0.5 \cdot d_{hY} = 1.44\ in$

Yoke Side Tearout $Cap_{BoltTearout.Y} := N_{sp} \cdot N_Y \cdot \phi \cdot 1.2 \cdot L_c \cdot t \cdot F_u = 336.37\ kip$ Eqn J3-6c

Plate Tensile Yielding

Strength Reduction Factor	$\phi := 0.90$	
Tensile Yielding Capacity	$Cap_{TensileYield} := \phi \cdot F_y \cdot A_g = 146.25\ kip$	Eqn J4-1

Plate Net Section Tensile Rupture

Test Side Net Area	$A_{netT} := \left(b - d_{hT}\right) t = 2.44\ in^2$	
Yoke Side Net Area	$A_{netY} := \left(b - d_{hY}\right) t = 2.12\ in^2$	
Strength Reduction Factor	$\phi := 0.90$	
Test Side Tensile Rupture Capacity	$Cap_{TensileRupt.T} := \phi \cdot F_u \cdot A_{netT} = 142.59\ kip$	Eqn J4-2
Yoke Side Tensile Rupture Capacity	$Cap_{TensileRupt.Y} := \phi \cdot F_u \cdot A_{netY} = 124.31\ kip$	Eqn J4-2

Block Shear Checks

Test Side Block Shear

Gross Shear Length $L_{gv} := (N_T - 1) \cdot S_T + L_h = 8\ in$

Net Shear Length $L_{nv} := L_{gv} - (N_T - .5) \cdot d_{hT} = 5.97\ in$

Gross Tension Length $L_{gt} := L_v = 1.63\ in$

Net Tension Length $L_{nt} := L_{gt} - \frac{d_{hT}}{2} = 1.21875\ in$

Gross Shear Area $A_{gv} := L_{gv} \cdot t = 8\ in^2$

Net Shear Area $A_{nv} := L_{nv} \cdot t = 5.97\ in^2$

Gross Tension Area $A_{gt} := L_{gt} \cdot t = 1.63\ in^2$

Net Tension Area $A_{nt} := L_{nt} \cdot t = 1.22 \cdot in^2$

Test Side Block Shear Capacity $Cap_{BlockShear.T} := F_u \cdot A_{nt} + min(0.6 \cdot F_u \cdot A_{nv}, 0.6 \cdot F_y \cdot A_{gv})$ Eqn J4-5

$Cap_{BlockShear.T} = 312\ kip$

Block Shear Checks

Yoke Side Block Shear

Gross Shear Length $L_{gv} := (N_Y - 1) \cdot S_Y + L_h = 5\ in$

Net Shear Length $L_{nv} := L_{gv} - (N_Y - .5) \cdot d_{hY} = 3.31\ in$

Gross Tension Length $L_{gt} := L_v = 1.63\ in$

Net Tension Length $L_{nt} := L_{gt} - \frac{d_{hY}}{2} = 1.0625\ in$

Gross Shear Area $A_{gv} := L_{gv} \cdot t = 5\ in^2$

Net Shear Area $A_{nv} := L_{nv} \cdot t = 3.31\ in^2$

Gross Tension Area $A_{gt} := L_{gt} \cdot t = 1.63\ in^2$

Net Tension Area $A_{nt} := L_{nt} \cdot t = 1.06 \cdot in^2$

Test Side Block Shear Capacity $Cap_{BlockShear.Y} := F_u \cdot A_{nt} + min(0.6 \cdot F_u \cdot A_{nv}, 0.6 \cdot F_y \cdot A_{gv})$ Eqn J4-5

Test Side	Yoke Side
$Cap_{BoltShear.T} = 107.35\ kip$	$Cap_{BoltShear.Y} = 127.23\ kip$
$Cap_{BoltBearing.T} = 526.5\ kip$	$Cap_{BoltBearing.Y} = 468\ kip$
$Cap_{BoltTearout.T} = 559.41\ kip$	$Cap_{BoltTearout.Y} = 336.37\ kip$
$Cap_{TensileRupt.T} = 142.59\ kip$	$Cap_{TensileRupt.Y} = 124.31\ kip$
$Cap_{BlockShear.T} = 312\ kip$	$Cap_{BlockShear.Y} = 198.25\ kip$

$Cap_{TensileYield} = 146.25\ kip$

Appendix D:

Shop Drawings

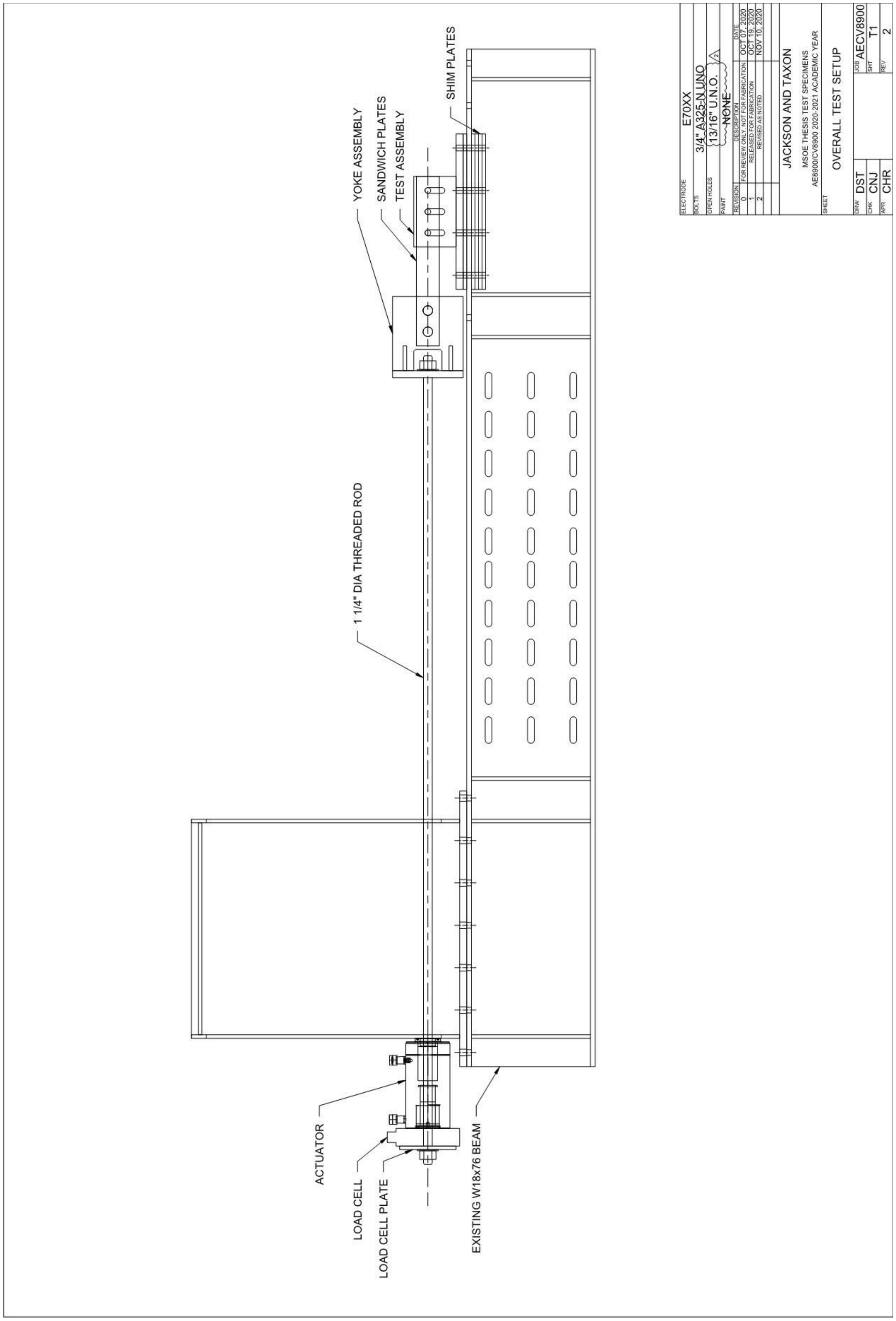
YOKE ASSEMBLY
SANDWICH PLATES
TEST ASSEMBLY
SHIM PLATES
1 1/4" DIA THREADED ROD
ACTUATOR
LOAD CELL
LOAD CELL PLATE
EXISTING W18x76 BEAM
ELECTRODE
E70XX
BOLTS
3/4" A325-N UNO
OPEN HOLES
13/16" U.N.O.
PAINT
NONE
REVISION
DESCRIPTION
DATE
0
FOR REVIEW ONLY, NOT FOR FABRICATION
OCT 07, 2020
1
RELEASED FOR FABRICATION
OCT 19, 2020
2
REVISED AS NOTED
NOV 10, 2020
JACKSON AND TAXON
MSOE THESIS TEST SPECIMENS
AE8900/CV8900 2020-2021 ACADEMIC YEAR
SHEET
OVERALL TEST SETUP
DRW DST
CHK CNJ
APR CHR
JOB AECV8900
SHT T1
REV 2

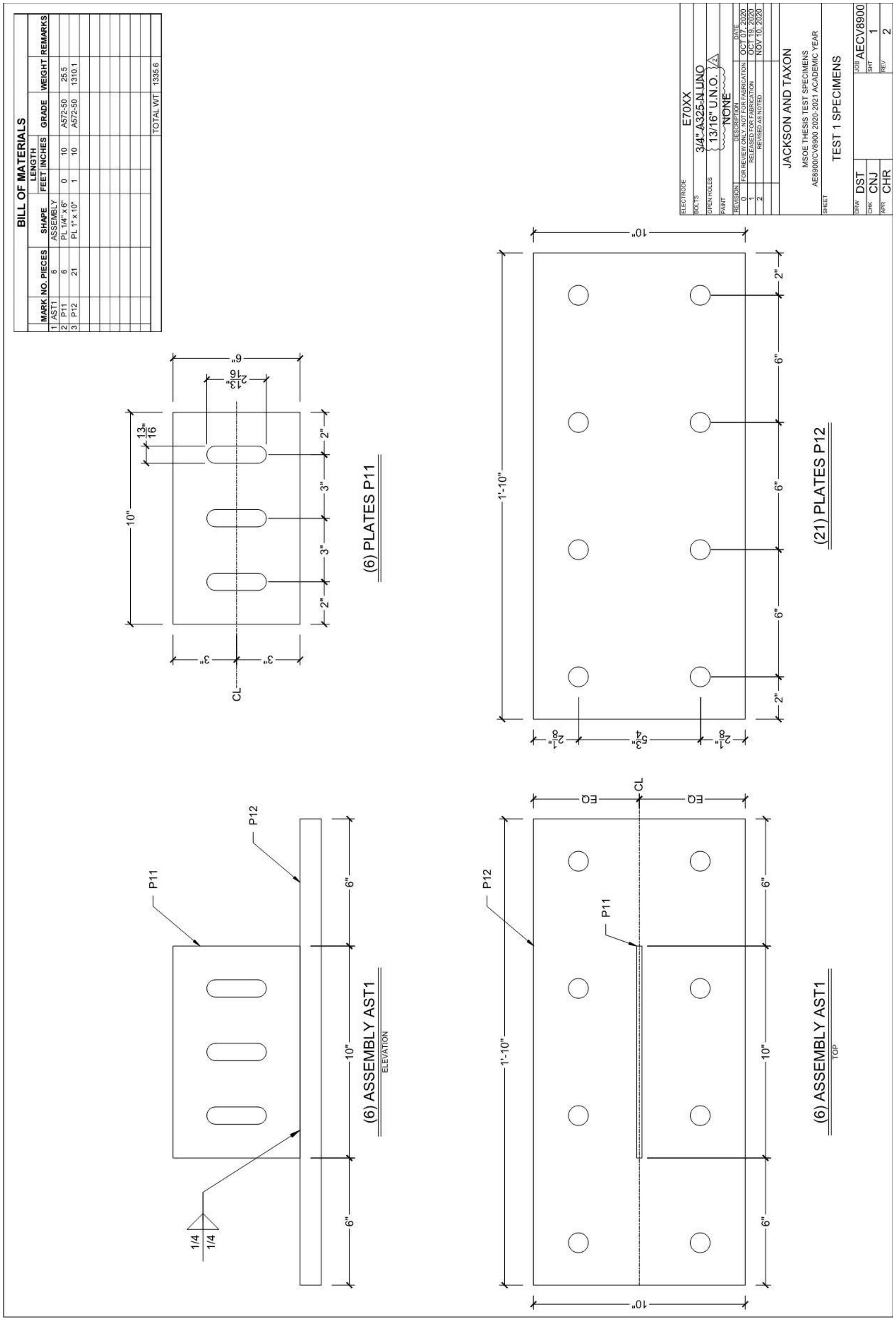
BILL OF MATERIALS
MARK NO. PIECES SHAPE LENGTH FEET INCHES GRADE WEIGHT REMARKS
1 AST1 6 ASSEMBLY
2 P11 6 PL 1/4" x 6" 0 10 A572-50 25.5
3 P12 21 PL 1" x 10" 1 10 A572-50 1310.1
TOTAL WT 1335.6
(6) ASSEMBLY AST1
ELEVATION
(6) PLATES P11
(6) ASSEMBLY AST1
TOP
(21) PLATES P12
ELECTRODE E70XX
BOLTS 3/4" A325-N UNO
OPEN HOLES 13/16" U.N.O.
PAINT NONE
REVISION DESCRIPTION DATE
0 FOR REVIEW ONLY, NOT FOR FABRICATION OCT 07, 2020
1 RELEASED FOR FABRICATION OCT 19, 2020
2 REVISED AS NOTED NOV 10, 2020
JACKSON AND TAXON
MSOE THESIS TEST SPECIMENS
AE8900/CV8900 2020-2021 ACADEMIC YEAR
SHEET TEST 1 SPECIMENS
DRW DST
CHK CNJ
APR CHR
JOB AECV8900
SHT 1
REV 2

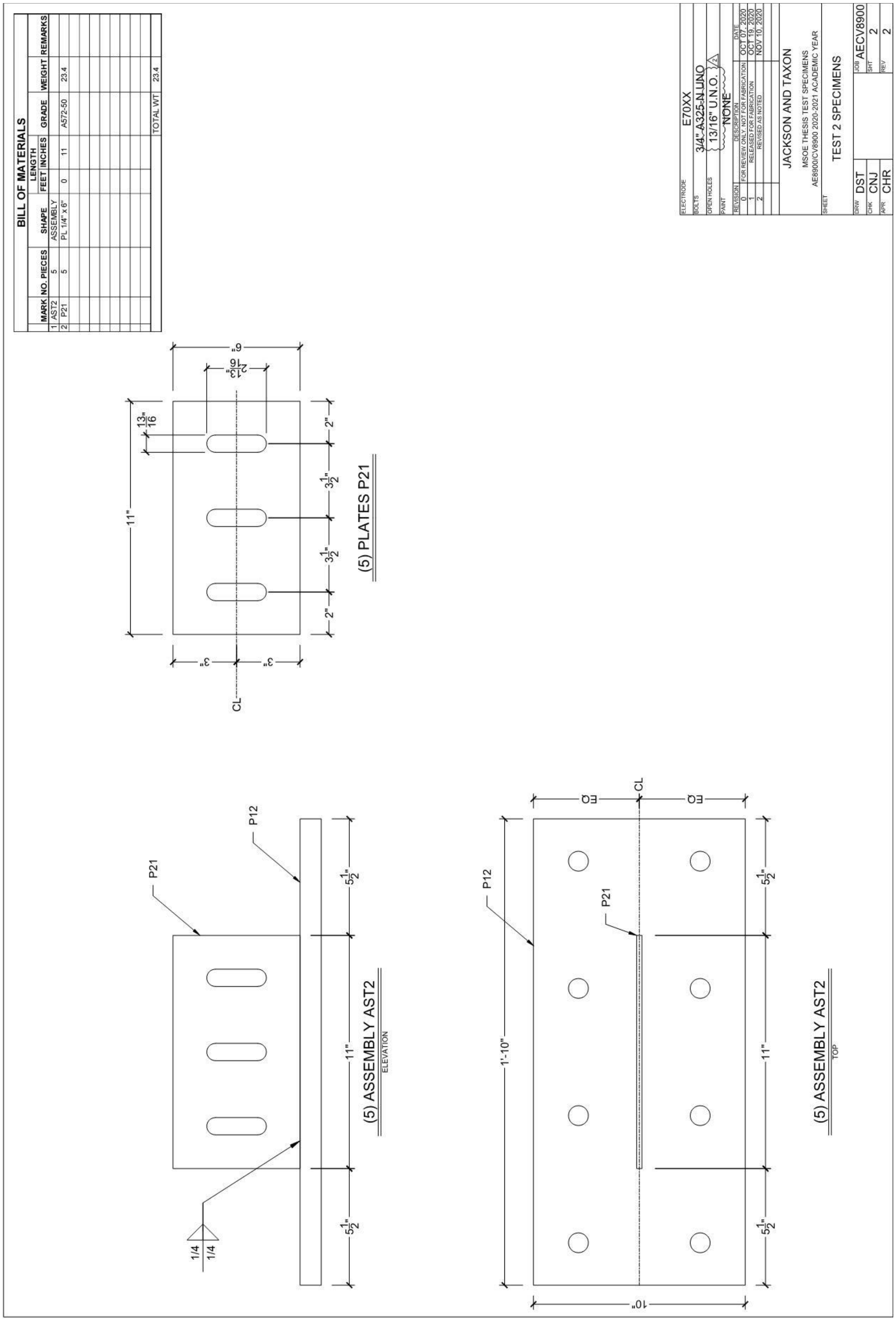
BILL OF MATERIALS
MARK | NO. PIECES | SHAPE | LENGTH FEET | LENGTH INCHES | GRADE | WEIGHT | REMARKS
1 AST2 | 5 | ASSEMBLY
2 P21 | 5 | PL 1/4" x 6" | 0 | 11 | A572-50 | 23.4
TOTAL WT 23.4
ELECTRODE E70XX
BOLTS 3/4" A325-N UNO
OPEN HOLES 13/16" U.N.O.
PAINT NONE
REVISION | DESCRIPTION | DATE
0 | FOR REVIEW ONLY, NOT FOR FABRICATION | OCT 07, 2020
1 | RELEASED FOR FABRICATION | OCT 19, 2020
2 | REVISED AS NOTED | NOV 10, 2020
JACKSON AND TAXON
MSOE THESIS TEST SPECIMENS
AE8900/CV8900 2020-2021 ACADEMIC YEAR
SHEET TEST 2 SPECIMENS
JOB AECV8900
SHT 2
REV 2
DRW DST
CHK CNJ
APR CHR
(5) PLATES P21
11"
13/16"
2 13/16"
6"
3"
3"
2"
3 1/2"
3 1/2"
2"
CL
(5) ASSEMBLY AST2
ELEVATION
P21
P12
1/4
1/4
5 1/2"
11"
5 1/2"
(5) ASSEMBLY AST2
TOP
P12
P21
1'-10"
EQ
EQ
CL
10"

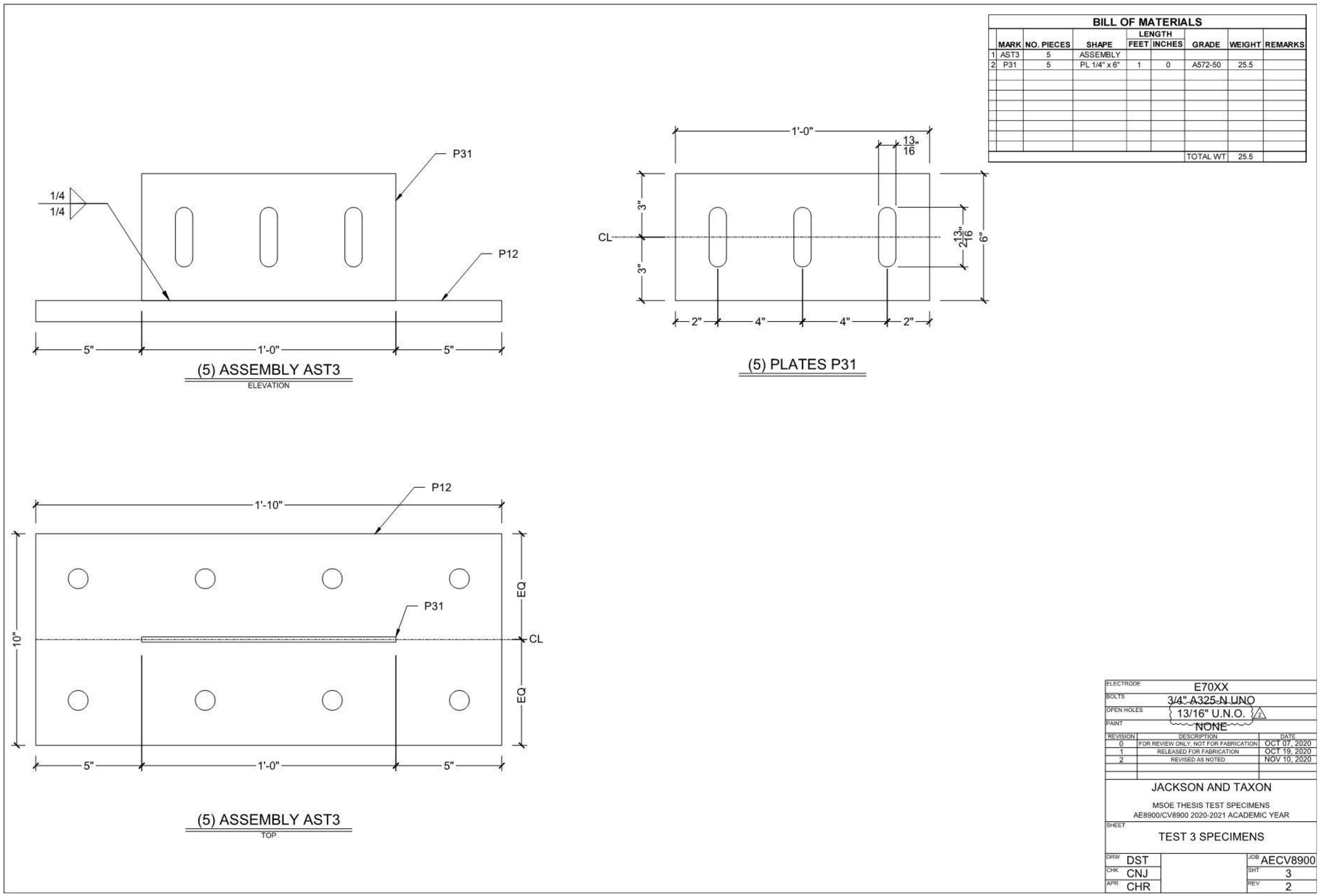
BILL OF MATERIALS
MARK | NO. PIECES | SHAPE | LENGTH FEET | LENGTH INCHES | GRADE | WEIGHT | REMARKS
1 AST3 | 5 | ASSEMBLY
2 P31 | 5 | PL 1/4" x 6" | 1 | 0 | A572-50 | 25.5
TOTAL WT 25.5
P31
P12
1/4
1/4
5"
1'-0"
5"
(5) ASSEMBLY AST3
ELEVATION
1'-0"
13/16"
CL
3"
3"
2 13/16"
6"
2"
4"
4"
2"
(5) PLATES P31
1'-10"
P12
P31
10"
EQ
CL
EQ
5"
1'-0"
5"
(5) ASSEMBLY AST3
TOP
ELECTRODE E70XX
BOLTS 3/4" A325-N UNO
OPEN HOLES 13/16" U.N.O.
PAINT NONE
REVISION | DESCRIPTION | DATE
0 | FOR REVIEW ONLY, NOT FOR FABRICATION | OCT 07, 2020
1 | RELEASED FOR FABRICATION | OCT 19, 2020
2 | REVISED AS NOTED | NOV 10, 2020
JACKSON AND TAXON
MSOE THESIS TEST SPECIMENS
AE8900/CV8900 2020-2021 ACADEMIC YEAR
SHEET
TEST 3 SPECIMENS
DRW DST
CHK CNJ
APR CHR
JOB AECV8900
SHT 3
REV 2

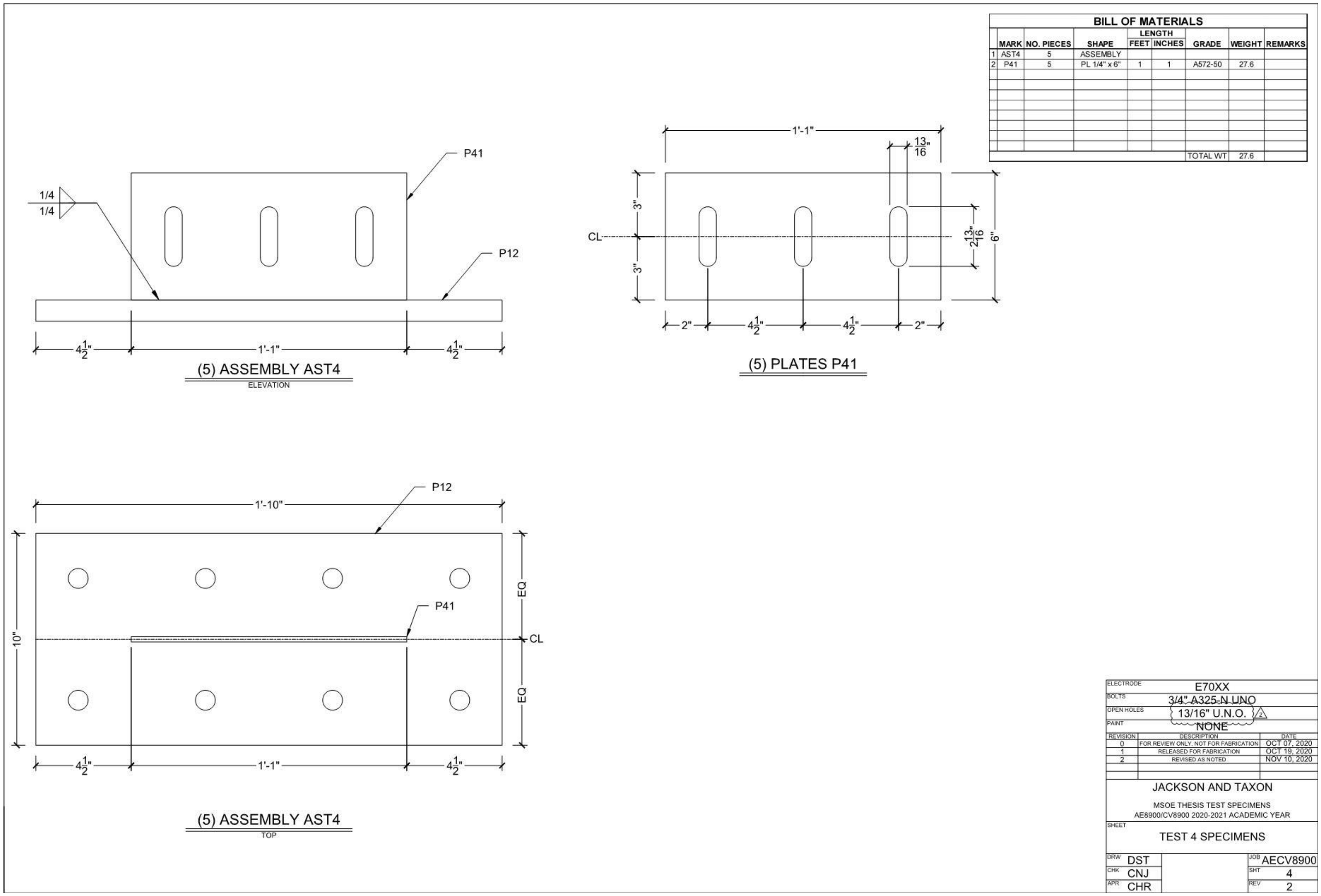
BILL OF MATERIALS
MARK | NO. PIECES | SHAPE | LENGTH FEET | LENGTH INCHES | GRADE | WEIGHT | REMARKS
1 AST4 | 5 | ASSEMBLY
2 P41 | 5 | PL 1/4" x 6" | 1 | 1 | A572-50 | 27.6
TOTAL WT 27.6
1/4
1/4
P41
P12
4½"
1'-1"
4½"
(5) ASSEMBLY AST4
ELEVATION
1'-1"
13/16"
CL
3"
3"
2 13/16"
6"
2"
4½"
4½"
2"
(5) PLATES P41
P12
1'-10"
P41
10"
EQ
CL
EQ
4½"
1'-1"
4½"
(5) ASSEMBLY AST4
TOP
ELECTRODE E70XX
BOLTS 3/4" A325-N UNO
OPEN HOLES 13/16" U.N.O.
PAINT NONE
REVISION | DESCRIPTION | DATE
0 | FOR REVIEW ONLY, NOT FOR FABRICATION | OCT 07, 2020
1 | RELEASED FOR FABRICATION | OCT 19, 2020
2 | REVISED AS NOTED | NOV 10, 2020
JACKSON AND TAXON
MSOE THESIS TEST SPECIMENS
AE8900/CV8900 2020-2021 ACADEMIC YEAR
SHEET
TEST 4 SPECIMENS
DRW DST
CHK CNJ
APR CHR
JOB AECV8900
SHT 4
REV 2

BILL OF MATERIALS

	MARK	NO. PIECES	SHAPE	LENGTH FEET	LENGTH INCHES	GRADE	WEIGHT	REMARKS
1	P51	5	PL 1" x 3 1/4"	2	0	A572-50	110.6	
2	P52	5	PL 1" x 3 1/4"	2	1	A572-50	115.2	
						TOTAL WT	225.8	

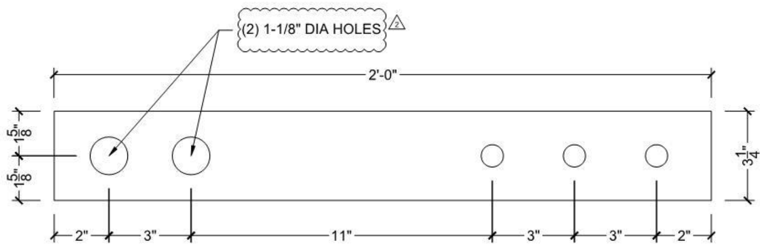

(2) PLATES P51

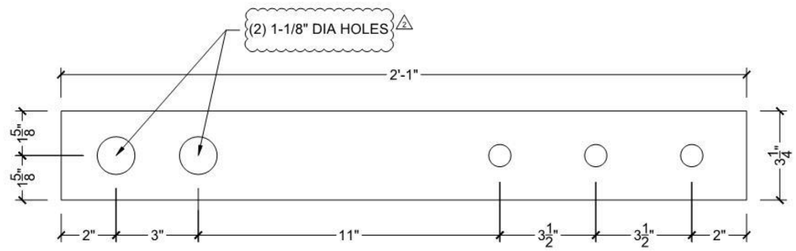

(2) PLATES P52

ELECTRODE	E70XX
BOLTS	~~3/4" A325-N UNO~~
OPEN HOLES	13/16" U.N.O.
PAINT	NONE

REVISION	DESCRIPTION	DATE
0	FOR REVIEW ONLY, NOT FOR FABRICATION	OCT 07, 2020
1	RELEASED FOR FABRICATION	OCT 19, 2020
2	REVISED AS NOTED	NOV 10, 2020

JACKSON AND TAXON

MSOE THESIS TEST SPECIMENS
AE8900/CV8900 2020-2021 ACADEMIC YEAR

SHEET: SANDWICH PLATES

DRW	DST	JOB	AECV8900
CHK	CNJ	SHT	5
APR	CHR	REV	2

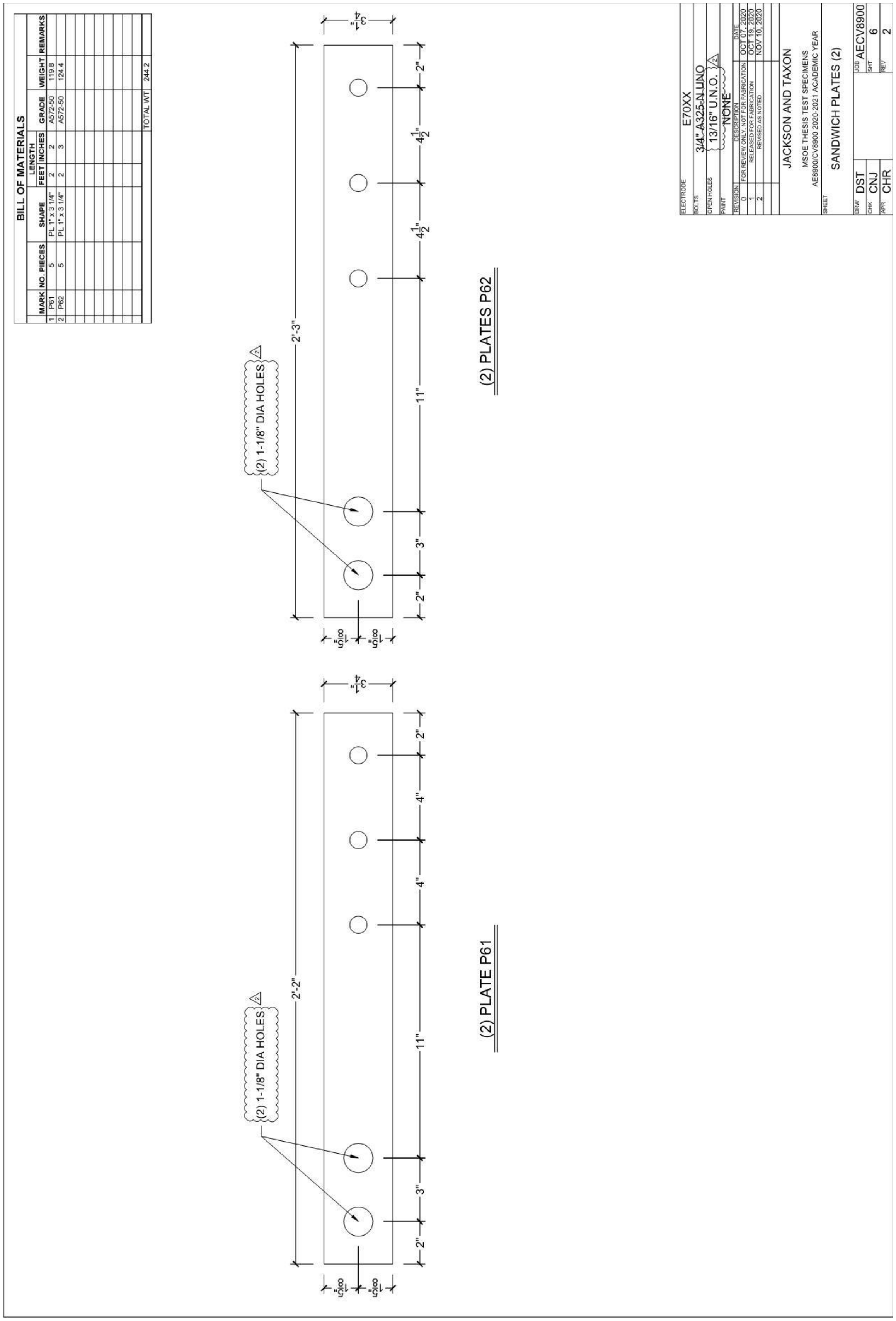

BILL OF MATERIALS

	MARK	NO. PIECES	SHAPE	LENGTH FEET	LENGTH INCHES	GRADE	WEIGHT	REMARKS
1	P61	5	PL 1" x 3 1/4"	2	2	A572-50	119.8	
2	P62	5	PL 1" x 3 1/4"	2	3	A572-50	124.4	
						TOTAL WT	244.2	

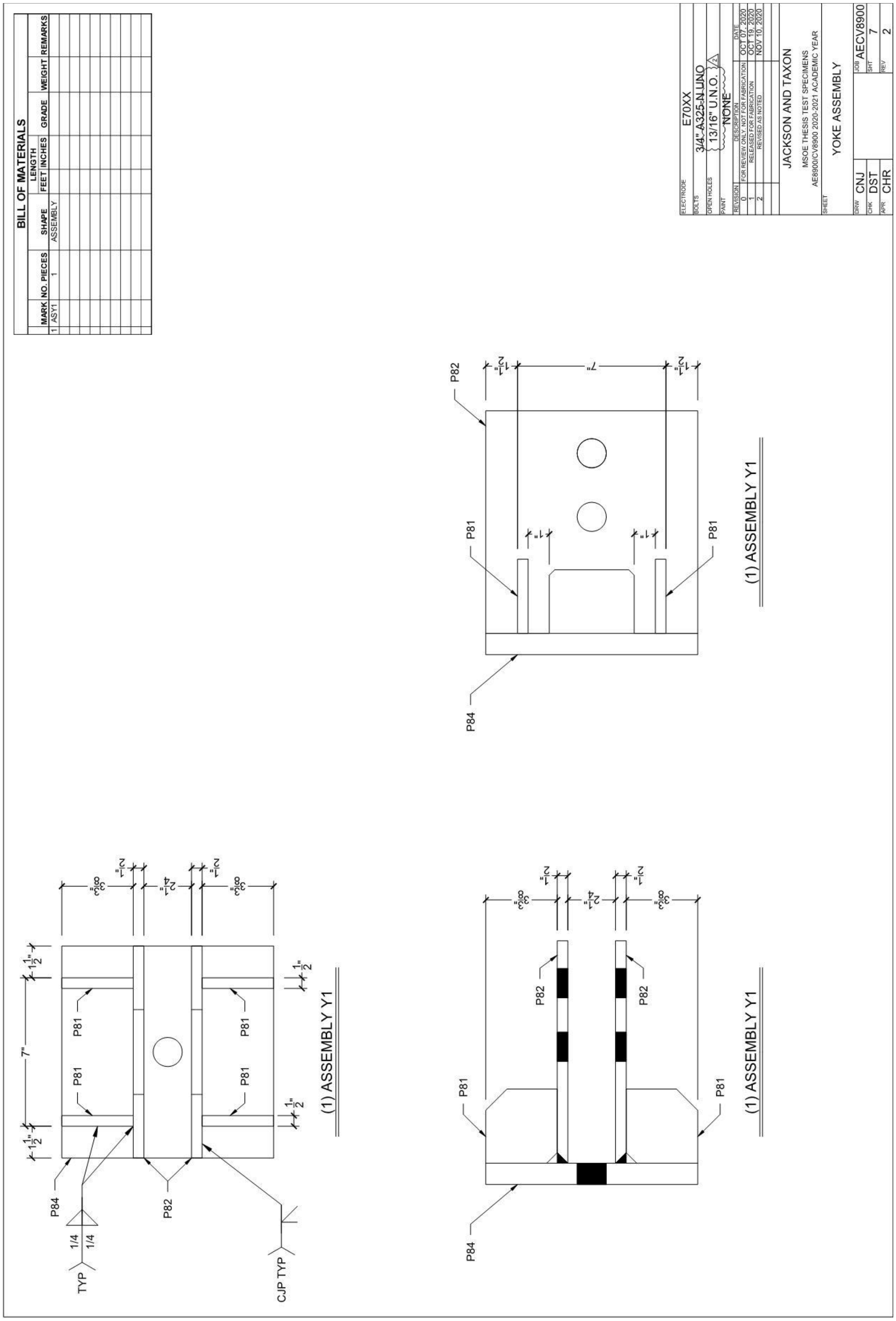

BILL OF MATERIALS
MARK
NO. PIECES
SHAPE
LENGTH
FEET
INCHES
GRADE
WEIGHT
REMARKS
1 ASY1
1
ASSEMBLY
ELECTRODE
E70XX
BOLTS
3/4" A325-N UNO
OPEN HOLES
13/16" U.N.O.
PAINT
NONE
REVISION
DESCRIPTION
DATE
0
FOR REVIEW ONLY, NOT FOR FABRICATION
OCT 07, 2020
1
RELEASED FOR FABRICATION
OCT 19, 2020
2
REVISED AS NOTED
NOV 10, 2020
JACKSON AND TAXON
MSOE THESIS TEST SPECIMENS
AE8900/CV8900 2020-2021 ACADEMIC YEAR
SHEET
YOKE ASSEMBLY
JOB
AECV8900
SHT
7
REV
2
DRW
CNJ
CHK
DST
APR
CHR
P81
P82
P84
TYP
1/4
1/4
CJP TYP
7"
(1) ASSEMBLY Y1
(1) ASSEMBLY Y1
(1) ASSEMBLY Y1

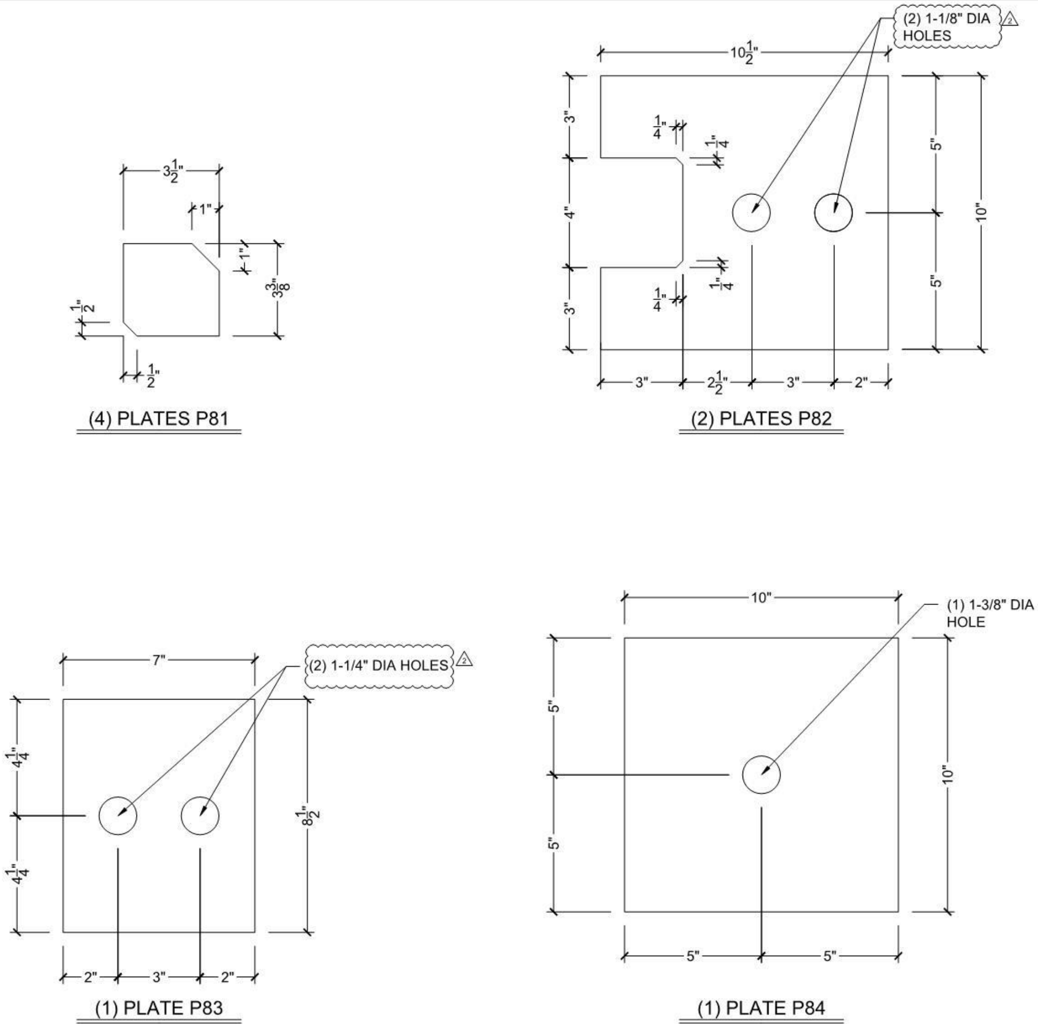

BILL OF MATERIALS

	MARK	NO. PIECES	SHAPE	LENGTH FEET	LENGTH INCHES	GRADE	WEIGHT	REMARKS
1	P81	4	PL 1/2" x 3 1/2"	0	3.375	A572-50	6.7	
2	P82	2	PL 1/2" x 10"	0	10.5	A572-50	29.8	BEVEL PLATE
3	P83	1	PL 1/4" x 8 1/2"	0	7	A572-50	4.2	
4	P84	1	PL 1" x 10"	0	10	A572-50	28.4	
						TOTAL WT	62.3	

ELECTRODE	E70XX	
BOLTS	~~3/4" A325-N UNO~~	
OPEN HOLES	13/16" U.N.O.	
PAINT	NONE	

REVISION	DESCRIPTION	DATE
0	FOR REVIEW ONLY, NOT FOR FABRICATION	OCT 07, 2020
1	RELEASED FOR FABRICATION	OCT 19, 2020
2	REVISED AS NOTED	NOV 10, 2020

JACKSON AND TAXON

MSOE THESIS TEST SPECIMENS

AE8900/CV8900 2020-2021 ACADEMIC YEAR

SHEET

YOKE PLATES

DRW	CNJ	JOB	AECV8900
CHK	DST	SHT	8
APR	CHR	REV	2

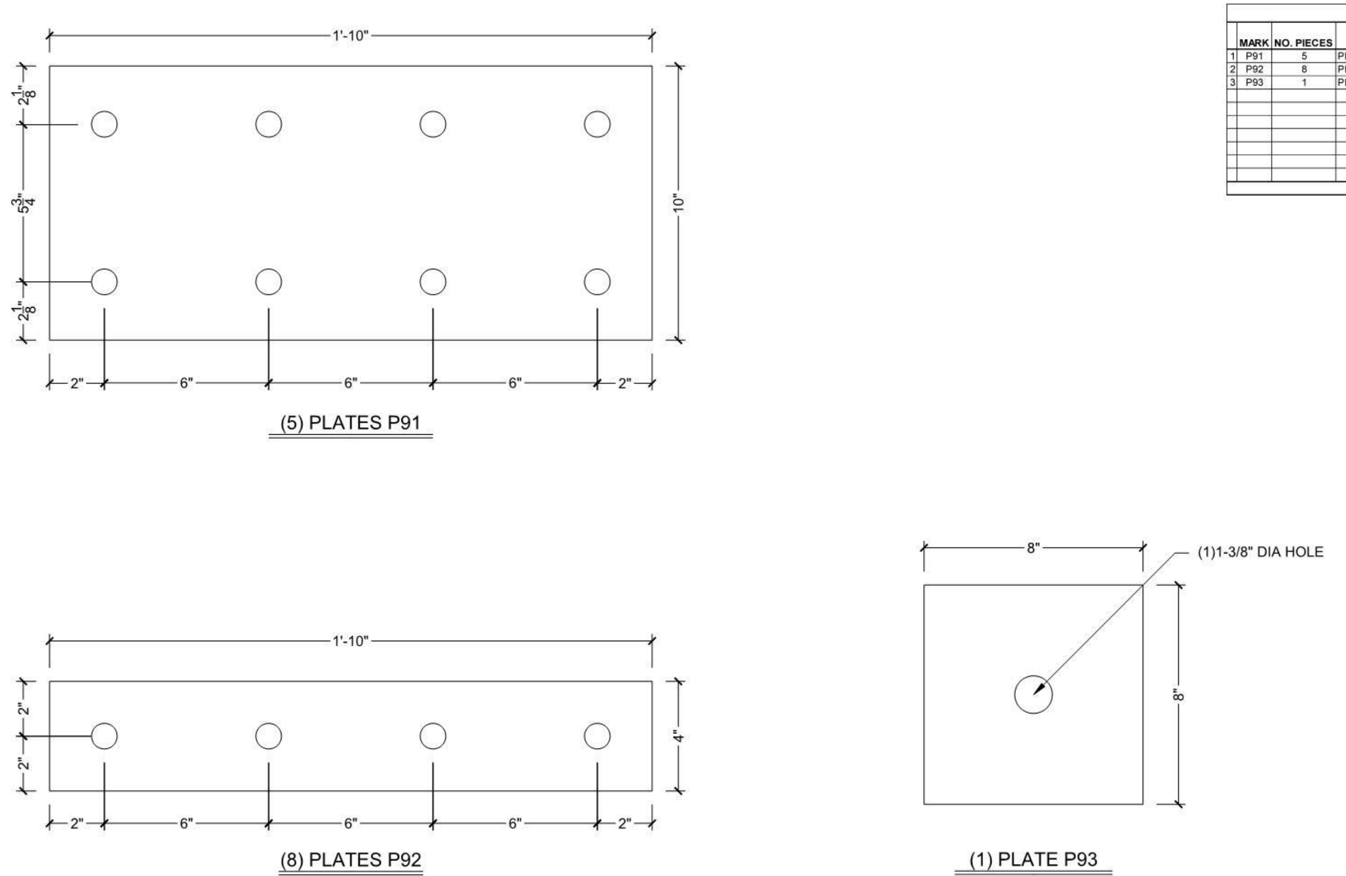

BILL OF MATERIALS

	MARK	NO. PIECES	SHAPE	LENGTH FEET	LENGTH INCHES	GRADE	WEIGHT	REMARKS
1	P91	5	PL 1/2" x 10"	1	10	A572-50	156.0	
2	P92	8	PL 1/2" x 4"	1	10	A572-50	99.8	
3	P93	1	PL 1" x 8"	0	8	A572-50	18.1	
						TOTAL WT	273.9	

ELECTRODE	E70XX
BOLTS	~~3/4" A325-N UNO~~
OPEN HOLES	13/16" U.N.O. (2)
PAINT	NONE

REVISION	DESCRIPTION	DATE
0	FOR REVIEW ONLY, NOT FOR FABRICATION	OCT 07, 2020
1	RELEASED FOR FABRICATION	OCT 19, 2020
2	REVISED AS NOTED	NOV 10, 2020

JACKSON AND TAXON

MSOE THESIS TEST SPECIMENS
AE8900/CV8900 2020-2021 ACADEMIC YEAR

SHEET: SHIM PLATES

DRW	DST	JOB	AECV8900
CHK	CNJ	SHT	9
APR	CHR	REV	2

	BILL OF MATERIALS							
				LENGTH				
	MARK	NO. PIECES	SHAPE	FEET	INCHES	GRADE	WEIGHT	REMARKS
1	P101	6	PL 1/4" x 1 1/2"	1	0	A572-50	7.7	
						TOTAL WT	7.7	

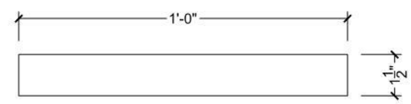

(6) PLATE P101

NOTE
THESE SPECIMENS SHALL BE CUT FROM THE SAME SHEET USED TO CREATE THE TEST ASSEMBLIES. PROVIDE MILL CERTIFICATION WITH MATERIAL.

ELECTRODE	E70XX
BOLTS	~~3/4" A325-N UNO~~
OPEN HOLES	13/16" U.N.O. (2)
PAINT	NONE

REVISION	DESCRIPTION	DATE
0	FOR REVIEW ONLY, NOT FOR FABRICATION	OCT 07, 2020
1	RELEASED FOR FABRICATION	OCT 19, 2020
2	REVISED AS NOTED	NOV 10, 2020

JACKSON AND TAXON

MSOE THESIS TEST SPECIMENS
AE8900/CV8900 2020-2021 ACADEMIC YEAR

SHEET: MATERIAL SAMPLE

DRW	DST	JOB	AECV8900
CHK	CNJ	SHT	10
APR	CHR	REV	2

Appendix E:

Material Testing Report

MAI METALLURGICAL ASSOCIATES, INC.

Tensile Test Report

MAI Report No:	220-3-235 REV1	**Date:**	January 15, 2021
Client:	Milwaukee School of Engineering	**Contact:**	Dr. Christopher Raebel
P.O. No:	Verbal	**Date Rec'd:**	December 22, 2020
Description:	Grade 50 Steel		

Property	11201407-P101 Sample1	11201407-P101 Sample2	112010407-P101 Sample3	112010407-P101 Sample4	ASTM A36
Test Bar Dimensions Width, inch Thickness, inch Gage Length, inches	 0.507 0.248 2.00	 0.500 0.247 2.00	 0.500 0.249 2.00	 0.488 0.248 2.00	 0.50 Material Thickness 2.0
Tensile Strength, psi	72,500	72,900	73,100	72,700	58,000 - 80,000
Yield Strength, psi (1)	62,600	62,200	63,200	62,200	36,000 min.
Yield/Tensile Ratio	0.86	0.86	0.86	0.86	Not Specified
Elongation, %	30	31	30	33	21 min.

Property	11201407-P101 Sample5	11201407-P101 Sample6	ASTM A36
Test Bar Dimensions Width, inch Thickness, inch Gage Length, inches	 0.481 0.247 2.00	 0.480 0.248 2.00	 0.50 Material Thickness 2.0
Tensile Strength, psi	73,000	72,900	58,000 - 80,000
Yield Strength, psi (1)	63,300	62,400	36,000 min.
Yield/Tensile Ratio	0.87	0.86	Not Specified
Elongation, %	31	31	21 min.

(1): at 0.2% offset

Notes: The tensile properties of all of the samples are in conformance with both ASTM A36, "Standard Specification for Carbon Structural Steel," and ASTM A992, "Standard Specification for Structural Steel Shapes."

The stress-strain curves for these samples are provided as separate Excel spreadsheets.

Respectfully submitted,

Anthony J. D'Antuono
Senior Metallurgical Engineer
Technical Manager

Appendix F:

Experimental Specimen Dimensions

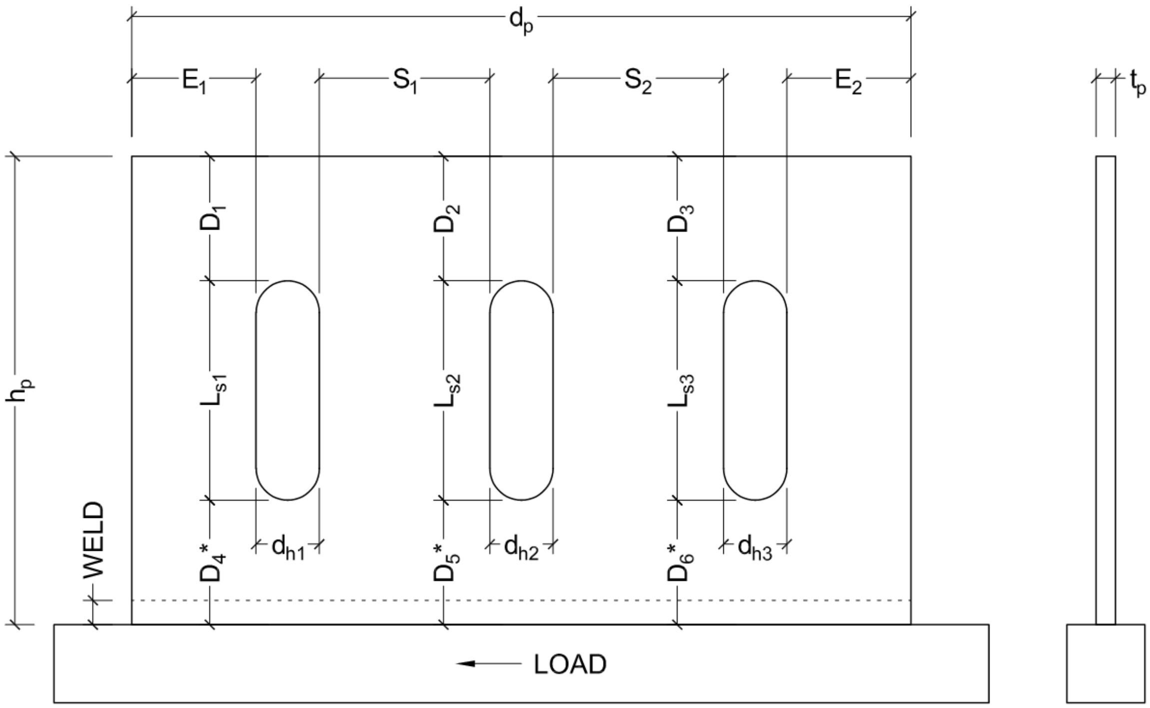

Figure F-1: Specimen Dimensions.

Table F-1: Experimental Specimen Dimensions.

Test Specimen	t_p	h_p	d_p	L_{s1}	L_{s2}	L_{s3}	WELD
	in. (mm)	*in. (mm)*	*in. (mm)*	*in. (mm)*	*in. (mm)*	*in. (mm)*	*in. (mm)*
S30P100	0.250 (6.35)	5.94 (151)	9.97 (253)	2.84 (72.2)	2.81 (71.4)	2.81 (71.4)	0.250 (6.35)
S35P100	0.249 (6.32)	5.97 (152)	10.9 (278)	2.81 (71.4)	2.81 (71.4)	2.84 (72.2)	0.250 (6.35)
S40P100	0.251 (6.36)	5.94 (151)	11.9 (303)	2.81 (71.4)	2.84 (72.2)	2.84 (72.2)	0.250 (6.35)
S45P100	0.250 (6.34)	5.94 (151)	12.9 (328)	2.84 (72.2)	1.84 (46.8)	2.84 (72.2)	0.250 (6.35)
S30P075	0.250 (6.34)	5.94 (151)	9.94 (252)	2.84 (72.2)	2.84 (72.2)	2.84 (72.2)	0.250 (6.35)
S35P075	0.249 (6.32)	5.94 (151)	10.9 (278)	2.84 (72.2)	2.84 (72.2)	2.84 (72.2)	0.250 (6.35)
S40P075	0.249 (6.32)	5.94 (151)	11.9 (303)	2.84 (72.2)	2.84 (72.2)	2.84 (72.2)	0.250 (6.35)
S45P075	0.249 (6.31)	5.94 (151)	12.9 (329)	2.84 (72.2)	2.84 (72.2)	2.84 (72.2)	0.250 (6.35)
S30P050	0.249 (6.31)	5.94 (151)	9.94 (252)	2.84 (72.2)	2.84 (72.2)	2.84 (72.2)	0.250 (6.35)
S35P050	0.249 (6.32)	5.94 (151)	10.9 (278)	2.84 (72.2)	2.84 (72.2)	2.84 (72.2)	0.250 (6.35)
S40P050	0.249 (6.32)	5.94 (151)	11.9 (303)	2.84 (72.2)	2.81 (71.4)	2.84 (72.2)	0.250 (6.35)
S45P050	0.249 (6.32)	5.94 (151)	12.9 (329)	2.84 (72.2)	2.84 (72.2)	2.84 (72.2)	0.250 (6.35)
S30P025	0.246 (6.25)	5.94 (151)	9.94 (252)	2.84 (72.2)	2.84 (72.2)	2.84 (72.2)	0.250 (6.35)
S35P025	0.249 (6.32)	5.94 (151)	10.9 (278)	2.88 (73.0)	2.88 (73.0)	2.88 (73.0)	0.250 (6.35)
S40P025	0.249 (6.31)	5.94 (151)	11.9 (303)	2.84 (72.2)	2.88 (73.0)	2.88 (73.0)	0.250 (6.35)
S45P025	0.248 (6.30)	5.94 (151)	12.9 (329)	2.88 (73.0)	2.88 (73.0)	2.88 (73.0)	0.250 (6.35)
S30P000	0.250 (6.34)	5.94 (151)	9.94 (252)	2.84 (72.2)	2.84 (72.2)	2.84 (72.2)	0.250 (6.35)
S35P000	0.249 (6.31)	5.94 (151)	10.9 (278)	2.84 (72.2)	2.84 (72.2)	2.84 (72.2)	0.250 (6.35)
S40P000	0.249 (6.32)	5.94 (151)	11.9 (303)	2.84 (72.2)	2.84 (72.2)	2.84 (72.2)	0.250 (6.35)
S45P000	0.249 (6.31)	5.94 (151)	12.9 (329)	2.84 (72.2)	2.84 (72.2)	2.84 (72.2)	0.250 (6.35)

Table F-1: Experimental Specimen Dimensions. (Continued)

Test Specimen	S_1 *in. (mm)*	S_2 *in. (mm)*	d_{h1} *in. (mm)*	d_{h2} *in. (mm)*	d_{h3} *in. (mm)*	E_1 *in. (mm)*	E_2 *in. (mm)*
S30P100	2.19 (55.6)	2.22 (56.4)	0.813 (20.6)	0.813 (20.6)	0.813 (20.6)	1.56 (39.7)	1.56 (39.7)
S35P100	2.69 (68.3)	2.69 (68.3)	0.813 (20.6)	0.813 (20.6)	0.813 (20.6)	1.56 (39.7)	1.56 (39.7)
S40P100	3.19 (81.0)	3.19 (81.0)	0.813 (20.6)	0.813 (20.6)	0.813 (20.6)	1.56 (39.7)	1.56 (39.7)
S45P100	3.69 (93.7)	3.66 (92.9)	0.813 (20.6)	0.813 (20.6)	0.813 (20.6)	1.56 (39.7)	1.56 (39.7)
S30P075	2.19 (55.6)	2.19 (55.6)	0.813 (20.6)	0.813 (20.6)	0.813 (20.6)	1.56 (39.7)	1.56 (39.7)
S35P075	2.69 (68.3)	2.69 (68.3)	0.813 (20.6)	0.813 (20.6)	0.813 (20.6)	1.56 (39.7)	1.56 (39.7)
S40P075	3.19 (81.0)	3.19 (81.0)	0.813 (20.6)	0.813 (20.6)	0.813 (20.6)	1.56 (39.7)	1.56 (39.7)
S45P075	3.69 (93.7)	3.69 (93.7)	0.813 (20.6)	0.813 (20.6)	0.813 (20.6)	1.56 (39.7)	1.56 (39.7)
S30P050	2.19 (55.6)	2.19 (55.6)	0.813 (20.6)	0.813 (20.6)	0.813 (20.6)	1.56 (39.7)	1.56 (39.7)
S35P050	2.69 (68.3)	2.69 (68.3)	0.813 (20.6)	0.813 (20.6)	0.813 (20.6)	1.56 (39.7)	1.56 (39.7)
S40P050	3.19 (81.0)	3.19 (81.0)	0.813 (20.6)	0.813 (20.6)	0.813 (20.6)	1.56 (39.7)	1.56 (39.7)
S45P050	3.69 (93.7)	3.69 (93.7)	0.813 (20.6)	0.813 (20.6)	0.813 (20.6)	1.56 (39.7)	1.56 (39.7)
S30P025	2.19 (55.6)	2.19 (55.6)	0.813 (20.6)	0.813 (20.6)	0.813 (20.6)	1.56 (39.7)	1.56 (39.7)
S35P025	2.69 (68.3)	2.69 (68.3)	0.813 (20.6)	0.813 (20.6)	0.813 (20.6)	1.56 (39.7)	1.56 (39.7)
S40P025	3.19 (81.0)	3.19 (81.0)	0.813 (20.6)	0.813 (20.6)	0.813 (20.6)	1.56 (39.7)	1.56 (39.7)
S45P025	3.69 (93.7)	3.69 (93.7)	0.813 (20.6)	0.813 (20.6)	0.813 (20.6)	1.56 (39.7)	1.56 (39.7)
S30P000	2.19 (55.6)	2.19 (55.6)	0.813 (20.6)	0.813 (20.6)	0.813 (20.6)	1.56 (39.7)	1.56 (39.7)
S35P000	2.69 (68.3)	2.69 (68.3)	0.813 (20.6)	0.813 (20.6)	0.813 (20.6)	1.56 (39.7)	1.56 (39.7)
S40P000	3.19 (81.0)	3.19 (81.0)	0.813 (20.6)	0.813 (20.6)	0.813 (20.6)	1.56 (39.7)	1.56 (39.7)
S45P000	3.69 (93.7)	3.69 (93.7)	0.813 (20.6)	0.813 (20.6)	0.813 (20.6)	1.56 (39.7)	1.56 (39.7)

Table F-1: Experimental Specimen Dimensions. (Continued)

Test Specimen	D_1	D_2	D_3	D_4*	D_5*	D_6*
	in. (mm)	*in. (mm)*	*in. (mm)*	*in. (mm)*	*in. (mm)*	*in. (mm)*
S30P100	1.56 (39.7)	1.56 (39.7)	1.56 (39.7)	1.53 (38.9)	1.56 (39.7)	1.56 (39.7)
S35P100	1.56 (39.7)	1.56 (39.7)	1.56 (39.7)	1.59 (40.5)	1.59 (40.5)	1.56 (39.7)
S40P100	1.56 (39.7)	1.56 (39.7)	1.56 (39.7)	1.56 (39.7)	1.53 (38.9)	1.53 (38.9)
S45P100	1.56 (39.7)	1.56 (39.7)	1.56 (39.7)	1.53 (38.9)	2.53 (64.3)	1.53 (38.9)
S30P075	1.56 (39.7)	1.56 (39.7)	1.56 (39.7)	1.53 (38.9)	1.53 (38.9)	1.53 (38.9)
S35P075	1.56 (39.7)	1.56 (39.7)	1.56 (39.7)	1.53 (38.9)	1.53 (38.9)	1.53 (38.9)
S40P075	1.56 (39.7)	1.56 (39.7)	1.56 (39.7)	1.53 (38.9)	1.53 (38.9)	1.53 (38.9)
S45P075	1.56 (39.7)	1.56 (39.7)	1.56 (39.7)	1.53 (38.9)	1.53 (38.9)	1.53 (38.9)
S30P050	1.56 (39.7)	1.56 (39.7)	1.56 (39.7)	1.53 (38.9)	1.53 (38.9)	1.53 (38.9)
S35P050	1.56 (39.7)	1.56 (39.7)	1.56 (39.7)	1.53 (38.9)	1.53 (38.9)	1.53 (38.9)
S40P050	1.56 (39.7)	1.56 (39.7)	1.56 (39.7)	1.53 (38.9)	1.56 (39.7)	1.53 (38.9)
S45P050	1.56 (39.7)	1.56 (39.7)	1.56 (39.7)	1.53 (38.9)	1.53 (38.9)	1.53 (38.9)
S30P025	1.56 (39.7)	1.56 (39.7)	1.56 (39.7)	1.53 (38.9)	1.53 (38.9)	1.53 (38.9)
S35P025	1.56 (39.7)	1.56 (39.7)	1.56 (39.7)	1.50 (38.1)	1.50 (38.1)	1.50 (38.1)
S40P025	1.56 (39.7)	1.56 (39.7)	1.56 (39.7)	1.53 (38.9)	1.50 (38.1)	1.50 (38.1)
S45P025	1.56 (39.7)	1.56 (39.7)	1.56 (39.7)	1.50 (38.1)	1.50 (38.1)	1.50 (38.1)
S30P000	1.56 (39.7)	1.56 (39.7)	1.56 (39.7)	1.53 (38.9)	1.53 (38.9)	1.53 (38.9)
S35P000	1.56 (39.7)	1.56 (39.7)	1.56 (39.7)	1.53 (38.9)	1.53 (38.9)	1.53 (38.9)
S40P000	1.56 (39.7)	1.56 (39.7)	1.56 (39.7)	1.53 (38.9)	1.53 (38.9)	1.53 (38.9)
S45P000	1.56 (39.7)	1.56 (39.7)	1.56 (39.7)	1.53 (38.9)	1.53 (38.9)	1.53 (38.9)

*Calculated dimension

Appendix G:

Post-Test Specimen Photos

Photos for each specimen include front elevation, profile at loaded edge, and any other features of interest. See the caption for a description of each photo. More photos taken during the experimental testing of the specimens and setup can be provided upon request.

Figure G-1: Specimen S30P100 Post-Test, Front.

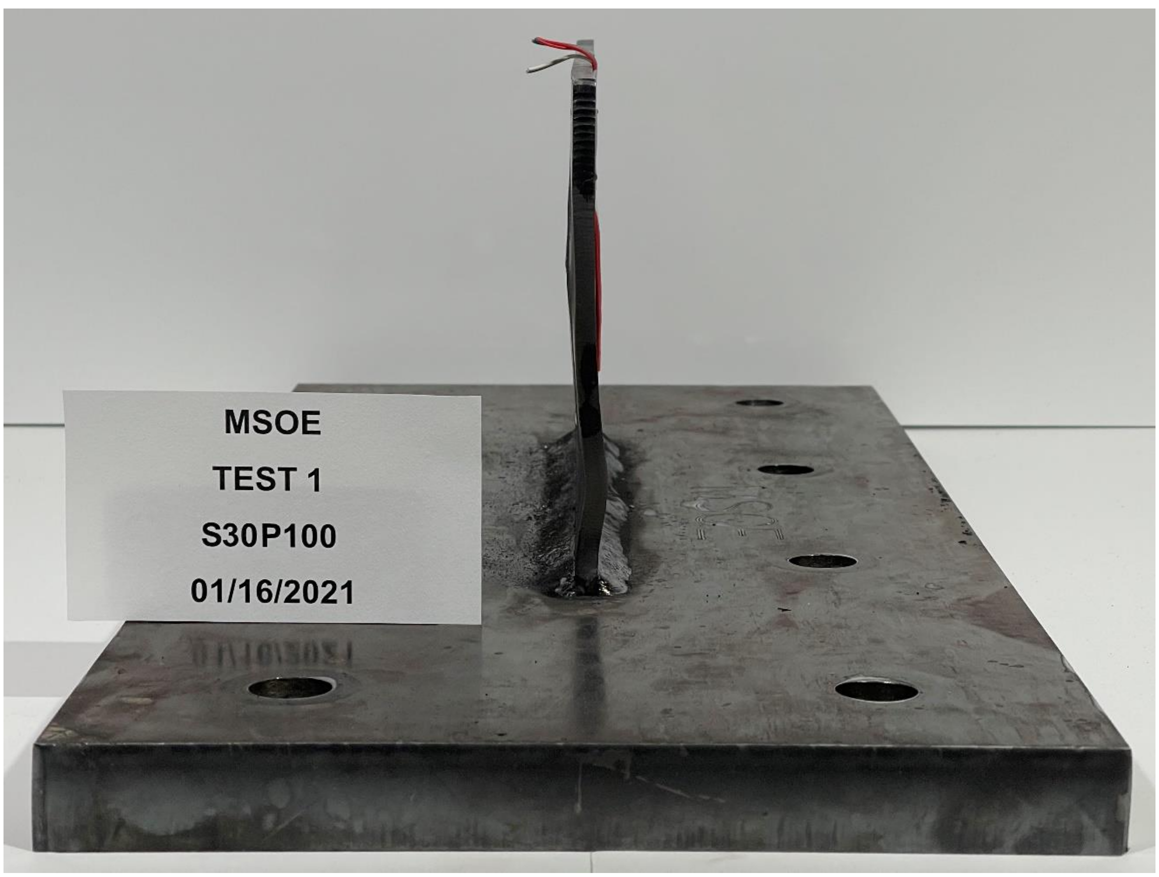

Figure G-2: Specimen S30P100 Post-Test, Loaded Edge.

Figure G-3: Specimen S35P100 Post-Test, Front.

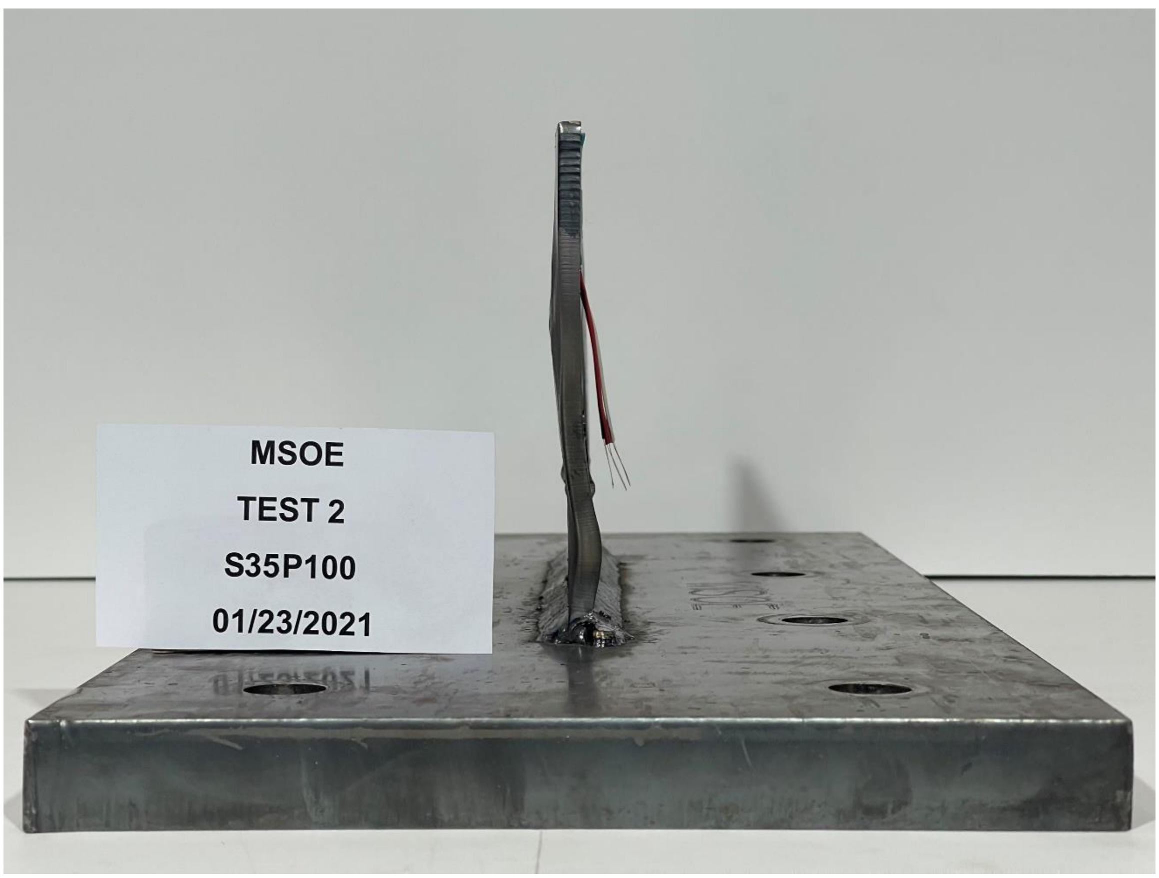

Figure G-4: Specimen S35P100 Post-Test, Loaded Edge.

Figure G-5: Specimen S40P100 Post-Test, Front.

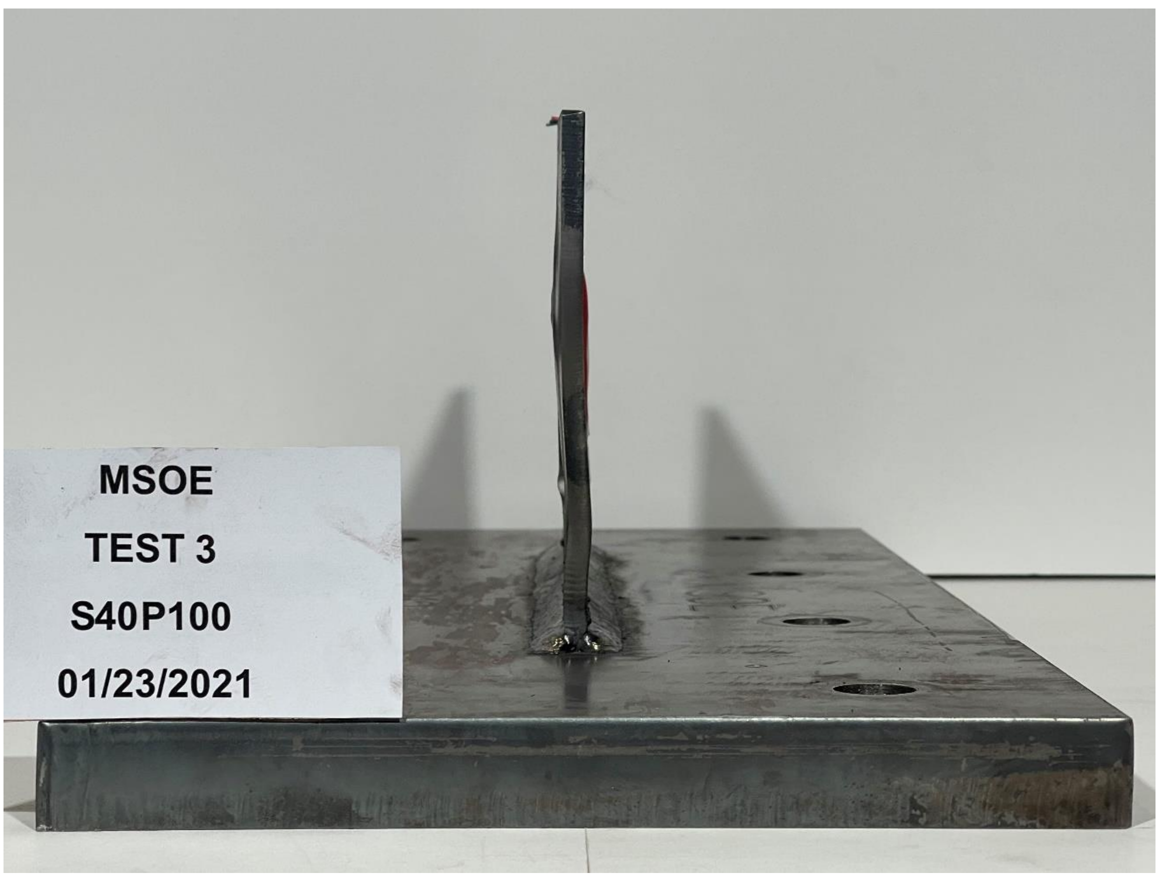

Figure G-6: Specimen S40P100 Post-Test, Loaded Edge.

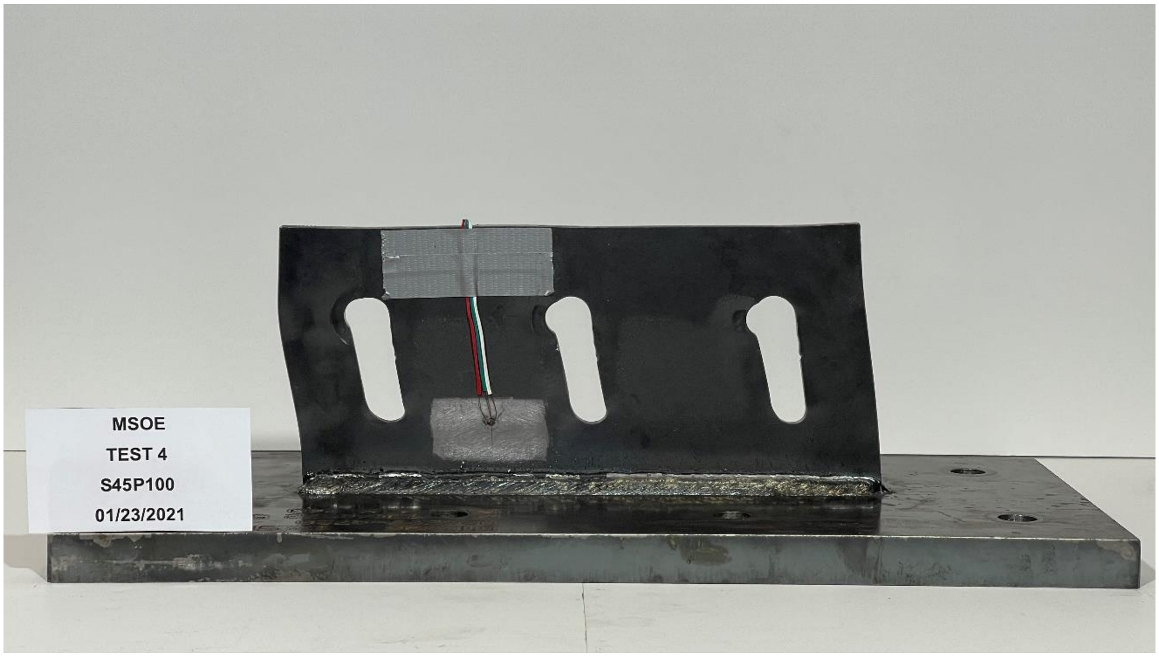

Figure G-7: Specimen S45P100 Post-Test, Front.

Figure G-8: Specimen S45P100 Post-Test, Loaded Edge.

Figure G-9: Specimen S30P075 Post-Test, Front.

Figure G-10: Specimen S30P075 Post-Test, Loaded Edge.

Figure G-11: Specimen S35P075 Post-Test, Front.

Figure G-12: Specimen S35P075 Post-Test, Loaded Edge.

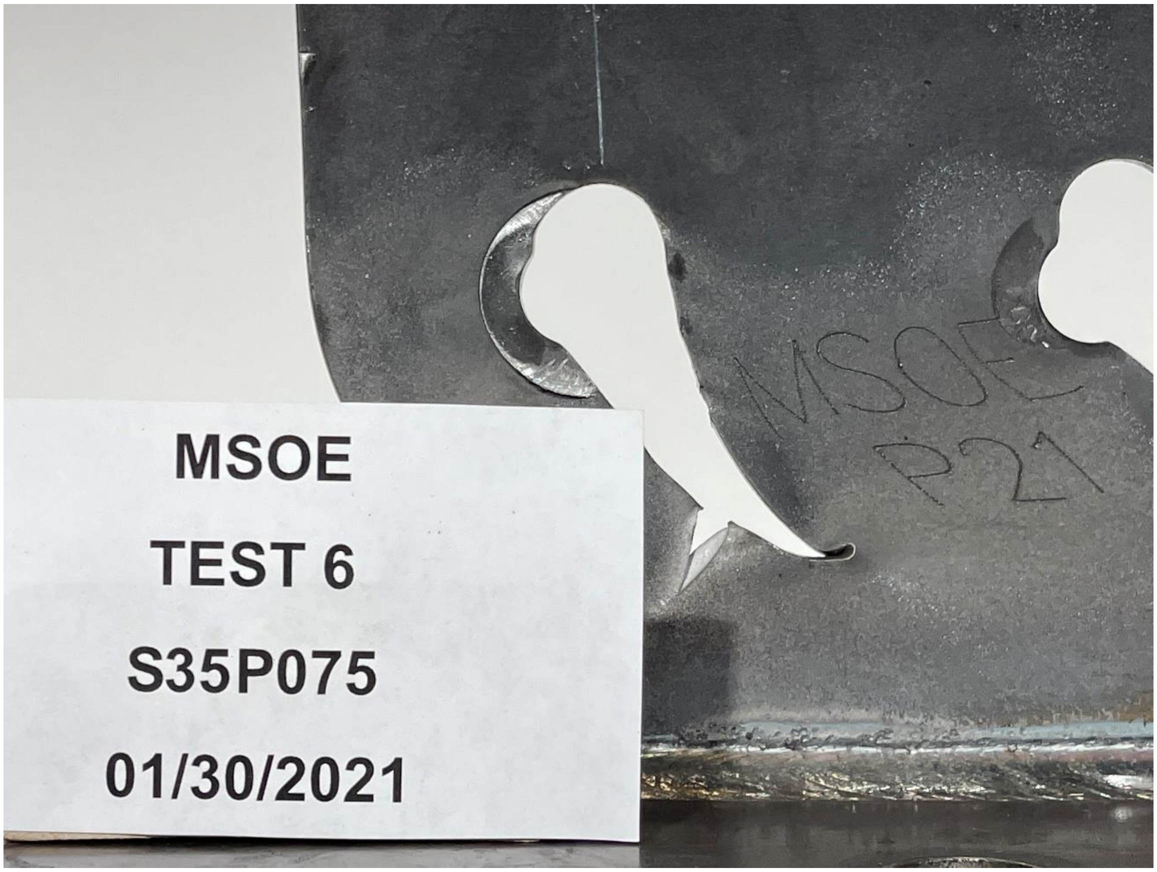

Figure G-13: Specimen S35P075 Post-Test, Plate Tearing.

Figure G-14: Specimen S40P075 Post-Test, Front.

Figure G-15: Specimen S40P075 Post-Test, Loaded Edge.

Figure G-16: Specimen S45P075 Post-Test, Front.

Figure G-17: Specimen S45P075 Post-Test, Loaded Edge.

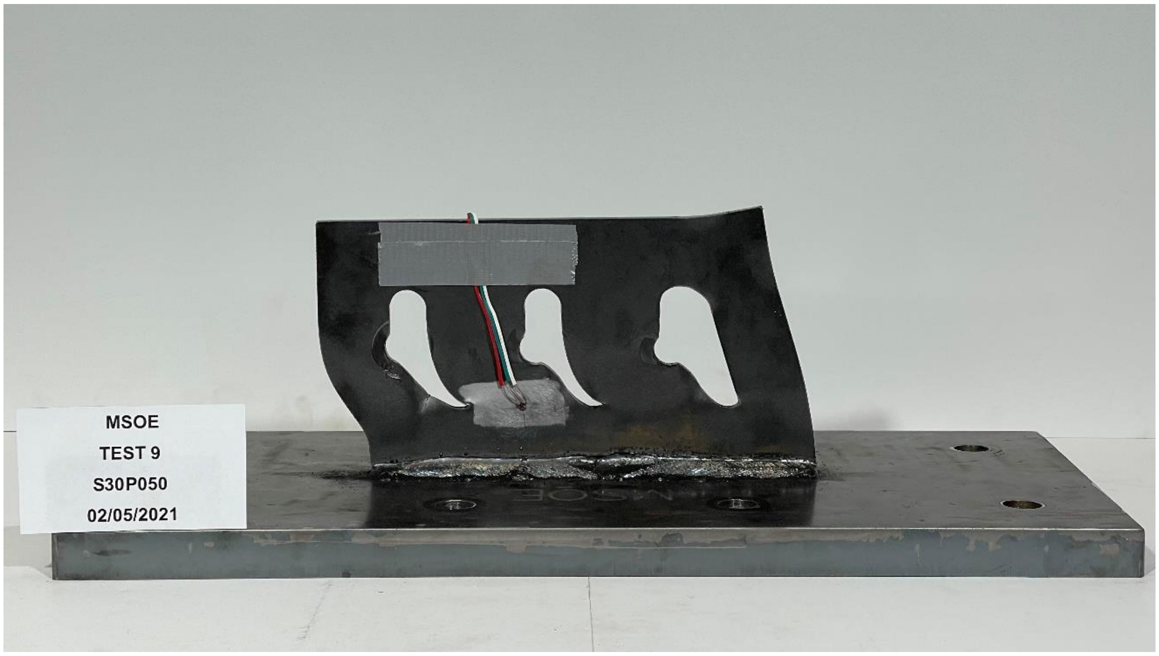

Figure G-18: Specimen S30P050 Post-Test, Front.

Figure G-19: Specimen S30P050 Post-Test, Loaded Edge.

Figure G-20: Specimen S30P050 Post-Test, Plate Tearing.

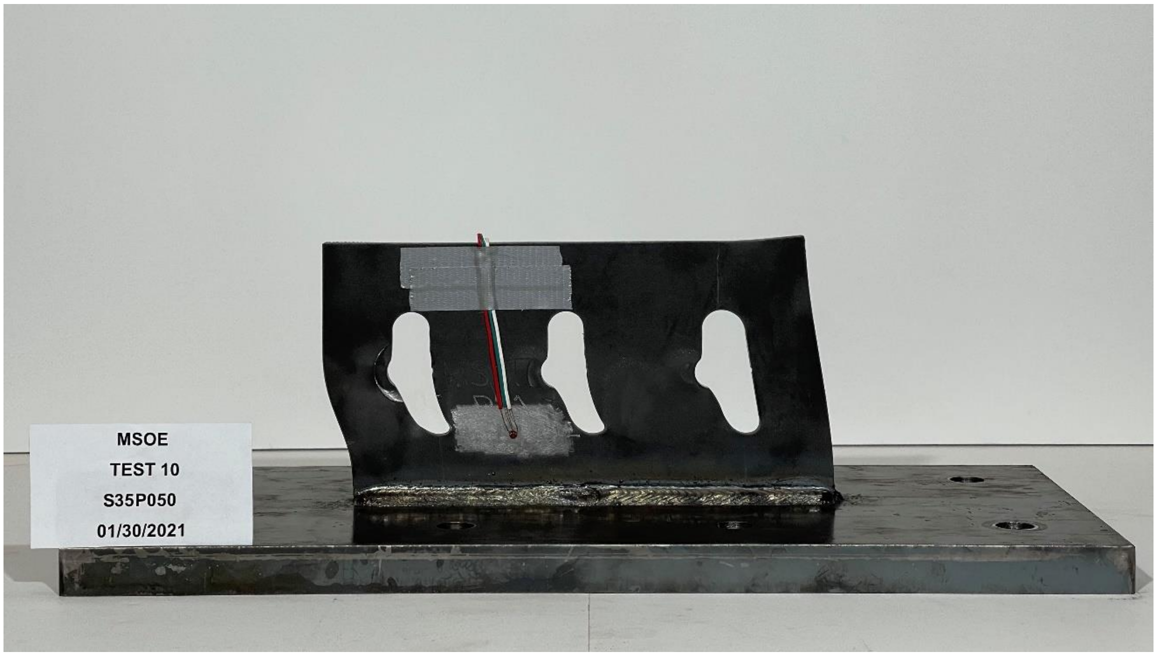

Figure G-21: Specimen S35P050 Post-Test, Front.

Figure G-22: Specimen S35P050 Post-Test, Loaded Edge.

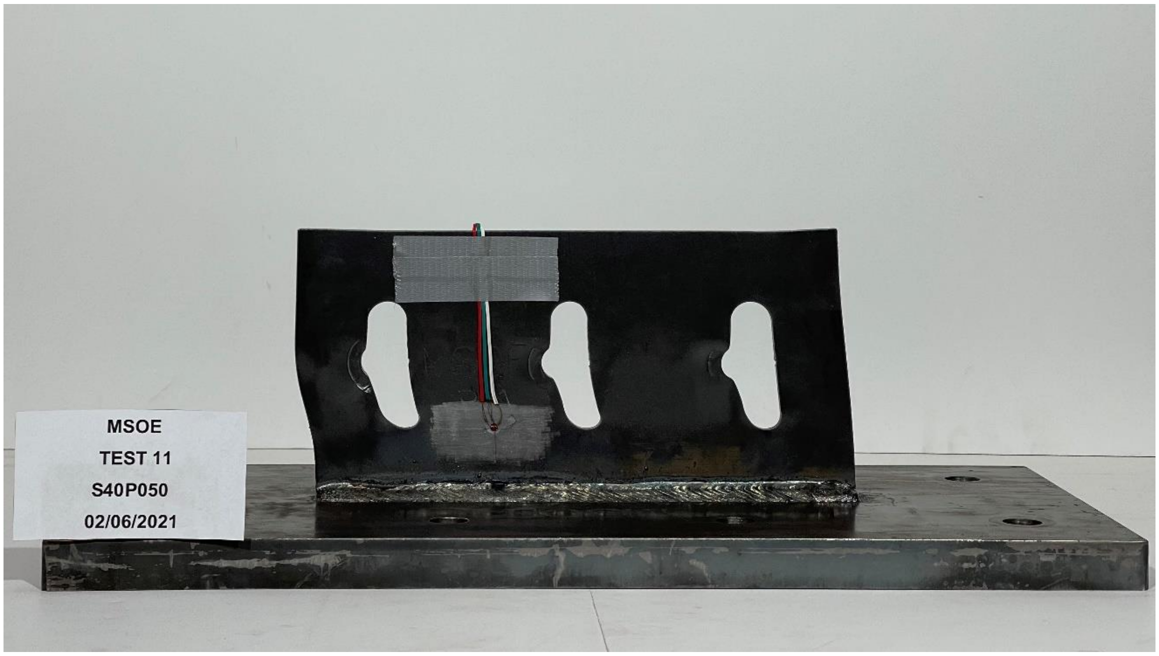

Figure G-23: Specimen S40P050 Post-Test, Front.

Figure G-24: Specimen S40P050 Post-Test, Loaded Edge.

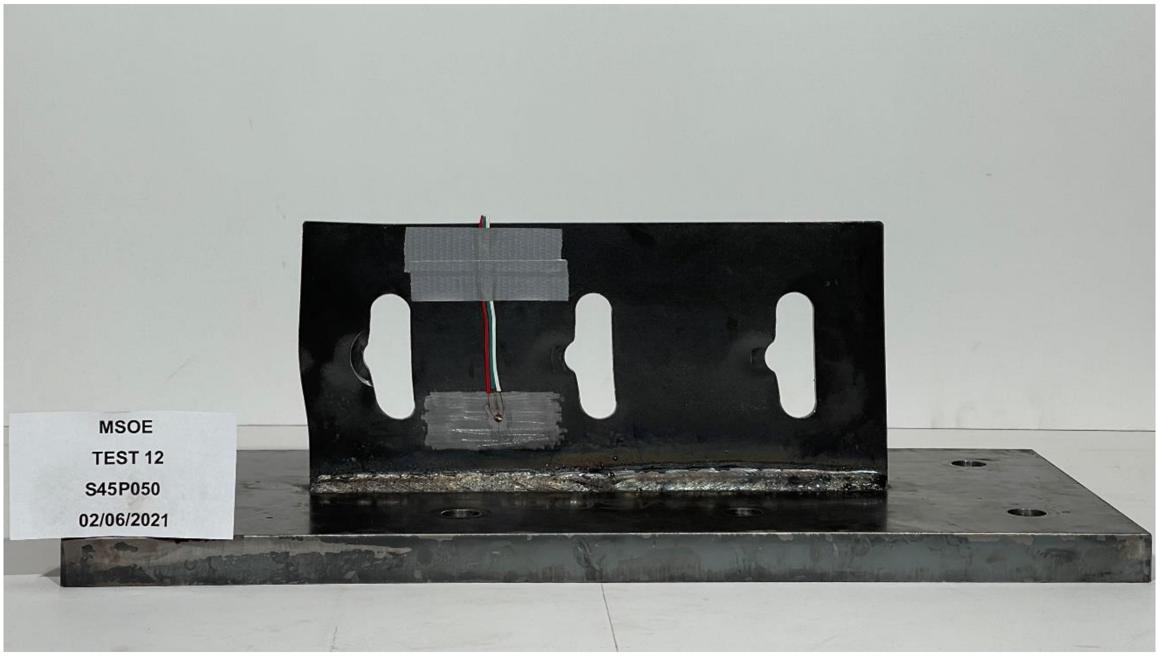

Figure G-25: Specimen S45P050 Post-Test, Front.

Figure G-26: Specimen S45P050 Post-Test, Loaded Edge.

Figure G-27: Specimen S30P025 Post-Test, Front.

Figure G-28: Specimen S30P025 Post-Test, Loaded Edge.

Figure G-29: Specimen S35P025 Post-Test, Front.

Figure G-30: Specimen S35P025 Post-Test, Loaded Edge.

Figure G-31: Specimen S40P025 Post-Test, Front.

Figure G-32: Specimen S40P025 Post-Test, Loaded Edge.

Figure G-33: Specimen S45P025 Post-Test, Front.

Figure G-34: Specimen S45P025 Post-Test, Loaded Edge.

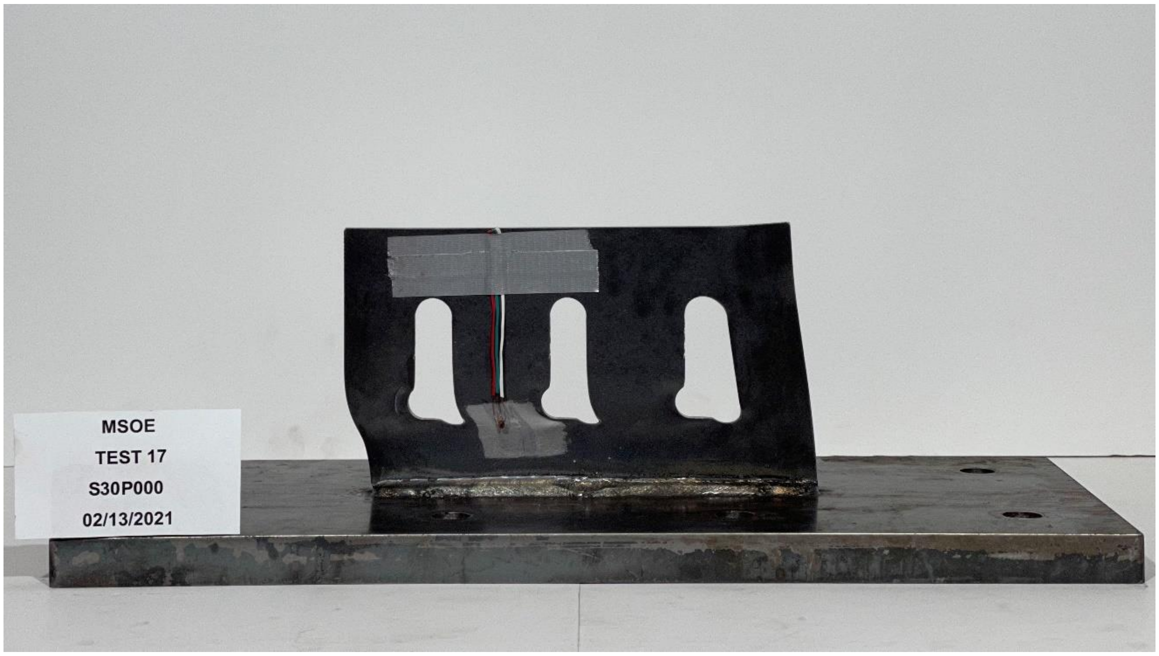

Figure G-35: Specimen S30P000 Post-Test, Front.

Figure G-36: Specimen S30P000 Post-Test, Loaded Edge.

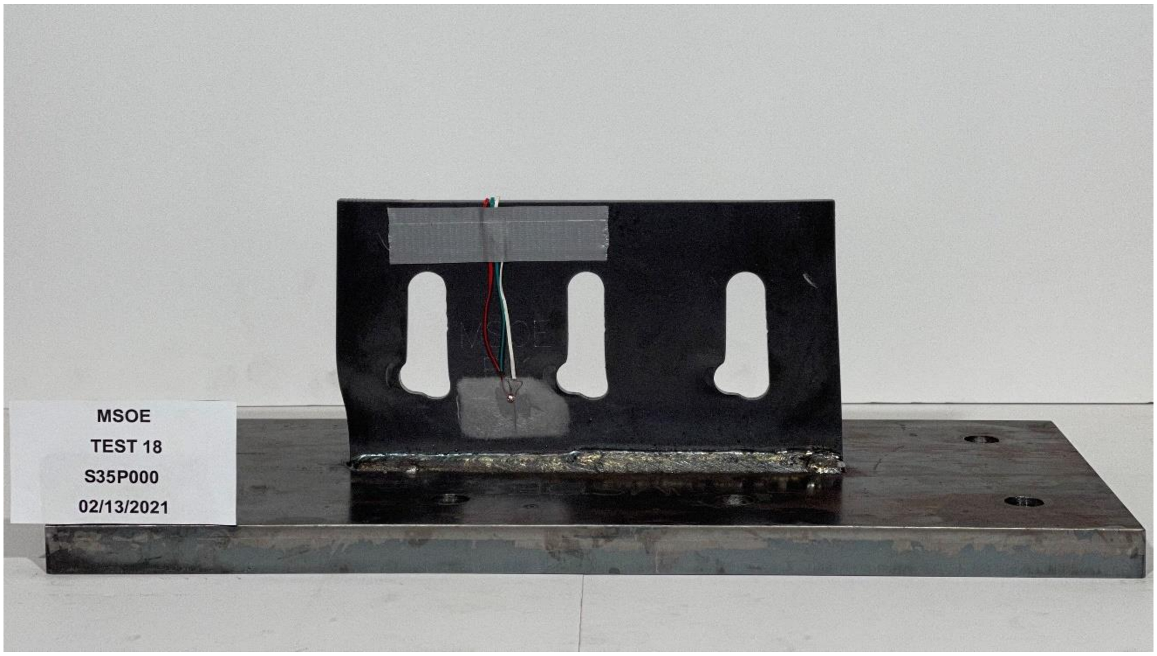

Figure G-37: Specimen S35P000 Post-Test, Front.

Figure G-38: Specimen S35P000 Post-Test, Loaded Edge.

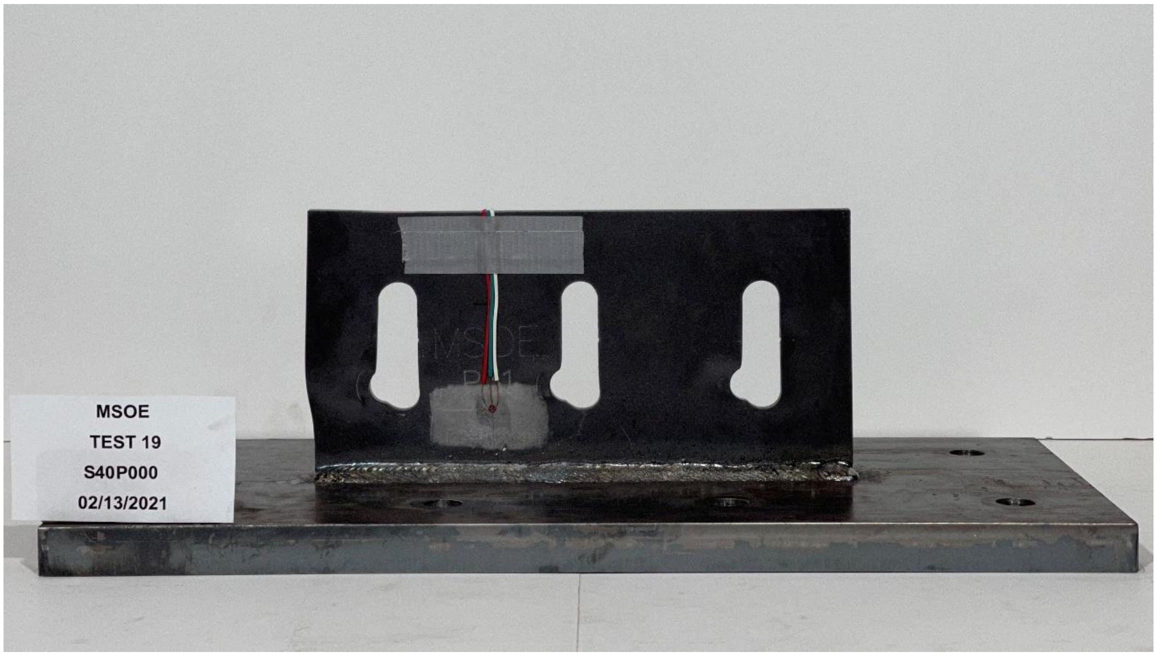

Figure G-39: Specimen S40P000 Post-Test, Front.

Figure G-40: Specimen S40P000 Post-Test, Loaded Edge.

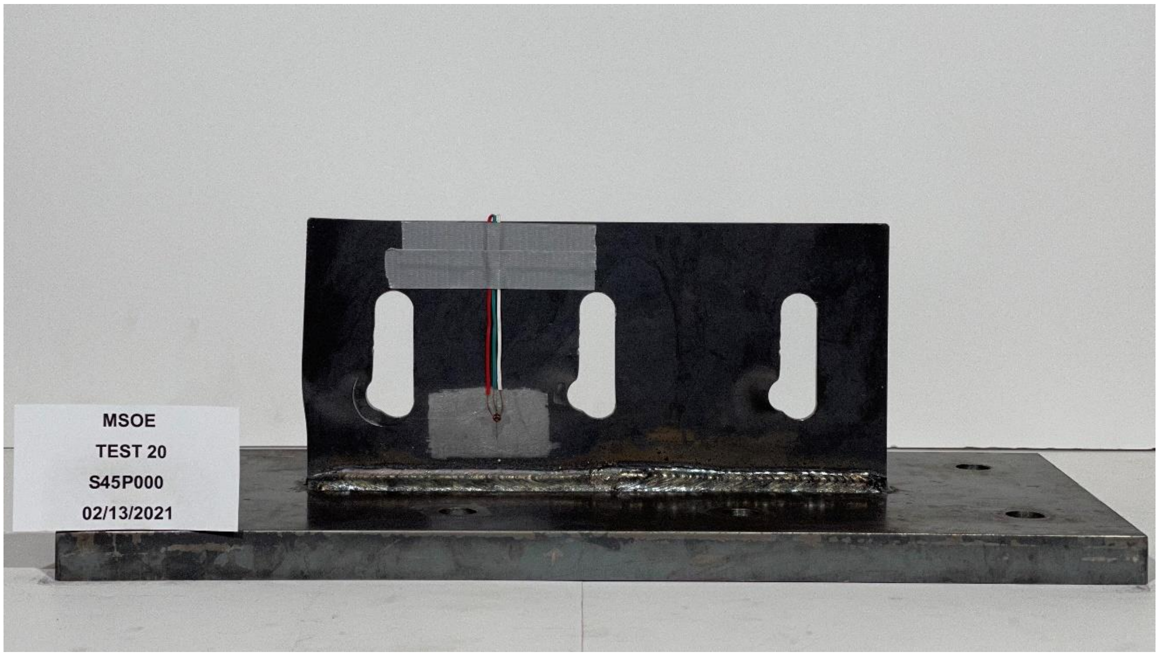

Figure G-41: Specimen S45P000 Post-Test, Front.

Figure G-42: Specimen S45P000 Post-Test, Loaded Edge.

Appendix H:

Load versus Strain Plots

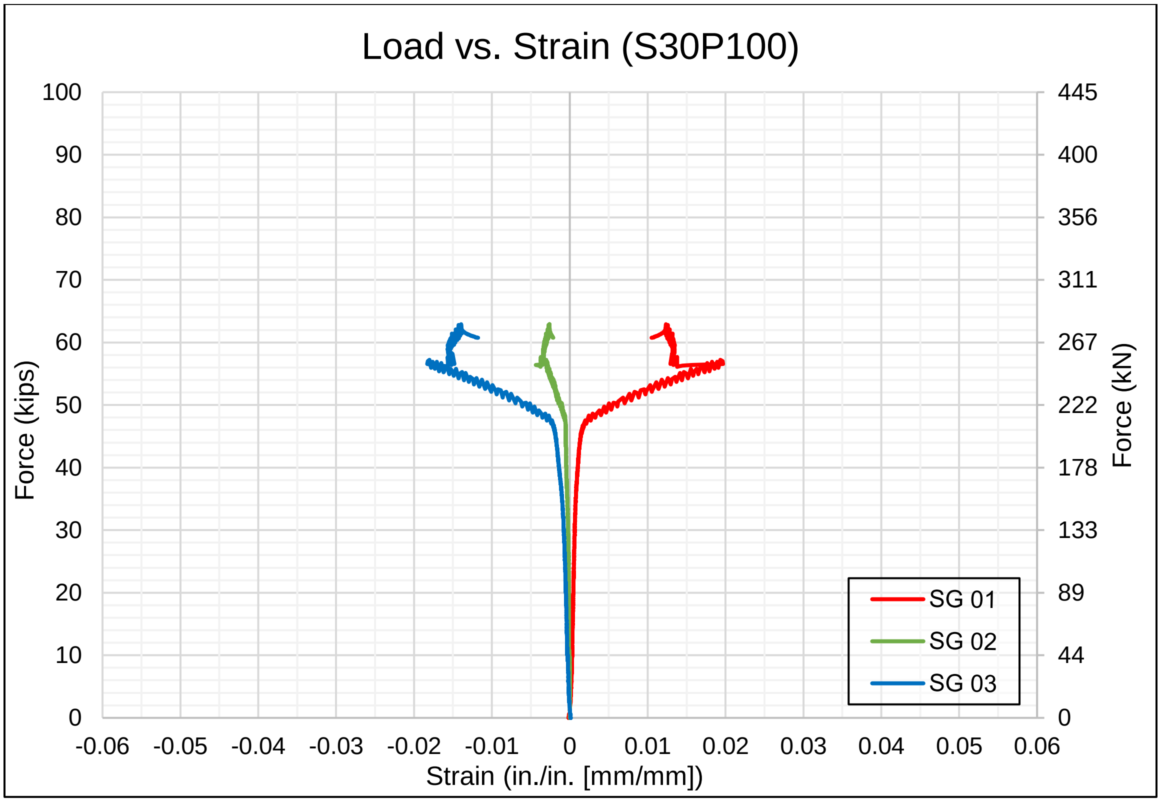

Figure H-1: Load Versus Strain Plot for Specimen S30P100.

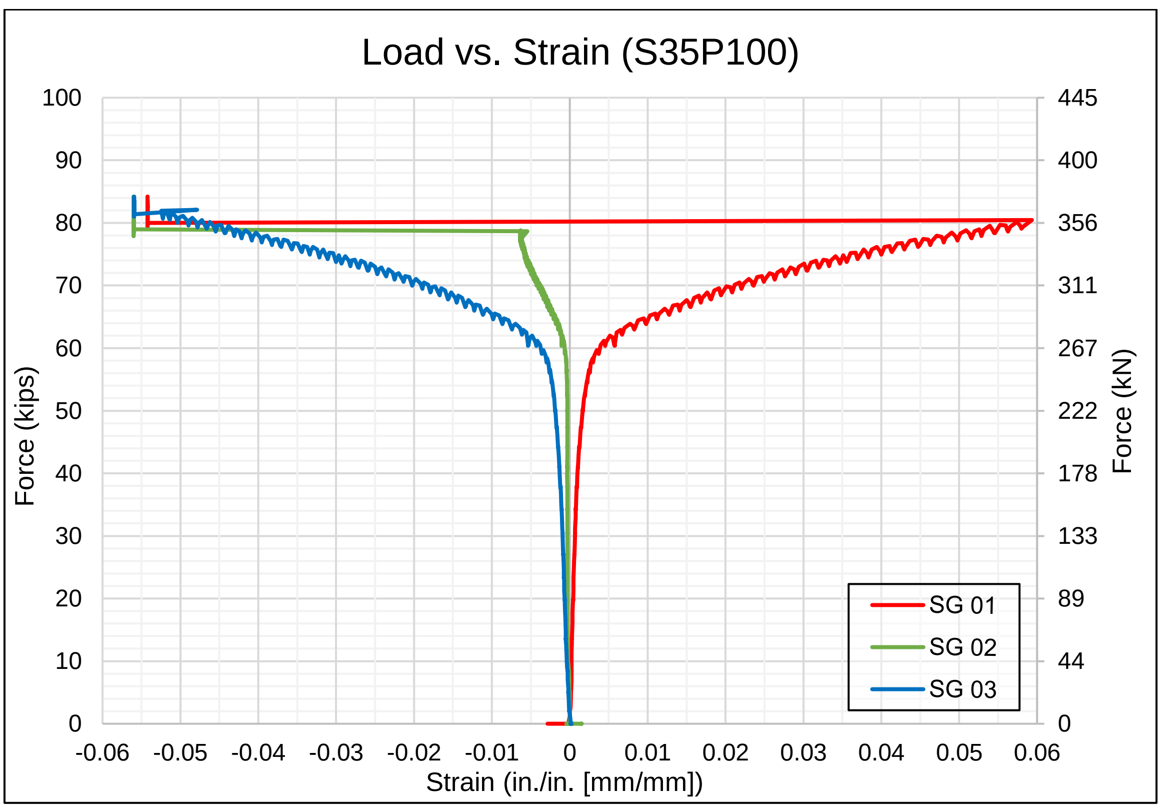

Figure H-2: Load Versus Strain Plot for Specimen S35P100.

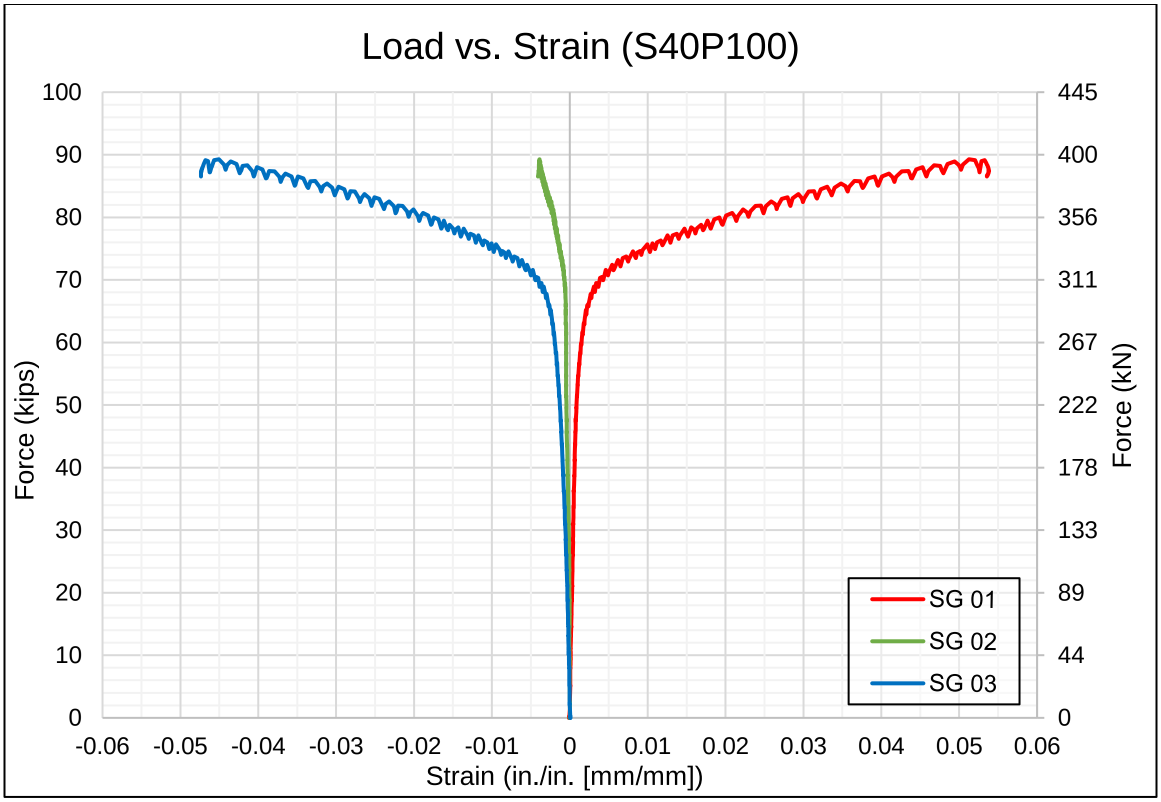

Figure H-3: Load Versus Strain Plot for Specimen S40P100.

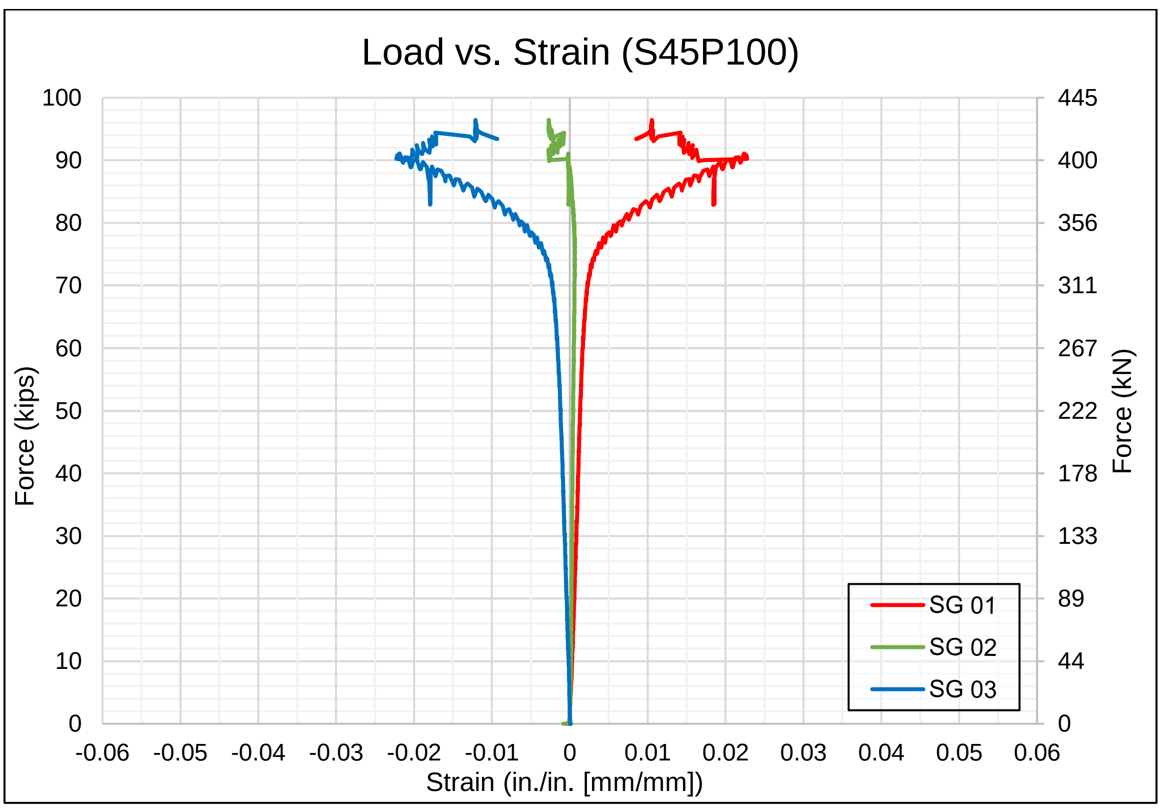

Figure H-4: Load Versus Strain Plot for Specimen S45P100.

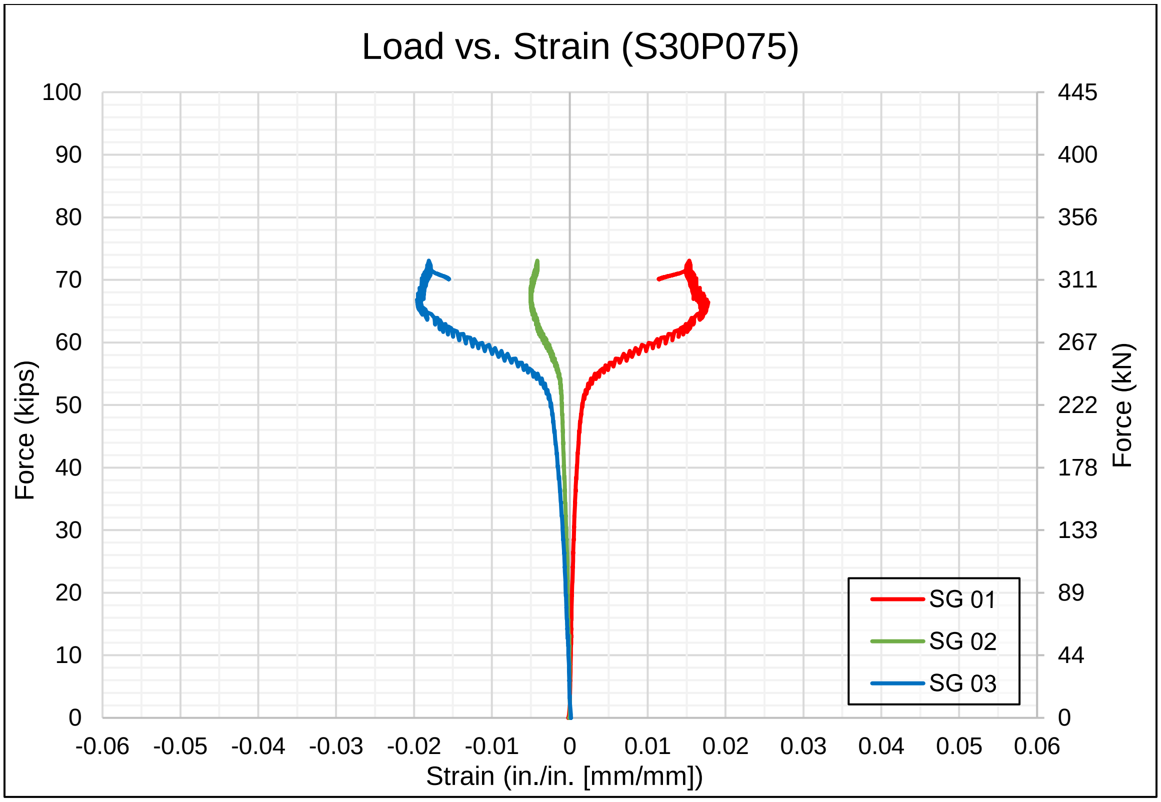

Figure H-5: Load Versus Strain Plot for Specimen S30P075.

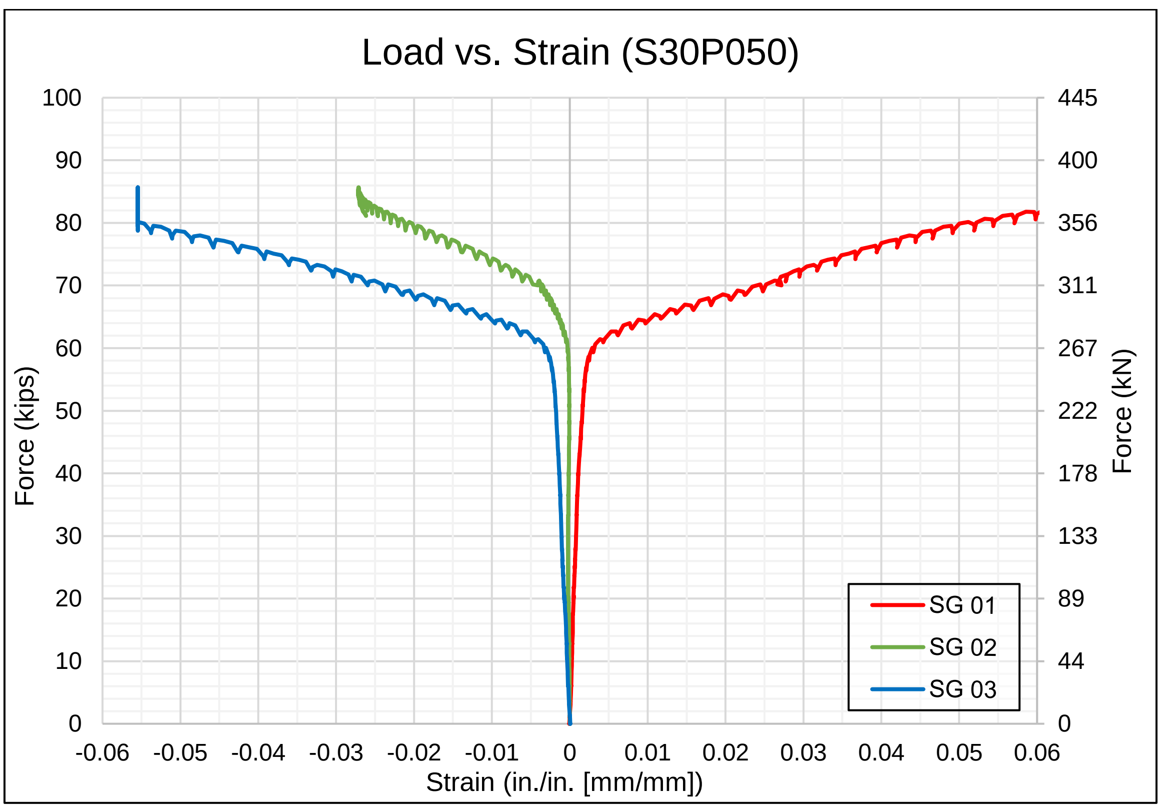

Figure H-6: Load Versus Strain Plot for Specimen S30P050.

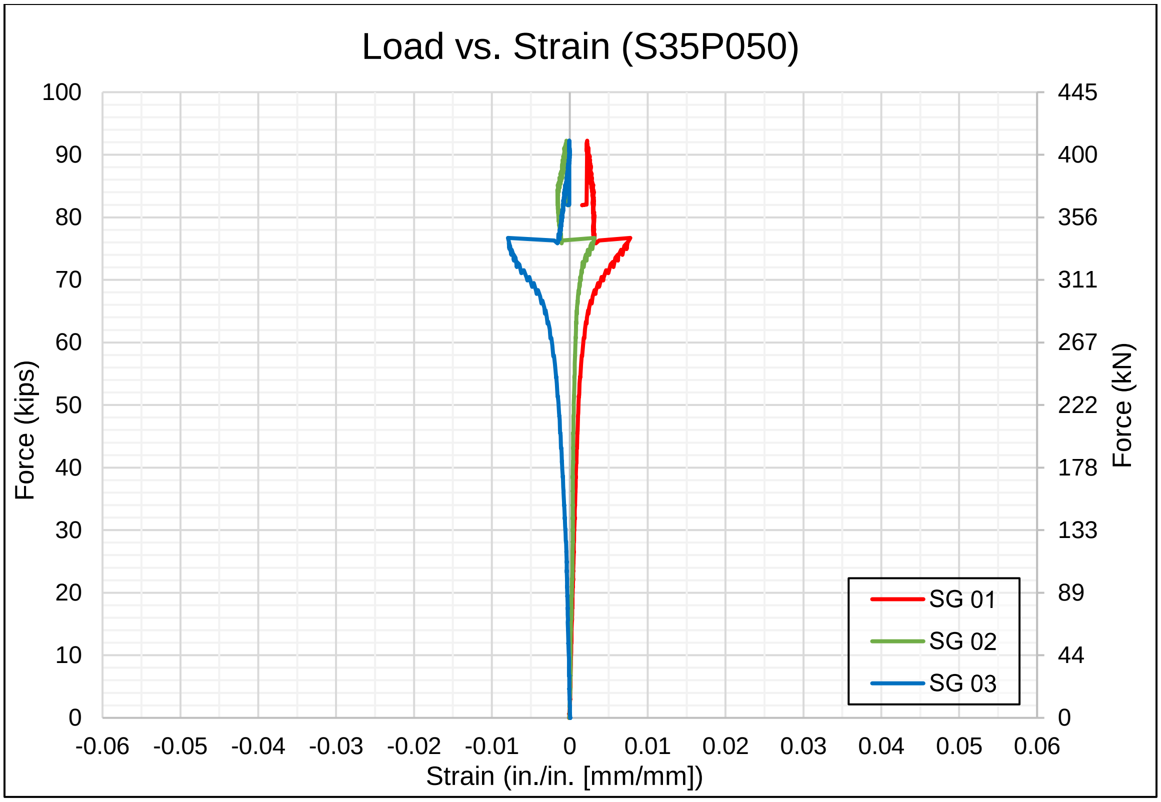

Figure H-7: Load Versus Strain Plot for Specimen S35P050.

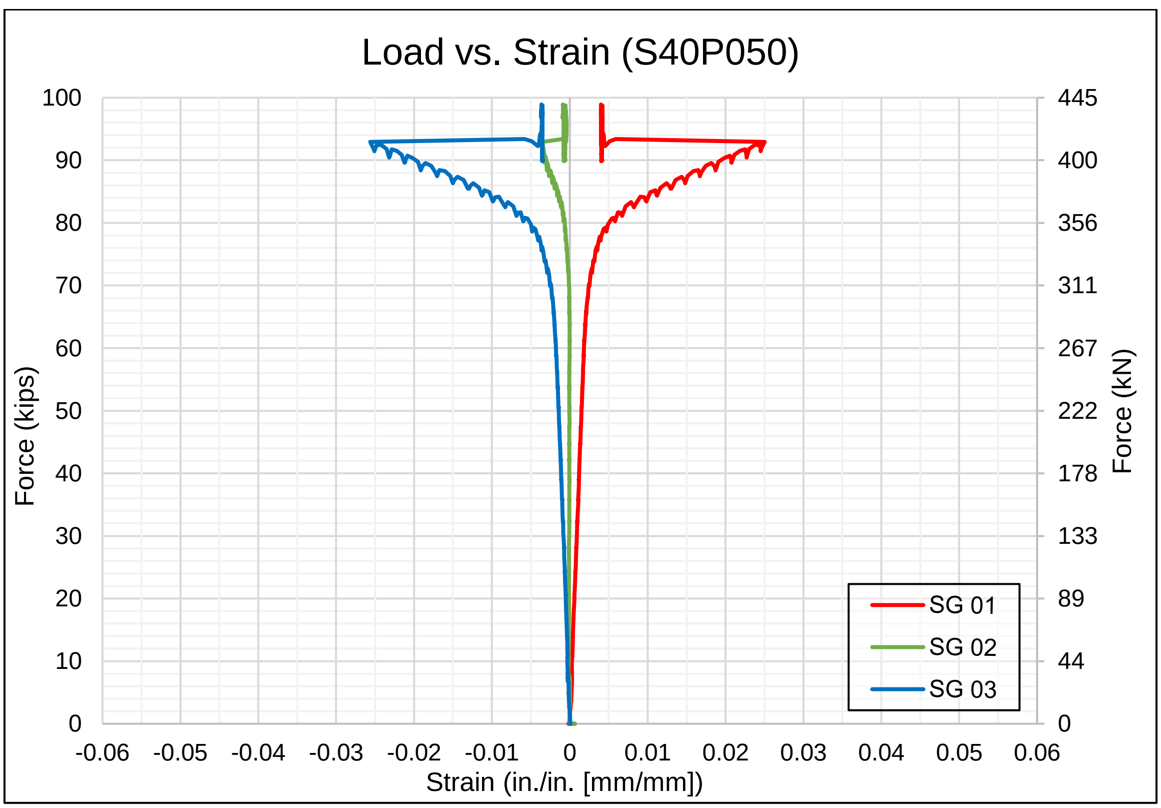

Figure H-8: Load Versus Strain Plot for Specimen S40P050.

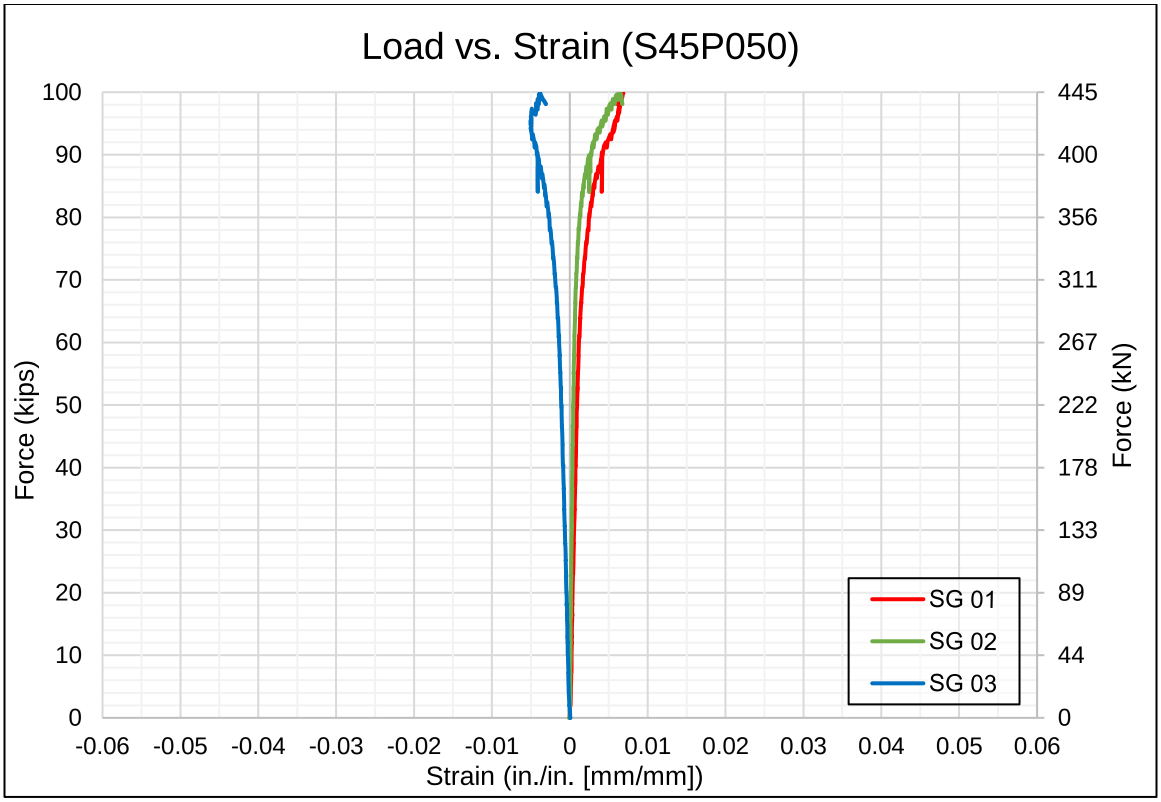

Figure H-9: Load Versus Strain Plot for Specimen S45P050.

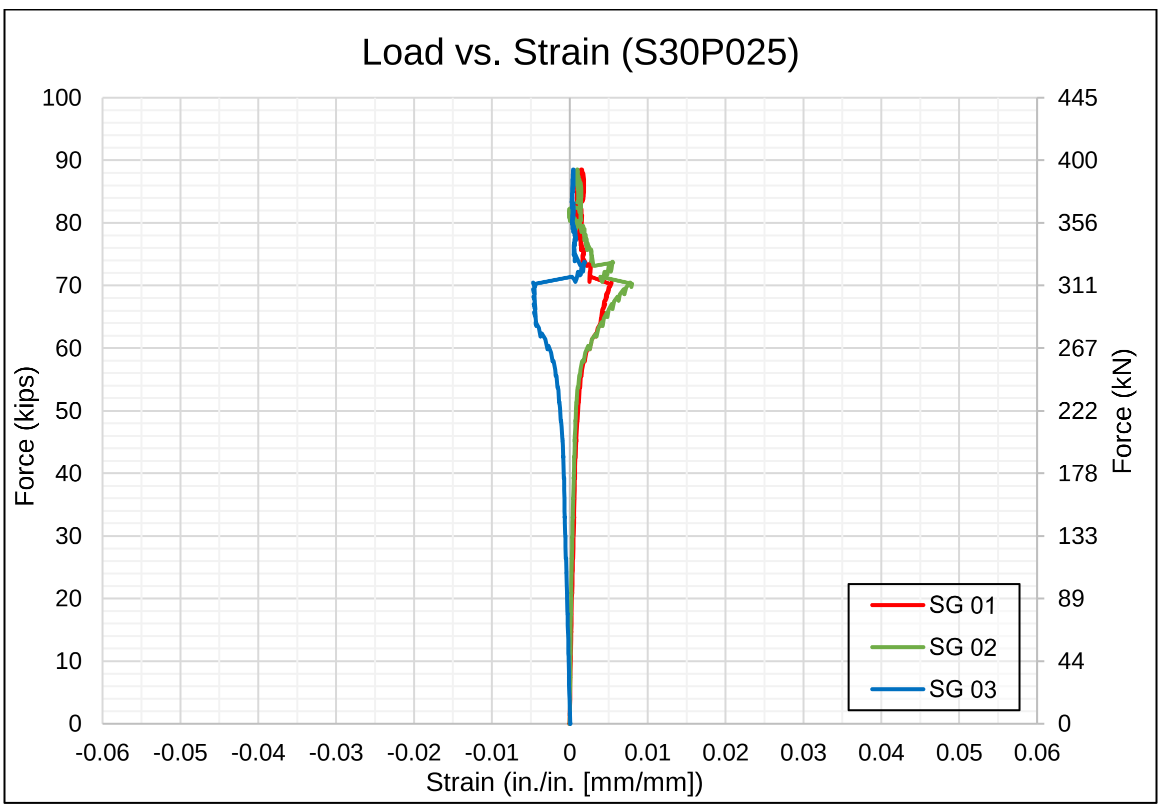

Figure H-10: Load Versus Strain Plot for Specimen S30P025.

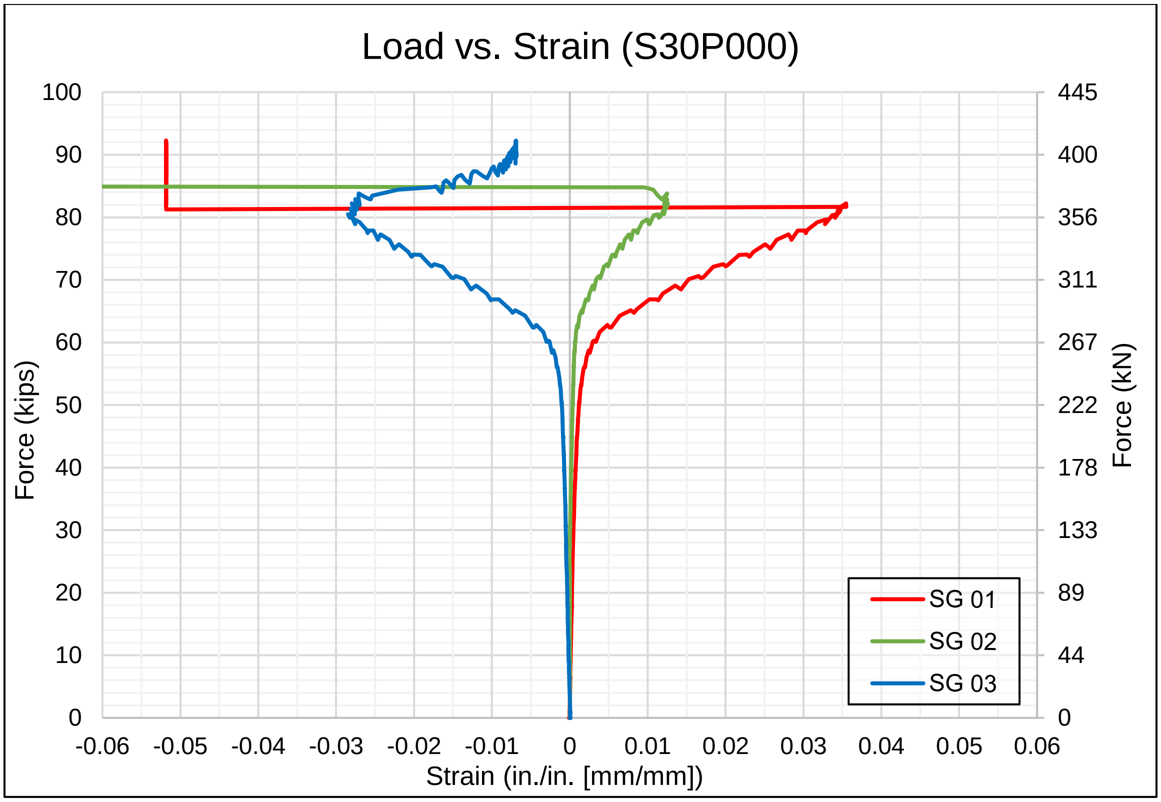

Figure H-11: Load Versus Strain Plot for Specimen S30P000.

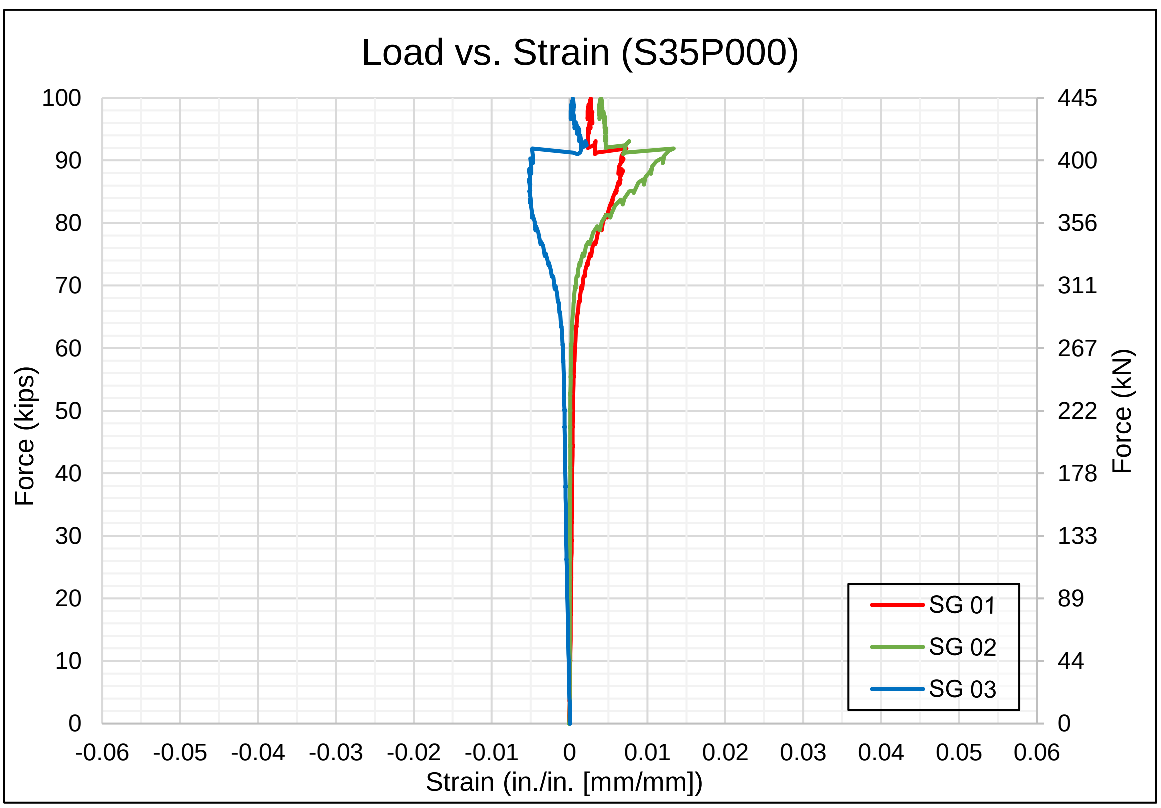

Figure H-12: Load Versus Strain Plot for Specimen S35P000.

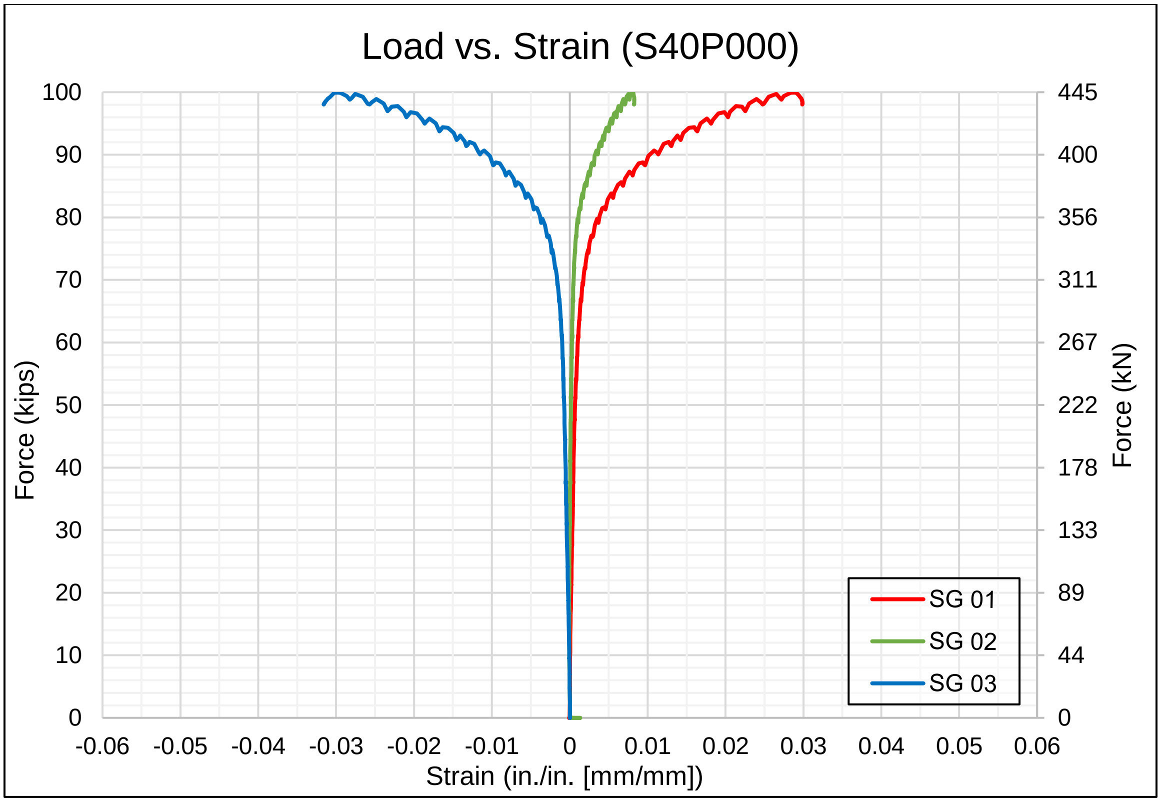

Figure H-13: Load Versus Strain Plot for Specimen S40P000.

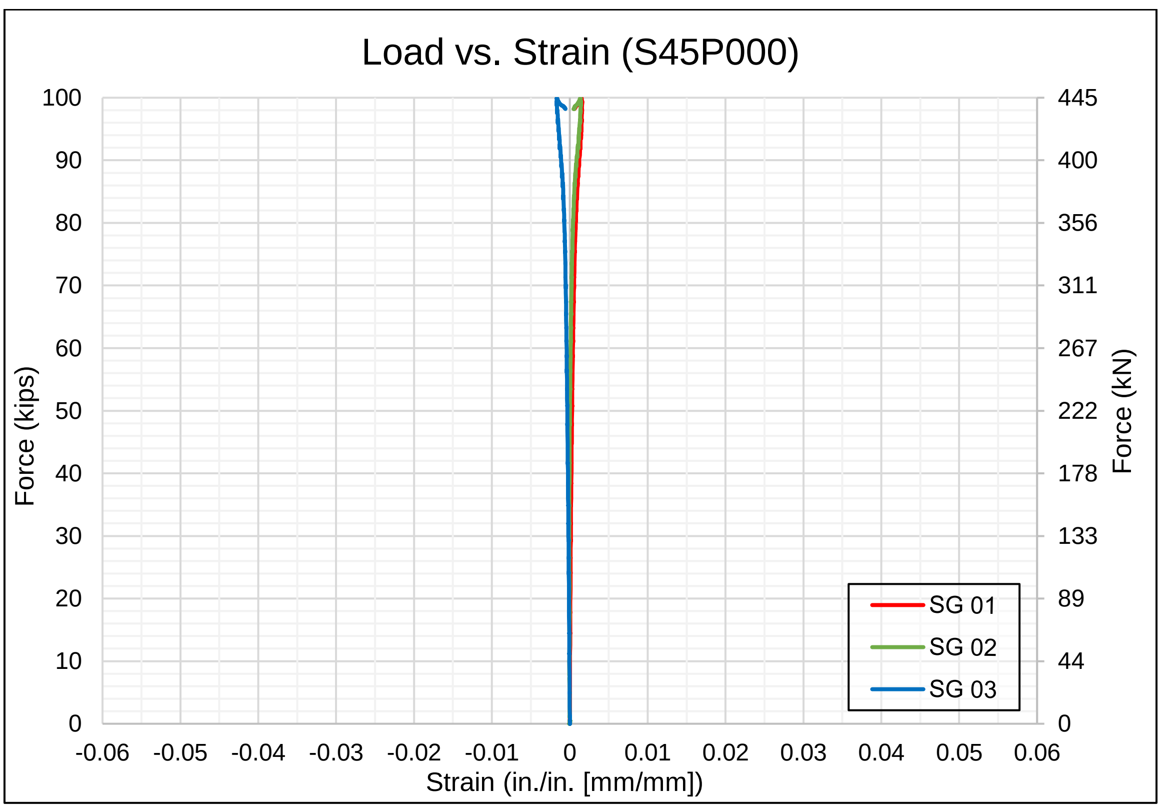

Figure H-14: Load Versus Strain Plot for Specimen S45P000.

Appendix I:

Summary of Changes Made to LVDT 1 Data During Prefilter Step

One note that is on every test except S30P100 is that the time steps were multiplied by four. Between specimen S30P100 and S35P100 (the first two tests in the experimental program), the sampling rate for the data was changed from 4 hertz to 16 hertz, except that there appeared to be an error and that the change only made the recorded time steps four times smaller and no additional data were gathered. This affects no part of the data analysis but is mentioned for the reader's understanding of the following summary.

Prefilter Notes

S30P100

- Deleted LVDT1 data from t = 0 to 22s to remove offset from start of test
- Deleted LVDT1 data from t = 175.5 to 179.75s to remove jump in LVDT
- Deleted LVDT1 data from t = 186.25-187.25, 212.5-213.75, 215.25-216.75, 233-233.75, 236.75s to remove noise from data
- Cut off data at t = 315.75 because LVDT came off specimen

S35P100

- Multiplied times by 4 to fix time range
- Removed outlier LVDT1 data at t= 61.25, 61.75 through 62.25, and 67.75s
- Deleted all data between t = 0 and 11.9375

S40P100

- Multiplied times by 4 to fix time range
- Deleted data from t=0 to 45.5s to remove noise at start of test
- Deleted outlier LVDT1 data at t = 57.25, 64.25, 69.25, 85, 85.25s

S45P100

- Multiplied times by 4 to fix time range
- Removed LVDT1 data Load less than 15,000 lbf to remove noise from beginning of test
- Removed outlier LVDT1 data from t = 60.25-60.75, 69.5-70.5, 76.5-76.75, 81.25, 85.5, 88.25-88.5, 95.5-95.75s
- Removed LVDT1 data from t = 97-103.75s because load was decreasing at the actuator

S30P075

- Multiplied times by 4 to fix time range

S35P075

- Multiplied times by 4 to fix time range
- Deleted t=0 through 29.25s to remove flickering of data at beginning of test when there was no load
- Deleted outlier LVDT1 data at t = 51.25, 62.5, 67.75-68, 68.75-69, 73.5-73.75, 80.25, 80.75-81.75s

S40P075

- Multiplied times by 4 to fix time range
- Deleted data from t=0 through 36s to remove noise at start of test
- Removed outlier LVDT1 data at t = 66.5, 67, 76, 85.25, 91, 91.75s

S45P075

- Multiplied times by 4 to fix time range
- Subtracted difference in LVDT1 readings at t=61.25 and 62.5s (0.082566in) from LVDT data from t = 0 to 61.25s to shift lower part of graph over. There was no observable reason for this jump in data and could have been caused by something internal to the LVDT
- Removed outlier LVDT1 data from t = 82.5, 83.5, 83.75, 84.25 through 85, 86.5s

S30P050

- Multiplied times by 4 to fix time range
- Removed data from t = 0 to 28.75s to remove extra data from before load was applied
- Removed outlier LVDT1 data from t = 30, 41.75-42.5, 49.75 and 64.5s

S35P050

- Multiplied times by 4 to fix time range
- Adjusted LVDT1 data for t=0 to24.75s to align data
- Removed outlier LVDT1 data at t = 25.25s
- Deleted data after t = 96.75s to remove noise at end of test

S40P050

- Multiplied times by 4 to fix time range
- Deleted data from t = 0 to 42.75 to remove noise at start of test
- Removed outlier LVDT1 data from t = 47.75, 59.5 through 60.25, 69.25, 79, 79.25, 88.75s

S45P050

- Multiplied times by 4 to fix time range
- Removed LVDT1 data from t = 0 to 17.25s to remove noise at start of test
- Removed outlier LVDT1 data from t = 49.5-50, 58.5, 61.5, 64.75-65, 67.5, 69.75-70.25, 72, 75.75-76, 79.25s
- Removed LVDT1 data from t = 81 to 91.75 s because load was not being applied during that time and was decreasing at the actuator

S30P025

- Multiplied times by 4 to fix time range
- Deleted data for t = 0 to 14s to reduce noise at start of test
- Remove outlier LVDT1 data at t = 21.25, 30, 37, 39.25s

S35P025

- Multiplied times by 4 to fix time range
- Deleted data from t = 0 to 16.5s to remove noise and offset from start of test
- Removed outlier LVDT1 data at t = 18.75, 19.5, 20, 40.75, 41.25-42.25, 42.75, 52.75-53, 59, 63.25, 67.25-67.5

S40P025

- Multiplied times by 4 to fix time range
- Adjusted LVDT1 data for t = 0 to 22.5s by 0.051243in to shift data.
- Removed outlier LVDT1 data from t = 23.25, 23.75, 33.75-34, 34.5-35, 35.5, 46-46.75, 53.75-54.25, 61.25, 62.25, 63, 70.25, 72.75

S45P025

- Multiplied times by 4 to fix time range
- Deleted data from t = 0 to 11.5s to remove noise at start of test
- Removed LVDT1 data from t = 29.75-31, 31.5, 44.25-44.75, 45.25-46, 57.25-57.75, 64.25-64.75, 70.5-70.75

S30P000

- Multiplied times by 4 to fix time range
- Deleted data for t=0 to 24.5s to remove noise at start of test
- Removed LVDT1 outlier data from t = 38.5, 39-39.75, 48-48.25, 53.5s

S35P000

- Multiplied times by 4 to fix time range
- Removed LVDT1 data from t = 0 t0 17.25s to remove noise at start of test
- Removed outlier LVDT1 data at t= 17.75, 23.5-24, 30.5-30.75, 35.5, 40-40;25, 43.25-43.5, 45.75, 51, 56.5, 61.25s

S40P000

- Multiplied times by 4 to fix time range
- Deleted data from t = 0 to 22.5s to remove noise at start of test
- Removed utlier LVDT1 data from t = 23-24, 29.25-29.75, 30.5, 31-31.5, 36.25, 40.75-41.25, 45.25-45.5, 49.5, 53, 57.75, 59.75, 61.5

S45P000

- Multiplied times by 4 to fix time range
- Deleted data after t = 70.5s because no more load was applied
- Removed outlier LVDT1 from t = 60.75, 61.5-61.75, 62.5, 64.25, 65.75, 66.5, 67, 68, 68.5, 69.25s
- Removed outlier LVDT1 from t = 60.75, 61.5-61.75, 62.5, 64.25, 65.75, 66.5, 67, 68, 68.5, 69.25s

Appendix J:

MATLAB Code

Two sets of code are provided. The first is for specimen S30P100 and has the additional median filter. The second is for the remaining specimens and does not have the additional median filter.

```
%Filtering and Curve-Fitting Operation for Specimen S30P100

clc
clear all

drive = "C:\Users\";
user = "taxonds";

% Location of data to be filtered
path = "\Box\2020-21 CDKS\DST\12 Experimental Data\Data Analysis\03↙
Analysis_02_Prefilter";


%Index of all test IDs in order of test number
TestIDs =↙
['S30P100';'S35P100';'S40P100';'S45P100';'S30P075';'S35P075';'S40P075';'S45P075';'S30P050↙
';'S35P050';'S40P050';'S45P050';'S30P025';'S35P025';'S40P025';'S45P025';'S30P000';'S35P00↙
0';'S40P000';'S45P000'];

for TestNumber = 1

%Convert Test Number to text string and add leading "0" if needed
TestNum = string(TestNumber);
if TestNumber <= 9
    TestNum = strcat('0',TestNum);
end

%Set Test ID Based on Test Num
TestID = TestIDs(TestNumber,:);

%Import Prefiltered Data file

%String together full file name
    datafile = strcat(drive, user, path, 'Test', TestNum, '_', TestID,↙
'_Analysis_Prefilter.xlsm');

    %Read unmodified columns
    RawData = xlsread(datafile,4,'B:G');
    T = RawData(:,1);
    P = RawData(:,2);
    D2 = RawData(:,3);
    SG1 = RawData(:,4);
    SG2 = RawData(:,5);
    SG3 = RawData(:,6);

    %Read Modified Columns
    Data = xlsread(datafile,4,'H:J');
    TMOD = Data(:,1);
    PMOD = Data(:,2);
    D1MOD = Data(:,3);
```

```
%Filtering and Curve-Fitting Operation for Specimen S30P100

clc
clear all

drive = "C:\Users\";
user = "taxonds";

% Location of data to be filtered
path = "\Box\2020-21 CDKS\DST\12 Experimental Data\Data Analysis\03↙
Analysis_02_Prefilter";


%Index of all test IDs in order of test number
TestIDs =↙
['S30P100';'S35P100';'S40P100';'S45P100';'S30P075';'S35P075';'S40P075';'S45P075';'S30P050↙
';'S35P050';'S40P050';'S45P050';'S30P025';'S35P025';'S40P025';'S45P025';'S30P000';'S35P00↙
0';'S40P000';'S45P000'];

for TestNumber = 1

%Convert Test Number to text string and add leading "0" if needed
TestNum = string(TestNumber);
if TestNumber <= 9
    TestNum = strcat('0',TestNum);
end

%Set Test ID Based on Test Num
TestID = TestIDs(TestNumber,:);

%Import Prefiltered Data file

%String together full file name
    datafile = strcat(drive, user, path, 'Test', TestNum, '_', TestID,↙
'_Analysis_Prefilter.xlsm');

    %Read unmodified columns
    RawData = xlsread(datafile,4,'B:G');
    T = RawData(:,1);
    P = RawData(:,2);
    D2 = RawData(:,3);
    SG1 = RawData(:,4);
    SG2 = RawData(:,5);
    SG3 = RawData(:,6);

    %Read Modified Columns
    Data = xlsread(datafile,4,'H:J');
    TMOD = Data(:,1);
    PMOD = Data(:,2);
    D1MOD = Data(:,3);
```

```
   FileName = strcat('Test',TestNum, '_', TestID, '_Filtered.xlsx');
   xlswrite(FileName,Output)

   cd(strcat(drive,user,path))
   clear Output

end

cd(strcat(drive,user,'\Box\2020-21 CDKS\DST\12 Experimental Data\Data Analysis\01 Matlab↙
Filtering Code'))
```

```
%Filtering and Curve-Fitting Operation for All Specimens EXCEPT S30P100

clc
clear all

drive = "C:\Users\";
user = "taxonds";

% Location of data to be filtered
path = "\Box\2020-21 CDKS\DST\12 Experimental Data\Data Analysis\03↙
Analysis_02_Prefilter\";


%Index of all test IDs in order of test number
TestIDs =↙
['S30P100';'S35P100';'S40P100';'S45P100';'S30P075';'S35P075';'S40P075';'S45P075';'S30P050↙
';'S35P050';'S40P050';'S45P050';'S30P025';'S35P025';'S40P025';'S45P025';'S30P000';'S35P00↙
0';'S40P000';'S45P000'];

for TestNumber = 2:20

%Convert Test Number to text string and add leading "0" if needed
TestNum = string(TestNumber);
if TestNumber <= 9
    TestNum = strcat('0',TestNum);
end

%Set Test ID Based on Test Num
TestID = TestIDs(TestNumber,:);

%Import Prefiltered Data file

%String together full file name
    datafile = strcat(drive, user, path, 'Test', TestNum, '_', TestID,↙
'_Analysis_Prefilter.xlsm');

    %Read unmodified columns
    RawData = xlsread(datafile,4,'B:G');
    T = RawData(:,1);
    P = RawData(:,2);
    D2 = RawData(:,3);
    SG1 = RawData(:,4);
    SG2 = RawData(:,5);
    SG3 = RawData(:,6);

    %Read Modified Columns
    Data = xlsread(datafile,4,'H:J');
    TMOD = Data(:,1);
    PMOD = Data(:,2);
    D1MOD = Data(:,3);
```

```
%Put data that does not need to be filtered into the Output matrix
    L = length(P);
    Output(1:L,1)= T(:,1);
    Output(1:L,2) = P(:,1);
    Output(1:L,3) = D2(:,1);
    Output(1:L,4) = SG1(:,1);
    Output(1:L,5) = SG2(:,1);
    Output(1:L,6) = SG3(:,1);
    L = length(TMOD);
    Output(1:L,7) = TMOD(:,1);
    Output(1:L,8) = PMOD(:,1);


%Isolate data to be filtered
    UnfiltData = D1MOD;

%Begin Filtering Operation

    f = 30;                                   % Sampling frequency -> Leave at 30
    f_cutoff = .9;                            % Cutoff frequency
    fnorm = f_cutoff/(f/2);
    [b1,a1] = butter(10,fnorm,'low');         % Low pass Butterworth Filter, 10th Order
    Filter1 = filtfilt(b1,a1,UnfiltData);     % Filter 1: Buterworth Filter

    count = round(L/15);                      %Sets window based on length of vector being↙
filtered
    Filter2 = medfilt1(Filter1,count);        % Filter 2: Median Filter


%Curve Fit Filtered Data

    %Runs curve fit function for filtered data, value of 0.9999999 is set
    %such that the curve smooths out roughness of data while still
    %following the trend of the data
        curvefit = fit(Filter2,PMOD,'smoothingspline','SmoothingParam', .9999999);
    %Returns Y values for function based on displacement input
        CurveFitY = curvefit(Filter2);

%Add filtered and curve fit data to output table
    Output(1:L,9) = Filter2;
    Output(1:L,10) = CurveFitY;

%Write Data to File
   savepath = "\Box\2020-21 CDKS\DST\12 Experimental Data\Data_03_Filtered";
   savefile = strcat(drive, user, savepath);
   cd (savefile)
   FileName = strcat('Test',TestNum, '_', TestID, '_Filtered.xlsx');
   xlswrite(FileName,Output)

   cd(strcat(drive,user,path))
   clear Output
```

```
end

cd(strcat(drive,user,'\Box\2020-21 CDKS\DST\12 Experimental Data\Data Analysis\01 Matlab
Filtering Code'))
```

Civil Engineering

Capstone Report Approval Form

Master of Science in Civil Engineering -- MSCVE

Milwaukee School of Engineering

This capstone report, entitled "Effect of Slot Spacing on Single Plate Connections with Long Slots" submitted by the student Drake S. Taxon, has been approved by the following committee:

Faculty Advisor: ________________________ Date: 5/25/2021

Dr. Christopher Raebel, Ph.D., PE, SE

Faculty Member: ________________________ Date: 5/25/2021

Dr. Pouria Bahmani, Ph.D., PE

Faculty Member: ________________________ Date: 5/25/21

Michael Kempfert, PE